Universidade de Brasília
Faculdade de Medicina
Programa de Pós-Graduação em Patologia Molecular

ANÁLISE PROTEÔMICA E TRANSCRICIONAL DE *Paracoccidioides* EM CONDIÇÕES QUE MIMETIZAM A INFECÇÃO

Tese de Doutorado

Aluna: Kelly Pacheco de Castro
Orientadora: Dra. Célia Maria de Almeida Soares

Brasília, DF 20/12/2012

KELLY PACHECO DE CASTRO

ANÁLISE PROTEÔMICA E TRANSCRICIONAL DE *Paracoccidioides* EM CONDIÇÕES QUE MIMETIZAM A INFECÇÃO

Tese apresentada ao Programa de Pós-Graduação em Patologia Molecular da Universidade de Brasília como requisito para obtenção do título de Doutor em Patologia Molecular

Orientadora: Profa. Dra. Célia Maria de Almeida Soares

TRABALHO REALIZADO NO LABORATÓRIO DE BIOLOGIA MOLECULAR DO DEPARTAMENTO DE BIOQUÍMICA E BIOLOGIA MOLECULAR, DO INSTITUTO DE CIÊNCIAS BIOLÓGICAS DA UNIVERSIDADE FEDERAL DE GOIÁS.

APOIO FINANCEIRO: CAPES/ CNPq/ SECTEC-GO/ FAPEG /PRONEX/FINEP

BANCA EXAMINADORA

TITULARES

Profa. Dra. Célia Maria de Almeida Soares, Instituto de Ciências Biológicas, Universidade Federal de Goiás.

Prof. Dr. Carlos André O. Ricart, Departamento de Biologia Celular, Universidade de Brasília.

Prof. Dr. Carlos Roberto Félix, Instituto de Ciências Biológicas, Universidade de Brasília

Dra. Luciana Casaletti, Instituto de Ciência Biológicas, Universidade Federal de Goiás.

Prof. Dr. Octávio Luiz Franco, Centro de Análises Proteômicas e Genômicas, Universidade Católica de Brasília.

SUPLENTE

Profa. Dra. Silvia Maria Salém Izacc Furlaneto, Instituto de Ciências Biológicas, Universidade Federal de Goiás.

Não sei... Se a vida é curta
Ou longa demais para nós,
Mas sei que nada do que vivemos
Tem sentido, se não tocamos o coração
Das pessoas.
Muitas vezes basta ser:
Colo que acolhe,
Braço que envolve,
Palavra que conforta,
Silêncio que respeita,
Alegria que contagia,
Lágrima que corre,
Olhar que acaricia,
Desejo que sacia,
Amor que promove.
E isso não é coisa de outro mundo,
É o que dá sentido à vida.
É o que faz com que ela
Não seja nem curta, Nem longa demais,
Mas que seja intensa,
Verdadeira, pura... Enquanto durar
(Saber viver – Cora Coralina)

Dedico este trabalho às pessoas mais importantes da minha vida...

Ao meu querido pai Adenil Alves de Castro pelo
exemplo de sabedoria e luta diante da vida.
Obrigada por acreditar em mim.

A minha mãe Elcione Ferreira Pacheco de quem
recebi grandes ensinamentos de vida,
coragem e perseverança.

Aos meus irmãos Eberton Pacheco de Castro (In
memorian) e Wemerson Pacheco de Castro.
Muito obrigado pelo apoio, carinho e amor
em todos os momentos.

Amo muito todos vocês!!!

Ao meu esposo Cleydson Henrique Siqueira, companheiro e amigo de tantos momentos felizes e conturbados, que soube com doação imensa e amor torná-los mais leves e mais prazerosos. Em quem encontrei compreensão pela ausência e amor para seguir adiante.

"O amor é força e poder, como o ferro no cimento: as duas naturezas fundem-se e transformam-se num só e único bloco inquebrantável, contra o qual em vão se abate a força daqueles que o queiram partir...".

Amo muito você.

AGRADECIMENTOS

À Deus, o Todo de Tudo. Se existem a Vida, a beleza, a sabedoria e o amor, é porque Ele está sempre presente. Obrigada por me dar forças nos momentos de fraqueza e cansaço e principalmente por sempre ter cuidado de mim. Sei que sempre posso contar Contigo.

À Profa. Dra. Célia Maria de Almeida Soares pela orientação, atenção, confiança e principalmente pelo grande exemplo de luta e dedicação na área de pesquisa. Você é um exemplo de profissionalismo e coragem. Sem a sua ajuda eu não teria conseguido terminar este trabalho. Obrigada por tudo, por me acolher em seu laboratório e por estes 10 anos de convivência e aprendizagem. Tenha sempre minha eterna admiração.

À Profa. Dra Maristela Pereira pelo apoio e pelas sugestões.

À Profa Silvia Maria Salém Izacc pela presença sempre alegre e amiga e pela disposição constante em ajudar.

Ao Prof. Alexandre, uma das pessoas mais extraordinárias que conheci. Sua inteligência é fora do comum. Obrigada pela ajuda, pela disponibilidade e por todos os momentos de aprendizagem.

Aos Profs. Clayton e Juliana. Pela disposição em sempre ajudar. Muito obrigada.

À minha amiga Tereza Cristina, também uma pessoa extraordinária. A sua ajuda foi essencial. Obrigada por todos os momentos de carinho, confiança, conselhos e amizade.

À Ana Flávia Parente. Obrigada por todo o profissionalismo e dedicação.

À Patrícia Zambuzzi e Dacie por todas as conversas, pela convivência e amizade. Vocês são pessoas especiais que sempre levarei no coração.

Ao meu amigo Ronney, que não tenho mais contato. Mas que foi muito importante na condução deste trabalho. Obrigada pelo apoio e ajuda.

Ao Leandro que sempre cuidou tão bem dos camundongos! Obrigada pela companhia e disposição em sempre ajudar. Admiro sua simplicidade e acredito no seu potencial.

Aos queridos amigos que fizeram parte desta história: Nathalie, Hellen,Sarah, Rodrigo, Amanda, Dayane, Luciane Almeida, Fabiana. Saudades!!

Aos amigos Mariana, Neto, Renata, Symone, Lucas, Priscila pela feliz convivência.

E a todos os colegas e companheiros do laboratório de Biologia Molecular: Simone Weber, Sheila, Elisa, Mirelle, Edilânia, Laura, Luciana, Marielle, Patrícia Lima, Karine.

Ao professor Bergmann e funcionários da Pós-Graduação pela boa vontade em ajudar os alunos de Goiânia.

Aos membros da Banca que aceitaram o convite para contribuir com nosso trabalho.

Aos Professores do Programa de Pós-Graduação em Patologia Molecular.

Aos agentes financiadores do trabalho.

À todos os meus familiares, amigos e colegas e as pessoas que, de alguma maneira, participaram desta jornada.

"Quem tem 'por que' viver pode suportar qualquer 'como' viver."

Nietzsche

SUMÁRIO

LISTA DE ABREVIATURAS E SÍMBOLOS

2D - gel bidimensional

2-DE - eletroforese bidimensional

ACN - acetonitrila

ADH – álcool desidrogenase

Badh - betaína aldeído desidrogenase

CAP20 - fator de virulência cap20

Cat - catalase

CDF- facilitador de difusão de cátions

CHAPS - 3-(colamidopropil)dimetilamônio-1-propanosulfonato

CHCA - ácido α-ciano- 4-hidroxicinamico

CoA - coenzima A

COEP - comissão de ética em pesquisa animal

Cot1 - transportador intracelular de zinco e cobalto

Crs1 - fator de transcrição zinco responsivo

Cs – citrato sintase

Ctf1B - C6 fator de transcrição

Ctr3 - transportador de cobre de alta afinidade

DDC - descarboxilase de aminoácidos aromáticos

DEPC - dietil pirocarbonato

Dfg5 - glicosil hidrolase

DIP5 – permease de aminoácido dicarboxílico

DP – produto diferencial

DTT - ditiotreitol

DIGE - eletroforese de fluorescência diferencial em gel 2D

E2 - 17β-estradiol

EBP - proteína que liga-se ao estradiol

EDTA - ácido etilenodiaminotetracético

Elf1B - fator de elongação 1B

ERG25 - C-4-esterol metil oxidase

ERO - espécie reativa de oxigênio

ESI - Ionização tipo eletrospray

EST - etiqueta de seqüência expressa

Fet4 - transportador de baixa afinidade de ferro

G - força centrífuga

Gata - fator de transcrição com dedos de zinco

gi - identificadores gerais de informação do banco de dados GenBank

Gln1- glutamina sintase

GP - glicoproteína

GPI - glicosilfosfatidilinositol

HPLC - cromatografia líquida de alta performance

HSF-1 - fator transcricional de choque térmico-1

Hsp - proteína de choque térmico

IAA - Iodoacetamida

Icl - Isocitrato liase

IEF - focalização isoelétrica

IL - interleucina

INF - interferon

IPG - gradiente de pH imobilizado

IPTG - isopropil-β-D-tiogalactopiranosídeo

ITS - sequência espaçadora interna

IVIAT - tecnologia de indução de antígenos *in vivo*

LS - lumasina sintase

MALDI - ionização à laser assistida por matriz

MALDI-TOF - ionização por dessorção a laser assistida por matriz e análise por tempo de vôo (TOF)

MALDI-TOF-TOF - fonte tipo MALDI com dois analisadores em série tipo TOF

MALDI-Q-TOF - fonte tipo MALDI com dois analisadores híbridos tipo quadrupolo e tempo de vôo (TOF)

MAPK - proteína quinase ativada por mitose

MIPS - centro de informação de sequências protéicas de Munique

MS - espectrometria de massas

Msc2 - transportador de zinco do retículo endoplasmático

m/z - razão massa-carga

NOKs - queratinócitos orais

NSdD - fator de transcrição tipo GATA

Q - quadrupolo

PA - persulfato de amônia

PAGE - eletroforese em gel de poliacrilamida

Pal1 - proteína de morfologia celular

pb - pares de base

PBS - solução de tampão fosfato

PCM - paracoccidioidomicose

PCR - reação em cadeia da polimerase

PMF - perfil de digestão tríptica

p/v - peso por volume

Qcr8 - subunidade do citocromo oxidase c

q.s.p - quantidade suficiente para

RDA - Análise de Diferença Representacional

ROS - espécies reativas ao oxigênio

RPD3 - histona deacetilase

RPM - rotações por minuto

qRT-PCR - PCR quantitativo acoplado a transcrição reversa

SAGE - análise serial de expressão gênica

SDS - dodecil sulfato de sódio

SDS - PAGE – gel de poliacrilamida em condições desnaturantes

Ser - serina proteinase

Skb1 - arginina N-metiltransferase

TCA - ciclo do ácido tricarboxílico

TFA - ácido trifluoracético

TNF - fator de necrose tumoral

TOF - tempo de vôo

TPEN - N,N,N_,N_-tetrakis (2-pyridyl-methyl) ethylenediamine

TRE - trealose fosfato sintase

Tris - tris(hidroximetil)aminometano.

UDP - uridina difosfato

UV - ultravioleta

v/v - volume por volume

Zap1- fator de transcrição zinco responsivo

Zip - Zrt- Irt-like Proteína

Zrc1 - transportador intracelular de zinco

Zre - elemento zinco responsivo

ZrfA - fator de transcrição para proteínas zinco-responsivas

ZrfB - zinco-permease de alta afinidade

Zrt1 - transportador de zinco/ferro de alta afinidade

Zrt2 - transportador de zinco de baixa afinidade

Zrt3 - transportador de zinco vacuolar

RESUMO

O fungo *Paracoccidioides* é um patógeno humano com ampla distribuição na América Latina. A infecção se inicia por inalação de conídios e ou propágulos da forma miceliana que ao atingirem o pulmão do hospedeiro se diferenciam na fase leveduriforme. Embora o perfil de expressão gênica em *Paracoccidioides* venha sendo estudado, pouco se conhece sobre o padrão de expressão de genes desta espécie durante o processo infeccioso. Durante a infecção, patógenos regulam o metabolismo em resposta a diferentes tipos de estresse e quantidades variadas de nutrientes disponíveis no hospedeiro, presumivelmente permitindo a sua adaptação e sobrevivência. Os íons metálicos são elementos essenciais para a manutenção de importantes vias metabólicas, e por esse motivo, a capacidade de adquiri-los pelos patógenos, a partir de fontes disponíveis no organismo hospedeiro, é considerada um fator de virulência. O zinco é considerado um íon metálico essencial para todos os organismos, por ser requerido para transcrição, tradução, replicação, resistência ao estresse oxidativo e virulência. Transportadores para este íons são altamente expressos em condições de infecção por *Paracoccidioides.* O presente trabalho descreve a análise de genes e proteínas diferencialmente expressos em células leveduriformes de *Paracoccidioides* em condições que mimetizam a infecção. Foi realizada a comparação do perfil proteômico de *Paracoccidioides* durante a privação de zinco e na disponibilidade desse metal com o objetivo de se descrever os mecanismos utilizados pelo fungo para sobreviver no ambiente com baixa disponibilidade de zinco, mimetizando a condição encontrada pelo patógeno durante a infecção. Adicionalmente, foi realizada a análise transcricional de *Paracoccidioides* recuperado de animais infectados. Os dados revelaram que proteínas relacionadas com resposta ao estresse, metabolismo de aminoácidos, gliconeogênese e ciclo do metilcitrato foram regulados durante a privação de zinco. Os transcritos induzidos durante a infecção no pulmão foram aqueles predominantemente relacionados com metabolismo de lipídios, ácidos graxos e isoprenóides, metabolismo de aminoácidos, resposta ao estresse e virulência e metabolismo de carboidratos. A expressão diferencial dos genes e proteínas identificados foi confirmada por ensaios de qRT-PCR. Os dados gerados podem facilitar estudos funcionais de novos genes e proteínas os quais podem ser importantes para estratégias de sobrevivência e adaptação do *Paracoccidioides* no hospedeiro.

Palavras Chave: *Paracoccidioides*, infecção, pulmão, deprivação de zinco, RDA, análise proteômica

ABSTRACT

Paracoccidioides is a fungal human pathogen with a wide distribution in Latin America. The fungus causes infection through host inhalation of airborne propagules of the mycelial phase of the organism. These particles reach the lungs and differ in the yeast phase. Although gene expression in *Paracoccidioides* had been studied, little is known about the genome sequences expressed by this species during the infection process. During infection, pathogens regulate the metabolism in response to different types of stress and varying amounts of nutrients available in the host, presumably allowing its adaptation and survival. Metal ions are essential elements for the maintenance of important metabolic pathways, and therefore, the ability to acquire them by pathogens from sources available in the host organism, is considered a virulence factor. Zinc is considered a metal ion essential for all organisms, being required for transcription, translation, replication, resistance to oxidative stress and virulence. Here we describe the analysis of genes and proteins differentially expressed in yeast cells of *Paracoccidioides* under conditions mimicking of infection. It was performed a comparison of the proteomic profile of *Paracoccidioides* during zinc deprivation and in the availability of the metal in order to describe the mechanisms used by the fungus to survive in the environment with low availability of zinc, mimicking the condition encountered by the pathogen during infection. Farther, was performed transcriptional analysis of *Paracoccidioides* recovered from lung of infected animals. The data revealed that proteins related to stress response, amino acid metabolism, gluconeogenesis and methylcitrate cycle were regulated during deprivation of zinc. The transcripts induced during infection in the lung were predominantly those related to lipid metabolism, fatty acid and isoprenoid, amino acid metabolism, carbohydrate metabolism and stress response and virulence. The differential expression of genes and proteins identified was confirmed by qRT-PCR assays. The data generated can facilitate functional studies of novel genes and proteins which may be important for survival strategies and adaptation of *Paracoccidioides* in the host.

Keywords: *Paracoccidioides*, infection, lung, zinc deprivation, RDA, proteomic analysis

Capítulo 1

Revisão Bibliográfica

1. INTRODUÇÃO

1.1. *Paracoccidioides* – Aspectos Gerais

Paracoccidioides, um fungo termodimórfico, é o agente etiológico da paracoccidioidomicose (PCM), uma micose humana sistêmica geograficamente restrita à América Latina (Restrepo & Tobón, 2005). O Brasil é responsável por 80% dos casos descritos na literatura, sendo a maioria reportados nas regiões Sul, Sudeste e Centro-Oeste (Blotta *et al*., 1999; Paniago *et al*., 2003).

O fungo se desenvolve como levedura nos tecidos infectados ou quando cultivado *in vitro* a 36°C, e como micélio (forma infectiva) em condições saprobióticas no meio ambiente, ou quando cultivado em temperaturas inferiores a 28°C (Bagagli *et al*., 2006). As leveduras de *Paracoccidioides* são caracterizadas por apresentarem brotamentos múltiplos, formados pela evaginação da célula-mãe, onde uma célula central é circundada por várias células periféricas, conferindo um aspecto de roda de leme de navio. A forma miceliana pode ser identificada por filamentos septados com conídios terminais ou intercalares (Restrepo-Moreno, 2003). A conversão morfogenética em *Paracoccidioides* está relacionada à mudança de temperatura (San-Blas, 1993), mas outros fatores foram identificados como influenciadores do dimorfismo, como o hormônio feminino 17β-estradiol capaz de inibir a transição de micélio para levedura (Restrepo, 1985; Sano *et al*.,1999). Acredita-se que a interação do hormônio com uma EBP (Estradiol Binding Protein), identificada em *Paracoccidioides*, iniba a transição morfológica do fungo, explicando abaixa incidência da PCM em mulheres (Shankar *et al*., 2011a). Pinzan e colaboradores (2010) evidenciaram que mecanismos imunológicos estão envolvidos na diferença de incidência de PCM entre homens e mulheres. Foi observada uma maior produção das citocinas IL-12, IFN-γ e TNF-α por células de baço de camundongos fêmeas em resposta à paracoccina, uma glicoproteína de *Paracoccidioides*, encontrada na superfície celular, capaz de estimular macrófagos a produzir TNF-α e óxido nítrico, podendo modular a resposta imune celular em modelo murino. Em contrapartida, células de camundongos machos apresentaram maior produção de IL-10, sugerindo assim uma resposta imunológica divergente entre os sexos. Os autores puderam também verificar que macrófagos provenientes de camundongos fêmeas apresentam maior produção de óxido nítrico, fato que, possívelmente, está relacionado com a maior mortalidade de leveduras internalizadas pelos macrófagos de fêmeas.

A PCM representa um sério desafio de saúde pública, com importância social eeconômica. Os indivíduos infectados compreendem principalmente trabalhadores rurais, do sexo masculino (Brummer *et al*., 1993; Barrozo *et al*., 2009). Prado e colaboradores (2009) demonstraram que as micoses sistêmicas estão em décimo lugar entre as doenças parasitárias e infecciosas que causam mais mortes no Brasil. Dados isolados mostraram que a PCM é a principal doença em causar mortes entre as micoses sistêmicas, seguida pela criptococose, candidíase e histoplasmose, representando um importante problema de saúde pública. Os Estados da região Sudeste e Sul tiveram as taxas de mortalidade mais altas, mais concentradas em São Paulo e Paraná. Em relação à idade e sexo, a maioria das mortes causadas pela doença ocorreu em indivíduos com idade entre 30-59 anos sendo a maioria do sexo masculino. A incidência da doença em homens foi de 13:1 quando comparada a das mulheres (Prado *et al*., 2009).

Alguns fungos termodimórficos como o *Paracoccidioides* tendem a ser restritos a regiões geográficas específicas, com determinadas características climáticas ou tipos específicos de solos que provavelmente auxiliam na adaptação do fungo ao habitat natural (Rappleye & Goldman, 2006). As diferentes condições de solos alteram a capacidade de crescimento da forma miceliana e a produção de conídios por *Paracoccidioides*. Sendo assim, Terçarioli e colaboradores (2007) verificaram que solos arenosos e argilosos, com alta umidade devem ser mais favoráveis para a produção de conídios, um fator importante por aumentar a eficiência de sobrevivência do fungo no meio ambiente e a capacidade de infectar animais e humanos. O nicho ecológico alternativo de *Paracoccidioides* são animais com temperatura corporal de 36 °C a 37 °C, onde a transição para a forma leveduriforme promove o estabelecimento da doença. O fungo tem sido freqüentemente isolado de tatus (*Dasypusnovem cinctus* no Brasil e *Cabassous centralis* na Colômbia) em áreas endêmicas, e esses animais são reconhecidos como reservatórios naturais do fungo (Corredor *et al*.,2005; Bagagli *et al*., 2008). O patógeno também tem sido relatado em cachorros (Canteros *et al*., 2010), pingüins (Garcia *et al*.,1993) e morcegos frugívoros (Grose & Tamsitt, 1965). Testes sorológicos e intradérmicos também sugeriram a presença do fungo em animais domésticos e primatas (Corte *et al*., 2007).

Avanços nas técnicas moleculares têm permitido a caracterização taxômica de espécies de microrganismos com base principalmente, no RNA ribossomal (rRNA) e seu correspondente DNA ribossomal (rDNA) (James *et al*., 1996). Leclerc e colaboradores (1994) e Bialek e colaboradores (2000), compararam sequências de

rDNA da subunidade ribossomal maior entre fungos dermatófitos e dimórficos e propuseram a classificação do *Paracoccidioides* como pertencente ao filo Ascomycota, a ordem Onygenales e a família Onygenaceae, junto com as formas teleomórficas de *Blastomyces dermatitidis*, *Histoplasma capsulatum* e *Histoplasma capsulatum var. duboissi*. Matute e colaboradores (2006), em estudos de polimorfismo genético, descreveram a existência de três diferentes espécies filogenéticas de *Paracoccidioides*: S1 (espécie 1), PS2 (espécie filogenética 2) e PS3 (espécie filogenética 3). A espécie filogenética PS3 está geograficamente restrita à Colômbia, enquanto S1 está distribuída no Brasil, Argentina, Paraguai, Peru e Venezuela. Alguns isolados da espécie filogenética PS2 foram encontrados no Brasil, nos estados de São Paulo e Minas Gerais, e ainda na Venezuela. Todas as três espécies foram capazes de induzir a doença em hospedeiros humanos e animais, no entanto, PS2 apresentou menor virulência. Em continuidade aos estudos sobre filogenia, Carrero e colaboradores (2008) realizaram análises comparando sequências de regiões codantes, não codantes e ITS (sequência espaçadora interna – "*internally transcribed sequence*") de 7 novos isolados e 14 isolados já estudados de *Paracoccidioides*, oriundos do Brasil, Colômbia e Venezuela, por meio do método de comparação genealógica GCPSR (*genealogical concordance phylogenetic species recognition*). Estas análises revelaram que a linhagem 01 de *Paracoccidioides* distancia-se das três espécies filogenéticas descritas anteriormente, sugerindo que Pb01 seja uma nova espécie do gênero *Paracoccidioides* (Carrero *et al*., 2008). Na tentativa de intensificar os estudos sobre a taxonomia do isolado Pb01, Teixeira e colaboradores (2009) usaram o método de GCPSR para investigar as diferenças genômicas do Pb01 com as outras três espécies filogenéticas anteriormente descritas (S1, PS2 and PS3). Foram utilizados 122 isolados, compreendendo o Pb01 e outros isolados da América Latina. As características morfológicas de conídio e de levedura dos isolados foram analisadas. De acordo com o método utilizado, o isolado Pb01 exibiu grande divergência em relação aos três grupos (S1, PS2 e PS3), inclusive diferenças morfológicas. De acordo com os autores, o Pb01 (referido como "Pb01-like") pode ser considerado uma nova espécie filogenética e sugerem a mudança do nome para *Paracoccidioides lutzii*, em homenagem a Adolfo Lutz.

Os genomas estruturais de três isolados de *Paracoccidioides* (Pb01, Pb03 e Pb18) foram finalizados por meio do projeto denominado "Genômica Comparativa de Coccidioides e outros Fungos Dimórficos". Assim, foram depositados o genoma completo de três diferentes isolados de *Paracoccidioides*, Pb01, Pb03 e Pb18 (Broad

Institute, http://www.broad.mit.edu/tools/data/seq.html). O genoma do isolado Pb01 é composto de 32,94 Mpb, com um total de 9.132 genes. Este isolado apresenta o maior genoma tanto em número de bases quanto em quantidade de genes comparado aos outros dois isolados analisados, que apresentaram genomas do tamanho de 29,06 e 29,95 Mpb, com número de genes de 7.875 e 8.741 (dados dos isolados Pb03 e Pb18, respectivamente).

1.2. Paracoccidioidomicose

A Paracoccidioidomicose (PCM) é uma micose humana sistêmica granulomatosa que é fatal se não tratada e freqüentemente leva a permanentes restrições no estilo de vida dos pacientes, uma vez que provoca extensivos danos fibróticos no pulmão. O fungo *Paracoccidioides* infecta hospedeiros humanos usualmente através das vias respiratórias, por inalação de propágulos do micélio e artroconídeos (Bagagli *et al*., 2006). No epitélio dos alvéolos pulmonares, conídios se diferenciam para a forma leveduriforrme, caracterizando a fase parasítica do fungo. *Paracoccidioides* é notavelmente um patógeno versátil, capaz de infectar numerosos nichos no hospedeiro, como a pele, as mucosas oral, nasal e gastrointestinal, baço, ossos, próstata, fígado, pâncreas e sistema nervoso central (Ramos-e-Silva & Saraiva, 2008; Lopes *et al*., 2009; Fortes *et al*., 2009; Goldani *et al*., 2011). A infecção ocorre inicialmente nos pulmões, de onde o fungo pode, através da via hematogênica e/ou sistema linfático, alcançar outros orgãos do hospedeiro, desenvolvendo uma forma disseminada da PCM (Franco, 1987).

A forma juvenil (aguda ou subaguda) da PCM representa 3 a 5% dos casos descritos da doença e afeta principalmente crianças e adultos jovens (Reis *et al*., 1986; Brummer *et al*., 1993). O quadro da doença caracteriza-se por um desenvolvimento rápido e por marcante envolvimento de órgãos como baço, fígado, gânglios linfáticos e medula óssea. A função imune mediada por células é gravemente deprimida nesses pacientes, provavelmente devido ao comprometimento medular (Londero & Melo, 1983; Brummer etal., 1993). Apesar de não haver manifestações clínicas ou radiológicas de comprometimento pulmonar evidente, pode-se isolar o fungo do lavado brônquico, evidenciando a participação do pulmão como porta de entrada do patógeno (Restrepo *et al*.,1989). Esta é a forma mais severa e com pior prognóstico (Brummer *et al*., 1993). A forma crônica ou adulta representa mais de 90% dos casos, sendo a maioria dos pacientes constituída por homens adultos. Ao contrário da forma aguda, o quadro

clínico apresenta um desenvolvimento lento com comprometimento pulmonar evidente (Brummer *et al*., 1993). Em aproximadamente 25% dos casos, o pulmão é o único órgão afetado-forma unifocal. Muitas vezes, com o desenvolvimento silencioso da doença, o paciente busca auxílio médico somente quando apresenta sintomas de comprometimento extrapulmonar. Nestes casos se constata o envolvimento de órgãos como pele, mucosas das vias aéreas superiores, tubo digestivo e linfonodos – forma multifocal (Londero, 1986; Brummer *et al*., 1993). A forma crônica apresenta notável tendência à disseminação, sendo pouco freqüentes os quadros onde há somente comprometimento pulmonar (Restrepo *et al*.,1983).

O grande número de tecidos que *Paracoccidioides* pode colonizar e infectar sugere que o fungo deve ter desenvolvido mecanismos que o capacitam a aderir, extravasar e invadir barreiras impostas pelos tecidos do hospedeiro (Mendes-Gianinni *et al*., 1994; Lenzi *et al*., 2000). Em *Paracoccidioides* alguns exemplos de moléculas de adesão à matriz extracelular, incluem, Gp43 (Vicentini *et al*., 1994), adesinas de 19 e 32 kDa (Gonzalez *et al*., 2005), 30 kDa (Andreotti *et al*., 2005), gliceraldeído-3-fosfato desidrogenase (Barbosa *et al*., 2006), triosefosfato isomerase (Pereira *et al*., 2007), DFG5 (Castro *et al*., 2007), malato sintase (Neto *et al*., 2009), enolase e Ctr3p (Nogueira *et al*., 2010; Bailão *et al*., 2012). Durante o processo de invasão tecidual, fungos patogênicos expressam moléculas que auxiliam na aderência celular, sendo fatores de colonização e disseminação.

1.3. Análises transcricionais em *Paracoccidioides*

Visando a descrição de genes, processos metabólicos, fatores de virulência, entre outros aspectos de *Paracoccidioides*, diferentes abordagens no estudo de transcriptomas têm sido aplicadas. O Projeto Genoma Funcional de *Paracoccidioides*, desenvolvido por um consórcio de laboratórios da região Centro - Oeste do Brasil (Projeto Genoma Funcional e Diferencial de *Paracoccidioides*) resultou no seqüenciamento de 25.511 clones derivados de bibliotecas de cDNA de levedura e micélio (Felipe *et al*., 2003; 2005). O projeto cobriu cerca de 80% do genoma estimado do fungo *Paracoccidioides* e possibilitou a detecção de genes diferencialmente expressos nas fases de *Paracoccidioides*. A análise do transcriptoma revelou alguns prováveis componentes das vias de sinalização e seqüências gênicas consideradas como potenciais alvos para antifúngicos em *Paracoccidioides*, não possuindo nenhum homólogo no genoma humano, como: quitina deacetilase, isocitrato liase e α-1,3-glucana sintase, todos

preferencialmente expressos na fase leveduriforme. Os autores descreveram ainda o perfil metabólico diferencial exibido por *Paracoccidioides* nas fases miceliana e leveduriforme. Em geral, micélio apresenta metabolismo aeróbio, uma vez que durante a fase saprofítica, genes que codificam enzimas que participam da fosforilação oxidativa, como a isocitrato desidrogenase e succinil coenzima A sintase, estão altamente expressos. Ao contrário, a fase leveduriforme apresenta metabolismo mais anaeróbio quando comparado a micélio; nesta fase, os altos níveis de expressão da álcool desidrogenase I favorecem a fermentação alcoólica e conseqüente produção de etanol (Felipe *et al*., 2005). A diferenciação celular em *Paracoccidioides* requer mudança na temperatura, o que pode ser associado com a resposta ao estresse. Dessa forma, foram identificados 48 transcritos codificando chaperonas ou proteínas envolvidas no processo de estresse, sendo oito diferencialmente expressos.

Outro projeto genoma funcional de *Paracoccidioides* foi desenvolvido por grupos do Estado de São Paulo. No banco de ESTs gerados, Goldman e colaboradores (2003), identificaram vários genes potenciais de virulência em *Paracoccidioides* homólogos à *Candida albicans*. A identificação de alguns genes de *Paracoccidioides* homólogos a genes envolvidos em vias de transdução de sinal e relacionados à virulência de *C. albicans*, sugere que estas vias possam estar atuando em *Paracoccidioides*, provavelmente controlando a diferenciação celular.

Marques e colaboradores (2004) identificaram genes preferencialmente expressos na fase leveduriforme de *Paracoccidioides* (isolado Pb18), utilizando técnicas de subtração (subtração por hibridização e supressão ou SSH) e microarranjos. Dentre os genes identificados como diferencialmente expressos estão α-1,3-glucana sintase, enzima relacionada ao metabolismo da parede celular, *ERG25* que codifica uma C-4 esterol metil oxidase e atua no primeiro passo enzimático da síntese de ergosterol em fungos, além de genes envolvidos no metabolismo de enxofre, tais como metionina permease o qual deve estar relacionado à manutenção no morfotipo de levedura, como descrito para *Histoplasma capsulatum*.

Nunes e colaboradores (2005) utilizaram microarranjos com seqüências de 4.692 genes do fungo *Paracoccidioides* para monitorar a expressão gênica em alguns pontos da transição morfológica micélio-levedura (5 a 12 h depois da mudança da temperatura). A hibridização por microarranjo cobriu cerca de 50% do número total de genes estimado do fungo *Paracoccidioides*. Foram identificados 2.583 genes diferencialmente expressos durante a transição morfológica. Estão inclusos entre esses, genes que

codificam enzimas envolvidas no metabolismo de aminoácidos, transdução de sinal, síntese de proteínas, metabolismo da parede celular, estrutura do genoma, resposta ao estresse oxidativo, controle do crescimento e desenvolvimento do fungo *Paracoccidioides*. Um desses genes que codifica para a enzima 4-hidroxil-fenil piruvato dioxigenase foi superexpresso durante a transição micélio-levedura e tem sido avaliado como um novo alvo para antifúngicos.

Andrade e colaboradores (2006), através das técnicas de subtração de ESTs *in silico* e microarranjos, e Ferreira e colaboradores (2006), através de microarranjos, realizaram análises da expressão de genes envolvidos na utilização de enxofre por *Paracoccidioides*. Neste estudo, os autores caracterizaram a expressão de cinco genes envolvidos no metabolismo do enxofre e avaliaram o acúmulo de mRNAs cognatos durante a transição de micélio para levedura e crescimento da fase leveduriforme, sugerindo que nestas situações ocorre mobilização e armazenamento de enxofre, além da ativação da via de assimilação inorgânica. Os autores sugerem que, embora *Paracoccidioides* não use enxofre inorgânico como única fonte para iniciar a transição e o crescimento da fase leveduriforme, este fungo pode de algum modo, utilizar ambas, a via orgânica e inorgânica durante o processo de crescimento.

O perfil transcricional de *Paracoccidioides* durante a diferenciação morfológica de micélio para levedura foi avaliado por Bastos e colaboradores (2007). Vários transcritos potencialmente relacionados com a síntese de membrana e parede celulares mostraram-se aumentados durante a diferenciação celular de micélio para levedura após 22 horas de indução da transição, sugerindo que *Paracoccidioides* favorece o remodelamento da membrana e de parede celular nos estágios iniciais da morfogênese. Neste estudo, genes envolvidos na via de assimilação do enxofre, como a sulfito redutase, mostrou-se superexpresso durante a transição, sugerindo o envolvimento do metabolismo do enxofre durante o processo de diferenciação em *Paracoccidioides*, como descrito anteriormente (Andrade *et al*., 2006; Ferreira *et al*., 2006). Durante a transição também foi verificada a presença de enzimas que participam do ciclo do glioxalato, como a isocitrato liase, malato desidrogenase, citrato sintase e aconitase. A presença destes transcritos durante a diferenciação indica que esta via é funcional durante esse processo. Também foram identificados genes envolvidos em vias de transdução de sinal tais como MAPK, serina/treonina quinase e histidina quinase, sugerindo que a transição morfológica em *Paracoccidioides* é mediada por vias de

transdução de sinal que controlam a adaptação ao ambiente para a sobrevivência do fungo dentro do hospedeiro (Bastos *et al*., 2007).

Com o objetivo de estudar genes possivelmente envolvidos na adaptação e sobrevivência de *Paracoccidioides* no hospedeiro durante a infecção, Bailão e colaboradores (2006), utilizaram a técnica de Análise de Diferença Representacional de cDNA (cDNA-RDA) para identificar genes de *Paracoccidioides* induzidos durante o processo infectivo e em condições que mimetizam a via hematológica de disseminação fúngica. No modelo de infecção experimental, em fígado, foi observada a alta freqüência do transcrito codificante da zrt1p (zinco/ferro permease). O mesmo foi observado para o transcrito *CTR3*, codificando um transportador de cobre de alta afinidade. Em adição, o transcrito codificante para a glutamina sintase (Gln1p) foi fortemente induzido após incubação com sangue humano sugerindo que a remodelação na parede/membrana celular possa ser um dos meios pelos quais *Paracoccidioides* responda às mudanças de osmolaridade externa encontrada pelo fungo na via de disseminação sanguínea.

Bailão e colaboradores (2007), utilizando a técnica de Análise de Diferença Representacional de cDNA (cDNA-RDA), analisaram genes preferencialmente expressos em leveduras de *Paracoccidioides* tratadas com plasma humano, simulando assim sítios de infecção, com inflamação. Foi observado um aumento significativo na expressão de transcritos associados com a degradação de ácido graxos, síntese de proteínas envolvidas no remodelamento da parede celular e síntese de proteínas relacionadas à mudança de osmolaridade. Assim como na incubação com sangue, o gene codificante da glutamina sintase também foi super expresso na condição de incubação com plasma, reforçando a hipótese já descrita anteriormente de que a superexpressão desta enzima esteja ligada ao aumento da síntese de quitina que ocorreria durante o estresse osmótico.

Tavares e colaboradores (2007), realizaram experimentos de hibridização em microarranjos de DNA, nos quais foi possível definir transcritos de *Paracoccidioides*, isolado Pb01, internalizado em macrófagos. Após a internalização, o patógeno promove adaptação metabólica induzindo a expressão de genes da biossíntese de aminoácidos, especificamente genes envolvidos na biossíntese de metionina, além de genes relacionados ao estresse como, por exemplo, a superóxido dismutase 3, *HSP60* e *QCR8* (subunidade do citocromo oxidase c).

Costa e colaboradores (2007) analisaram o transcriptoma de *Paracoccidioides*, fase leveduriforme, recuperado de fígado de animais experimentais (camundongos B10). Foram seqüenciadas 4.932 ESTs no processo infectivo, sendo 37,47% relacionadas a novos genes e 23,75% pertencentes a genes super expressos. Os genes identificados foram categorizados em processos metabólicos, transporte celular e energia. Do total de ESTs geradas neste estudo, 65,53% das seqüências identificadas, também estavam presentes no transcriptoma de levedura e micélio de células obtidas de cultura *in vitro*, descrito por Felipe e colaboradores. (2005). A demonstração do perfil gênico das células leveduriformes de *Paracoccidioides* recuperadas de animais infectados é um requisito essencial para o estudo do genoma funcional de modo a esclarecer os mecanismos de patogenicidade e virulência fúngica.

Uma análise global dos transcritos superexpressos em células leveduriformes derivadas de fígado de camundongos infectados, plasma e sangue humano (Costa *et al*.,2007; Bailão *et al*., 2006, 2007) sugere que *Paracoccidioides* apresenta um metabolismo nicho específico durante a infecção, onde o ciclo do glioxalato, a glicólise e a biossíntese de etanol apresentam-se mais ativos no fígado, enquanto que no plasma e no sangue humano as vias metabólicas que demonstram atividade elevada são as vias de resposta a estresse osmótico, ciclo do metilcitrato e gliconeogênese (Pereira *et al*., 2009).

Shankar e colaboradores (2011b), utilizando a técnica de microarranjo, analisaram o perfil transcricional de *Paracoccicidioides* durante a transição de micélio-levedura na presença de 17β-estradiol (E2). O tratamento com E2 afetou a expressão de 550 transcritos, sendo que 331 foram induzidos e 219 reprimidos. Genes potencialmente envolvidos na sinalização, tais como aqueles codificantes da palmitoil transferase, da GTPase RhoA, fosfatidilinositol-4-quinase, proteína-quinase, e genes envolvidos na resposta ao estresse mostraram baixa expressão na presença de E2. Genes relatados com a degradação de proteínas e resposta ao estresse oxidativo foram induzidos. Portanto, o estudo foi capaz de caracterizar o efeito de E2, a nível molecular, na inibição da transição micélio-levedura e essa ação inibitória ocorre através de genes de sinalização que regulam o dimorfismo.

Peres da Silva e colaboradores (2011), através da técnica de RDA, avaliaram o perfil de expressão diferencial em *Paracoccidioides* durante infecção em queratinócitos orais (NOKs). O perfil de expressão gênica do fungo foi determinado após contato com as células, no intuito de caracterizar os genes diferencialmente expressos durante

infecção por *Paracoccidioides*. Após o contato com as células NOKs, o fungo pareceu induzir alterações nestas células, as quais apresentaram extensões celulares e cavitações, provavelmente resultantes de alterações no citoesqueleto de actina. Nas análises transcricionais de *Paracoccidioides* durante a infecção em queratinócitos pode-se ainda identificar genes induzidos envolvidos em diferentes processos biológicos, como metabolismo de proteínas, metabolismo alternativo de obtenção carbono, resposta ao estresse e transporte de zinco. A indução do transcrito para o transportador de zinco pode indicar, indiretamente, a necessidade de eliminar espécies reativas de oxigênio através de proteínas como superóxido dismutase, uma enzima dependente de cobre/zinco, que é importante para detoxificação celular durante o metabolismo oxidativo.

Ensaios *in vitro* de ligação de células leveduriformes de *Paracoccidioides* a colágeno tipo I e fibronectina foram realizados com o objetivo de identificar novas adesinas. Através da técnica de RDA foram encontrados vários genes induzidos, entre eles aqueles codificantes da enolase e do transportador de cobre Ctr3p. Ensaios de imunofluorescência demonstraram que a enolase se liga à superfície de macrófagos, reforçando a função desta molécula na interação de *Paracoccidioides* a células do hospedeiro (Bailão *et al*., 2012).

1.4. Estudos proteômicos

Proteômica tem sido definida como a análise em grande escala de proteínas expressas por uma determinada célula, tecido ou organismo numa condição específica (Wilkins *et al*., 1996). O padrão de expressão das proteínas é variável - enquanto o genoma é uma característica relativamente fixa de um organismo o proteoma muda continuamente, conforme o estágio de desenvolvimento, tecido, condições ambientais, variações na expressão gênica, "splicing" de RNA e modificações pós-traducionais.

Em fungos patogênicos humanos a proteômica têm contribuído para um melhor conhecimento dos processos envolvidos na morfogênese, virulência, resposta ao hospedeiro, bem como para o desenvolvimento de alvos antifúngicos potenciais e abordagens terapêuticas (Pitarch *et al*., 2003). Marcadores biológicos de um determinado patógeno podem ser identificados e caracterizados por técnicas proteômicas, ajudando no diagnóstico precoce de doenças e no acompanhamento do tratamento (Cash *et al*., 2002).

Os primeiros trabalhos pós-genômicos foram os estudos de proteínas associadas ao envelope celular de *Trichoderma reesei* (Lim *et al*., 2001), e de proteínas GPI (glicosilfosfatidilinositol) em *Aspergillus fumigatus* (Bruneau *et al*., 2001). Melin e colaboradores (2002) realizaram a análise proteômica com o fungo patogênico *Aspergillus nidulans* em resposta ao antibiótico concanamicina A. Strom e colaboradores (2005) detectaram alterações específicas na expressão de proteínas e inibição do crescimento celular causados quando *A. fumigatus* foi cultivado em associação com uma bactéria produtora de ácido lático. Num trabalho posterior realizado também em *A. fulmigatus*, Kniemeyer e colaboradores (2006) identificaram 52 proteínas da gliconeogênese, ciclo do glioxalato e enzimas de degradação do etanol induzidas durante crescimento em glicose e etanol como fonte de carbono. Carberry e colaboradores (2006) identificaram 54 proteínas envolvidas com energia e biossíntese de proteínas, mostrando pela primeira vez que o fator de elongação 1B (elf1Bp) exibe atividade de glutationa transferase em *A. fumigatus*. Em estudos realizados com *A. nidulans* durante a osmoadaptação, Kim e colaboradores (2007) demostraram que enzimas do ciclo do ácido tricarboxílico estão reprimidas e aquelas envolvidas com a biossíntese de glicerol estão induzidas. Além disso, observaram um aumento no acúmulo de proteínas de choque térmico, sugerindo um aumento de *turnover* protéico. Análises proteômicas da adaptação do fungo *A. fumigatus* a altas temperaturas permitiram identificar proteínas envolvidas principalmente com o remodelamento protéico, resposta ao estresse oxidativo, transdução de sinal, transcrição, tradução e metabolismo de carboidratos e nitrogênio. Além disso, foram fornecidas evidências de regulação dependente de HSF-1(fator transcricional de choque térmico-1) da síntese de manitol, tradução, organização do citoesqueleto e divisão celular (Albrecht *et al*., 2010).

Para elucidar as proteínas do fungo *A. fumigatus* induzidas durante a aspergilose invasiva, Asif e colaboradores (2010) utilizaram extratos de proteínas de conídios do fungo e inocularam em animais. Após a infecção o soro desses animais foi então utilizado como anticorpo primário para identificar antígenos de *A. fumigatus*. Foram identificadas proteínas relacionadas à via glicolítica e ao estresse oxidativo, bem como proteínas associadas à parede celular. Teutschbein e colaboradores (2010) compararam o perfil de proteínas intracelulares entre conídios e micélio de *A. fumigatus*. Entre as 57 proteínas mais expressas em conídio, estão enzimas envolvidas na eliminação de espécies reativas de oxigênio (EROs), biossíntese de pigmentos e morfologia celular .

Análises proteômicas comparativas entre a forma de biofilme e planctônica do fungo *Candida glabrata* foram realizadas para se explorar os mecanismos que contribuem para a virulência desse organismo e resistência a antifúngicos (Seneviratne et. al., 2010). As análises demonstraram um aumento de proteínas relacionadas ao estresse e uma diminuição das enzimas da via glicolítica.

Análise da expressão de proteínas de *C. albicans* envolvidas com a transição dimórfica de levedura para hifas foi realizada. Utilizando-se a técnica 2D-DIGE, Monteoliva e colaboradores (2010) detectaram proteínas citoplasmáticas de diferentes vias metabólicas envolvidas no estabelecimento e na manutenção de cada morfologia celular. Foram identificadas, dentre as proteínas induzidas durante a transição do fungo *C. albicans* a enzima fosfoglicomutase. Os autores sugerem que a fosfoglicomutase esteja envolvida na conversão de glicose-6-fosfato em glicose-1-fosfato, que depois poderia ser convertida em UDP-glicose. A glicose pode então ser utilizada na síntese de proteínas N-glicosiladas e de β-glicana. Outra proteína encontrada como abundante nas hifas de *C. albicans* foi a Hsp90p e foi descrita como uma proteína que orquestra a morfogênese em *C. albicans* sob condições de mudança de temperatura (Shapiro *et al*., 2009). As análises permitiram uma visão integrada do metabolismo e da reorganização celular durante a transição levedura-hifa.

Micronutrientes são essenciais para o patógeno e para o hospedeiro. Portanto, a habilidade de capturar nutrientes do meio é fundamental para o crescimento de fungos patogênicos, assim a redução da disponibilidade de ferro, e outros micronutrientes, consistem em um mecanismo de defesa do hospedeiro para eliminar patógenos e combater a doença (Doherty, 2007). Neste sentido, os patógenos precisaram desenvolver eficientes sistemas de captura de ferro, devido à ausência de ferro livre nos tecidos infectados e para competir com mecanismos de restrição desse micronutriente pelo hospedeiro (Johnson, 2008). Winters e colaboradores (2008) realizaram análises proteômicas de *H. capsulatum* em condições de depleção de ferro e detectaram 35 proteínas reprimidas, dentre elas enolase, malato desidrogenase, sacaropina desidrogenase, Hsp70p, asparaginil-tRNA sintetase. Esses resultados sugerem que *H. capsulatum* induz funções metabólicas específicas para competir com alterações no ambiente do hospedeiro. No intuito de avaliar a adaptação de *Paracoccidioides* a condições de restrição de ferro, Parente e colaboradores (2011) avaliaram o perfil protéico do fungo em condições de depleção de ferro. Foi identificado aumento da expressão de proteínas relacionadas à via glicolítica e aquisição de ferro. Enzimas do

ciclo do ácido tricarboxílico (TCA), ciclo do glioxalato, ciclo do metilcitrato e cadeia transportadora de elétrons foram reprimidas em decorrência da limitação do micronutriente. Estas análises sugerem que em condições de baixa concentração de ferro, *Paracoccidioides* aumentaria a expressão de proteínas relacionadas ao sistema de captura do metal e direcionaria seu metabolismo energético para vias independentes de ferro (Parente *et al*., 2011).

Rezende e colaboradores (2011) realizaram a comparação entre perfis proteômicos das formas de micélio, transição de micélio para levedura e levedura de *Paracoccidioides*. As análises proteômicas indicaram uma reorganização do metabolismo de carboidratos em *Paracoccidioides* durante a transição. Enzimas envolvidas nas reações não oxidativas da via das pentoses fosfato, como transcetolase e transaldolase, foram induzidas durante transição de micélio para levedura, sugerindo que a indução da via durante a transição poderia fornecer substratos para as enzimas da glicólise, que se mostrou induzida na forma de levedura (Rezende *et al*., 2011). Outra mudança detectada através deste estudo foi o aumento de expressão da enzima álcool desidrogenase, após 22 horas de transição, sugerindo um direcionamento para o metabolismo mais anaeróbio na fase de levedura (Rezende *et al*., 2011).

1.5. Homeostase de zinco

Os íons metálicos são elementos vitais que participam de inúmeros processos metabólicos em todos os tipos celulares, sendo ligados diretamente ao metabolismo do DNA e ao processamento pós-traducional da maioria das proteínas. Em microrganismos patogênicos os íons metálicos ainda garantem uma colonização bem sucedida do parasita no hospedeiro. Dessa forma, é de extrema importância para o bom funcionamento celular que haja tanto a distribuição correta dos metais, quanto sua concentração adequada nos compartimentos intracelulares, já que aparentemente qualquer distúrbio na concentração de íons metálicos em meio intracelular pode causar danos a elementos metabólicos vitais, geralmente levando a morte celular (Nelson, 1999).

Zinco, ferro e cobre, são elementos essenciais aos sistemas biológicos, embora em grandes quantidades em meio intracelular, se tornam agentes potencialmente tóxicos. Dessa forma, as células em geral desenvolveram mecanismos homeostáticos que garantem as concentrações necessárias dos metais para a sobrevivência celular. Uma série desses mecanismos homeostáticos já foram identificados e estudados, dentre

eles o controle da transcrição de genes envolvidos na aquisição, distribuição e armazenamento de metais (Rutherford & Bird *et al*., 2004).

O zinco é considerado um íon metálico essencial para todos os organismos, por ser requerido para transcrição, tradução, replicação, resistência ao estresse oxidativo e virulência, mas como para outros metais, é vital para os organismos e tóxico em altas concentrações (Llull *et al*., 2011). Em humanos, foi observado que mais de 3% das proteínas identificadas possui motivos de ligação a zinco, o que confere importância metabólica a esse metal (Dainty *et al*., 2008). Além disso, a aquisição de zinco é reconhecida como chave nos processos infectivos para qualquer patógeno (Silva *et al*., 2011).

Dois fatores de transcrição que controlam a expressão gênica em resposta à concentração de zinco são bem caracterizados. Esses são: o fator de transcrição zinco responsivo, Zap1p, presente em *S.cerevisiae*, que ativa a expressão gênica dos transportadores de alta e baixa afinidade de zinco mediante a deficiência do metal e o fator de transcrição zinco-responsivo, Mtf-1p (metal-regulatory transcription factor 1), em humanos, que é ativado por íons zinco. Para ambos os fatores, os ativadores transcricionais possuem mecanismos em comum, dentre eles, domínios de ligação ao DNA ricos em motivos de dedo de zinco, conhecidos por C_2H_2 (Rutherford & Bird, 2004).

Ainda não é bem estabelecido como íons zinco regulam o fator Zap1p. Bird e colaboradores (2000), observaram dois domínios de ativação com regiões dedo de zinco presentes na proteína Zap1p: ADI e ADII, que possivelmente estão ligados a esse processo de regulação. Já Gaither & Eide (2001), sugeriram que o produto do gene *ZAP1* é um sensor direto de zinco que possui em sua topologia um ou mais sítios de regulação de baixa afinidade para o metal que se ligam ao domínio de ligação do DNA, em adição a dedos de zinco Cys2His2 de alta afinidade. Dessa forma, a ligação de zinco nesses sítios regulatórios pode estabilizar a conformação da interface de ligação ao DNA proporcionando a regulação de Zap1p. Lyons e colaboradores (2000), através de estudos por microarranjos de DNA, em levedura, sugeriram que o gene *ZAP1* é responsável por controlar a expressão de mais 42 genes relacionados à homeostase de zinco celular.

Em eucariotos, duas famílias de transportadores estão envolvidas na captação de zinco: ZIP e CDF. A família ZIP desempenha importante função no transporte de zinco

para o citoplasma. Um segundo grupo de transportadores, a família CDF, transporta o zinco para o interior das organelas (Gaither & Eide, 2001).

Muito do conhecimento a respeito do transporte de zinco e de sua regulação, foi proveniente de estudos com *S. cerevisiae*. As atividades dos transportadores de zinco, pertencentes à família ZIP, em *S.cerevisiae* podem ser reguladas tanto em nível transcricional, quanto pós-traducional (Gaither & Eide, 2001). A nível transcricional, os mecanismos de captação de zinco são regulados em resposta a concentração de zinco intracelular, através do produto gênico gerado por *ZAP1* que por sua vez se liga a elementos zinco-responsivos (ZREs) presentes nas regiões promotoras dos genes *ZRT1*, *ZRT2* e *FET4* que codificam respectivamente, os transportadores de alta e de baixa afinidade de zinco e o transportador de baixa afinidade de ferro (Zhao & Eide, 1997; Zhao *et al*., 1998; Waters & Eide, 2002). Vale ressaltar que cada gene envolvido no transporte de alta e de baixa afinidade pode ter mais de um elemento zinco-responsivo (ZRE) em sua respectiva região promotora o que diferencia a resposta em relação à disponibilidade de zinco intracelular entre os genes envolvidos na captação do metal (Gaither & Eide, 2001). Zap1p pode se ligar também a elementos zinco responsivos localizados em sua própria região promotora por um mecanismo de autoregulação. A diferença de sensibilidade dos promotores de *ZRT1*, *ZRT2* e *ZAP1* ao zinco pode estar relacionada às diferentes funções desempenhadas por cada proteína envolvida nos processos de captação e regulação de zinco e sugere o seguinte cenário: a expressão basal (i.e., Zap1-independente) do transportador de zinco de baixa afinidade Zrt2p é suficiente para suprir as células na presença de zinco (Zhao & Eide 1997). Assim, quando as células entram em períodos iniciais de escassez de zinco, a primeira resposta celular gerada é o aumento da atividade da permease de baixa afinidade, Zrt2p. Se a escassez de zinco ficar mais severa então é induzida a expressão do transportador de alta afinidade, Zrt1p (Gaither & Eide, 2001). Finalmente, a indução da expressão de Zap1p, permitindo a máxima expressão de seus genes alvos, somente será necessária sob condições de extrema limitação de zinco (Gaither & Eide, 2001). O segundo mecanismo de regulação do transporte de zinco é a nível pós-traducional. Em condições de limitação de zinco, Zrt1p é estável na membrana plasmática. Exposição a altos níveis de zinco extracelular leva a uma rápida diminuição da atividade de Zrt1p. Essa inativação ocorre através da endocitose de Zrt1p e sua subseqüente degradação no vacúolo (Gitan *et al*., 1998; Van Ho *et al*., 2002). Gitan e colaboradores (1998), observaram que o sistema de regulação a nível pós-traducional é independente do

sistema de controle transcricional,visto que em células mutadas para o gene *ZAP1*, a inativação de Zrt1p ocorre normalmente. Contudo, esses processos devem acontecer de forma harmônica para que haja a manutenção da homeostasia celular.

A família das proteínas facilitadoras da difusão de cátions (CDF), assim como a família ZIP, está presente em todos os organismos, embora seu mecanismo de transporte ainda não tenha sido examinado detalhadamente. Sabe-se que esses grupos de transportadores promovem o transporte de zinco do citoplasma para o interior de vacúolos, ou do citoplasma para o lúmen de organelas (Gaither & Eide, 2001). *Em S. cerevisiae* foram descritos três transportadores potenciais para zinco que transportam esse metal do citoplasma para o interior dos vacúolos e do Retículo Endoplasmático, os quais pertencem à família CDF, Zrc1p (*intracellular* Zn^{2+} *transporter*), Cot1p (*intracellular* Zn^{2+}*/Co2+transporter*) e Msc2p (Gaither & Eide, 2001). Zrc1p foi isolado como um determinante de resistência ao zinco, pois a superexpressão de *ZRC1* resulta em um aumento da habilidade das células em tolerar altos níveis de zinco (Kamizono *et al*. 1989). O gene *COT1* foi isolado como um supressor da toxicidade de cobalto, mas posteriormente foi descrito que ele também confere resistência ao zinco (Conklin *et al*. 1994; Conklin *et al*. 1992). As duas proteínas estão localizadas no vacúolo, o que sugere que estes transportadores são responsáveis pelo transporte do zinco para o interior desta organela (Li & Kaplan, 1998). A função de Msc2p no transporte de zinco foi sugerida por Li & Kaplan, 2000. A proteína está localizada no envelope nuclear. Uma hipótese é que Msc2p media o transporte de zinco para o espaço intermembrana deste compartimento (Gaither & Eide, 2001). MacDiarmid e colaboradores (2000) identificaram um gene adicional *ZRT3*, em *S. cerevisiae,* o qual codifica uma permease responsável por transportar íons zinco do interior dos vacúolos quando há escassez do metal no meio intracelular. Esse transportador, ao contrário dos demais, pertence à família ZIP, assim como os transportadores de alta e baixa afinidade, e possivelmente são regulados pelo mesmo fator de transcrição, Zap1p.

Uma vez que o zinco é transportado através da membrana plasmática e chega ao meio intracelular, primeiramente esse íon é utilizado para suprir organelas, como o Retículo Endoplasmático e para auxiliar na síntese de metaloproteínas dependentes desse metal. Conklin e colaboradores (1994), demonstraram que em leveduras, os átomos excedentes de zinco presentes no meio intracelular, são em sua maioria mobilizados e estocados em vacúolos, sendo essas organelas o principal sítio de estoque de zinco presente nesses microrganismos. Dessa forma, essas estruturas auxiliam nos

processos de desintoxicação celular gerada pelo excesso do íon no citoplasma (Simm *et al*., 2007). Por serem sítios de estoque de zinco, os vacúolos se tornam uma organela de extrema importância na atuação e sobrevivência de fungos patogênicos (Lulloff *et al*., 2004; Liuzzi *et al*., 2005).

Vicentefranqueira e colaboradores (2005) demonstraram que em *A. fumigatus* a captação de zinco também é dependente do pH e da concentração do íon no meio. Oito genes codificando proteínas da família ZIP de transportadores de zinco foram descritas (Amich *et al*., 2010). ZrfAp e ZrfBp funcionam sob pH ácido e em condições de limitação de zinco (Amich *et al*, 2009; Amich *et al*., 2010). Foi demonstrado que ZrBp representa uma zinco-permease de alta afinidade, visto que o transcrito foi inibido em altas concentrações de zinco (Vicentefranqueira *et al*., 2005). ZrfCp participa na captação de zinco em condições de pH neutro ou alcalino e meio pobre em zinco (Amich *et al*., 2010). Moreno e colaboradores (2007), discutiram o papel do gene *ZFAA* que possivelmente codifica um fator de transcrição para proteínas zinco-responsivas, homólogo ao gene *Zap1* de *S.cerevisiae*, na regulação da homeostase de zinco e aumento da virulência em *A. fumigatus*. Foi observado que cepas com deleção do gene *ZFAA*, quando inoculadas em modelos murinos, não eram capazes de estabelecer um processo infeccioso.

Outros estudos investigam os mecanisos de homeostase de zinco em microrganismos. Em *C. albicans* estudos realizados por Kim e colaboradores (2008), demonstraram a existência do fator de transcrição zinco-responsivo, Crs1p (Candida Supressor of ROK1/zinc-responsive transcription factor), que é codificado por um gene homólogo ao gene *Zap1*de *S. cerevisiae*, que regula a expressão dos genes *ZRT1* e *ZRT2*, sendo de extrema importância para o crescimento filamentoso e patogenicidade do fungo. Dainty e colaboradores (2008), ao avaliarem os níveis de mRNA em *Schizossacharomyces pombe* cultivado sob condições limitantes de zinco, observaram que apenas 2,5% dos transcritos identificados por microarranjo são regulados em condições de deficiência de zinco,dentre eles estão, *ZRT1*, *ZRT2* e *ZAP1*.

Análisis *in silico* do genoma demostraram que *Cryptococcus neoformas var. grubbi* e *Cryptococcus gattii* possuem homólogos aos transportadores Zrt1p e Zrt2p de *S. cerevisiae*. Um homólogo ao fator de transcrição Zap1p também está presente em C*ryptococcus* (Silva *et al*., 2011). Estas análises sugerem que *C. neoformans var. grubbi* e *C. gattii* podem obter o zinco por rotas similiares as que são descritas para *S. cerevisiae* (Silva *et al*., 2011). Schneider e colaboradores (2012), caracterizaram o gene

ZAP1 e sua função como um regulador transcricional do metabolismo de zinco em *C. gatti*. Foi demonstrado que a expressão de *ZAP1* é altamente induzida durante deprivação de zinco. A inativação de *ZAP1* compromete o crescimento do fungo em condições de limitação de zinco, *ZAP1* regula a expressão dos transportadores de zinco ZIP e de proteínas de ligação ao zinco e finalmente Zap1p regula a concentração de zinco intracelular. Em adição, foi demonstrado que a inativação de *ZAP1* reduz a virulência de *C. gatti* em modelo de infecção murino.

Alguns estudos descrevem transportadores de zinco em *Paracoccidioides*. Com o propósito de identificar genes potencialmente envolvidos na adaptação e sobrevivência de *Paracoccidioides* no hospedeiro durante a infecção, Bailão e colaboradores (2006), utilizaram a Análise de Diferença Representacional de cDNA (cDNA-RDA) para identificar genes de *Paracoccidioides* induzidos durante o processo infectivo e em condições que mimetizam a via hematológica de disseminação fúngica. No modelo de infecção experimental foi observada alta freqüência dos transcritos homólogos à *ZRT1* e *ZRT2*. Bailão e colaboradores (2007), ao continuarem os estudos de avaliação do perfil transcricional, através da técnica de cDNA-RDA utilizando dessa vez, células de *Paracoccidioides* incubadas com plasma novamente observaram a expressão dos genes que codificam os transportadores de alta e baixa afinidade de ferro e zinco. Análises *in silico* do genoma de *Paracoccidioides* demonstram a presença de ortólogos aos transportadores de zinco descritos em *S. cerevisiae*, que são localizados nas membranas plasmática, vacuolar e do retículo endoplasmático. Genes codificando os transportadores da família ZIP, ortólogos dos transportadores Zrt1p e Zrt2p, estão presentes no genoma de *Paracoccidioides* (Silva *et al*., 2011). O isolado Pb01 possui dois transportadores de zinco vacuolares, codificados pelos genes *ZRC1* e *COT1*, enquanto os isolados Pb03 e Pb 18 possuem ortólogos apenas para *COT1*. Um ortólogo ao fator de transcrição Zap1p também está presente nos três isolados de *Paracoccidioides* (Silva *et al*., 2011). Portanto, a assimilação de zinco em *Paracoccidioides* pode ser similar a *S. cerevisiae*. Bailão e colaboradores (2012) demonstraram que o transcrito ZRT2, mas não ZRT1, foi altamente expresso em pHs alcalino e neutro sob condições de depleção de zinco, como observado para *ZRFC* de *A. fumigatus.*

1.6. Interação patógeno-hospedeiro

A patogenicidade de microrganismos está relacionada com a complexa interação entre o patógeno e o hospedeiro. Esta interação é um processo dinâmico, envolvendo a capacidade do organismo em atravessar o epitélio, disseminar para diversos tecidos e resistir à defesa imune. Portanto, o sucesso da infecção requer uma rápida adaptação do patógeno através de mudanças na expressão de determinados repertórios gênicos requeridos frente às diferenças de micro-ambientes (Kumamoto, 2008). Estudos da patogenicidade de fungos estão ainda na sua fase inicial (Albrecht *et al*., 2008). Os primeiros passos foram tomados em sistemas de pesquisa biológica de infecções causadas por *Candida albicans*, pela modelagem teórica da interação patógeno-hospedeiro (Hummert *et al*., 2010).

O fungo patogênico *C. albicans* comumente causa infecções superficiais em mucosas, porém em pacientes imunocomprometidos este fungo pode se disseminar para outros sítios causando infecções sistêmicas (Walker *et al*., 2009). Para elucidar a resposta de *C. albicans* durante disseminação na corrente sanguínea, foi utilizada a técnica de microarranjo conjuntamente com os ensaios de subtração de cDNA para traçar o perfil transcricional do fungo exposto ao sangue humano. Foram encontrados diferentes grupos de genes diferencialmente expressos: relacionados ao estresse, resposta antioxidante, virulência e genes envolvidos na obtenção de energia através da via glicolítica e ciclo do glioxalato. As análises forneceram informações a respeito dos mecanismos pelos quais *C. albicans* pode sobreviver e adaptar ao ambiente hostil do sangue como um passo essencial para a disseminação (Fradin *et al*., 2003; Fradin *et al*., 2005). Após romper a barreira hematogênica, *C. albicans* pode provocar processos infecciosos em diversos órgãos como rins, fígado e baço. Em modelos de infecção por *C. albicans* em rins de coelhos pode-se observar uma resposta transcricional adaptativa relacionada com a indução de genes envolvidos na adesão, adaptação ao estresse e vias alternativas de produção de carbono (Walker *et al*., 2009). Thewes e colaboradores (2007) avaliaram, através de modelos de infeção *in vivo* e *ex vivo*, o perfil transcricional de *C. albicans*. Através de análises de microarranjos foram identificados genes relacionados a processos metabólicos para obtenção de fontes alternativas de carbono e nitrogênio, resposta ao estresse, captura de nutrientes, genes de regulação morfológica e também relacionados à formação da hifa. Utilizando ensaios de microarranjo em modelos de infecção *in vitro* e de amostras fúngicas de pacientes com candidíase na mucosa oral, foi observada a importância da expressão de genes associados a

manutenção da morfologia celular, essencial para adesão e invasão celular e a indução de genes envolvidos na resposta a diferentes condições de estresse, tais como estresse oxidativo, limitação de fontes de carbono e nitrogênio e estresse nitrosativo (Martin *et al*., 2011).

Lorenz e colaboradores (2004) verificaram que, no interior de fagossomos, *C. albicans* apresenta um aumento na expressão de genes codificantes para proteínas envolvidas na captura e biossíntese de aminoácidos, enquanto que genes relacionados à via glicolítica não são induzidos neste ambiente. Estes resultados indicam que durante a fagocitose por macrófagos o fungo é submetido a um ambiente pobre em fontes de nitrogênio e glicose. Estas análises revelaram ainda que durante a fagocitose, transcritos para enzimas do metabolismo de lipídios são hiper regulados, uma vez que os lipídios seriam a principal fonte de carbono para o fungo neste nicho. Ainda analisando a resposta de *C. albicans* ao sistema mononuclear fagocítico observou-se que as células do fungo ativam uma maior resposta ao estresse oxidativo em consequência da fagocitose por neutrófilos, do que por macrófagos. Assim, sugere-se que a resposta ao estresse oxidativo durante o estabelecimento e progressão da infecção sistêmica de *C. albicans* seja um fenômeno nicho-específico (Enjalbert *et al*., 2007).

O fungo patogênico *Cryptococcus neoformans* possui a habilidade de disseminar-se na corrente sanguínea e então cruzar a barreira hemato-encefálica causando a meningoencefalite. Para se ter uma visão sobre a adaptação do fungo ao sistena nervoso central, a estratégia de análise serial de expressão gênica (SAGE) foi utilizada para caracterizar células de *C. neoformans* isoladas de fluído cerebroespinhal (CSF) de coelhos. Os dados revelaram que os transcritos mais expressos foram aqueles relacionados com resposta a estresse, sinalização celular, transporte celular, metabolismo de lipídios e carboidratos (Steen *et al*., 2003). Da mesma forma que em *C. albicans,* a capacidade de resistir às células fagocíticas caracteriza uma importante adaptação para sobrevivência de *C. neoformans* no hospedeiro. Os mecanismos utilizados pelo fungo para evadir os processos de fagocitose, envolve alterações morfológicas que dificultam a sua internalização, aumentando a resistência ao estresse oxidativo e nitrosativo (Okagaki *et al*., 2010). Após a fagocitose de *C. neoformans*, o fungo pode ser expelido sem causar danos às células, um processo chamado de exocitose. Nicola *et al* (2011), demonstraram através da técnica de citometria de fluxo que este processo depende do pH fagossomal.

Análises de *Aspergillus fumigatus* recuperado do pulmão de camundongos infectados revelaram a expressão de vários genes relacionados a virulência, entre eles genes codificantes para proteínas reguladoras do desenvolvimento, biossíntese de micotoxinas e resposta a estresse térmico (Gravelat *et al*., 2008). Nesse patógeno, a avaliação da resposta gênica diferencial em conídios e hifas em resposta a interação com neutrófilos envolveu a ativação de processos metabólicos relacionados com a degradação de ácidos graxos, proliferação peroxissomal, ciclo do glioxalato e assimilação de ferro/cobre (Sugui *et al*., 2008). O perfil transcricional, acompanhado pela análise de mutantes tem mostrado que a privação nutricional, estresse oxidativo, hipóxia, estresse térmico e perturbações na membrana plasmática representam os maiores desafios enfrentados por *A. fumigatus* durante a infecção. O conhecimento sobre as vias celulares e perfis adaptativos do patógeno na tentativa de neutralizar as defesas do hospedeiro são cruciais para identificação de novos alvos de drogas (Hartmann *et al*., 2011). Thywißen e colabordores (2011), investigaram a interação de conídios de *A. fumigatus* com macrófagos e neutrófilos. Foi demonstrado que as células conidiais são capazes de inibir a acidificação dos fagolisossomos e que a melanina é essencial neste processo.

Bailão e colaboradores (2006) identificaram, através da técnica de RDA, genes induzidos durante o processo infectivo e em condições que mimetizam a via de disseminação fúngica em *Paracoccidioides*. Por estas análises, identificou-se transcritos codificantes para proteínas relacionadas à virulência, transportadores de nutrientes, proteínas de choque térmico e síntese de melanina em células leveduriformes de *Paracoccidioides* recuperadas de fígado de animais infectados experimentalmente (Bailão *et al*., 2006). Já no tratamento de *Paracoccidioides* com sangue humano, observou-se uma maior abundância de transcritos codificantes para proteínas do metabolismo de aminoácidos, remodelagem da parede celular, regulação da osmolaridade e moléculas relacionadas à defesa celular (Bailão *et al*., 2006). Ainda utilizando a técnica de cDNA-RDA, Bailão e colaboradores (2007), analisaram genes preferencialmente expressos em leveduras de *Paracoccidioides* tratadas com plasma humano, simulando sítios de infecção, com inflamação. Foi observado um aumento na expressão de transcritos codificantes de proteínas de degradação de ácidos graxos, remodelamento da parede celular e resposta à mudança de osmolaridade.

O transcriptoma de células leveduriformes de *Paracoccidioides* recuperadas de fígado de camundongos infectados foi descrito por Costa e colaboradores (2007) com o

objetivo de se avaliar as estratégias desenvolvidas por este fungo durante a infecção. Foram encontrados transcritos codificantes para transportadores de membrana, proteínas relacionadas com estresse, moléculas envolvidas no metabolismo de nitrogênio e enzimas que participam do metabolismo de carboidratos e lipídios. Este estudo possibilitou um maior esclarecimento das adaptações metabólicas realizadas por *Paracoccidioides* durante o processo infeccioso, sugerindo que em tecidos do hospedeiro os processos significativamente favorecidos são metabolismo de nitrogênio, carboidratos e lipídios. A interpretação geral dos processos que ocorrem durante a infecção sugere que o fungo utiliza múltiplas fontes de carbono durante acolonização do fígado, incluindo glicose e substratos do ciclo do glioxalato (Costa *et al*., 2007; Pereira *et al*., 2009).

Ainda com o intuito de avaliar a resposta de *Paracoccidioides* à espécies reativas de oxigêncio (EROs) produzidas pelo próprio metabolismo fúngico ou pelas células fagocitárias do hospedeiro, foram realizados ensaios de atividade em gel para catalases. Através destas análises pode-se identificar três catalases em *Paracoccidioides*: *Pb*CATA, *Pb*CATP e *Pb*CATC. A expressão da catalase *Pb*CATA está relacionada à condições de estresse oxidativo endógeno, enquanto que a catalase peroxissomal *Pb*CATP é induzida em condições de estresse oxidativo exógeno. Já *Pb*CATC responde a condições de estresse osmótico e térmico. Durante a fagocitose de *Paracoccidioides* por macrófagos observou-se um aumento de expressão dos transcritos para a catalase A e catalase P, sugerindo que estas enzimas possam estar envolvidas na resposta e proteção do fungo contra EROs produzidas nesta condição (Chagas *et al*., 2008).

Utilizando a tecnologia de indução de antígenos *in vivo* (IVIAT), Dantas e colaboradores, (2009) identificaram proteínas imunogênicas expressas em altos níveis durante a infecção por *Paracoccidioides*. Antígenos relacionados à via de melanização (*Pb*DDC), síntese de riboflavina (*Pb*LS) e um transportador de cobre de alta afinidade (*Pb*CTR3) foram identificados. Análises de expressão por RT-PCR quantitativa (qRT-PCR) mostraram um aumento de expressão dos transcritos codificantes para estes antígenos, 15 dias após infecção em fígado e baço e durante infecção em macrófagos, sugerindo um papel importante destas proteínas como antígenos nos processos de interação de *Paracoccidioides* com o hospedeiro.

No intuito de avaliar a adaptação de *Paracoccidioides* a condições de restrição de ferro no hospedeiro, Parente e colaboradores (2011) avaliaram o perfil protéico do fungo em condições de depleção de ferro em comparação com condições de ferro em

abundância. As proteínas identificadas que apresentaram um aumento de expressão em condições de depleção de ferro estavam relacionadas com a via glicolítica e aquisição de ferro. Enzimas do ciclo do ácido tricarboxílico (TCA), ciclo do glioxalato, ciclo do metilcitrato e cadeia transportadorade elétrons foram reprimidas em decorrência da limitação do micronutriente.

1.7. RDA

Várias são as técnicas utilizadas a fim de estudar a expressão diferencial de genes em um determinado organismo ou identificar quais genes estão envolvidos em um determinado processo ou tratamento. Essas técnicas permitem detectar as mudanças na expressão de mRNAs sem qualquer conhecimento prévio de informações da sequência dos genes específicos em questão. Dentre os métodos utilizados para clonar genes diferencialmente expressos encontra-se a técnica do RDA (Hubank and Schatz 1994).

A Análise Representacional Diferencial (RDA) é um processo de subtração acoplado à amplificação, originalmente desenvolvido para uso com DNA genômico como um método capaz de isolar as diferenças entre dois genomas complexos. Esta técnica elimina aqueles fragmentos presentes em ambas as populações, deixando apenas as diferenças. O RDA genômico se baseia na geração, por digestão com enzima de restrição e amplificação por PCR (reação em cadeia da polimerase), de versões simplificadas dos genomas sob investigação conhecidas como "representações". Se um fragmento de restrição amplificável (o alvo) existe numa representação (*tester*) e está ausente em outra (*driver* – controle), um enriquecimento cinético do alvo pode ser alcançado por hibridização subtrativa do *tester* na presença de um excesso de *driver*. Seqüências com homólogos no *driver* não são amplificadas, enquanto o alvo hibridiza apenas com ele mesmo e retém a habilidade de ser amplificável por PCR. Interações sucessivas da subtração e o processo de PCR produzem fragmentos de DNA visíveis num gel de agarose correspondendo ao alvo enriquecido (Fig 1) (Hubank & Schatz, 1994). A técnica de RDA é flexível porque as populações de cDNA podem ser fracionadas por um número de enzimas de restrição com seqüências curtas de reconhecimento para produzir conjuntos de cDNAs. Este aspecto do RDA melhora grandemente as chances de se clonar com sucesso espécies diferencialmente expressas. Além disso, pelo fato de que cada cDNA é restringido no seu comprimento para produzir fragmentos menores, o procedimento de RDA oferece múltiplas chances de se recuperar um gene de interesse (Pastorian *et al*., 2000).

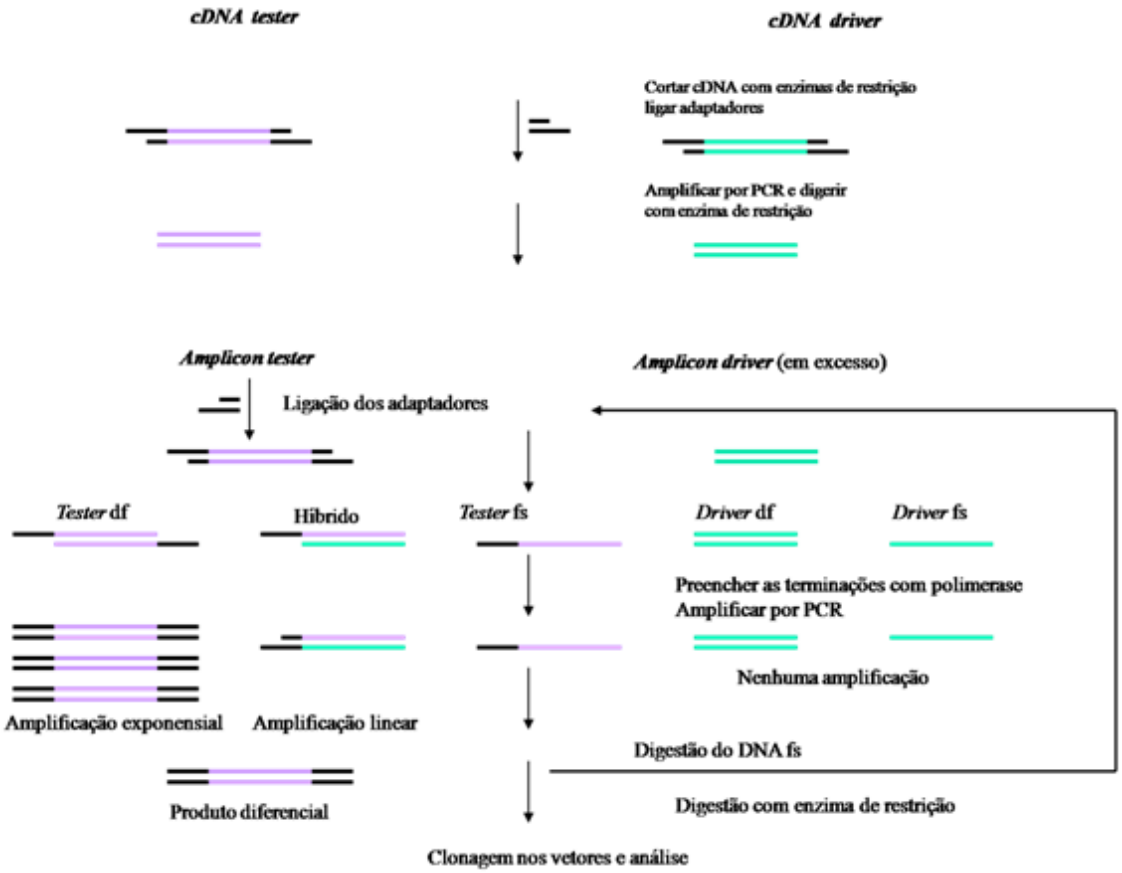

Fig 1. Diagrama esquemátio da metodologia do RDA (adaptado de Hubank & Schatz, 1994). Os cDNAs são digeridos com enzima de restrição Sau3AI para gerar fragmentos menores para serem mais eficientemente amplificáveis por PCR e com sítios de restrição para ligar os adaptadores. Os produtos da digestão são purificados em sistema comercial GFX (GE Healthcare, Chalfont St. Giles, UK), ligados aos adaptadores (16 h a 16 °C) e amplificados por PCR (25 ciclos de 45 s a 95 °C e 4 min a 72°C, cada). Os produtos finais da reação de PCR são purificados com o sistema comercial GFX. Ambos, tester e driver são digeridos com Sau3AI para remoção dos adaptadores e purificados antes da ligação de um novo par de adaptadores somente no tester. Para a geração do primeiro produto diferencial, driver e tester são hibridizados, numa relação de 10:1, por 16 h a 67 °C e amplificados por PCR (7 ciclos de 45 s a 95 °C e 3 min a 72 °C, cada). Os produtos são submetidos a uma nova etapa de amplificação (20 ciclos) para remoção dos cDNAs fita simples não desejados. Para geração de um segundo produto diferencial, novos adaptadores são ligados ao primeiro produto diferencial, que é hibridizado ao driver numa relação de 100:1.

No intuito de se conhecer genes que poderiam contribuir para a adaptação e sobrevivência de *Paracoccidioides* durante a infecção, Bailão e colaboradores (2006) utilizaram a técnica de RDA para identificar genes induzidos durante o processo infectivo num modelo murino de infecção e em condições que mimetizam a rota hematológica da disseminação fúngica. Os transcritos diferencialmente expressos nesse

estudo eram predominantemente relacionados com remodelamento de parede celular e síntese da parede celular. Através de RDA foi também observada a influência do plasma humano na expressão gênica de *Paracoccidioides*, sugerindo genes que poderiam ser essenciais na adaptação do fungo no hospedeiro (Bailão *et al*., 2007). O grupo mostrou que o plasma ativa significativamente a expressão de transcritos associados com biossíntese de proteínas, facilitadores de transporte, degradação de ácidos graxos, remodelamento de parede e defesa celular.

Os genes envolvidos no processo infeccioso de *Trichophyton rubrum* foram analisados por Baeza *et al*. (2007), utilizando a técnica do RDA a partir de duas populações de cDNA, uma proveniente de RNA extraído do fungo exposto à queratina e outra obtida de RNA extraído do fungo cultivado em meio mínimo. Genes relacionados à transdução de sinal, proteína de membrana, resposta a estresse oxidativo e alguns prováveis fatores de virulência se apresentaram super-expressos.

Faganello e colaboradores (2009) utilizaram a técnica de RDA a fim de isolar sequências que representam diferenças no DNA genômico de *C. neoformans var. grubii* e *Cryptococcus gattii*. Nesse estudo foram sequenciados, cerca de 200 clones, que permitiram a identificação de 19 sequências diferentes em relação ao genoma de *C. neoformans*. Dentre as sequências identificadas, genes envolvidos com o polimorfismo em espécies de *Cryptococcus* foram observados, como o gene codificante para quitina sintase.

Borges *et al*. (2010), utilizaram a técnica do RDA a fim de identificar genes diferencialmente expressos entre as células leveduriformes de dois isolados diferentes de *Paracoccidioides*, isolados Pb01, que se apresenta com morfologia características de células leveduriformes, e o isolado Pb4940, que se apresenta tipicamente na forma miceliana, sem a presença de conversão para a fase leveduriforme ao se alterar a temperatura de cultivo. A técnica foi utilizada a fim de compreender os eventos moleculares que ocorrem no fungo durante a resposta ao aumento de temperatura e estabelecimento da fase leveduriforme do isolado Pb01. Nesse trabalho, o isolado Pb01 foi utilizado como tester e o isolado Pb4940 como driver. Um total de 258 clones se mostram super-expressos para o isolado Pb01, comparado ao isolado Pb4940, que correspondem a proteínas de membrana/parede celular, HSP30, C6 fator de transcrição (Ctf1b) e fator de transcrição Gata (NSdD).

2. JUSTIFICATIVA

A complexidade de interações entre *Paracoccidioides* e o hospedeiro humano sugere que o fungo tenha desenvolvido mecanismos que o possibilitam adaptar-se à diversidade de sítios, regulando a expressão gênica de forma nicho específica, a exemplo de outros patógenos. Apesar de esforços terem sido feitos no estudo da complexa interação *Paracoccidioides*-hospedeiro, bem como no estudo da resposta do fungo a diferentes condições biológicas, as estratégias que este patógeno utiliza para sobrevivência nos sítios de infecção permanecem pouco conhecidas.

Em função do exposto observa-se a relevância do conhecimento espacial e temporal de aspectos metabólicos de patógenos durante a infecção. Acredita-se que em microrganismos patogênicos a utilização preferencial de vias metabólicas em decorrência de sítios do hospedeiro possa ser importante para o conhecimento da biologia e patogenia dos organismos. Estudos anteriores, revelaram algumas estratégias do *Paracoccidioides* para adaptação a condições do hospedeiro durante o processo infeccioso no fígado (Bailão *et al*., 2006; Costa *et al*., 2007), durante disseminação no sangue (Bailão *et al*., 2006) e plasma (Bailão *et al*., 2007). Neste contexto, a identificação de ESTs de *Paracoccidioides* recuperado de animais experimentais é um importante requisito para fornecer dados necessários na elucidação dos mecanismos de virulência e patogênese. Pelo pulmão ser o primeiro órgão-alvo da paracoccidioidomicose em humanos, o estudo da resposta do fungo a esse nicho permitiria ampliar o conhecimento das diferentes estratégias adaptativas utilizadas pelo fungo para escapar e sobreviver às defesas do hospedeiro.

Sabe-se que micronutrientes, como zinco, ferro e cobre são essenciais para o metabolismo de organismos, por participarem de processos bioquímicos vitais. Estudos recentes evidenciam que os mecanismos ligados à captação e à homeostase de metais estão fortemente ligados entre si e são, por sua vez, fatores de virulência para patógenos. Estudos em nosso laboratório identificaram transportadores de alta e baixa afinidade de zinco (*Pb*Zrt1p/*Pb*Zrt2p), como moléculas altamente expressas em condições que mimetizam o processo infeccioso por *Paracoccidioides*. Essas análises tornaram-se o ponto de partida para o início dos estudos de genes envolvidos na homeostase de micronutrientes nesse patógeno.

3. OBJETIVOS

1 - Caracterizar o perfil proteômico de *Paracoccidioides* em condições limitantes de zinco, comparando com o perfil proteômico do fungo na presença desse metal.

2 - Obtenção de bibliotecas subtraídas de ESTs de *Paracoccidioides*, através da técnicade cDNA-RDA, na seguinte condição experimental:
- *Paracoccidioides* recuperado do pulmão de camundongos, após 7 e 15 dias de infecção;

3 - Caracterização e categorização das sequências obtidas através de anotação utilizando o programa BLAST2GO;

4 - Confirmação, por qRT-PCR ,da expressão diferencial de genes identificados.

5 - Análise e compreensão das possíveis estratégias moleculares utilizadas por *Paracoccidioides* durante infecção no pulmão.

Capítulo 2

Proteoma em condições de depleção de zinco

1. MATERIAIS E MÉTODOS

1.1. Microrganismo e condições de crescimento

Paracoccidioides, *Pb* 01 (ATCC MYA-826), foi utilizado em todos os experimentos. A fase leveduriforme do fungo foi crescida em meio Fava Netto semi-sólido [1% (w/v) peptona, 0.5% (w/v) extrato de levedura, 0.3% (w/v) proteose peptona, 0.5% (w/v) extrato de carne, 0.5% (w/v) NaCl, 4% (w/v) glicose, 1.2% (w/v) agar, pH 7.2] à 36 ^{o}C por 7 dias. Um esquema experimental de todas as técnicas desenvolvidas é mostrado na Fig 1.

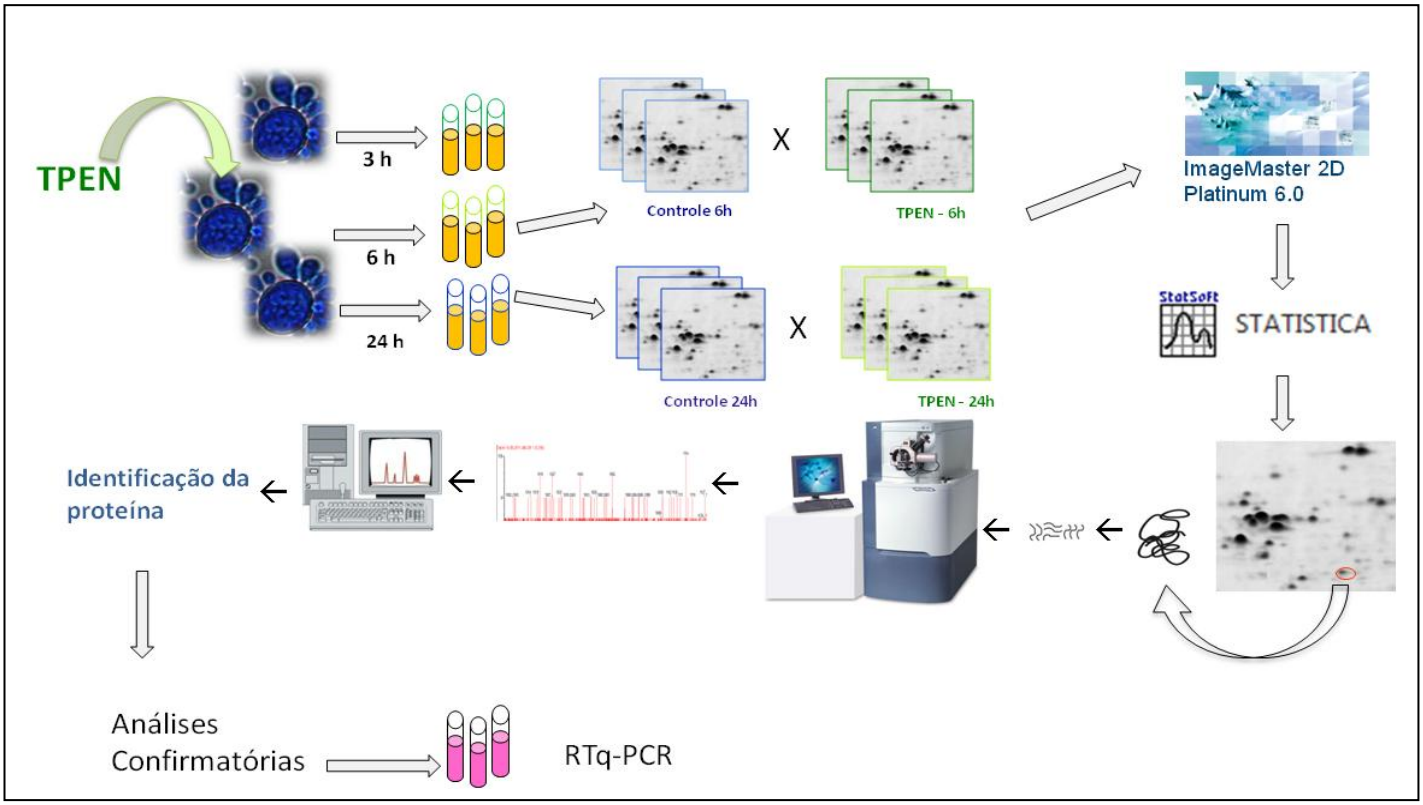

Fig 1 – Desenho experimental. *Paracoccidioides*, Pb01 (ATCC MYA-826) foi utilizado em todos os experimentos. Células leveduriformes foram incubadas por 3, 6 e 24 h na ausência de zinco e na presença de 50 µM de TPEN (tratadas) e 30 µM de $ZnSO_4$ (controle). Extratos protéicos foram obtidos após 6 e 24 h de incubação e fracionados por 2-DE. Triplicatas de cada condição foram obtidas. Análise de imagem utilizando-se o software ImageMaster 2D Platinum 6.0 e análises estatísticas por one-way ANOVA ($p < 0.05$) foram realizadas. Os spots de interesse foram submetidos à digestão tríptica. Espectros de MS e MS/MS foram adquiridos. Após 3, 6 e 24 h de incubação foi realizada extração de RNA. Os RNAs obtidos foram submetidos à análise por RT-PCR em tempo real.

1.2. Experimentos de depleção de zinco

Para os experimentos de depleção intra e extracelular de zinco, células leveduriformes de *Paracoccidioides* foram incubadas em meio McVeigh/Morton (MMcM) (Restrepo e Jiménez 1980) na presença e ausência de zinco, como descrito a seguir. O meio MMcM foi preparado sem a adição de $ZnSO_4$ e suplementado com o quelante de zinco N,N,N_,N_-tetrakis (2-pyridyl-methyl) ethylenediamine (TPEN 0.05 mM; Sigma Aldrich, Co., St. Louis, MO). As culturas foram mantidas a 36 °C, 150 rpm. Para que fossem realizadas análises de viabilidade celular, com a finalidade de padronizar o tempo de incubação na presença do quelante que não fossem letais às células leveduriformes, foram retiradas alíquotas em vários tempos de incubação (1, 2, 3, 4, 6, 8 and 24 h). As células coletadas foram diluídas na proporção de 1:10 em corante Trypan Blue 0,4% e analisadas em câmara de Neubauer.

Para a obtenção dos extratos protéicos, 10^8 células/mL of *Paracoccidioides* foram inoculadas em 50 mL de meio Fava Netto líquido. As culturas foram mantidas a 36 ^oC sob agitação por 72 h. Após o período de incubação, a cultura foi centrifugada a 3,500 g por 10 min, as células foram lavadas em tampão PBS estéril 1 X (1.4 mM KH_2PO_4, 8 mM Na_2HPO_4, 140 mM NaCl, 2.7 mM KCl; pH 7.3), em seguida foram ressuspensas em meio de cultura MMcM e mantidas 18 h a 36 ºC sob agitação. Após este período as células foram centrifugadas a 3,500 x g por 5 min e lavadas em PBS 1 X. Um inóculo de $2x10^6$ células foi introduzido em meio MMcM, suplementado com 0.05 mM do quelante zinco-específico TPEN (Sigma Aldrich, Germany). As culturas foram incubadas por 6 e 24 h sob agitação a 36 ° C. Para a condição controle, células leveduriformes de *Paracoccidioides* foram incubadas em meio MMcM contendo 0.03 mM de $ZnSO_4$, por 6 e 24 h. Para obtenção do RNA para análises por RT-qPCR, as células foram incubadas, como descrito acima, por 3, 6 e 24 h.

1.3. Preparação dos extratos protéicos

Células leveduriformes foram coletadas após 6 e 24 de depleção de zinco e submetidas a extração de proteínas. As células foram centrifugadas a 3,500 x g por 15 min a 4 ºC e rompidas por agitação vigorosa com glass beads em solução contendo 20 mM Tris-HCl, pH 8.8, 2 mM $CaCl_2$ (Fonseca CA *et al*. 2001) e uma mistura de inibidores de proteases (serine, cisteína and calpain) (GE Healthcare, Uppsala, Sweden).

Após centrifugação o sobrenadante foi coletado e a concentração protéica determinada por reagente de Bradford (Sigma Aldrich). Soro albumina bovina (BSA) foi utilizada como padrão (Bradford 1976). As amostras foram estocadas em alíquotas a - 80 ºC.

1.4. Eletroforese Bidimensional de Proteínas (2-DE)

Todos os reagentes e equipamentos utilizados na eletroforese bidimensional foram da empresa GE Healthcare. Um total de 300 μg de proteínas foi utilizado para cada condição e aplicado em tiras de gradiente de pH imobilizado (IPG) de 13 cm com separação não linear (NL) de pH 3-11. Antes da focalização isoelétrica (IEF) os extratos celulares foram precipitados utilizando-se o sistema comercial 2-D Clean-Up™. Após a centrifugação o precipitado foi lavado para retirada de contaminantes não protéicos como detergentes, sais, lipídeos e ácidos nucléicos. A mistura foi centrifugada novamente e o precipitado resultante foi ressuspendido em tampão de reidratação [7 M uréia, 2 M tiouréia, 0,5 % (v/v) tampão para IPG 3-11 NL, 65 mM DTT, 2 % (p/v) CHAPS e traços de azul de bromofenol] até se obter o volume final de 250 μL. Após incubação por 1 h, sob agitação, o material foi centrifugado a 3,500 x g, 10 min a 4 ^{0}C. O sobrenadante foi aplicado em um suporte apropriado e a tira de IPG foi colocada sobre o tampão de reidratação. As tiras de IPG foram cobertas com óleo mineral e deixadas por 30 min a temperatura ambiente. Em seguida, as tiras foram incubadas (reidratadas) por 14 h sendo as seguintes as condições para a focalização das proteínas: 500 V por 1 h (step), 500 -1000 V por 1 h (gradiente),1000 - 8000 por 12,5 h (gradiente) e 8000 V por 2,5 h (step), com total de 15980 V/h. Tanto a reidratação quanto a focalização isoelétrica foram realizados no sistema Ettan IPGphor III e a temperatura da corrida foi mantida à 20 ^{0}C. Após a focalização isoelétrica as tiras de IPG foram reduzidas com 0,5% (p/v) de DTT em 5 mL de tampão de equilíbrio contendo 6 M uréia; 0,5 M Tris-HCl; pH 8,8; 30% (v/v) glicerol, 2% (p/v) SDS e azul de bromofenol durante 40 min com suave agitação. Em seguida, a solução foi descartada e as tiras foram alquiladas com 2,5% (p/v) de iodocetamida no mesmo tampão de equilíbrio e deixadas por 40 min com suave agitação e sob proteção da luz. Após isso, o tampão de equilíbrio foi retirado e as tiras IPGs foram lavadas com tampão de corrida (25 mM Tris pH 8.8, 192 mM glicina, 0,1% [p/v] SDS) por 5 min. A separação na segunda dimensão

foi realizada na cuba de eletroforese vertical, Hoefer SE-600 em géis homogêneos de 10%, (1,5 mm de espessura). Um marcador de proteínas com massa molecular conhecida foi colocado na extremidade ácida da tira IPG. As tiras IPG foram colocadas e seladas nos géis SDS-PAGE com 0,5% de agarose em tampão de corrida e traços de azul de bromofenol. A separação eletroforética da segunda dimensão foi realizada segundo a descrição de Laemmli (1970) com tampão de corrida nos compartimentos superior e inferior da cuba. A corrida teve duas etapas: na primeira hora de corrida a voltagem foi mantida a 100 V e após esse tempo foi aumentada para 250 V até que a linha de frente atingisse o final do gel. A temperatura foi mantida à 10 ^{0}C e após o término da corrida os géis foram retirados da cuba e corados utilizando-se o azul de comassie (PlusOne Coomassie Tablets PhastGel Blue R-350, GE Healthcare), de acordo com instruções do fabricante. As imagens dos géis foram capturadas utilizando-se o scanner ImageScan III e posteriormente, digitalizadas com o software ImageMaster 6.0.

1.5. Aquisição e análise das imagens

Os géis corados foram capturados em modo transparência utilizando-se o programa Labscan v 3.0 e as imagens foram importadas no formato TIFF (Tag Image File Format) e convertidas para o formato do programa Image Master Platinum 6.0 (.mel). Os spots detectados automaticamente pelo software do programa foram conferidos manualmente e os sinais falsos positivos foram removidos, também, manualmente. Foram analisadas triplicatas de géis para cada condição estudada, utilizando-se uma referência para alinhamento (ponto de referência) e pareamento automático. Um spot foi considerado reprodutível quando estava presente em todas as triplicatas dos géis de cada condição. Para se comparar spots entre os géis das três condições (pareamento intra classes) uma pasta de pareamento (*matchSet*) foi criada. Um gel referência (*master*) de cada condição foi escolhido como sendo a imagem com o maior número de spots e com melhor resolução. O pareamento automático entre os géis *master* (pareamento inter classes) foi realizado pelo programa e uma inspeção manual de cada spot foi realizada para aumentar a confiabilidade do pareamento (Figura 2). A porcentagem de volume de cada spot foi determinada e utilizada para cálculos estatísticos dos níveis de expressão de proteínas. Para comparar proteínas com múltiplas isoformas, a soma da porcentagem dos volumes, relativa a proteína total, de

cada isoforma foi obtida em triplicata. A soma da porcentagem dos volumes foi utilizada para os testes estatísticos. As análises estatísticas foram realizadas com o software STATISTICA version 7.0 (Statsoft Inc., 2005). Os testes de análise de variância (one-way ANOVA) e comparações múltiplas com teste de Tukey foram realizados para identificação de diferenças significativas entre as três condições analisadas. Os resultados foram considerados significantes quando $p \leq 0,05$.

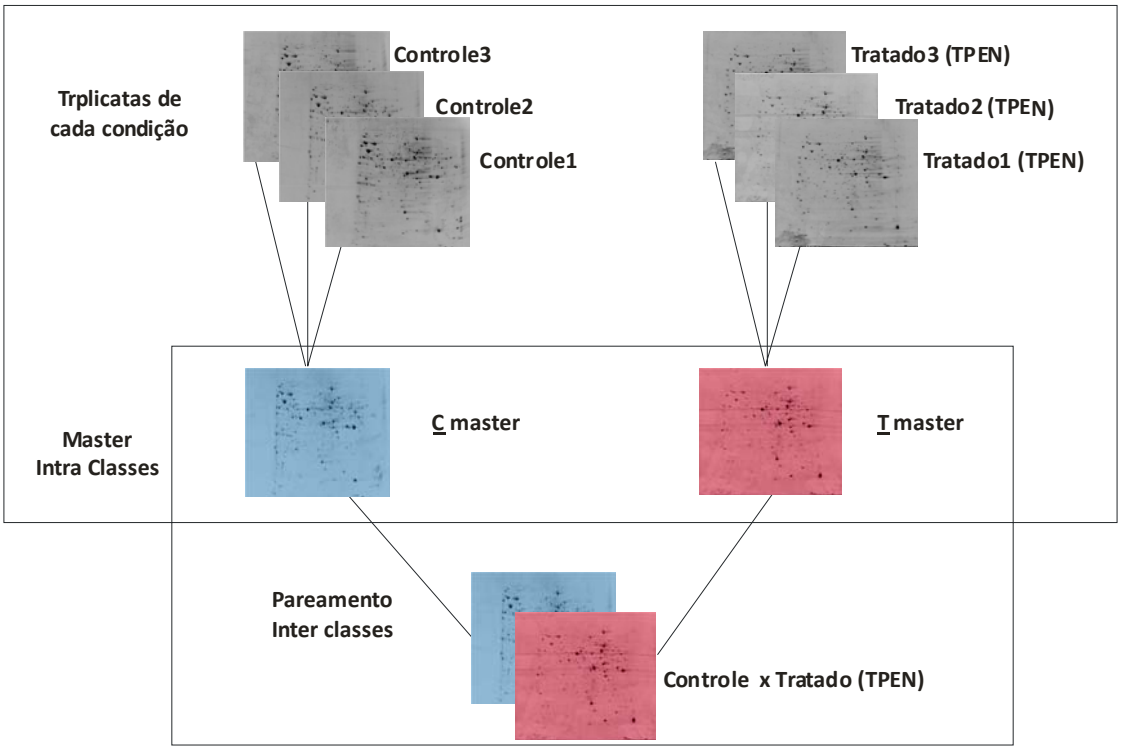

Fig 2 – Fluxograma das análises de imagens realizadas entre as duas condições: Controle x depleção de zinco.

1.6. Digestão das proteínas para espectrometria de massa tipo MALDI

Os spots de proteínas com diferença significativa de expressão foram selecionados e excisados do gel 2-D. O procedimento para a digestão das proteínas foi realizado manualmente como previamente descrito (Parente *et al*, 2011 e Rezende *et al*, 2011). Os spots foram desidratados com 100 µL de acetonitrila (ACN) por 5 min e, após a solução ser retirada, os spots de proteínas foram deixados no *speed vacuum* até secar completamente. Os spots de géis foram então reduzidos com 10 mM DTT por 1 h. O sobrenadante foi retirado e os spots foram alquilados com 55 mM de iodoacetamida ao

abrigo da luz. Os spots foram lavados com 100 µL de solução contendo 25 mM de NH_4HCO_3 por 10 min agitando em vortex. Em seguida o sobrenadante foi retirado e foram adicionados 100 µL de uma solução contendo 25 mM de NH_4HCO_3/50% ACN (v/v), deixando sob agitação em vortex por 5 min. Esse procedimento foi repetido. Após a solução ser retirada as amostras foram desidratadas no *speed vacuum*. Finalmente, as amostras foram reidratadas em 30 µl de tripsina a 10 ng/µL (Sequencing Grade Modified Trypsin Promega, Madison, WI, USA) durante 10 min a 4 ^{0}C. Após a remoção do excesso de tripsina foi adicionado 25 µL de solução de 25 mM de NH_4HCO_3 às amostras em gel e prosseguiu-se a incubação à 37 ^{0}C por 16 h. Após a digestão, o sobrenadante foi retirado e colocado em tubos novos e limpos. Aos spots de géis foi adicionado 50 uL de solução de 50% (v/v) de ACN, 5% (v/v) de ácido trifluoroacético (TFA). A solução foi misturada em vortex por 10 min e depois sonicada por 3 min a 4 ^{0}C. O sobrenadante foi adicionado aos tubos anteriores contendo a mistura de peptídeos. Os tubos contendo os peptídeos trípticos foram deixados no *speed vacuum* até secarem completamente e, em seguida, os peptídeos foram reconstituídos em água. Para concentrar e dessalinizar algumas amostras de spots pequenos foi utilizada a ponteira de cromatografia ZipTip C18 (Millipore, Bedford, MA, USA). Foi adicionado 2 µL da amostra na placa MALDI e deixado secar à temperatura ambiente até a completa evaporação. Em seguida, 2 µL da solução de matriz CHCA [α ácido α-ciano-4-hidroxicinamico em 50% (v/v) de acetonitrila e 5% (v/v) de TFA] a 10 ng/µL foi adicionado à placa e deixado secar à temperatura ambiente.

1.7. Identificação das proteínas por PMF e por MS/MS e pesquisa em banco de dados

As análises foram realizadas no espectrômetro de massa MALDI-Synapt MSTM (Waters-Micromass, Manchester, UK) e UltraFlex III MALDI-TOF/TOF mass spectrometer (Bruker, Bremen, Germany). Para realização das análises por MS os espectros foram adquiridos em modo positivo e refletido. O instrumento foi calibrado com uma acurácia de <10 ppm utilizando-se uma mistura de padrões de peptídeos sintéticos conhecidos com uma variação de m/z de 800 to 4000 Da. O instrumento foi configurado para adquirir os espectros MS e os picos com intensidade acima de 15 counts foram automaticamente fragmentados com argônio na célula de colisão, resultando nos espectros MS/MS, utilizando se o software Masslynx 4.0.

A identificação das proteínas por PMF foi realizada submetendo-se as listas de massas monoisotópicas dos espectros MS (*.txt) ao programa MASCOT (MASCOT 2.1.02; Matrix Science, London, U.K.), usando o banco de dados não redundante do National Center for Biotechnology Information (NCBI) para identificar proteínas candidatas. Os parâmetros de busca para PMF foram: (i) taxonomia, fungi; (ii) enzima, tripsina; (iii) modificações fixas: carbamidometilação das cisteínas; (iv) modificações variáveis: oxidação das metioninas; (v) tolerância de peptídeos: 20-100 ppm; (vi) permissão de clivagem perdida para peptídeos: máximo de 1. Para confirmação da identificação das proteínas por PMF, os espectros de ions MS/MS processados e convertidos nos arquivos *pkl e a lista de picos foram confrontados novamente no banco de dados não redundante do NCBI (fungi). Os parâmetros de busca foram os mesmos descritos para o PMF, exceto para tolerância de massa do fragmento (MS/MS), que foi entre 0.2-0.6 Da. As análises por MS/MS confirmaram as proteínas identificadas com base nos PMFs, validando as identificações.

As ORFs das proteínas identificadas foram analisadas utilizando o Pedant-Pro Sequence Analysis Suite of Biomax GmbH (http://pedant.gsf.de.) e categorizadas de acordo com o Catálogo Funcional (FunCat2).

1.8. Extração de RNA, síntese de cDNA e RT-qPCR

Todos os procedimentos envolvendo a manipulação de RNA foram realizados em condições livres de RNAses. Os RNAs foram isolados por disrupção mecânica das células e agitação com pérolas de vidro por 10 min na presença de Trizol (GIBCO^{TM} Invitrogen Corporation), seguindo o protocolo do fabricante. Os oligonucleotídeos iniciadores foram desenhados na junção exon-exon, amplificando amplicons de aproximadamente 100 a 200 pares de base. A Tabela 1 mostra a lista dos oligonucleotídeos utilizados na reação de qRT-PCR. As reações de qRT-PCR foram realizadas utilizando-se a mistura SYBR green (Applied Biosystems, FosterCity, CA) no sistema StepOnePlusTM real time PCR (Applied Biosystems) em triplicatas biológicas. A especificidade de cada par de oligonucleotídeos utilizados foi confirmada pela visualização de um único produto de PCR em gel de agarose 1,2%. A reação de PCR em tempo real foi realizada em 40 ciclos de 95 °C por 15 s e 60 °C por 1 min. A mistura SYBR Green PCR foi utilizada adicionada de 10 pmol de cada oligonucleotídeo

e 40 ng de cDNA molde, em um volume final de 20 µl. As curvas padrões foram geradas utilizando-se uma alíquota de cDNA de cada amostra, serialmente diluídas (1:5 da diluição original). Os dados foram normalizados com o transcrito codificante para a proteína alfa tubulina amplificado em cada conjunto de experimentos de qRT-PCR. Os níveis de expressão relativa dos genes de interesse foram calculados utilizando-se o método de curva padrão para quantificação relativa (Bookout et al., 2006). Os resultados foram validados pelo teste *t* de *student*, sendo consideradas diferenças significativas as amostras que apresentaram valor de $p \leq 0.05$.

Tabela 1: Oligonucleotídeos utilizados na RT-qPCR

Oligonucleotídeos	**Sequencia**	**Número de acesso[a]**
Tubulina sense	5' ACAGTGCTTGGGAACTATACC 3'	PAAG_01647.1
Tubulina anti-sense	5' GGGACATATTTGCCACTGCC 3'	PAAG_01647.1
Zrt1 sense	5' CTATCCGCTGTGTTCGTCAT 3'	PAAG_08727.1
Zrt1 anti-sense	5' GGAGATGGATGAAAGCTGTG 3'	PAAG_08727.1
Zrt2 sense	5' GCAAAATCCCCCAATGGTAGT3'	PAAG_03419.1
Zrt2 anti-sense	5' GGGTAAGGCCGATTATGATAG3'	PAAG_03419.1
Álcool desidrogenase sense	5' ACCTTGTTGTGCTGGAGTAGA 3'	PAAG_06715.1
Álcool desidrogenase anti-sense	5' GGAGTCTGGAATCGGGGTG 3'	PAAG_06715.1
Isocitrato liase sense	5' ATGGGAACCGACCTCCTGG 3'	PAAG_06951.1
Isocitrato liase anti-sense	5' CGTTCTTGCCTGCTTGCTCA 3'	PAAG_06951.1
Citrato sintase sense	5' ACTGAGCACGGCAAGACGG 3'	PAAG_08075.1
Citrato sintase anti-sense	5' TTCCCAATGCACGGTCGATAA 3'	PAAG_08075.1
Catalase peroxisomal sense	5' AGGTGCAGGAGCTTACGGTG 3'	PAAG_01454.1
Catalase peroxisomal anti-sense	5' CCCAATTTCCTTGCTCGGTG 3'	PAAG_01454.1

[a]Número de acesso – número de acesso das proteínas identificadas na database do Broad Institute of MIT and Harvard: (http://www.broadinstitute.org/annotation/genome/*Paracoccidioides*_brasiliensis/MultiHome.html)

2. RESULTADOS

2.1. Análise de expressão de genes de *Paracoccidioides* envolvidos com aquisição de zinco durante depleção de zinco

Para investigar o perfil de trancrição de genes responsivos ao zinco em *Paracoccidioides* foi utilizada a técnica de RT-qPCR. As análises incluíram os ortólogos aos tranportadores de zinco *ZRT1* e *ZRT2* de *Paracoccidioides* (Fig 3 e tabela 1). Embora os dois transportadores de zinco tenham sido induzidos após 3, 6 e 24 h de tratamento, um maior nível expressão para *ZRT2* foi observado em 6 e 24 h de depleção de zinco, com valores de indução maiores que 20 vezes comparando com o controle (Fig 3). O transcrito codificante para o transportador *ZRT1* apresentou uma indução da

expressão em torno de 10 vezes maior que o controle, em 24 h de depleção. A partir desses resultados, os tempos de 6 e 24 h foram escolhidos para extração protéica e análises proteômicas.

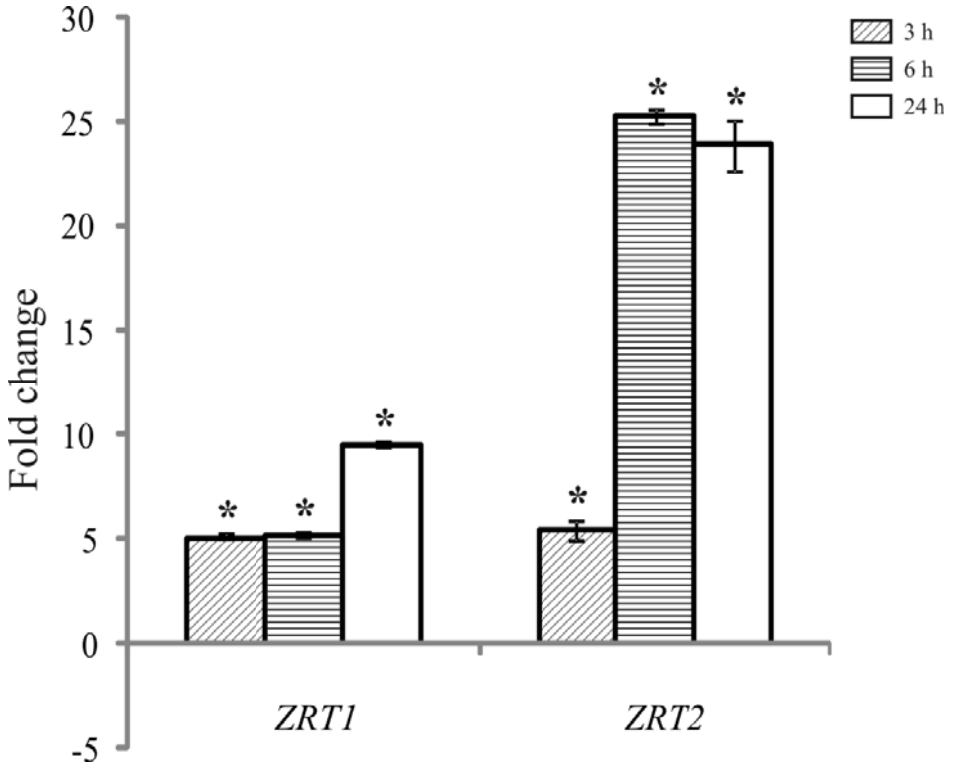

Fig 3. Quantificação da expressão dos transportadores de zinco de *Paracoccidioides* por PCR em tempo real. RT-qPCR em tempo real dos transcritos *ZRT1* e *ZRT2* de *Paracoccidioides* durante depleção de zinco. Os dados foram normalizados para o transcrito codificante para α-tubulina e apresentados como fold change em relação ao controle. Análises estatísticas para avaliar o nível de significância foram realizadas, utilizando o teste *t* de Student, adotando $p \leq 0,05$ (*).

2.2. Análise dos géis-2D de *Paracoccidioides* durante depleção de zinco

Utilizando o corante azul de trypan, foi observado que cerca de 90% das células continuavam viáveis após 24 h de depleção de zinco (dados não mostrados). A técnica de gel bidimensional foi realizada para separar proteínas citosólicas do fungo e análises de imagem permitiram a quantificação das proteínas/isoformas.

Três experimentos independentes geraram três replicatas, os quais incluem: controle 6h, depleção de zinco 6h, controle 24 h e depleção de zinco 24 h (Fig 4A-D, respectivamente). Utilizando um software de análise de gel um total de 845 spots foi detectado (Fig 4 e Fig 5). Análises estatísticas revelaram que 127 e 296

proteínas/isoformas foram diferencialmente acumuladas em 6 e 24 h de depleção de zinco, respectivamente, totalizando 423 proteínas/isoformas diferencialmente reguladas (Fig 5).

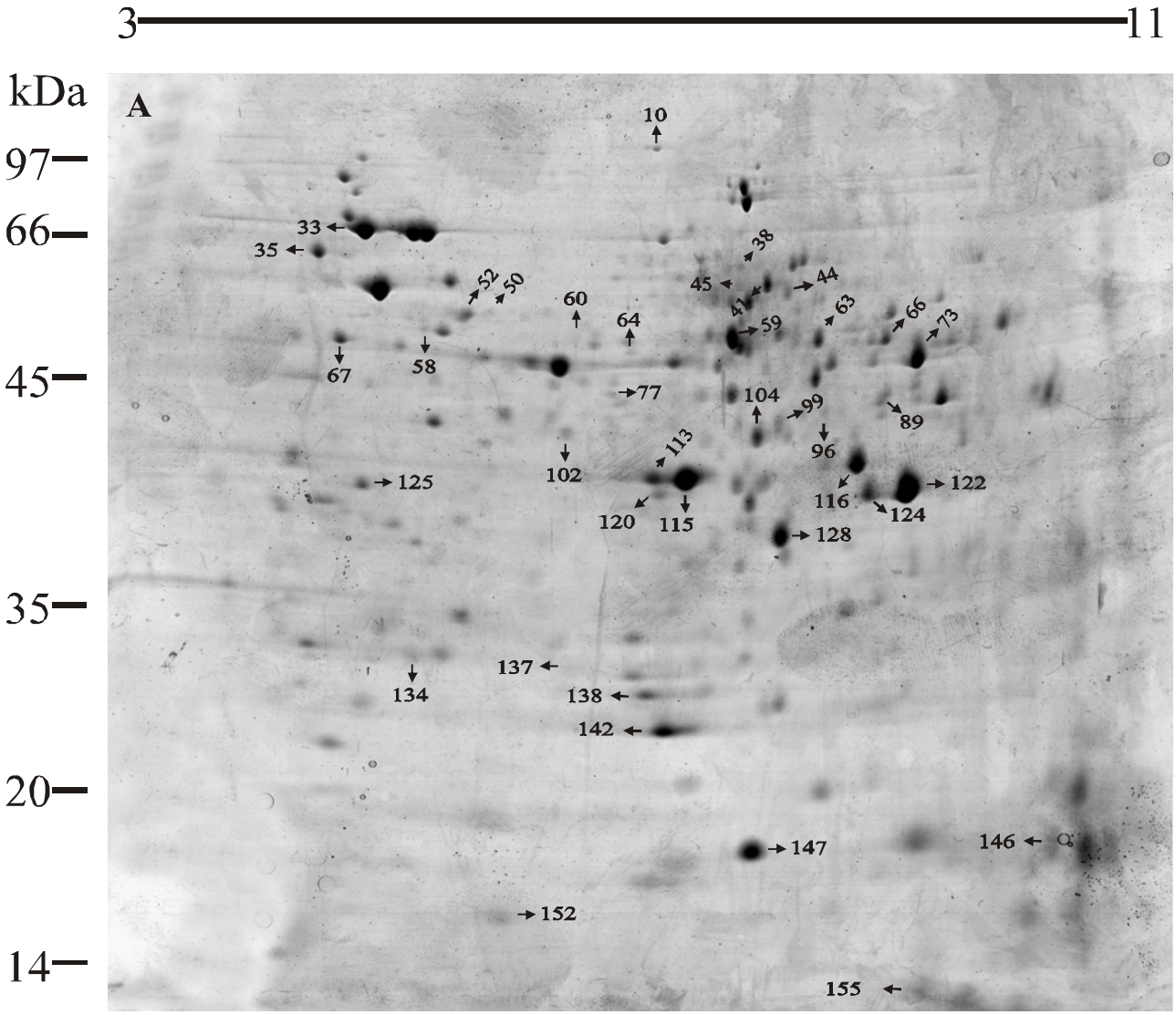

Fig 4A. Análise do gel bidimensional de proteínas de *Paracoccidioides* extraídas de células leveduriformes incubadas por 6h na condição controle. Os spots identificados são numerados e listados de acordo com a tabela 2.

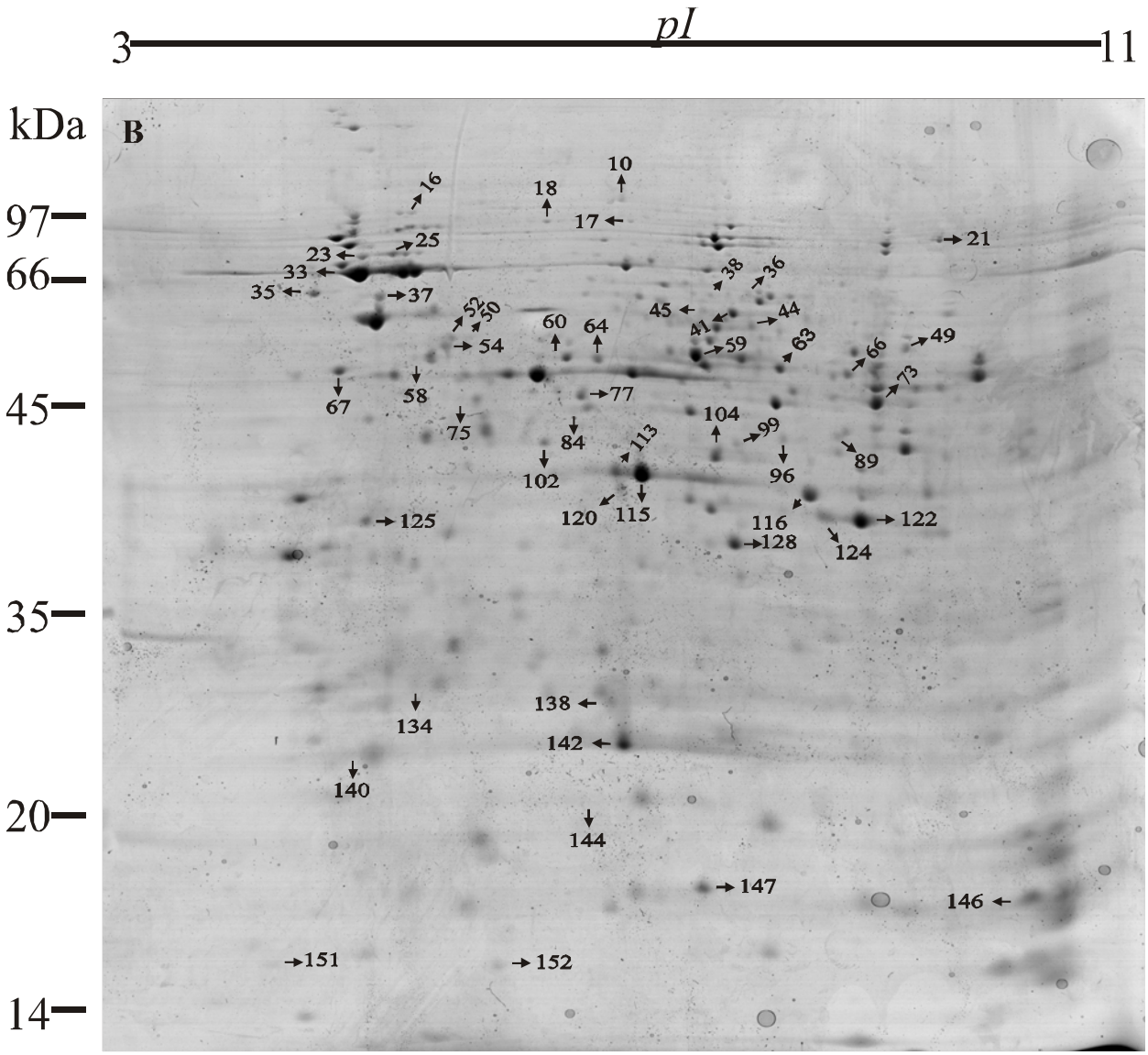

Fig 4B. Análise do gel bidimensional de proteínas de *Paracoccidioides* extraídas de células leveduriformes incubadas por 6h na condição de depleção de zinco. Os spots identificados são numerados e listados de acordo com a tabela 2.

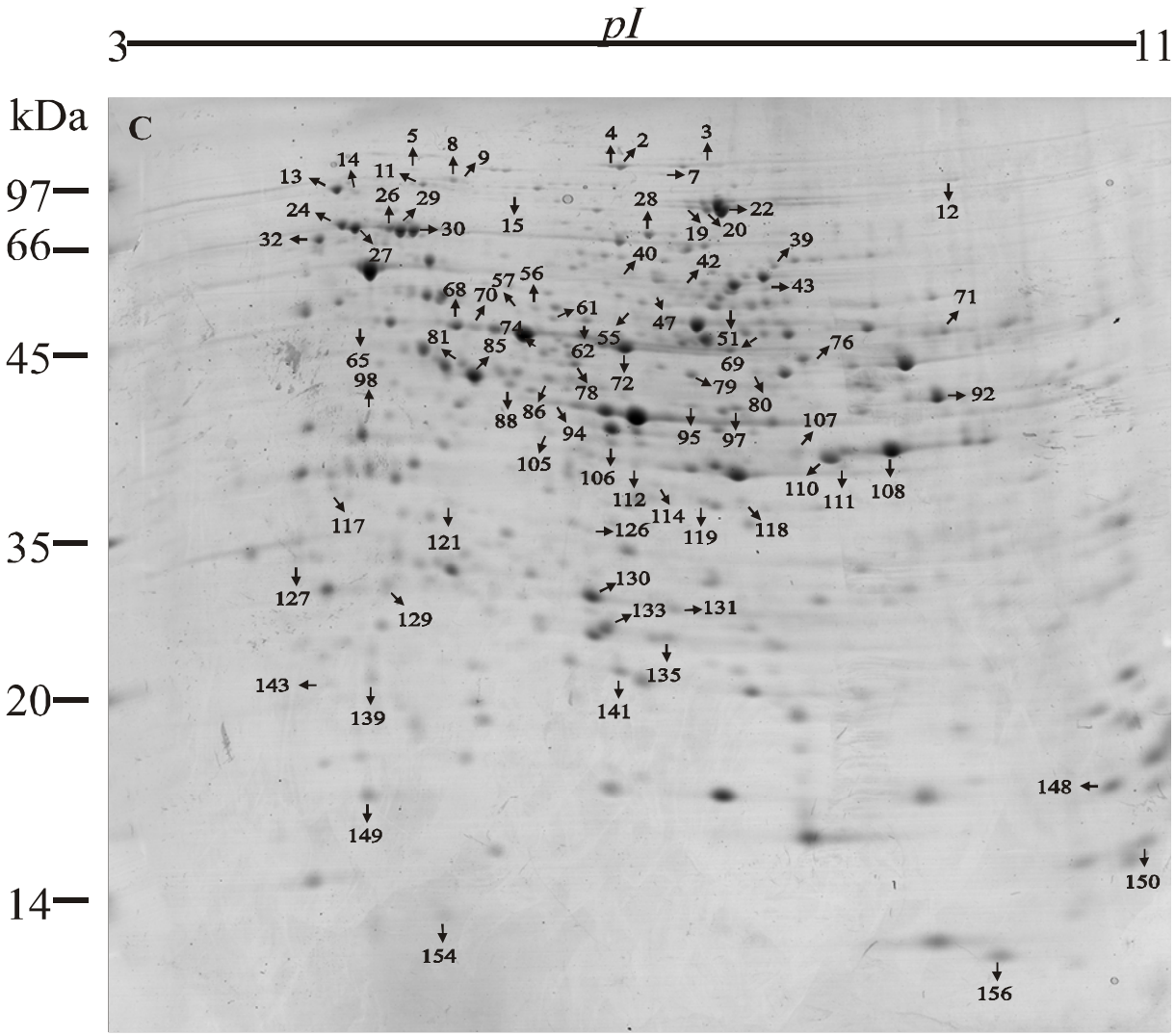

Fig 4C. Análise do gel bidimensional de proteínas de *Paracoccidioides* extraídas de células leveduriformes incubadas por 24h na condição controle. Os spots identificados são numerados e listados de acordo com a tabela 2.

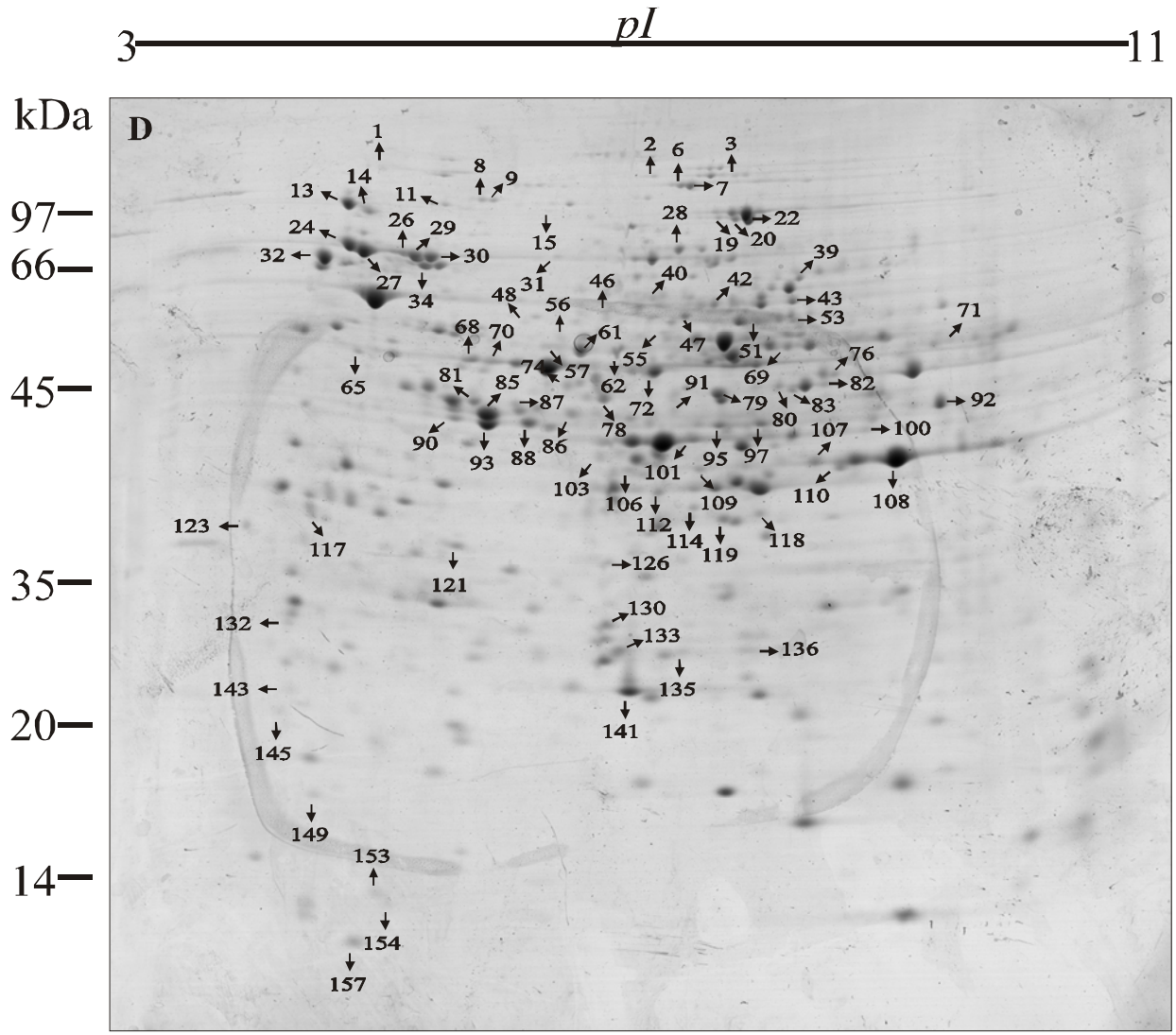

Fig 4D. Análise do gel bidimensional de proteínas de *Paracoccidioides* extraídas de células leveduriformes incubadas por 24h na condição de depleção de zinco. Os spots identificados são numerados e listados de acordo com a tabela 2.

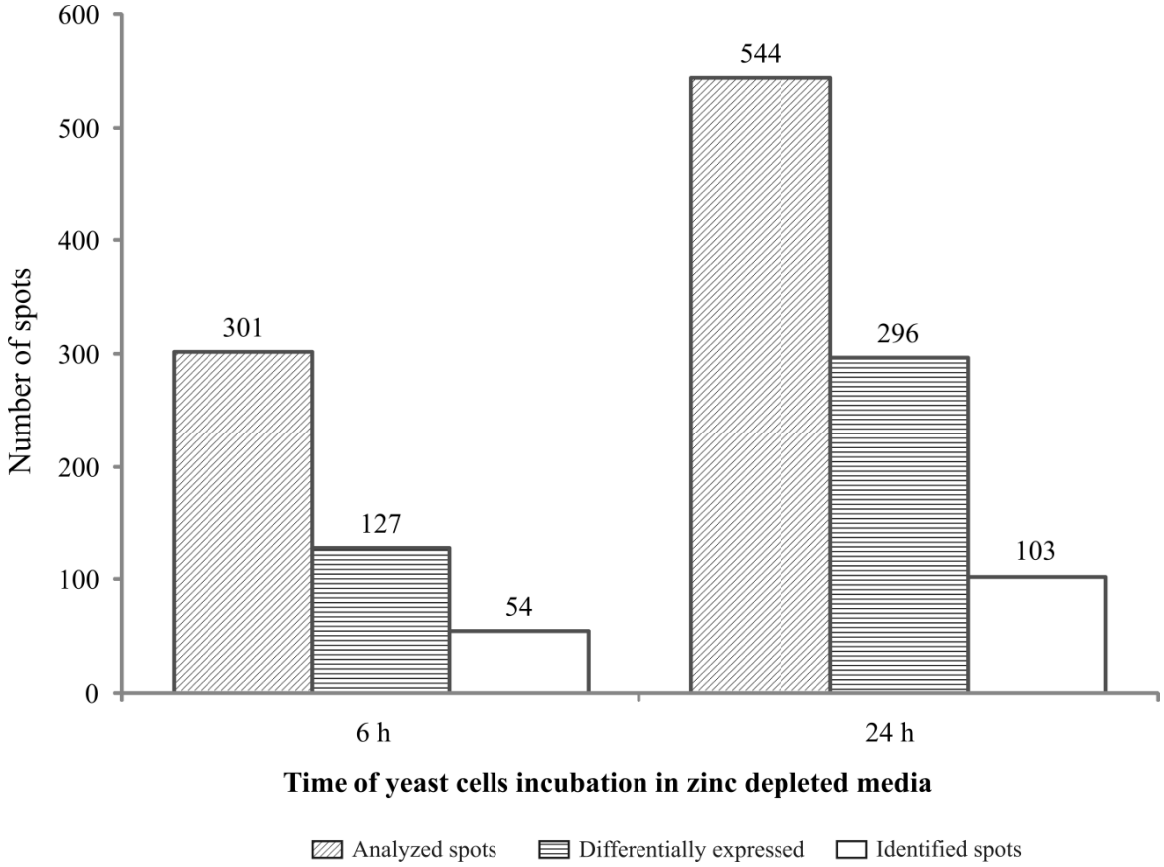

Fig 5. Gráfico resumo das análises proteômicas de *Paracoccidioides* em condições de depleção de zinco. O número de spots diferencialmente expressos foi determinado utilizando software de análise de imagem de gel bidimensional. Análise estatística foi realizada utilizando o ANOVA.

2.3. Identificação de proteínas zinco-reguladas

Para identificação das proteínas diferencialmente reguladas, foi realizada digestão in-gel dos spots utilizando tripsina, seguida pelas análises de espectrometria de massa.

Análises por espectrometria de massa seguida por procura em bancos de dados resultou na identificação de 157 proteínas/isoformas diferencialmente expressas (Fig 4, Fig 5 e tabela 2). Cento e vinte proteínas/isoformas foram identificadas por PMF e confirmadas por análises de MS/MS, enquanto 37 proteínas/isoformas foram identificadas apenas por PMF. Todas as proteínas identificadas estão listadas na tabela 2. Os gi, score de PMF e MS/MS do mascot, massa molecular e ponto isoelétrico de cada spot são listados na tabela 2.

Table 2: *Paracoccidioides* identified protein upon 6 and 24 hours of zinc starvation

Accession number[a]/Protein description	Spot number[b]	Time[c]	PMF		MS/MS	Exp/Theo pI[g]	Exp/Theo MW[h]
			Score[d]	Seq. Cov (%)[e]	Matched Peptides[f]		
gi|295673162 - Disulfide isomerase Pdi1	35	6 h	195	49	14	4.44/4.80	63.67/59.31
gi|295673162 - Disulfide isomerase Pdi1	32	24 h	265	55	4	4.53/4.80	69.67/59.3
gi|295664022 - Glutathione reductase	63	6 h	154	44	15	8.42/6.74	50.83/51.96
gi|295664022 - Glutathione reductase	69	24 h	94	23	2	8.06/6.74	49.67/51.9
gi|295674755 - Glutathione synthetase	55	24 h	158	35	1	7.09/6.14	53.33/56.7
gi|295671569 - Heat shock protein SSC1	30	24 h	239	43	8	5.32/5.92	72.83/73.82
gi|295671569 - Heat shock protein SSC1	26	24 h	168	49	12	5.12/5.92	74.33/73.82
gi|295671569 - Heat shock protein SSC1	29	24 h	175	59	7	5.21/5.92	73.0/73.82
gi|295671569 - Heat shock protein SSC1	16	6 h	173	60	7	5.21/5.92	97.33/73.82
gi|295671569 - Heat shock protein SSC1	25	6 h	98	65	6	4.99/5.92	76.0/73.82
gi|295671569 - Heat shock protein SSC1	34	24 h	104	20	1	5.40/5.92	67.0/73.82
gi|295671569 - Heat shock protein SSC1	81	24 h	86	16	2	5.69/5.92	44.67/73.8
gi|295671569 - Heat shock protein SSC1	87	24 h	108	16	1	6.12/5.92	43.67/73.82
gi|295671569 - Heat shock protein SSC1	86	24 h	**	**	2	6.41/5.92	43.83/73.8
gi|295671569 - Heat shock protein SSC1	117	24 h	**	**	1	4.56/5.92	38.0/73.8
gi|295658865 - Heat shock protein	127	24 h	106	47	**	4.24/5.51	35.0/62.27
gi|295658865 - Heat shock protein	37	6 h	177	52	4	4.87/5.51	63.33/62.27
gi|295658865 - Heat shock protein	1	24 h	**	**	1	5.09/5.51	130.33/62.27
gi|4164594 - Heat shock protein 70	33	6 h	**	**	5	4.82/5.43	68.5/65.3
gi|14538021 - Heat shock protein 70	27	24 h	143	26	5	4.84/5.05	74.0/70.9
gi|14538021 - Heat shock protein 70	95	24 h	100	21	1	7.52/5.05	42.67/70.9

gi|14538021 - Heat shock protein 70	93	24 h	183	25	5	5.92/5.05	42.67/70.9
gi|14538021 - Heat shock protein 70	88	24 h	207	35	**	6.09/5.05	43.17/70.9
gi|295659116 - Hsp70-like protein	23	6 h	182	49	11	4.72/5.08	76.0/70.92
gi|295659116 - Hsp70-like protein	123	24 h	**	**	2	4.05/5.08	36.67/70.9
gi|295659116 - Hsp70-like protein	85	24 h	187	28	3	5.79/5.08	43.83/70.9
gi|295659116 - Hsp70-like protein	90	24 h	148	23	1	5.67/5.08	43.0/70.92
gi|295673716 - Hsp70-like protein	24	24 h	234	36	5	4.73/5.39	76.0/68.8
gi|295673716 - Hsp70-like protein	91	24 h	85	23	1	7.34/5.39	43.0/68.86
gi|295659787 - Heat shock protein Hsp88	13	24 h	201	35	4	4.69/4.92	97.83/80.7
gi|295659787 - Heat shock protein Hsp88	14	24 h	157	30	4	4.85/4.92	95.5/80.7
gi|295665077 - Hsp90 binding co-chaperone (Sba1)	143	24 h	**	**	1	4.49/4.23	22.5/21.3
gi|295665077 - Hsp90 binding co-chaperone (Sba1)	145	24 h	**	**	1	4.38/4.23	20.0/21.3
gi|295659837 - Heat shock protein SSB1	65	24 h	96	22	2	4.85/5.47	50.5/60.6
gi|295672932 - 30 kDa heat shock protein	138	6 h	109	53	11	7.06/9.75	24.83/28.64
gi|295672932 - 30 kDa Heat shock protein	133	24 h	170	48	**	6.80/9.75	27.0/28.64
gi|295672932 - 30 kDa Heat shock protein	135	24 h	120	57	**	7.28/9.75	26.5/28.64
gi|295664909 - 10 kDa heat shock protein, mitochondrial	156	24 h	102	58	1	9.41/8.79	12.67/11.19
gi|295668244 - Mitochondrial peroxiredoxin PRX1	132	24 h	**	**	1	4.45/5.28	28.33/24.9
gi|295668244 - Mitochondrial peroxiredoxin PRX1	132	24 h	**	**	1	4.45/5.28	28.33/24.9
gi|295662873 - Mitochondrial co-chaperone GrpE	134	6 h	**	**	6	5.30/8.89	26.5/28.51
gi|225681400 - Peroxisomal catalase	45	6 h	121	41	**	7.73/6.42	57.0/57.66
gi|295661107 - Thioredoxin reductase	103	24 h	87	29	1	6.77/5.51	41.0/38.19
gi|295670221 - Thioredoxin	153	24 h	77	56	1	5.21/5.24	13.33/12.9
gi|17980998 - Y20 protein	142	6 h	60	33	1	7.19/6.09	22.83/21.64
gi|17980998 - Y20 protein	141	24 h	**	**	2	6.90/6.09	23.0/21.6

gi|295657024 - Puromycin sensitive aminopeptidase	18	6 h	283	58	12	6.31/5.65	90.0/100.71
gi|295669794 - Elongation factor Tu	75	6 h	73	44	3	5.57/6.11	45.67/48.71
gi|295675019 - Elongation factor 2	112	24 h	116	16	2	7.08/6.46	39.17/92.6
gi|295675019 - Elongation factor 2	118	24 h	**	**	2	7.85/6.46	37.83/92.7
gi|295674319 - Polyadenylate binding protein	17	6 h	74	37	**	6.99/6.31	92.0/86.92
gi|295672445 - Alanyl-tRNAsynthetase	9	24 h	121	18	**	5.76/5.52	103.83/108.4
gi|295660511 - Glycyl-tRNAsynthetase	31	24 h	**	**	2	6.40/5.77	70.67/74.9
gi|146762537 - Enolase	70	24 h	89	27	**	5.82/5.67	49.5/47.4
gi|146762537 - Enolase	68	24 h	205	64	6	5.66/5.67	50.17/47.41
gi|295671152 - Phosphoglucomutase	42	24 h	**	**	1	7.48/6.59	58.33/83.6
gi|295669690 - Phosphoglyceratekinase	79	24 h	91	27	2	7.51/6.48	44.83/45.3
gi|295658778 - Phosphoenolpyruvate carboxykinase	40	24 h	128	27	2	6.99/6.10	60.5/63.9
gi|295671120 - Fructose-1,6-bisphosphate aldolase	101	24 h	133	43	1	7.48/6.09	41.67/39.72
gi|295671120 - Fructose-1,6-bisphosphate aldolase	113	6 h	190	69	7	7.08/6.09	38.67/39.72
gi|295671120 - Fructose1,6-bisphosphate aldolase	115	6 h	**	**	1	7.32/6.09	38.5/39.72
gi|295671120 - Fructose1,6-bisphosphate aldolase	94	24 h	153	58	**	6.33/6.09	42.67/39.72
gi|295658119 - Glyceraldehyde-3-phosphate dehydrogenase	122	6 h	286	85	8	9.13/8.26	36.83/36.62
gi|295658119 - Glyceraldehyde-3-phosphate dehydrogenase	111	24 h	88	50	**	8.47/8.26	39.67/36.62
gi|295658119 - Glyceraldehyde-3-phosphate dehydrogenase	108	24 h	140	42	**	8.95/8.26	40.17/36.6
gi|295658119 - Glyceraldehyde-3-phosphate dehydrogenase	107	24 h	193	69	3	8.28/8.26	40.17/36.6
gi|295658897 - Citrate synthase	80	24 h	84	26	2	7.99/8.75	44.83/52.2
gi|295658897 - Citrate synthase	82	24 h	**	**	1	8.51/8.75	44.67/52.20
gi|295658897 - Citrate synthase	83	24 h	**	**	1	8.25/8.75	44.33/52.20
gi|295669416 - 2-oxoglutarate dehydrogenase E1	10	6 h	122	20	1	7.11/6.68	103.5/121.6
gi|295669416 - 2-oxoglutaratedehydrogenase E1	6	24 h	91	13	1	7.36/6.68	110.0/121.63

gi|295669416 - 2-oxoglutarate dehydrogenase E1	7	24 h	221	27	4	7.30/6.68	108.67/121.6
gi|295669416 - 2-oxoglutarate dehydrogenase E1	46	24 h	83	10	**	6.79/6.68	56.33/121.63
gi|295673931 - Pyruvate dehydrogenase protein X complex	54	6 h	98	33	6	5.46/6.45	53.67/52.71
gi|295673931 - Pyruvate dehydrogenase protein X component	58	6 h	79	55	5	5.31/6.45	51.83/52.71
gi|295673937 - Malate dehydrogenase	128	6 h	185	49	10	8.10/8.99	34.17/36.02
gi|295664721 - Aconitase	20	24 h	146	47	13	7.64/6.49	86.5/79.20
gi|295664721 - Aconitase	19	24 h	109	24	12	7.51/6.49	88.17/79.20
gi|295664721 - Aconitase	22	24 h	131	50	13	7.75/6.49	85.5/79.20
gi|295665542 - Osmotic growth protein	71	24 h	159	50	**	9.37/6.90	49.33/68.04
gi|295669416 - 2-oxoglutarate dehydrogenase E1	4	24 h	84	39	**	6.79/6.68	114.0/121.63
gi|295658595 - Pyruvate dehydrogenase E1 component subunit alpha	78	24 h	130	28	2	6.63/8.62	44.83/45.3
gi|295660969 - Isocitrate lyase	36	6 h	215	74	12	8.05/6.79	63.67/60.17
gi|295660969 - Isocitrate lyase	43	24 h	161	27	2	8.10/6.79	57.83/60.2
gi|295660969 - Isocitrate lyase	41	6 h	364	46	13	8.01/6.79	59.67/60.17
gi|295665123 - Aldehyde dehydrogenase	57	24 h	170	41	2	6.19/5.87	52.33/54.5
gi|295665123 - Aldehyde dehydrogenase	60	6 h	106	55	7	6.51/5.87	51.5/54.56
gi|295665123 - Aldehyde dehydrogenase	61	24 h	140	38	3	6.46/5.87	51.17/54.5
gi|295665123 - Aldehyde dehydrogenase	157	24 h	**	**	3	5.08/5.87	12.0/54.5
gi|295672968 - Phosphomannomutase	121	24 h	**	**	2	5.57/5.60	37.17/30.6
gi|295663567 - 6-phosphogluconolactonase	126	24 h	148	40	3	6.70/5.86	36.17/29.3
gi|295661432 - UTP-glucose-1-phosphate uridylyltransferase	49	6 h	93	42	7	9.37/9.11	55.0/58.87
gi|295674635 - Alcohol dehydrogenase	116	6 h	178	84	7	8.72/7.55	38.33/38.00
gi|295674635 - Alcohol dehydrogenase	110	24 h	134	61	6	8.5/7.55	39.83/38.00
gi|295662360 - Mannitol-1-phosphate 5-dehydrogenase	102	6 h	138	26	1	6.44/5.66	41.5/43.12

gi|295666179 - 2- Methylcitrate synthase	73	6 h	127	66	12	9.23/9.02	47.17/51.52
gi|295666197 - 2-Methylcitrate dehydratase	59	6 h	**	**	3	7.72/8.55	51.67/62.26
gi|295672652 - Bifunctional purine biosynthesis protein ADE17	39	24 h	98	20	1	8.15/6.70	62.83/67.2
gi|295672652 - Bifunctional purine biosynthesis protein ADE17	47	24 h	153	29	2	7.26/6.70	56.17/67.2
gi|295665468 - Nucleic acid-binding protein	130	24 h	79	26	**	6.70/9.40	30.0/30.41
gi|295665468 - Nucleic acid-binding protein	131	24 h	101	41	**	7.18/9.40	30.0/30.41
gi|295666938 - Nucleoside diphosphate kinase	147	6 h	187	71	**	7.89/6.84	17.5/16.88
gi|225681397 - Conserved hypotetical protein	129	24 h	78	50	**	4.93/5.25	32.33/23.11
gi|295665131 - Delta-1-pyrroline-5-carboxylate dehydrogenase	53	24 h	**	**	1	8.25/7.68	54.0/62.9
gi|225683481 - Cysteinyl-tRNAsynthetase	15	24 h	81	22	**	6.18/6.09	95.5/89.20
gi|295672027 - Glycine dehydrogenase	3	24 h	106	36	5	7.64/8.84	115.0/129.88
gi|295668479 - Formamidase	72	24 h	**	**	5	7.02/6.06	47.17/46.10
gi|295674273 - Acetolactate synthase	38	6 h	95	35	5	7.81/8.93	62.83/74.16
gi|295674767 - 4-aminobutyrate aminotransferase	66	6 h	75	29	**	8.98/9.21	50.5/32.28
gi|295668370 - Aminopeptidase	11	24 h	158	58	6	5.41/6.20	100.67/73.39
gi|295661139 - Methylmalonate-semialdehyde dehydrogenase	44	6 h	168	51	8	8.17/8.99	57.67/63.11
gi|295658698 - Fumarylacetoacetase	74	24 h	99	26	2	6.36/5.95	45.83/46.7
gi|295667902 - Aminomethyltransferase	76	24 h	110	31	**	8.44/9.59	45.5/53.1
gi|295669670 - Adenosylhomocysteinase	77	6 h	129	26	1	6.76/5.83	45.17/49.0
gi|295669240 - Kynurenine-oxoglutarate transaminase	84	6 h	82	39	6	6.54/7.05	44.0/50.88
gi|295662426 - Aspartate aminotransferase	96	6 h	88	30	5	8.46/8.39	42.5/50.91
gi|295662426 - Aspartate aminotransferase	100	24 h	89	26	**	8.83/8.39	42.0/50.91
gi|295672504 - Inorganic pyrophosphatase	2	24 h	99	59	4	7.0/5.13	115.67/33.55
gi|295672504 - Inorganic pyrophosphatase	98	24 h	121	61	**	4.82/5.13	42.0/33.55
gi|295672504 - Inorganic pyrophosphatase	125	6 h	187	63	11	4.84/5.13	36.5/33.55
gi|225678712 - Ketol-acid reductoisomerase	104	6 h	192	60	10	7.92/9.12	40.83/44.86

gi|226294930 - Ketol-acidreductoisomerase	136	24 h	**	**	1	7.92/9.12	26.0/44.8
gi|295658312 - L-PSP endoribonuclease family protein (Hmf1)	152	6 h	77	46	1	5.98/8.96	15.17/18.72
gi|295670601 - 3-hydroxyisobutyryl-CoA hydrolase	56	24 h	80	62	**	6.30/7.09	53.17/57.35
gi|295657225 - Peroxisomal multifunctional enzyme	12	24 h	93	38	**	9.37/8.98	100.33/97.15
gi|295657225 - Peroxisomal multifunctional enzyme	21	6 h	**	**	2	9.59/8.98	86.33/97.15
gi|295665414 - Short chain dehydrogenase family protein	137	6 h	63	18	**	6.62/6.77	25.67/32.09
gi|295666416 - Short-chain-fatty-acid-CoA ligase	124	6 h	51	11	**	8.82/7.09	36.67/55.37
gi|295666416 - Short-chain-fatty-acid-CoA ligase	144	6 h	51	11	**	6.55/7.09	20.33/55.37
gi|295666416 - Short-chain-fatty-acid-CoA ligase	151	6 h	46	11	**	3.96/7.09	15.33/55.37
gi|295668707 - Acetyl-CoA acetyltransferase	97	24 h	**	**	1	7.85/8.98	42.33/46.6
gi|295668707 - Acetyl-coA acetyltransferase	99	6 h	**	**	4	8.09/8.98	42.0/46.65
gi|295664927 - ATP-citrate-lyase	64	6 h	**	**	3	6.91/5.99	50.67/52.9
gi|295664927 - ATP citrate lyase	62	24 h	**	**	1	6.73/5.99	51.17/52.9
gi|295658821 - ATP synthase subunit beta	67	6 h	233	57	18	4.54/5.28	50.33/55.18
gi|295658923 - Citochrome b-c1 complex subunit 2	89	6 h	138	45	5	8.92/9.10	43.17/49.01
gi|295669073 - 12-oxophytodienoate reductase	92	24 h	250	71	13	9.31/8.69	42.83/43.25
gi|295657369 - Nicotinate-nucleotide pyrophosphorylase	119	24 h	101	33	1	7.56/6.55	37.67/33.7
gi|295660716 - UDP-galactopyranose mutase	51	24 h	100	22	**	7.82/6.81	54.5/58.3
gi|295661741 - 3- demethylubiquinone 9,3-methyltransferase	149	24 h	96	40	**	4.74/4.93	17.0/22.42
gi|295660455 - Pyridoxine biosynthesis protein PDX1	105	24 h	94	70	**	6.26/6.04	40.67/34.41
gi|295663887 - 40S ribosomal protein S19	146	6 h	129	80	5	10.45/9.69	17.67/16.41
gi|295663887 - 40S ribosomal protein S19	148	24 h	121	77	**	10.32/9.69	17.33/16.41
gi|295664112 - 40S ribosomal protein S22	150	24 h	94	92	**	10.50/9.99	16.0/14.73
gi|295672445 - Alanyl-tRNA synthetase	8	24	242	50	10	5.67/5.52	104.33/108.48
gi|295666766 - Vacuolar aminopeptidase	48	24 h	62	18	**	6.17/5.75	55.33/56.65
gi|295657201 - Glutamate carboxypeptidase	50	6 h	**	**	5	5.81/6.23	54.83/64.62

gi|295674421 - Ubiquitin carboxyl-terminal hydrolase	5	24 h	154	46	4	5.21/5.33	111.67/88.03
gi|295660102 - Dipeptidyl- peptidase	28	24 h	226	66	**	7.21/7.99	73.50/86.55
gi|295662102 - Rab GDP-dissociation inhibitor	52	6 h	158	64	9	5.64/5.44	54.33/52.54
gi|295657091 - Tropomyosin-1	140	6 h	80	50	1	4.52/4.99	23.0/18.83
gi|295673184 - Actin-interacting protein	109	24 h	93	23	1	7.53/6.48	40.0/65.9
gi|295669061 - Arp2/3 complex subunit Arc16	120	6 h	**	**	5	7.13/5.87	37.5/36.15
gi|295669061 - Arp2/3 complex subunit Arc16	106	24 h	**	**	2	6.87/5.87	40.5/36.15
gi|295660405 - Hypotetical protein	155	6 h	152	64	7	9.26/10.06	13.33/14.97
gi|295661500 - Conserved hypothetical protein	114	24 h	**	**	2	7.28/6.36	38.5/33.1
gi|295673506 - Conserved hypothetical protein	154	24 h	113	95	6	5.3/5.36	13.33/13.55
gi|295659253 - Conserved hypothetical protein	139	24 h	86	61	**	4.81/5.15	23.67/17.35

**Spots visualized only in zinc-depleted or zinc replete conditions;
[a]GenBank general information identifier**;**
[b]Spot numbers as depicted in Fig 2;
[c] Time of exposure to zinc starvation;
[d]Mascot score;
[e]Amino acid sequence coverage for the identified protein;
[f]Number of matched peptides on MS/MS searching;
[g]Experimental/theoretical isoelectric point;
[h]Experimental/theoretical molecular weight;

2.3.1. Proteínas induzidas na condição de depleção de zinco

Algumas proteínas foram detectadas em mais de um spot. Para melhorar o entendimento e caracterizar a abundância global das proteínas, foi realizada a soma da porcentagem dos volumes de todos os spots de cada proteína.

A categorização das proteínas preferencialmente expressas após a depleção de zinco comparada à condição controle permitiu a identificação de um total de 55 proteínas (tabela 3). As proteínas induzidas foram classificadas principalmente em resgate, defesa e virulência, representando um total de 18 proteínas, correspondendo a 33% das proteínas identificadas (Fig 6). Nessa categoria funcional estão proteínas envolvidas na resposta antioxidante, tais como tioredoxina, glutationa redutase, glutationa sintetase, disulfide isomerase, Y20 e peroxiredoxina mitocondrial, todas induzidas após 24 h de depleção de zinco, apresentando um fold change variando de 1.58 a 3.17. Adicionalmente, 11 proteínas, pertencentes à família de proteínas heat shock foram superexpressas, principalmente após 24 h de limitação de zinco (tabela 3).

Enzimas da via da gliconeogênese, incluindo fosfoenolpiruvato carboxiquinase, fosfoglicerato quinase, gliceraldeído-3-fosfato desidrogenase e frutose-bifosfato aldolase foram upreguladas. A indução ocorreu principalmente em 24 h de depleção de zinco (tabela 3). Enzimas do metabolismo de aminoácidos, tais como aspartato aminotransferase e delta-1-pirrolina-5-carboxilato desidrogenase foram induzidas em 24h de deprivação de zinco (tabela 3).

A Fig 7 resume alguns aspectos metabólicos que podem estar ocorrendo em 24h de depleção de zinco, sugerido pelas análises proteômicas. Prolina e arginina podem ser convertidos em glutamato pela ação da enzima delta-1-pirrolina-5-carboxilato desidrogenase. O glutamato pode então ser utilizado para a síntese de glutationa através da ação da enzima glutationa sintetase. A peroxiredoxina metaboliza peróxido de hidrogênio em uma reação na qual resíduos da enzima tornam-se oxidados, requerendo tioredoxina para reduzir a molécula de volta ao seu estado ativo. Tioredoxina, por sua vez, requer tioredoxina redutase para ser restaurada ao seu estado reduzido (Wu *et al*. 2009).

Table 3: *Paracoccidioides* proteins with increased expression upon 6 and 24 h of zinc starvation and their predicted biological function-FunCat2[†]

Accession number[a]/Protein description	Time[b]	Number of isoforms in *Paracoccidioides*[c]	Average of amount of isoform abundances in zinc starvation[d]	Average of amount of isoform abundances in control[e]	ANOVA (p-value)[f]	Fold Change[g]
Cell rescue, defense and virulence						
gi|295670221 - Thioredoxin	24 h	1	0.52	**	**	**
gi|295664022 - Glutathione reductase	24 h	1	0.19	0.12	0.033	1.58
gi|295674755 - Glutathione synthetase	24 h	1	0.07	0.04	0.006	1.61
gi|295661107 - Thioredoxin reductase	24 h	1	0.16	**	**	**
gi|295668244 - Mitochondrial peroxiredoxin PRX1	24 h	1	0.08	**	**	**
gi|17980998 - Y20 protein	24 h	1	0.89	0.28	0.001	3.17
gi|295673162 - Disulfide isomerase Pdi1	24 h	1	0.94	0,33	0.003	2.83
gi|295658865 - Heat shock protein	6 h	1	0.14	**	**	**
gi|4164594 - Heat shock protein 70	6 h	1	1.75	1.51	0.044	1.16
gi|14538021 - Heat shock protein 70	24 h	3	2.43	0.94	0.0012	2.58
gi|295659116 - Hsp70-like protein	6 h	1	0.14	**	**	**
gi|295673716 - Hsp70-like protein	24 h	2	1.06	0.53	0.0014	2.00
gi|295659116 - Hsp70-like protein	24 h	3	1.68	1.0	0.0013	1.68
gi|14538021 - Heat shock protein 70	24 h	1	0.63	0.20	0.046	3.19
gi|295671569 - Heat shock protein SSC1	6 h	2	0.20	**	**	**
gi|295659837 - Heat shock protein SSB1	24 h	1	0.11	0.09	0.020	1.81
gi|295659787 - Heat shock protein Hsp88	24 h	2	0.99	0.61	0.0052	1.64
gi|295665077 - Hsp90 binding co-chaperone (Sba1)	24 h	2	0.25	0.11	0.00005	2.32
Protein synthesis and Fate						
gi|295657024 - Puromycin-sensitive aminopeptidase	6 h	1	0.06	**	**	**
gi|295669794 - Elongation factor Tu	6 h	1	0.08	**	**	**
gi|295675019 - Elongation factor 2	24 h	2	0.37	0.28	0.001	1.34
gi|295674319 - Polyadenylate-binding protein	6 h	1	0.05	**	**	**
gi|295660511 - Glycyl-tRNA synthetase	24 h	1	0.07	**	**	**
Glycolysis and Gluconeogenesis						
gi|295671152 - Phosphoglucomutase	24 h	1	0.22	0.04	0.013	5.54
gi|295658119 - Glyceraldehyde-3-phosphate dehydrogenase	24 h	3	3.95	2.14	0.0061	1.85
gi|295669690 - Phosphoglycerate kinase	24 h	1	0.37	0.25	0.032	1.50
gi|295671120 - Fructose-1,6-bisphosphate aldolase	24 h	2	0.33	0.19	0.05	1.73
gi|295658778 - Phosphoenolpyruvate carboxykinase	24 h	1	0.13	0.05	0.000	2.59
Citric acid cycle						
gi|295658897 - Citrate synthase	24 h	3	0.39	0.10	0.0008	3.84
gi|295669416 - 2-oxoglutarate dehydrogenase E1	6 h	1	0.16	**	0.018	1.86

gi|295669416 - 2-oxoglutarate dehydrogenase E1	24 h	4	0.41	0.17	0.003	2.42
gi|295658595 - Pyruvate dehydrogenase E1 component subunit alpha	24 h	1	0.31	0.20	0.002	1.60
Glyoxylate cycle						
gi|295660969 - Isocitrate lyase	24 h	1	0.25	0.11	0.001	2.36
Oxidation of fatty acids						
gi|295665123 - Aldehyde dehydrogenase	24 h	3	1.22	0.15	0.0002	8.25
Carbohydrate metabolism						
gi|295672968 - Phosphomannomutase	24 h	1	0.25	0.05	0.000	4.74
gi|295663567 - 6-phosphogluconolactonase	24 h	1	0.15	0.08	0.016	1.87
gi|295661432 - UTP-glucose-1-phosphate-uridylyltransferase	6 h	1	0.14	**	**	**
Nucleotide metabolism						
gi|295672652 - Bifunctional purine biosynthesis protein ADE17	24 h	2	0.37	0.17	0.004	2.17
Amino acid and nitrogen metabolism						
gi|295669240 - Kynurenine-oxoglutarate transaminase	6 h	1	0.16	**	**	**
gi|295669670 - Adenosylhomocysteinase	6 h	1	0.19	0.07	0.033	2.67
gi|295667902 - Aminomethyltransferase	24 h	1	0.10	0.05	0.014	1.96
gi|226294930 - Ketol-acid reductoisomerase	24 h	1	0.19	**	**	**
gi|295658698 - Fumarylacetoacetase	24 h	1	0.19	0.15	0.028	1.30
gi|295665131 - Delta-1-pyrroline-5-carboxylate dehydrogenase	24 h	1	0.07	**	**	**
gi|295662426 - Aspartate aminotransferase	24 h	1	0.16	**	**	**
Lipid, fatty acid and isoprenoid metabolism						
gi|295657225 - Peroxisomal multifunctional enzyme	6 h	1	0.14	**	**	**
gi|295668707 - Acetyl-CoA acetyltransferase	24 h	1	0.32	0.20	0.002	1.58
gi|295664927 - ATP-citrate-lyase	6 h	1	0.17	0.05	0.003	3.31
gi|295664927 - ATP citrate lyase	24 h	1	0.26	0.17	0.011	1.50
Metabolism of vitamins, cofactors and prosthetic groups						
gi|295657369 - Nicotinate-nucleotide pyrophosphorylase	24 h	1	0.25	0.13	0.011	1.88
gi|295660716 - UDP-galactopyranose mutase	24 h	1	0.18	0.10	0.046	1.69
Protein/peptide degradation						
gi|295666766 - vacuolar aminopeptidase	24 h	1	0.04	**	**	**
Cell growth / morphogenesis						
gi|295657091 - Tropomyosin-1	6 h	1	0.26	**	**	**
gi|295673184 - Actin-interacting protein	24 h	1	0.23	**	**	**
Unclassified Proteins						
gi|295661500 - Conserved hypothetical protein	24 h	1	0.11	0.07	0.016	1.62

**Spots visualized only in zinc-starvation condition;

[a]GenBank general information identifier**;**
[b]Time of exposure to zinc starvation;
[c]Number of identified isoforms of protein in *Paracoccidioides*. Pb01 during zinc starvation
[d,e]The average of amount of values of abundances of all identified isoforms used to statistical test
[f]$p < 0.05$ was used to considerer statistically significant differences
[g]Fold change increase in protein expression in zinc starvation.
[†]Functional classification by FunCat2 (http://pedant.helmholtzmuenchen.de/pedant3htmlview/pedant3view?Method=analysis&Db=p3_r48325_Par_brasi_Pb01)

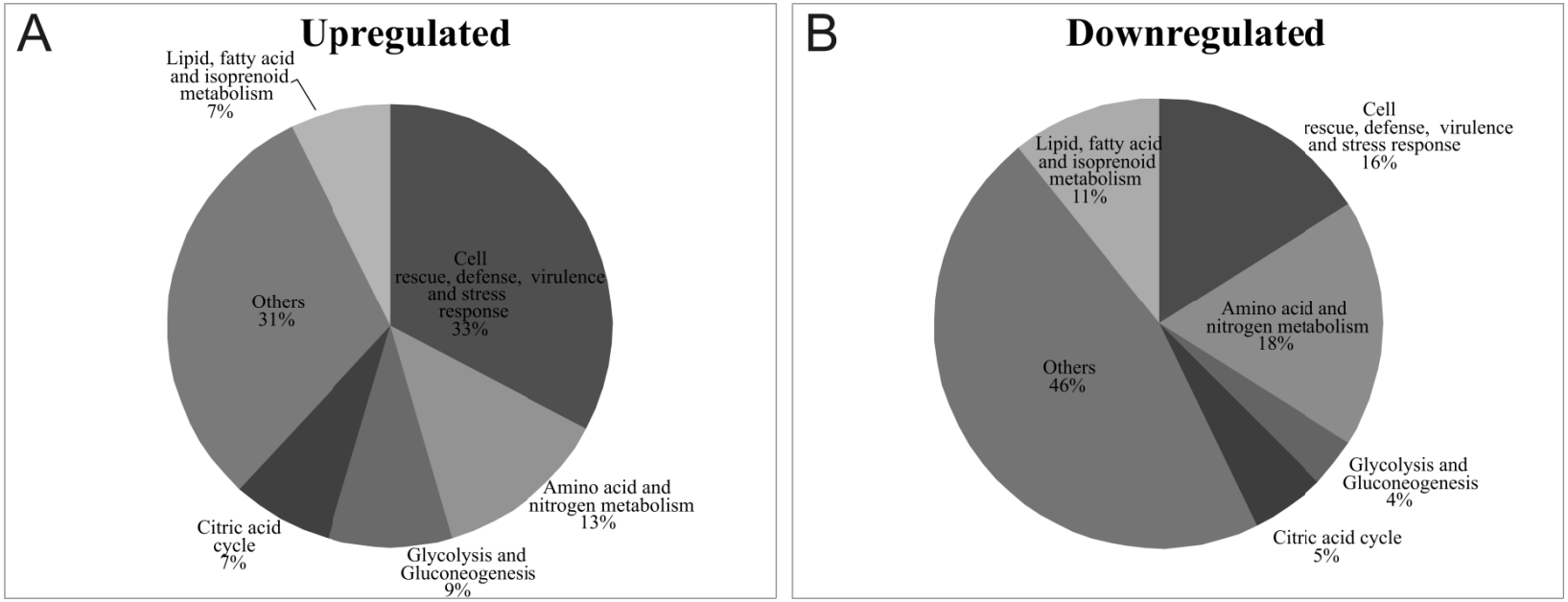

Fig 6. Representação da classificação funcional das proteínas de *Paracoccidioides* reguladas durante a depleção de zinco. As proteínas identificadas foram classificadas de acordo com o FunCat2. Classificação das proteínas com expressão induzida (A) e reprimida (B) em condições de limitação de zinco.

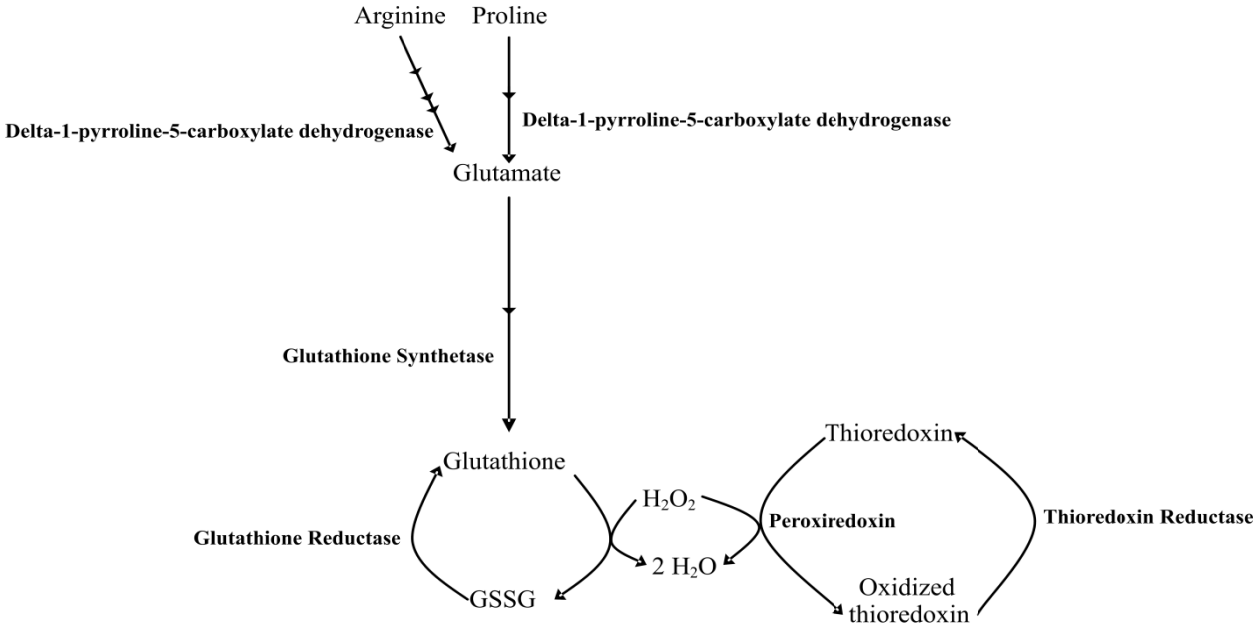

Fig 7. Esquema metabólico da possível resposta de *Paracoccidioides* ao estresse gerado pela depleção de zinco revelado pelas análises proteômicas. GSSG representa glutationa oxidada.

2.3.2. Proteínas com expressão reprimida após depleção de zinco

A categorizacão das proteínas reprimidas durante a depleção de zinco permitiu a identificação de um total de 56 proteínas (tabela 4), apresentando um fold change de 1.17 a 7.93. Em 6 h de privação de zinco, algumas proteínas antioxidantes, tais como glutationa redutase, Y20 e catalase peroxissomal foram reprimidas. É importante notar que glutationa redutase e Y20 foram induzidas em 24 h, como descrito acima.

Três enzimas de *Paracoccidioides* envolvidas com o ciclo do metilcitrato foram menos abundantes na condição de depleção de zinco: aconitase, 2-metilcitrato desidratase e 2-metilcitrato sintase. A enzima álcool desidrogenase, envolvida na fermentação, também foi downregulada em células leveduriformes após privação de zinco (tabela 4).

Enzimas do metabolismo de aminoácidos também foram reprimidas durante depleção de zinco, principalmente aquelas envolvidas com o metabolismo de valina e isoleucina, tais como acetolactato sintase e metilmalonato-semialdeído desidrogenase (tabela 4).

Table 4: *Paracoccidioides* proteins with decreased expression upon 6 and 24 h of zinc starvation and their predicted biological function-FunCat2[†]

Accession number[a]/Protein description	Time[b]	Number of isoforms in *Paracoccidioides*[c]	Average of amount of isoform abundances in zinc starvation[d]	Average of amount of isoform abundances in control[e]	ANOVA (*p*-value)f	Fold Change[g]
Cell rescue, defense and virulence						
gi|295664022 - Glutathione reductase	6 h	1	0.19	0.34	0.024	1.83
gi|225681400 - Peroxisomal catalase	6 h	1	0.12	0.21	0.027	1.69
gi|295662873 - Mitochondrial co-chaperone GrpE	6 h	1	0.13	0.30	0.003	2.35
gi|295673162 - Disulfide isomerase Pdi1	6 h	1	0.22	0.36	0.013	1.66
gi|17980998 - Y20 protein	6 h	1	0.80	1.31	0.025	1.64
gi|295672932 - 30 kDa heat shock protein	6 h	1	0.29	0.59	0.03	2.02
gi|295672932 - 30 kDa Heat shock protein	24 h	2	0.49	0.88	0.00072	1.80
gi|295658865 - Heat shock protein	24 h	2	0.06	0.13	0.009	2.28
gi|295664909 - 10 kDa heat shock protein. mitochondrial	24 h	1	**	0.52	**	**
Protein synthesis and Fate						
gi|295663887 - 40S ribosomal protein S19	6 h	1	0.45	0.90	0.007	2.01
gi|295663887 - 40S ribosomal protein S19	24 h	1	**	0.47	**	**
gi|295664112 - 40S ribosomal protein S22	24 h	1	**	0.53	**	**
Glycolysis and Gluconeogenesis						
gi|295671120 - Fructose1,6-bisphosphate aldolase	6 h	2	1.56	2.35	0.0054	1.5
gi|295658119 – Glyceraldehyde 3-phosphate dehydrogenase	6 h	1	0.78	2.18	0.001	2.80
Citric acid cycle						
gi|295673937 - Malate dehydrogenase	6 h	1	0.36	0.77	0.004	2.12
gi|295664721 - Aconitase	24 h	3	0.47	1.17	0.005	2.48
gi|295665542 - Osmotic growth protein	24 h	1	0.10	0.28	0.029	2.7
Oxidation of fatty acids						
gi|295665123 - Aldehyde dehydrogenase	6 h	1	0.03	0.07	0.022	2.49
Carbohydrate metabolism						
gi|295662360 - Mannitol-1-phosphate 5-dehydrogenase	6 h	1	0.14	0.20	0.042	1.41
Nucleotide metabolism						
gi|295666938 - Nucleoside diphosphate kinase	6 h	1	0.82	0.52	0.001	3.12
gi|225681397 - Conserved hypotetical protein	24 h	1	**	0.32	**	**
Amino acid and nitrogen metabolism						
gi|295661139 - Methylmalonate-semialdehyde dehydrogenase	6 h	1	0.11	0.23	0.005	2.15
gi|295662426 - Aspartate aminotransferase	6 h	1	0.08	0.15	0.009	1.83

gi|295674273 - Acetolactate synthase	6 h	1	0.04	0.12	0.031	3.17
gi|295658312 - L-PSP endoribonuclease family protein (Hmf1)	6 h	1	0.17	0.34	0.006	2.00
gi|225678712 - Ketol-acid reductoisomerase	6 h	1	0.27	0.38	0.014	1.40
gi|295674767 - 4-aminobutyrate aminotransferase	6 h	1	0.03	0.02	0.047	1.77
gi|295668370 - Aminopeptidase	24 h	1	0.08	0.13	0.025	1.7
gi|225683481 - Cysteinyl-tRNA synthetase	24 h	1	0.02	0.03	0.05	1.17
gi|295672027 - Glycine dehydrogenase	24 h	1	0.05	0.10	0.009	2.2
gi|295668479 - Formamidase	24 h	1	0.75	1.21	0.020	1.6
Lipid, fatty acid and isoprenoid metabolism						
gi|295668707 - Acetyl-coA acetyltransferase	6 h	1	0.09	0.24	0.002	2.65
gi|295665414 - Short chain dehydrogenase family protein	6 h	1	**	0.15	**	**
gi|295666179 - 2-Methylcitrate synthase	6 h	1	0.55	1.10	0.004	1.99
gi|295666197 - 2-Methylcitrate dehydratase	6 h	1	0.52	0.82	0.028	1.58
gi|295657225 - Peroxisomal multifunctional enzyme	24 h	1	**	0.09	**	**
gi|295670601 - 3-hydroxyisobutyryl-CoA hydrolase	24 h	1	0.06	0.11	0.013	1.7
Metabolism of vitamins, cofactors and prosthetic groups						
gi|295661741- 3-demethylubiquinone 9,3-methyltransferase	24 h	1	0.20	0.39	0.019	1.9
gi|295660455 - Pyridoxine biosynthesis protein PDX1	24 h	1	**	0.09	**	**
Protein/peptide degradation						
gi|295657201 - Glutamate carboxypeptidase	6 h	1	0.07	0.11	0.005	1.69
gi|295674421 - Ubiquitin carboxyl-terminalhydrolase	24 h	1	**	0.03	**	**
gi|295660102 - Dipeptidyl- peptidase	24 h	1	0.20	0.28	0.039	1.4
Transcription						
gi|295665468 - Nucleic acid-binding protein	24 h	2	0.33	1.01	0.00073	3.10
Electron transport and membrane-associated energy conservation						
gi|295658821 - ATP synthase subunit beta	6 h	1	0.22	0.32	0.037	1.48
gi|295658923 - Citochrome b-c1 complex subunit 2	6 h	1	0.12	0.16	0.026	1.42
gi|295669073 - 12-oxophytodienoate reductase	24 h	1	0.56	0.96	0.013	1.7
Fermentation						
gi|295674635 - Alcohol dehydrogenase	6 h	1	0.44	0.81	0.002	1.85
gi|295674635 - Alcohol dehydrogenase	24 h	1	0.37	1.0	0.001	2.7
Phosphate Metabolism						
gi|295672504 - Inorganic pyrophosphatase	6 h	1	0.19	0.25	0.044	1.32
gi|295672504 - Inorganic pyrophosphatase	24 h	2	0.041	0.32	0.002	7.93
Signal transduction						
gi|295662102 - Rab GDP-dissociation inhibitor	6 h	1	0.13	0.29	0.002	2.24
Cytoskeleton/structural proteins						
gi|295669061 - Arp2/3 complex subunit Arc16	6 h	1	0.13	0.18	0.003	1.42

gi|295669061 - Arp2/3 complex subunit Arc16	24 h	1	0.11	0.18	0.006	1.7
DNA synthesis and replication						
gi|295660405 - Hypotetical protein	6 h	1	0.41	0.76	0.011	1.8
Unclassified Proteins						
gi|295673506 - Conserved hypothetical protein	24 h	1	0.10	0.21	0.008	2.0
gi|295659253 - Conserved hypothetical protein	24 h	1	**	0.21	**	**

**Spots visualized only in zinc-replete condition;
[a]GenBank general information identifier**;**
[b]Time of exposure to zinc starvation;
[c]Number of identified isoforms of protein in *Paracoccidioides*. Pb01 in zinc replete conditions
[d,e]The average of amount of values of abundances of all identified isoforms used to statistical test
[f]$p < 0.05$ was used to considerer statistically significant differences
[g]Fold change increase in protein expression in zinc availability.
[†]Functional classification by FunCat2 (http://pedant.helmholtzmuenchen.de/pedant3htmlview/pedant3view?Method=analysis&Db=p3_r48325_Par_brasi_Pb01)

2.4. Correlação entre os dados proteômicos e transcricionais

Para validar a significância dos resultados encontrados na análise proteômica, foi avaliado se as mudanças nos níveis protéicos teriam correlação com as mudanças nos níveis transcricionais. Por meio de análises por RT-PCR em tempo real de transcritos codificantes para isocitrato liase (*ICL*), citrato sintase (*CS*), catalase peroxissomal (*CATP*) e álcool desidrogenase (*ADH*) foi encontrado que os dados proteômicos estão de acordo os transcricionais (Fig 8). Os níveis de proteínas e transcritos diminuíram após a limitação de zinco, como apresentado na Fig 8 e tabela 4. Os níveis transcricionais de *CS* e *ICL* estão aumentados e também correlacionados com os níveis transcricionais (Fig 8 e tabela 3).

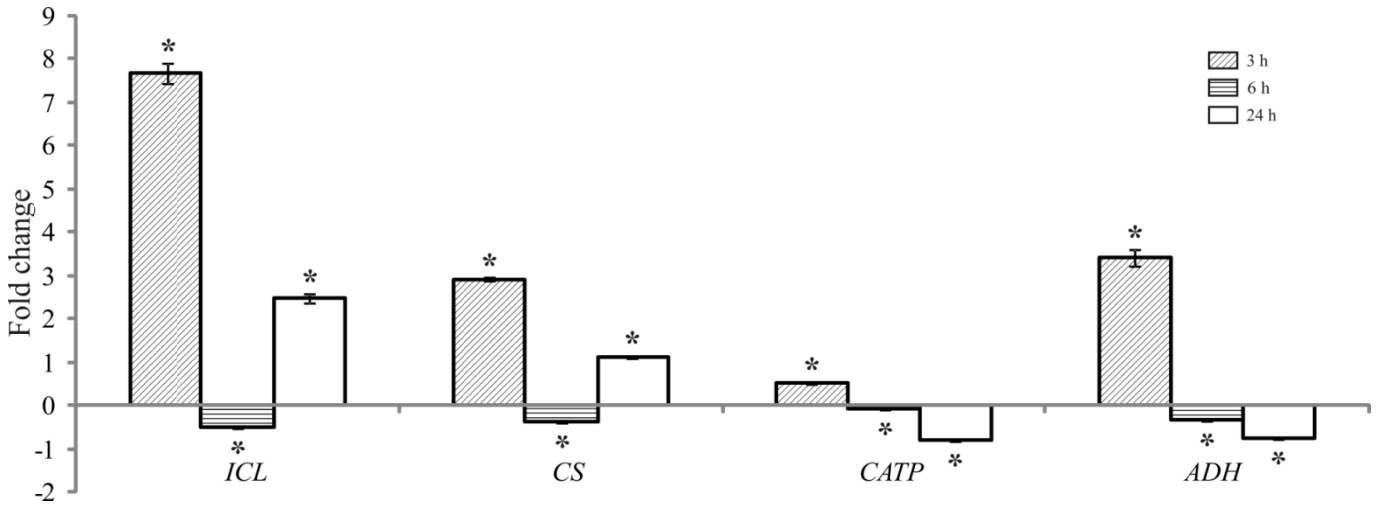

Fig 8. Validação dos dados proteômicos por RT-PCR em tempo real. Os níveis de transcritos de *Paracoccidioides* codificantes para isocitrato liase (*ICL*), citrato sintase (*CS*), catalase peroxissomal (*CATP*) e álcool desidrogenase (*ADH*) foram quantificados por meio de RT-qPCR. Os dados foram normalizados utilizando o transcrito codificante para a proteína α-tubulina e apresentados como fold change Análises estatísticas para avaliar o nível de significância foram realizadas utilizando o teste *t* de Student, adotando $p \leq 0,05$ (*).

3. DISCUSSÃO

Sabe-se que componentes da resposta celular a depleção de zinco operam por meio da indução de vários transcritos (Amich *et al*. 2010; Zhao and Eide 1996a; Zhao and Eide 1996b). Sob condições de restrição de zinco foi observada a indução de transcritos de *Paracoccidioides* que são dependentes de zinco. Os resultados obtidos pela RT-qPCR utilizando cDNAs derivados de células leveduriformes de *Paracoccidioides* crescidas em meio depletado demonstrou que houve superexpressão de *PbZRT2*, sugerindo que Zrt2p comporta-se como um transportador de alta-afinidade. Bailão *et al*. (2012) demonstrou que *ZRT2*, mas não *ZRT1*, foi altamente expresso em pH neutro e alcalino durante depleção de zinco, como observado para *ZRFC* de A. *fumigatus*, sugerindo que a expressão desse gene pode ser regulada pelo zinco e pelo pH em *Paracoccidioides*.

Nós analisamos o proteoma de células leveduriformes de *Paracoccidioides* após privação de zinco. As análises proteômicas resultaram na identificação de 157 proteínas. Destas, 19 foram detectadas em mais de um spot e 9 foram observadas nas formas reprimida e induzida, mas em diferentes tempos de limitação de zinco. As descrições aqui apresentadas, embora não exaustivas, fornecem as primeiras informações a respeito do comportamento de *Paracoccidioides* durante a depleção de zinco.

Nossos resultados demonstraram superexpressão de proteínas relatadas com a resposta ao estresse em condições de privação de zinco. Espécies reativas de oxigênio (ROS), incluindo o ânion superóxido, peróxido de hidrogênico (H_2O_2), e radical hidroxila, podem causar vários tipos de danos biológicos. A deficiência de zinco está associada com altos níveis de óxido nítrico (NO) e H_2O_2 em células PC12 originadas da medula adrenal de ratos, H_2O_2 em células humanas IMR-32 originadas de neuroblastomas (Mackenzie *et al*. 2006), e NO em células C6 de glioma de ratos (Ho and Ames 2002). Adicionalmente, através de estudos *in vitro* e *in vivo* foi demonstrado que a deficiência de zinco leva a um aumento do estresse oxidativo em células de mamíferos (Wu *et al*. 2009). Em leveduras de *S. cerevisae* há indução do estresse oxidativo quando elas são crescidas em condições de limitação de zinco (Wu *et al*. 2007). Nessas condições, Zap1p de *S. cerevisae* ativa a expressão do gene *TSA1,* que codifica uma peroxiredoxina citosólica responsável por metabolizar H_2O_2 (Rhee *et al*., 2005). Os resíduos de cisteína tornam-se oxidados durante essa reação e requer

tioredoxina para ser reduzida ao seu estado ativo. Tioredoxina, por sua vez, requer tioredoxina redutase para ser restaurada ao seu estado reduzido (Wu *et al*. 2009). De acordo com os dados proteômicos aqui apresentados, as proteínas tioredoxina, glutationa redutase, peroxiredoxina e tioredoxina redutase são induzidas durante a depleção de zinco, sugerindo fortemente que durante a privação de zinco há aumento do estresse oxidativo. Genes e proteínas de *Paracoccidioides* relacionados ao estresse oxidativo (catalase, superóxido dismutase (SOD), peroxiredoxina, citocromo C peroxidase, glutationa e tioredoxina) tem sido descritos, indicando que *Paracoccidioides* utiliza vários sistemas antioxidantes para combater as ROS (Campos *et al*. 2005; Chagas *et al*. 2008; Dantas *et al*. 2008).

As chaperonas moleculares são responsáveis por manter a conformação das proteínas (Hartl 1996). Elas mantêm a sinalização, regulam a proliferação, diferenciação e apoptose (Sõti *et al*. 2005). As chaperonas ainda (ou proteínas do estresse) conferem citoproteção e asseguram a sobrevivência celular após vários tipos de estresses. Neste estudo 15 proteínas de *Paracoccidioides*, incluindo isoformas, pertencentes à família de proteínas heat shock foram alteradas em abundância após limitação de zinco. Esses resultados podem ser uma indicação do envolvimento das chaperonas na proteção do fungo durante o estresse gerado pela depleção de zinco.

A deficiência de zinco leva a um aumento do estresse oxidativo, como citado acima. Sob condições de estresse oxidativo o fungo *Aspergillus niger* reduz a captação de glicose (Li *et al*. 2008). Nesse caminho, foi observado que enzimas da gliconeogênese, tais como fosfoenolpiruvato carboxiquinase e fosfoglicerato quinase são induzidas em resposta ao estresse oxidativo causado pela limitação de zinco em *Paracoccidioides*.

Três enzimas de *Paracoccidioides* envolvidas com o ciclo do metilcitrato foram reprimidas durante a restrição de zinco. O ciclo do metilcitrato é um sistema alternativo de fornecimento de carbono através da produção de piruvato (Bramer *et al*. 2002). Uma das maiores vias de metabolismo de propionil-CoA é o ciclo do metilcitrato. Propionil-CoA é gerado pela quebra de cadeias ímpares de ácidos graxos e dos aminoácidos valina e isoleucina (Fleck and Brock 2008). De acordo com as análises proteômicas aqui apresentadas, foi observada uma redução na expressão de enzimas envolvidas no metabolismo de valina e isoleucina, bem como enzimas do metabolismo de lipídios,

possivelmente reduzindo a produção de propionil-CoA. Os dados sugerem que há um ajustamento global do metabolismo de *Paracoccidioides* sob depleção de zinco.

A enzima álcool desidrogenase catalisa a oxidação de etanol a acetaldeído. Essa enzima é dependente de zinco e é altamente expressa em condições de repleção de zinco, mas reprimida durante condições de depleção em *S. cerevisiae* (Bird *et al*. 2006). Nós demonstramos que a álcool desidrogenase é downregulada durante privação de zinco em *Paracoccidioides*, novamente sugerindo que a expressão gênica diferencial auxilia na adaptação de *Paracoccidioides* à deficiência de zinco.

As análises proteômicas de *Paracoccidioides* revelaram que a maior resposta celular afetada pela restrição de zinco foi a resposta ao estresse oxidativo. Os dados também sugerem que resgate, defesa e virulência foram a vias mais favorecidas. Nossos resultados fornecem a primeira visão proteômica da resposta de *Paracoccidioides* à depleção de zinco.

Capítulo 3

Análises transcricionais de *Paracoccidioides* durante o processo infectivo no pulmão

1. MATERIAIS E METODOS

1.1. Microrganismo e condições de crescimento

Foi utilizado o isolado Pb01 (ATCC MYA-826) de *Paracoccidioides* já caracterizado e padronizado em nosso laboratório. O fungo na fase leveduriforme foi cultivado por 7 dias em meio Fava Netto sólido (Fava-Netto, 1961) à temperatura de 37 °C. Após este período as células foram transferidas para o meio Fava Netto líquido e incubadas à 36 °C por 3 dias. As células foram coletadas por centrifugação a 3000 x *g* por 10 min, e lavadas três vezes com PBS 1X. A viabilidade celular foi avaliada por microscopia óptica utilizando-se azul de trypan 0,05%.

1.2. Infecção Experimental

O presente trabalho foi submetido para apreciação pelo COEP-UFG (comissão de ética em pesquisa animal) sendo aprovado em novembro de 2008 (Protocolo COEP/UFG n. 131/2008). Doze fêmeas de camundongos da linhagem Balb/C de 8 a 12 semanas de idade foram utilizadas para os experimentos de infecção. Deste total 06 camundongos foram infectados e 6 usados como controle. Os camundongos foram infectadas por via intranasal com 5 x 10^6 células de *Paracoccidioides* na forma de levedura e foram eutanaziados, por deslocamento cervical, 7 e 15 dias após a infecção. Nos animais controle foi utilizado solução salina [0,9% (p/v) NaCl]. Pulmões dos animais infectados e controle, foram removidos e homogeneizados em 5 mL de PBS 1 X. Alíquotas de 100 µl do material homogeneizado foram plaqueadas em meio BHI Ágar, suplementado com 4% (p/v) de glicose e 0,1% (p/v) do antibiótico gentamicina (10 µg/mL).

1.3. Recuperação de *Paracoccidioides* do pulmão de animais infectados

Os pulmões obtidos de camundongos infectados com *Paracoccidioides* por via intranasal foram solubilizados em 1 mL de água, por maceração, com ajuda de grinders. A solução foi filtrada para remoção de restos celulares que não foram homogeneizados. O sobrenadante foi rapidamente congelado em nitrogênio líquido para bloqueio de transcrição. Após descongelamento, o sobrenadante foi adicionado de triton X-100 [1% (v/v)] e incubado por 20 min a 37 °C, a seguir o material foi centrifugado a 500 x *g* por 5 min. O sobrenadante coletado foi centrifugado novamente a 7000 x *g* por 15 min e o precipitado foi submetido à extração do RNA.

1.4. Extração de RNA

Todos os procedimentos envolvendo a manipulação de RNA foram realizados em condições livres de RNAses. As vidrarias foram embaladas em papel alumínio, autoclavadas e tratadas em estufa a 180 ^{o}C por um período de 4 h. Os materiais plásticos utilizados eram novos. As cubas de eletroforese foram tratadas com peróxido de hidrogênio 3 % (v/v), durante 4 h. As soluções foram feitas com água previamente tratada com DEPC 0,01 % (p/v).

Para a extração de RNA de *Paracoccidioides* foi utilizado Trizol (GIBCO^{TM} Invitrogen Corporation), segundo o protocolo do fabricante. Células leveduriformes de *Paracoccidioides* derivadas do pulmão de animais infectados e células controle, foram misturadas com Trizol na proporção de 3,5 mL para 1,5 mg de células. Foi então adicionado o mesmo volume de pérolas de vidro. O material foi agitado em aparelho tipo vórtex por 10 min, mantido em repouso por 10 min à temperatura ambiente e centrifugado a 3.000 x *g* por 10 min a 4 ºC. Com o auxílio de uma pipeta, a fase superior foi transferida para um tubo novo. A essa fase foi adicionado clorofórmio (200 µL para cada 0,75 mL de trizol). O material foi homogeneizado por 1 min em aparelho tipo vórtex, incubado durante 10 min à temperatura ambiente e centrifugado a 3.000 x *g* por 15 min a 4°C. A fase aquosa foi recolhida, sendo adicionada à mesma, uma mistura de clorofórmio: fenol: álcool isoamílico (25:24:1). O material foi agitado, incubado durante 10 min à temperatura ambiente e centrifugado a 3.000 x *g* por 15 min a 4 ^{o}C. A fase aquosa foi recolhida e o RNA nela contido foi precipitado pela adição da solução de citrato de sódio 1,2 M e cloreto de sódio 0,8 M e de isopropanol (0,25 mL para cada 0,75 mL de Trizol). O material foi homogeneizado, incubado à temperatura ambiente por 10 min e centrifugado a 3.000 x *g* por 30 min a 4 ºC. O sedimento obtido foi lavado com etanol 75 % (v/v) na proporção de 1 mL para cada 0,75 mL de Trizol e centrifugado a 3.000 x *g* por 5 min a 4 °C. O RNA resultante foi seco à temperatura ambiente por 10 min e ressuspendido em água. O RNA foi quantificado por espectrofotometria, aliquotado e estocado a -80°C.

1.5. Síntese de cDNA

A síntese da primeira fita de cDNA foi realizada com a enzima transcriptase reversa (RT Superscrip II, Invitrogen, CA, USA), utilizando 1µg de RNA nas condições a seguir: 72 °C por 2 min e 42 °C por 1 h e 50 min, seguida da adição de tampão 10 mM Tris/1 mM EDTA e incubação a 72 °C por 7 min. A primeira fita de cDNA foi utilizada

como molde para síntese da segunda fita (25 ciclos de 95 °C por 1 min e 15 s e 55 °C por 30 s, cada) . O cDNA foi preparado utilizando-se o sistema comercial para síntese de cDNA SMART PCR da Clonetech Laboratories (Palo Alto, CA, USA). Os oligonucleotídeos utilizados estão listados na Tabela 1.

1.6. Construções de bibliotecas subtraídas (RDA)

Bibliotecas subtraídas de cDNA foram construídas a partir de RNAs obtidos de células leveduriformes derivadas do pulmão de animais infectados ("*tester"*) e aquelas mantidas por repiques sucessivos ("*driver"*). Foi utilizada a estratégia subtrativa de RDA, anteriormente padronizada em nosso laboratório (Bailão *et al*., 2006; 2007).

O cDNA dupla-fita foi digerido com a enzima de restrição Sau3AI (GE Healthcare, Chalfont St. Giles, UK). Os produtos resultantes foram purificados utilizando-se o sitema comercial GFX (GE Healthcare), e ligados a adaptadores (um de 24 mer e outro de 12 mer). Para a geração dos produtos diferenciais, os cDNAs do *driver* e do *tester* foram hibridizados à 67 °C por 18 h e amplificados por PCR com o adaptador de 24 mer. Para se obter uma amplificação seletiva subtrativa, a hibridização foi realizada de acordo com Pastorian e colaboradores (2000). Foram realizadas duas etapas sucessivas de subtração e amplificação por PCR usando as relações de hibridização *tester-driver* de 1:10, para gerar o primeiro produto diferencial (DP1) e 1:100, para gerar o segundo produto diferencial (DP2). Os adaptadores foram trocados entre cada etapa de hibridização e os produtos diferenciais foram purificados com o sistema comercial GFX (GE Healthcare, Chalfont St. Giles, UK) (Dutra *et al*, 2004). Os produtos diferenciais de cDNAs amplificados foram purificados e clonados em vetor pGEM-T Easy (Promega, Madison, WI, USA).

1.7. Sequenciamento dos cDNAs, Processamentos de dados das EST, Anotação e Análises de Expressão diferencial

Uma alíquota dos produtos finais do RDA (fragmentos DP2) foi ligada ao vetor pGEM-T Easy (Promega Co., Madison, USA). Células competentes *Escherichia coli* DH5α foram transformadas com os produtos da ligação pelo método de eletroporação conforme descrito por Löfblom *et al* (2007). Os DNAs plasmidiais foram preparados a partir dos clones selecionados das bibliotecas subtraídas e seqüenciados com o kit Dyenamic ET Dye Terminator no seqüenciador MegaBace (Amershan Pharmacia Biotech, Amershan Place, UK), usando o oligonucleotídeo T7 correspondente ao vetor

pGEM-T Easy (Tabela 1). As ESTs foram processadas com os programas Phred e Crossmatch (HTTP://www.genome.washington.edu/UWGC/analysistools/Swat.cfm). As seqüências de, no mínimo, 100 nucleotídeos e com qualidade Phred maior ou igual a 20 foram consideradas para a montagem. As ESTs foram submetidas ao programa de montagem de seqüências CAP3 (Huang and Madan, 1999) para serem agrupadas (*clusters*) e gerar *contigs* e *singlets*, os quais foram analisados. A anotação foi realizada utilizando-se o BLAST2GO (http://www.blast2go.org), o qual compara os *clusters* montados com as seqüências disponíveis em bancos de dados públicos (Conesa *et al*., 2005). Os programas BLAST do NCBI (*National Center for Biotechnology Information*) (http://www.ncbi.lm.nih.gov/BLAST) processado com seqüências não-redundantes (nr) do GenBank, COG (*Cluster of Ortologous Genes*) (http://www.ncbi.nlm.nih.gov) e GO (*Gene Ontology Consortium*) (http://www.geneontology.org) foram usados para a anotação das ESTs.

1.8. Análise da expressão gênica por RT- PCR quantitativa em Tempo Real (qRT-PCR)

Para validação dos resultados, RNAs do fungo crescido em condições *in vitro* e recuperado da infecção em pulmão foram extraídos e submetidos às análises por PCR em tempo real. As qRT-PCR foram realizadas utilizando-se a mistura SYBR green (Applied Biosystems, Foster City, CA) no sistema StepOnePlus™ real time PCR (Applied Biosystems). As reações foram realizadas em triplicatas. As curvas padrões foram geradas utilizando-se uma alíquota de cDNA de cada amostra, serialmente diluídas (1:5 da diluição original). Os dados foram normalizados com o transcrito codificante para a proteína alfa-tubulina amplificado em cada conjunto de experimentos de qRT-PCR. Para os experimentos com transcritos de *Paracoccidioides* recuperado diretamente do órgão foi utilizada a gama-tubulina. Os níveis de expressão relativa dos genes de interesse foram calculados utilizando-se o método de curva padrão para quantificação relativa (Bookout *et al*., 2006). Os resultados foram validados pelo teste *t* de *Student*, sendo consideradas diferenças significativas as amostras que apresentaram $p \leq 0,05$. Os oligonucletídeos utilizados no experimento, assim como as seqüências correspondentes estão descritos na Tabela 1.

1.9. Análises estatísticas

Os experimentos foram realizados em triplicata. Os resultados são apresentados como médias ± o desvio padrão. As comparações estatísticas foram realizadas utilizando o teste *t* de Student. Foi considerado com diferença estatisticamente significante valores com $p \leq 0.05$.

Tabela 1: Oligonucleotídeos utilizados nas etapas do RDA, seqüenciamento e qRT-PCR

Oligonucleotídeos	Sequência	Número de acesso[a]
cDNA	5' AGCAGTGGTATCAACGACAGAGTACGCGGG 3'	--
CDS	5' AAGCAGTGGTATCAACGCAGAGTACT(30)N1N 3'	--
PCRII	5' AAGCAGTGGTATCAACGCAGAGT 3'	--
JBam12	5' GATCCGTTCATG 3'	--
JBam24	5' ACCGACGTCGACTATCCATGAACG 3'	--
NBam12	5' GATCCTCCCTCG 3'	--
NBam24	5' AGGCAACTGTGCTATCCGAGGGAG 3'	--
RBam12	5' GATCCTCGGTGA 3'	--
RBam24	5' AGCACTCTCCAGCCTCTCTCACCGAG 3'	--
T7	5' GTAATACGACTCACTATAGGGC 3'	--
ICL[b] sense	5'GAACCGACCTCCTGGCTGT 3'	PAAG_06951.1
ICL antisense	5'CGTTCTTGCCTGCTTGCTCA 3'	PAAG_06951.1
TRE[c] sense	5'AGTGGCAAGACAAGGTGGTT 3'	PAAG_06703.1
TRE antisense	5'CAACGCAATATACTGAGGGA 3'	PAAG_06703.1
BADH[d] sense	5'GTTGAAGAGCCATTTGGTCC 3'	PAAG_05392.1
BADH antisense	5'CAGATCATTGGACCACACAGA 3'	PAAG_05392.1
SKB1[e] sense	5'CGCAGGAGGGGGATTATGA 3'	PAAG_02402.1
SKB1 antisense	5'GGTGTCAAAAAGGTATCATCAG 3'	PAAG_02402.1
RPD3[f] sense	5'TGGCTTCTGCTATGTAAATGAT 3'	PAAG_06742.1
RPD3 antisense	5'AGGCTTCTTCCACTCCATCT 3'	PAAG_06742.1
PAL1[g] sense	5'TGCTGCGGAACTCTTTGAA 3'	PAAG_02031.1
PAL1 antisense	5'GGGCTTATCGTCGGAGAGTC 3'	PAAG_02031.1
CAP20 sense	5'CCTTCACGAACTCGCCACTAT 3'	PAAG_06538.1
CAP20 antisense	5'TCGCTGCTTAGGGAGTCTGC 3'	PAAG_06538.1
MFS[h] sense	5'CTAATTATGTTCTTTTGGGGTAC 3'	PAAG_06077.1
MFS antisense	5'GCATCGCCTATACCAACAAGA 3'	PAAG_06077.1
C_2H_2[i] sense	5'AAATGGCCGAAAAGAACTCCC 3'	PAAG_02842.1
C_2H_2 antisense	5'GTTCTGACAGTCATTCGACAG 3'	PAAG_02842.1
CCCH[j] sense	5'GATTGGACAACTTGCTGGGC 3'	PAAG_04844.1
CCCH antisense	5'GTGTCTACTCCTTCCACGGT 3'	PAAG_04844.1
GATA[k] sense	5'GGCCAAAGCGGAAACCAAAT 3'	PAAG_00610.1
GATA antisense	5'AGTTTGGTGTATTGGTGCGG 3'	PAAG_00610.1
CTF1B[l] sense	5'CAAACCACTCGTCAACACAATC 3'	PAAG_01359.1
CTF1b antisense	5'GATTGCCTTGAGTCTGATAGAG 3'	PAAG_01359.1
DIP5[m] sense	5'TGTTTACATGGGGAAGTATCTG 3'	PAAG_04187.1
DIP5 antisense	5'CGCGGCGTCCAGAATCAAC 3'	PAAG_04187.1
SER[n] sense	5'GGCCTCTCCACACGTTGCTG 3'	PAAG_07237.1
SER sense	5'GTTCCAGATAAGAACGTTAGC 3'	PAAG_07237.1
Tub[o] sense	5'ACAGTGCTTGGGAACTATACC 3'	PAAG_01647.1
Tub antisense	5'GGGACATATTTGCCACTGCC 3'	PAAG_01647.1

[a]Número de acesso/descrição da proteína – número de acesso da proteína identificada no banco de dados do *Paracoccidioides*: (http://www.broadinstitute.org/annotation/genome/*Paracoccidioides*_brasiliensis/MultiHome.html); [b]Isocitrato Liase; [c]Trealose fosfato sintase; [d]Betaína aldeído desidrogenase; [e]Arginina N-metiltransferase; [f]Histona deacetilase; [g]Pal1 proteína de morfolgia celular; [h]Maior superfamília de transportadores; [i]Ativador transcricional zinco responsivo c_2h_2; [j]CCCH zinc finger proteína; [k]Fator de transcrição tipo Gata; [l]Fator de transcrição C6; [m]Permease de aminoácido dicarboxílico; [n]Serina proteinase; [o]alpha-tubulina

2. RESULTADOS

2.1. Perfil transcricional de *Paracoccidioides* no processo infectivo

A análise de cDNA-RDA foi realizada utilizando 2 condições "*testers*" que incluem: *Paracoccidioides* recuperado do pulmão de camundongos infectados após 7 e 15 dias de infecção. O fungo cultivado *in vitro* foi utilizado como "*driver*" nas subtrações. Um total de 1728 clones foram seqüenciados sendo 864 originados de RNAs de células leveduriformes recuperadas de camundongos após 7 dias de infecção e 864 de células recuperadas após 15 dias de infecção. A natureza das estratégias adaptativas utilizadas pelo fungo nas condições analisadas foi obtida através da classificação das ESTs em categorias funcionais MIPS (Munich Information Center for Protein Sequences) (Fig 1 e 2; Tabela 2).

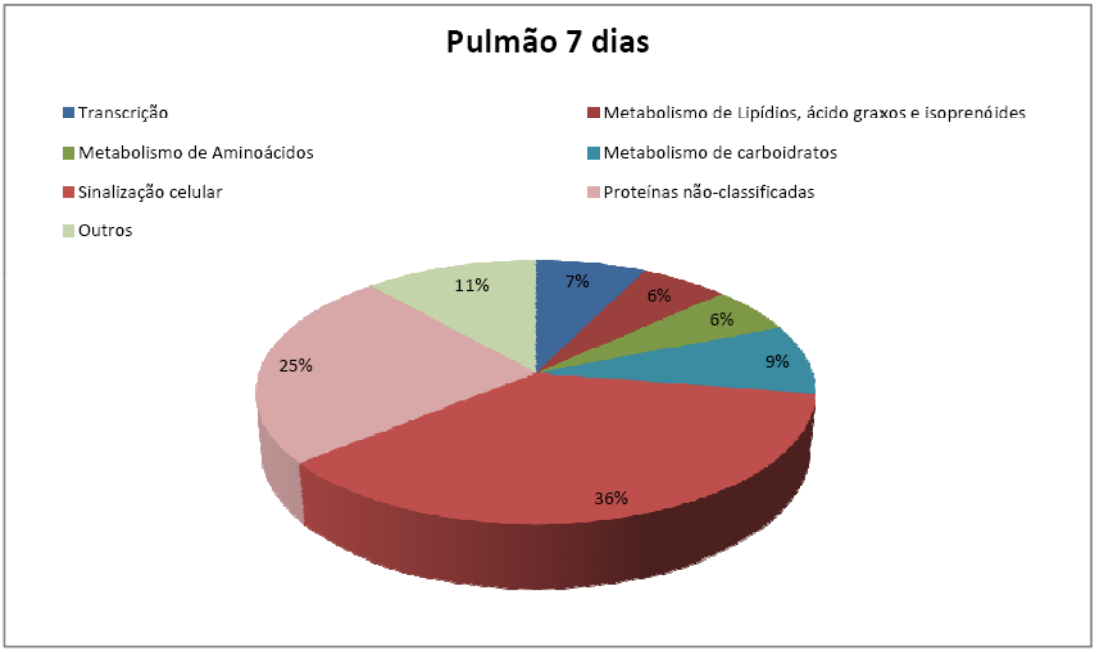

Fig 1: Classificação funcional das ESTs de *Paracoccidioides* derivados dos experimentos de RDA usando como *tester* o cDNA obtido de RNA de *Paracoccidioides* recuperado do pulmão de animais infectados por 7 dias. A classificação foi realizada segundo as categorias funcionais desenvolvidas no esquema de anotação funcional MIPS (http://mips.gsf.de/). Cada classe funcional está representada por um segmento colorido e expressa por porcentagem do número total de ESTs na biblioteca.

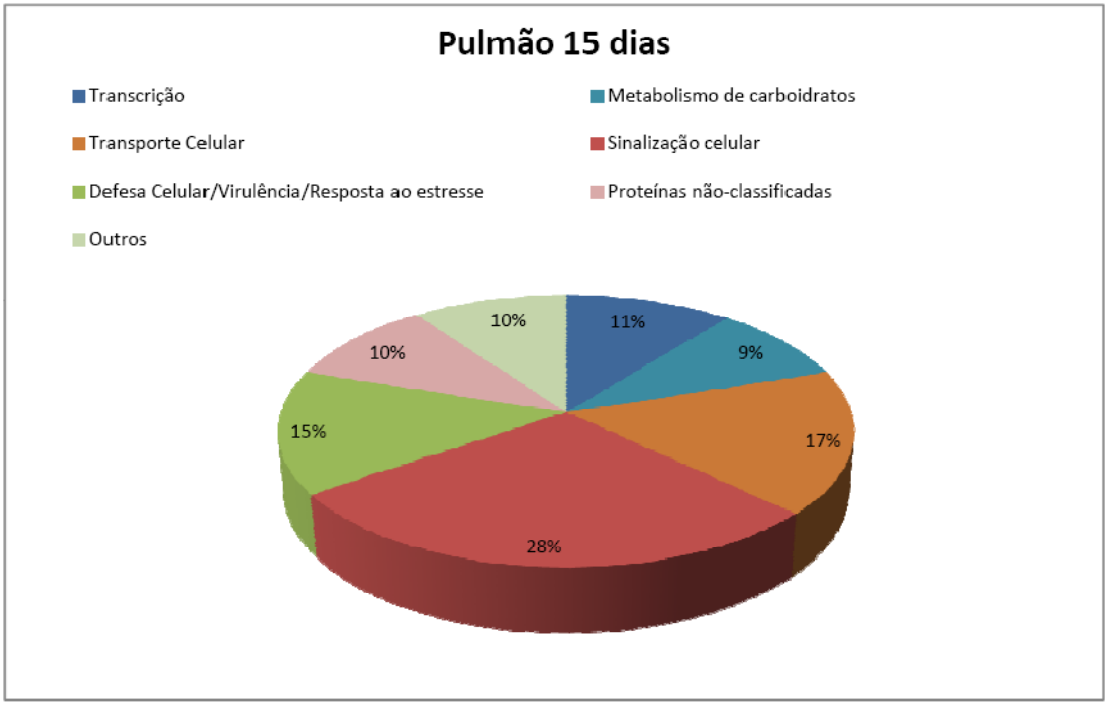

Fig 2: Classificação funcional das ESTs de *Paracoccidioides* derivados dos experimentos de RDA usando como *tester* o cDNA obtido de RNA de *Paracoccidioides* recuperado do pulmão de animais infectados por 15 dias.

Os dados ilustram a diversidade funcional dos fatores expressos, demonstrando as categorias funcionais específicas que dominam a resposta adaptativa de *Paracoccidioides* ao hospedeiro e a diferença temporal de expressão desses fatores (Tabela 2). Pode-se observar um maior número de transcritos relacionados com a sinalização celular (36%), não-classificados (25%), transcrição (11%), metabolismo de carboidratos (9%), metalismo de aminoácidos (6%) e metabolismo de lipídios (6%) com 7 dias de infecção (Fig 1) e sinalização celular (28%), transporte celular (17%), defesa celular/virulência/resposta ao estresse (15%), transcrição (11%) e metabolismo de carboidratos (9%) com 15 dias de infecção (Fig 2).

A figura 3 esquematiza os principais eventos metabólicos que estariam ocorrendo durante o processo de infecção no pulmão.

2.2. Validação da expressão diferencial de transcritos por PCR em Tempo Real

Para confirmação e validação dos dados, análises de expressão por RT-PCR em tempo real foram realizadas (fig 4). Os resultados encontrados corroboram os resultados do RDA confirmando esta técnica como uma boa estratégia para análises de expressão gênica diferencial. Dessa maneira os transcritos da isocitrato liase (*ICL*), trealose fosfato sintase (*TRE*), betaína aldeído desidrogenase (*BADH*), *PAL1*, fator de transcrição tipo

gata (*GATA*) foram aumentados 7 e 15 dias após a infecção. Os transcritos de arginina N-metiltransferase (*SKB1*), C_2H_2 e *CAP20* apresentaram-se aumentados em 7 dias e reprimidos em 15 dias de infeção, ao passo que histona deacetilase (*RPD3*), transportador MFS (*MFS*), *CCCH* e permease de aminoácido dicarboxílico (*DIP5*) foram reprimidos em 7 e induzidos em 15 dias após a infeção.

As análises de RDA e a comparação entre o repertório de genes induzidos em cada uma das condições experimentais sugerem que *Paracoccidioides* apresenta uma resposta de adaptação e sobrevivência no ambiente encontrado no hospedeiro que compõem as diferentes etapas do processo infeccioso.

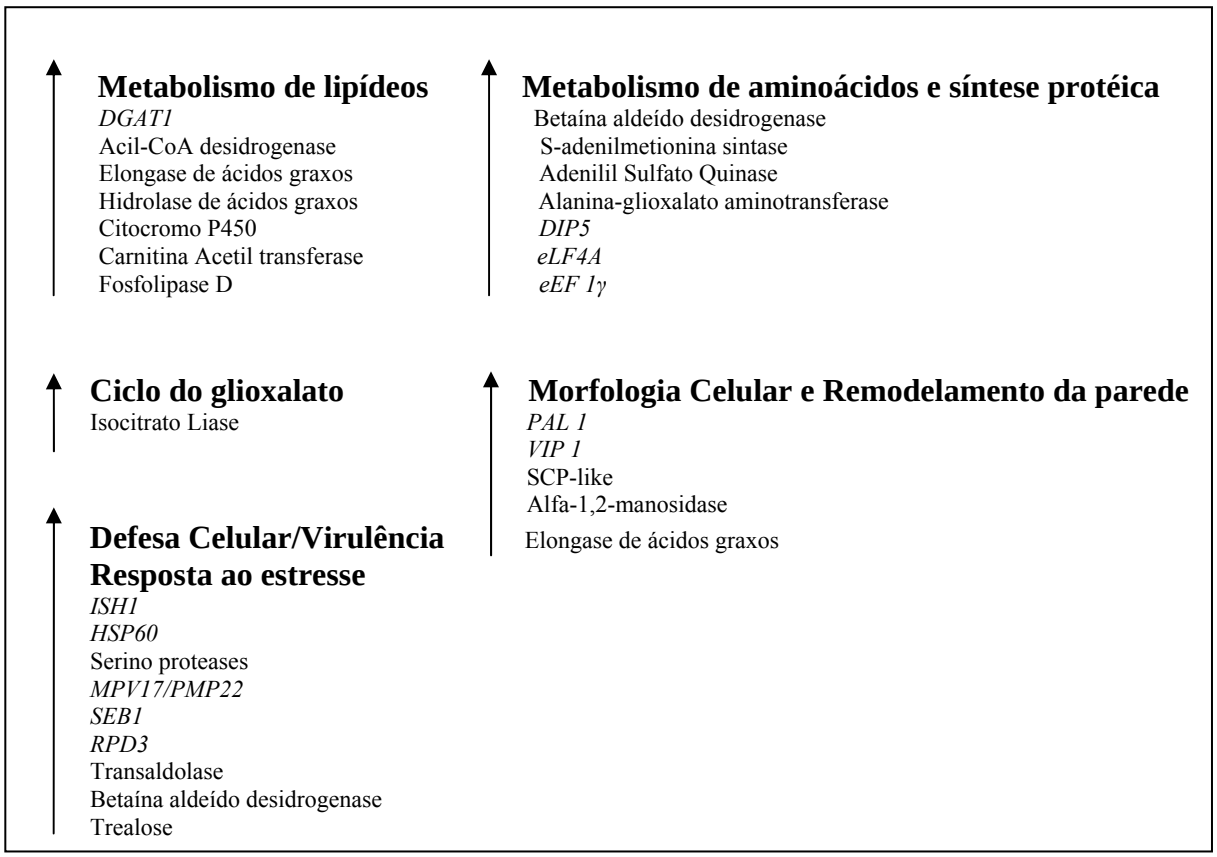

Fig 3: Eventos metabólicos predominantes durante o processo infectivo no pulmão.

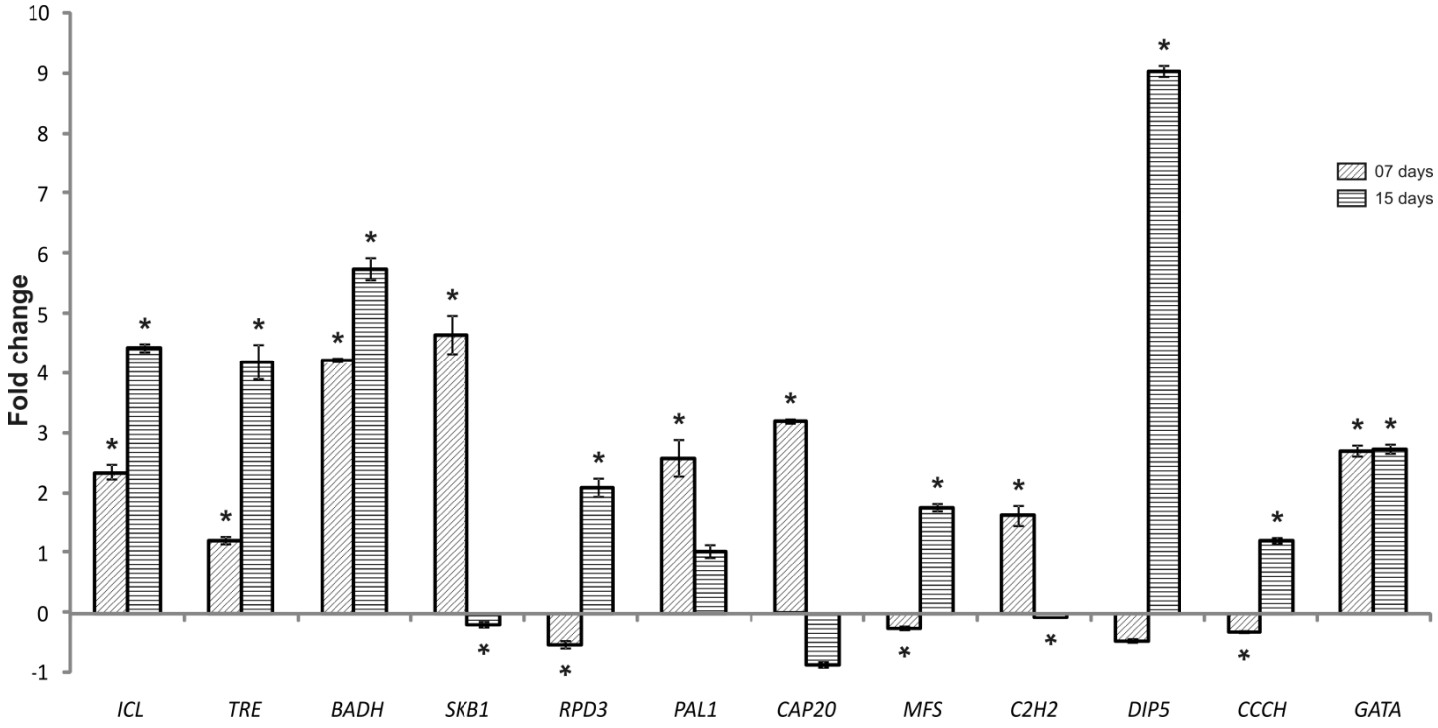

Fig 4: Análise dos transcritos por RT-PCR em tempo real. A expressão dos transcritos encontrados no RDA isocitrato liase (*ICL*), trealose fosfato sintase (*TRE*), betaína aldeído desidrogenase (*BADH*), arginina N-metiltransferase (*SKB1*), histona deacetilase (*RPD3*), Pal1 proteína de morfolgia celular (*PAL1*), maior superfamília de transportadores (*MFS*), ativador transcricional zinco responsivo c_2h_2 (*C_2H_2*), CCCH zinc finger proteína (*CCCH*), fator de transcrição tipo Gata (*GATA*), permease de aminoácido dicarboxílico (*DIP5*) e serina proteinase (*SER*) foi avaliada através de qRT-PCR. Os valores da expressão dos genes foram normalizados utilizando-se os valores de expressão do gene constitutivo codificante para a proteína alfa-tubulina. Análises estatísticas para avaliar o nível de significância foram realizadas, utilizando o teste *t* Student, adotando $p \leq 0,05$ (*).

2.3.Expressão gênica em *Paracoccidioides* recuperado diretamente do pulmão

Com o intuito de avaliar e validar os resultados do RDA foi realizada análise da expressão gênica *in vivo* de *Paracoccidioides* recuperado do pulmão de animais experimentais após 15 dias de infecção. Foi avaliada a expressão, por qRT-PCR, dos transcritos codificantes para fator de transcrição C6 (*CTF1b*), permease de aminoácido dicarboxílico (*DIP5*), betaína aldeído desidrogenase (*BADH*) e serino-proteinase (*SER*). Verificou-se concordância com os dados obtidos nas bibliotecas subtrativas (fig 5). Não se verificou a expressão dos transcritos acima citados no pulmão de animais controle (fig 5).

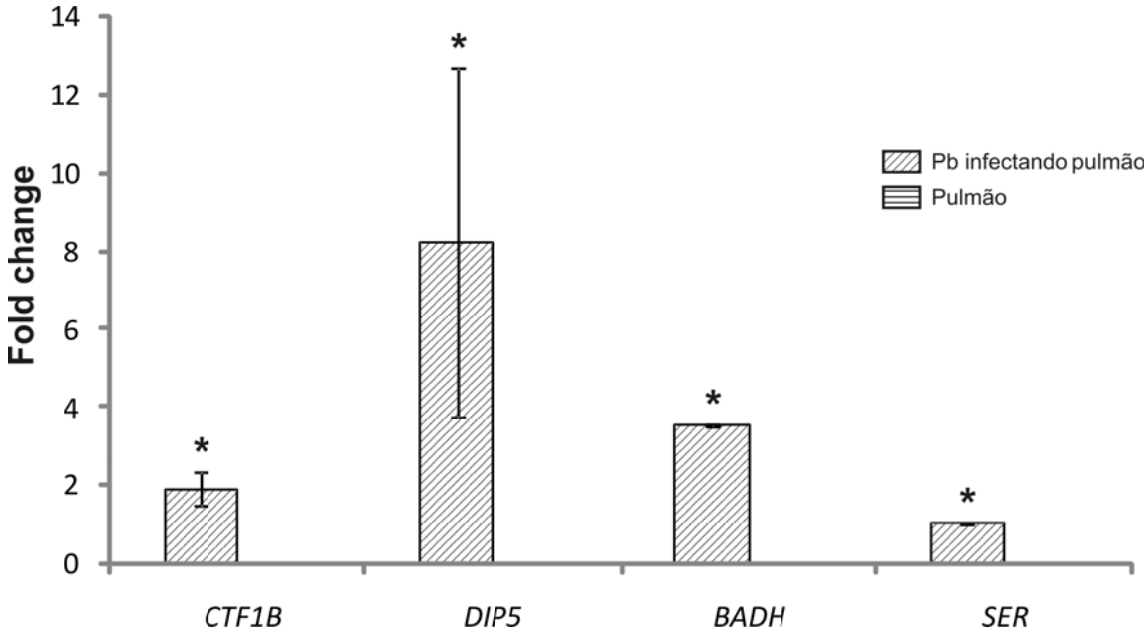

Fig 5: Análise por RT-PCR em tempo real de transcritos de células leveduriformes de *Paracoccidioides* recuperado de pulmão infectado. A expressão dos transcritos do fator de transcrição C6 (*CTF1B*), permease de aminoácido dicarboxílico (*DIP5*), betaína aldeído desidrogenase (*BADH)* e serina proteinase (*SER*) foi avaliada através de qRT-PCR. Os valores da expressão dos genes foram normalizados utilizando-se os valores de expressão do gene constitutivo codificante para a proteína gama-tubulina. Análises estatísticas para avaliar o nível de significância foram realizadas, utilizando o teste *t* Student, adotando $p \leq 0,05$ (*).

Tabela 2: Transcritos induzidos em células leveduriformes de *Paracoccidioides* recuperadas de pulmão de camundongos infectados

Categoria Funcional/MIPS[a]	Produto gênico	Organismo/número de acesso[b]	e-value	Frequência	
				P7	P15
Transcrição	Fator de transcrição Tipo GATA (NsDd)	*Paracoccidioides*/PAAG_05818.1	1e-57	31	54
	Histona deacetilase rpd3	*Paracoccidioides*/PAAG_06742.1	1e-49	1	11
	Fator de transcrição C6 (Ctf1B)	*Paracoccidioides*/PAAG_01359.1	1e-53	3	5
	Fator transcrição tipo CCCH	*Paracoccidioides*/PAAG_02735.1	1e-82	4	---
	Ribonuclease P/MRP, subunidade POP1	*Paracoccidioides*/PABG_06487.1	1e-78	1	---
	Fator de transcrição SteA	*Paracoccidioides*/PAAG_00406.1	1e-39	---	1
	Fator de transcrição C_2H_2 (seb1)	*Paracoccidioides*/PAAG_03287.1	1e-10	1	---
Metabolismo de Lipídios, ácido graxos e isoprenóides	Diacilglicerol o-aciltransferase (DGAT1)	*Paracoccidioides*/PAAG_07527.1	1e-99	21	24
	Acil-Coa desidrogenase	*Paracoccidioides*/PAAG_03490.1	1e-80	6	6
	Elongase de ácidos graxos	*Paracoccidioides*/PAAG_08553.1	1e-67	5	---
	Hidrolase de ácidos graxos	*Paracoccidioides*/PAAG_06825.1	1e-65	1	---
	Citocromo P450	*Paracoccidioides*/PAAG_01137.1	1e-14	---	1
	Carnitina Acetil transferase	*Paracoccidioides*/PAAG_06224.1	1e-30	---	1
Metabolismo de Aminoácidos	S-Adenosilmetionina Sintase	*Paracoccidioides*/PAAG_02901.1	1e-88	28	11
	Adenilil Sulfato Quinase	*Paracoccidioides*/PAAG_03043.1	1e-80	2	---
	Alanina-glioxalato aminotransferase	*Paracoccidioides*/PAAG_03138.1	1e-30	2	---
Ciclo do Glioxalato	Isocitrato liase	*Paracoccidioides*/PAAG_06951.1	1e-69	3	14
Metabolismo de carboidratos	Betaína aldeído desidrogenase	*Paracoccidioides*/PAAG_05392.1	1e-69	38	47
	Trealose fosfato sintase	*Paracoccidioides*/PAAG_06703.1	1e-40	3	10
	Transaldolase	*Paracoccidioides*/PAAG_04166.1	1e-74	5	3
	Fosfomanomutase	*Paracoccidioides*/PAAG_00889.1	1e-16	2	---
Transporte Celular	Permease de aminoácido dicarboxílico (dip5)	*Paracoccidioides*/PAAG_04187.1	1e-24	---	87

	Transportador Succinato/fumarato	*Paracoccidioides*/PAAG_06563.1	1e-38	11	14
	Transportador MFS	*Paracoccidioides*/PAAG_01353.1	1e-56	1	10
Transporte de elétrons e conservação de energia	ATP sintase subunidade Beta	*Paracoccidioides*/PAAG_08037.1	1e-75	8	---
Sinalização celular	Proteína com domínio PYP-like (domínio PAS)	*Paracoccidioides*/PAAG_06301.1	1e-104	196	170
	Fosfolipase D	*Paracoccidioides*/PAAG_00220.1	1e-61	3	8
	serina/threonina proteína kinase srk1	*Paracoccidioides*/PAAG_06726.1	1e-35	1	5
	Fosfatase/subunidade regulatória	*Paracoccidioides*/PAAG_00128.1	1e-46	2	---
	Inositol-pentaquisfosfato 2-quinase	*Paracoccidioides*/PABG_03477.1	1e-20	1	---
	Proteína pleckstrina-like	*Paracoccidioides*/PAAG_03092.1	1e-14	---	1
	Arginina N-metiltransferase (skb1)	*Paracoccidioides*/PAAG_02402.1	1e-84	2	---
Defesa Celular/Virulência/Resposta ao estresse	Proteína responsiva ao stress Ish1	*Paracoccidioides*/PAAG_01860.1	1e-116	---	12
	HSP60 - mitocondrial	*Paracoccidioides*/PAAG_08059.1	1e-84	1	11
	Serina proteinase	*Paracoccidioides*/PAAG_07237.1	1e-88	8	---
	CAP20	*Paracoccidioides*/PAAG_06538.1	1e-85	6	---
	Protease da família Rombóide	*Paracoccidioides*/PAAG_06616.1	1e-52	---	4
	Mpv17Pmp22	*Paracoccidioides*/PAAG_02868.1	1e-40	4	67
	Proteína extracellular SCP-like	*Paracoccidioides*/PAAG_03057.1	1e-27	---	1
Síntese Protéica	Fator de iniciação da tradução 4A (Elf4A)	*Paracoccidioides*/PAAG_00689.1	1e-79	10	7
	Fator de elongação 1 gama (eEF 1-γ)	*Paracoccidioides*/PAAG_03556.1	1e-85	2	---
Endereçamento de proteínas	alpha-1,2-manosidase	*Paracoccidioides*/PAAG_04552.1	1e-38	2	---
Divisão celular/Síntese de DNA	Ribonucleotídeo redutase – cdc22	*Paracoccidioides*/PAAG_02210.1	1e-36	2	---
	Protéina de controle da divisão celular MCM4	*Paracoccidioides*/PAAG_01035.1	1e-62	1	---

Crescimento/Morfologia Celular	Pal1	*Paracoccidioides*/PAAG_02031.1	1e-41	3	---
	Actina VIP1	*Paracoccidioides*/PAAG_01347.1	1e-29	2	---
	Rho-GDP	*Paracoccidioides*/PAAG_02377.1	1e-16	---	1
Proteínas não-classificadas	Proteína Hipotética	*Paracoccidioides*/PAAG_05009.1	1e-53	59	1
	Proteína Hipotética Conservada	*Paracoccidioides*/PAAG_04190.1	1e-102	19	49
	Proteína Hipotética Conservada	*Paracoccidioides*/PABG_02511.1	1e-45	---	14
	Proteína Predita	*Paracoccidioides*/PADG_00817.1	1e-20	27	---
	Proteína Hipotética	*Paracoccidioides*/PAAG_07684.1	1e-40	32	1

[a]Categoria funcional – baseado no MIPS e GO;
[b]Número de acesso/descrição da proteína – número de acesso da proteína identificada no banco de dados do *Paracoccidioides*: (http://www.broadinstitute.org/annotation/genome/*Paracoccidioides*_brasiliensis/MultiHome.html);

3. DISCUSSÃO

O objetivo do trabalho foi identificar transcritos regulados em células leveduriformes de *Paracoccidioides* derivados de pulmão de animais infectados experimentalmente. A patogenicidade de microrganismos está relacionada com a complexa interação entre o patógeno e o hospedeiro. Esta interação é um processo dinâmico, envolvendo a capacidade do organismo em atravessar o epitélio, disseminar para diversos tecidos e resistir à defesa imune. Portanto, o sucesso da infecção requer uma rápida adaptação do patógeno através de mudanças na expressão de determinados repertórios gênicos requeridos frente mudanças no ambiente (Kumamoto, 2008).

Neste estudo foram identificados vários genes diferencialmente expressos em células leveduriformes de *Paracoccidioides* derivadas do pulmão de animais infectados. Quarenta e dois transcritos foram induzidos após 7 dias de infecção, enquanto trinta e um após 15 dias de infecção. Os transcritos identificados foram agrupados de acordo com suas categorias funcionais (MIPS). Algumas categorias funcionais observadas nas análises dos dados obtidos pelos ensaios de RDA são listadas e discutidas abaixo.

Controle transcricional

Entre os transcritos identificados, com maior abundância, relacionados com o processo de transcrição, destacam-se o fator de transcrição do tipo gata, fator de transcrição *CTF1B*, fator de transcrição do tipo CCCH e histona deacetilase. A família conservada de reguladores transcricionais que apresentam dedo de zinco, conhecidos como fatores-GATA asseguram a utilização eficiente de fontes de nitrogênio por fungos, fator importante para a virulência (Limjindaporn *et al.*, 2003; Liao *et al.*, 2008). Adicionalmente, o gene *GLN3* codificante para um fator de transcrição do tipo GATA de *Pichia pastoris*, é fator responsável pelo controle do sistema de captação de ferro deste fungo (Miele *et al.*, 2007). Genes envolvidos com o controle trancricional, tais como C_2H_2, fatores-GATA e *CTF1B*, foram encontrados induzidos durante ensaios *in vitro* de ligação de *Paracoccidioides* a fibronectina (Bailão *et al*., 2012).

Os fatores de transcrição *SEB1* (C_2H_2) e *STEA* foram induzidos em *Paracoccidioides* em condições de infecção no pulmão (Fig 5). Esses genes são induzidos em *Schizosaccharomyces pombe*, *Trichoderma atroviride* em resposta ao estresse osmótico (Sansó *et al*., 2008; Peterbauer *et al*., 2002) e em resposta a estresse hidrostático em *S. pombe* (George *et al*., 2007). Além disso, o fator de transcrição ctf1B está envolvido na regulação de genes codificantes de proteínas da β-oxidação e

biogênese peroxissomal, sendo essencial à virulência em diversos patógenos, incluindo *C. albicans* (Ramírez and Lorez, 2009). O fator de transcrição histona deacetilase (Rpd3) é conhecido por se ligar a diferentes promotores sobre condições variadas, tais como choque térmico e tratamento com o antibiótico rapamicina (Kurdistani *et al*., 2003; Robert *et al.,* 2004). Histona deacetilase é requerida para ativação de genes envolvidos em estresse osmótico (Proft and Struhl, 2002; De Nadal *et al*., 2004; Alejandro-Osorio *et al*., 2009), genes induzidos por galactose (Wang *et al*., 2002), genes induzidos durante danos causados ao DNA (Sharma *et al*., 2007) e genes codificantes para manoproteínas de parede celular (Sertil *et al*., 2007). Pode-se observar um aumento da freqüência do transcrito da histona deacetilase *RPD3* ao longo do tempo de infecção (Tabela 2) sugerindo que *Paracoccidioides* poderia responder ao ambiente do hospedeiro por remodelagem da cromatina, regulando processos metabólicos necessários a adaptação do fungo nessa condição.

Metabolismo

Durante a infecção, nutrientes com glucose e aminoácidos não estão facilmente disponíveis, portanto os fungos patogênicos devem devem flexibilizar seu metabolismo para serem capazes de sobreviver de adaptar no interior do hospedeiro (Fleck *et al*., 2011).

Através das análises subtrativas de cDNA-RDA observou-se abundância de ESTs codificando para proteínas relacionadas com o metabolismo de aminoácidos, β-oxidação e ciclo do glioxalato (Tabela 2). O gene codificante para betaína aldeído desidrogenase foi induzido em *Paracoccidioides* durante a infecção em pulmão, tanto em condições *in vitro* quanto *in vivo*. Em *Pseudomonas aeruginosa*, a atividade dessa enzima é crucial para o crescimento durante infecção, estresse osmótico, bem como na presença de colina ou precursores (Velasco-Garcia *et al*., 1999; Brocker *et al*., 2010). Betaína (N, N, N-trimetil glicina) é um composto amônio quaternário anfotérico, produzido durante os passos de oxidação da colina, reação catalisada pela colina monooxigenase (Cmo) e betaína aldeído desidrogenase (Badh) (Boch *et al*., 1994; Vijaranakul *et al*. 1997; Weretilnyk and Hanson, 1990; Landfald and Strom, 1986). Betaína é um importante osmoprotetor presente em bactérias, fungos, cianobactérias, algas, animais e várias famílias de plantas (Rhodes and Hanson, 1993), atuando na estabilização de estruturas e atividades de complexos enzimáticos e de proteínas, mantendo a integridade de membranas contra os efeitos danosos do excesso de sal e temperatura (Hayashi *et al*., 1998; Alia *et al*., 1998; Chen *et al*., 2000). Nas análises do

cDNA-RDA de *Paracoccidioides* durante adesão *in vitro* a fibronectina o transcrito codificante para esta proteína foi encontrado induzido (Bailão *et al*., 2012). A betaína aldeído desidrogenase também está envolvida do equilíbrio redox através da utilização do aldeído. O aldeído é o produto final da oxidação de lipídios. A oxidação do aldeído pela *Badh* produz NADH e consequentemente pode promover o equilíbrio redox. Esta estratégia adaptativa é inerente em muitos processos de infecção incluindo infecção do baço por *M. tuberculosis* (Shin *et al*., 2011).

O gene codificante para S-adenosilmetionina sintase apresentou alta freqüência em *Paracoccidioides* recuperado do pulmão tanto em 7 quanto em 15 dias de infecção. Esta proteína catalisa a conversão de metionina em S-adenosilmetionina, sendo este produto o principal doador de grupos metil, em reações essenciais para todos os organismos. Genes envolvidos no metabolismo de metionina são importantes para o desenvolvimento de infecções. Em *Helicobacter pylori*, S-adenosilmetionina sintase é um dos importantes fatores de virulência responsáveis por exacerbar a severidade da infecção levando ao desenvolvimento de câncer gástrico (Lin *et al*., 2006). A enzima S-adenosilmetionina sintase está envolvida na síntese dos cofatores tetrahidrofolato e indica um metabolismo ativo de compostos nitrogenados durante a infecção no pulmão.

A síntese protéica foi um dos processos apresentando transcritos induzidos em *Paracoccidioides* recuperado do pulmão de camundongos infectados. Os transcritos encontrados foram o fator de elongação da tradução, subunidade 1-gama (*eEF-1γ*), e fator de iniciação da tradução, subunidade 4A (*eIF-4A*). A expressão de genes que compõem a maquinaria de síntese protéica pode refletir a adaptação molecular a uma nova condição celular. Resultados similares foram descritos para o fungo patogênico *C. albicans* (Fradin *et al.,* 2003), na incubação de *Paracoccidioides* com sangue e plasma humanos (Bailão *et al*, 2006, 2007) e *Paracoccidioides* derivado do fígado de animais infectados (Costa *et al*., 2007).

Outra condição de limitação nutricional encontrada por organismos patogênicos durante a infecção consiste na privação de carbono. Como observado em outros fungos, *Paracoccidioides* regula suas vias metabólicas para obtenção de carbono durante a infecção: β-oxidação, ciclo do glioxalato e gliconeogênese (Bailão *et al*., 2006, 2007; Costa 2007; Peres da Silva *et al*., 2011). O aumento na expressão de enzimas da β-oxidação durante a infecção foi descrito para outros microrganismos patogênicos (Strijbis and Distel, 2010; Farhana *et al*., 2010; Shin *et al*., 2011).Um intermediário dessas vias alternativas é acetil-CoA, molécula que pode ser produzida pelo

metabolismo de etanol, ácido-graxos e alguns aminoácidos, sendo requerida para os ciclos do glioxalato e ácido tricarboxílico. Estas vias metabólicas são compartimentalizadas nas células fúngicas entre os peroxissomos, mitocôndrias e citoplasma, necessitando do transporte intracelular de acetil-CoA que é facilitado pela carnitina acetil transferase. A identificação de ESTs para as proteínas acil-CoA desidrogenase, isocitrato liase, carnitina acetil transferase e o transportador mitocondrial succinato-fumarato sugere que *Paracoccidioides* direcione seu metabolismo para obtenção e captação de fontes alternativas de carbono para sobrevivência no hospedeiro. Em *Mycobacterium avium* foi observado que a proteína acil-Coa desidrogenase é induzida quando no interior de macrófagos e que ela é importante para o metabolismo de ácidos graxos e para a sua adaptação nestas condições (Brunori *et al*., 2004). Esta enzima também foi encontrada como sendo importante para o desenvolvimento de *M. tuberculosis* durante a infecção por estar envolvida no metabolismo de colesterol do hospedeiro (Thomas *et al*., 2011).

A isocitrato liase é uma enzima do ciclo do glioxalato e converte isocitrato em succinato e glioxalato e é importante para a patogenicidade de vários fungos (Dunn *et al*., 2009; Padilla-Guerrero *et al.,* 2011). Análises por northern blot revelaram que a enzima de *C. albicans* é induzida quando o fungo está na presença de macrófagos (Lorenz and Fink, 2001; Prigneau *et al*., 2003) e neutrófilos humanos (Fradin *et al*., 2005). Superexpressão do gene codificante da isocitrato liase também foi observada em *Paracoccidioides* durante infecção no pulmão (Tabela 2 e Fig 5). Análises por RT-PCR demonstraram que o transcrito é induzido durante a fagocitose por macrófagos murinos (Derengowski *et al*., 2008). Estudos sugerem que o ciclo do glioxalato está envolvido na virulência de *Penicillium marneffei*. Experimentos de northern blot demonstraram que após a internalização de conídios há um aumento de expressão do gene codificante da isocitrato liase, sugerindo uma potencial função deste ciclo na adaptação do patógeno no interior de macrófagos (Thirach *et al.*, 2008)**.** Durante infecção crônica por *Mycobacterium tuberculosis* a glicólise é diminuída e o ciclo do glioxalato é aumentado para permitir a manutenção anaplerótica do ciclo do ácido tricarboxílico e assimilação de carbono via gliconeogênese (Wheeller and Ratledge, 1988; Sharma *et al*., 2000).

Sob condições de hipóxia, estresse nitrosativo e outras condições de estresse, *M. tuberculosis* pode sintetizar e estocar triacilgliceróis como reserva de energia (Sirakova *et al*., 2006). A diacilglicerol aciltransferase, está envolvida na transferência de grupamentos acil para um esqueleto de glicerol formando assim os triacilgliceróis (Shi

and Cheng., 2009). Além do transcrito codificante para esta enzima, pôde-se também identificar o transcrito para uma fosfolipase D. Em células eucarióticas a fosfolipase D está envolvida em vários processos celulares, tais como secreção celular, transporte de proteínas através da membrana celular, crescimento celular polarizado, remodelamento do citoesqueleto, metabolismo de lipídios (Ktistakis *et al*., 2003; McDermott *et al*., 2004; Jenkins and Frohman, 2005; Roth, 2008; Mendonsa and Engebrecht, 2009; Harkins *et al*., 2010). Esta enzima está relacionada à conversão de fosfatidilcolina ou fosfatidiletanolamina em diacilglicerol-3-fosfato que poderia também ser convertido em triacilglicerol, sugerindo que os triacilgliceróis poderiam ser utilizados como fonte de energia para crescimento do *Paracoccidioides* no pulmão. Nessa reação metabólica há também a produção de colina que pode estar sendo utilizada por *Paracoccidioides* como fonte alternativa de carbono e nitrogênio. Pôde-se ainda observar que a expressão o transcrito para fosfolipase D aumentou no decorrer da infecção, sugerindo que a síntese de triacilgliceróis seria uma alternativa de *Paracoccidioides* para garantir a sua sobrevivência durante a fase de persistência da infecção. Em *M. tuberculosis* a diacilglicerol aciltranferase tem uma importante função na formação de estoques de lipídios que é uma característica importante para manutenção e persistência da tuberculose (Elamin *et al*., 2011)

A indução do transcrito codificando a enzima elongase de ácido-graxo em 7 dias de infecção corrobora também a sugestão de que a biossíntese de lipídios pode ser induzida durante infecção, o que poderia estar relacionada com formação de moléculas de reserva energética ou lipídios estruturais de membranas celulares.

A via das pentoses fosfato é uma via alternativa de oxidação de glicose. Ela não requer oxigênio e não produz ATP, está presente no citosol de todas as células e tem duas principais funções: (1) produção de NADPH, o qual é utilizado como agente redutor em muitas vias biossintéticas e que é também importante na proteção contra danos oxidativos, e (2) síntese de ribose 5-fosfato que é utilizado na síntese de nucleotídeos e ácidos nucléicos (Wamelink *et al*., 2008). O NADPH é uma molécula de grande importância na proteção de células contra danos causados por ROS (Pocsi *et al*., 2004; Muller, 2004) e é também utilizado em muitas vias anabólicas, tais como síntese de lipídios e elongação de ácidos graxos (Pollak *et al*., 2007). Uma das enzimas chaves dessa via é a transaldolase, que é induzida em *Cryptococcus neoformans* em resposta ao estresse nitrosativo (Missall *et al*., 2006). Em *M. avium* esta enzima faz parte de um complexo que foi encontrado exclusivamente em modelos murinos durante a infecção

por este fungo, sendo, portanto um importante alvo para diagnóstico da doença (Gupta *et al*., 2011). Em *Paracoccidioides* o transcrito codificante para a transaldolase também é induzido quando o fungo é incubado com sangue e plasma humanos (Bailão *et al*., 2006 e 2007).

Trealose é um dissacarídeo não-redutor que consiste de duas unidades de glicose (α-D-glicopiranosil-1,1-α-D-glicopiranosideo), sendo amplamente distribuída em uma variedade de organismos, tais como bactérias, fungos, assim como em insetos e outros invertebrados (Elbein *et al*., 2003). Em fungos, a trealose desempenha função na tolerância aos estresses osmótico (Hounsa *et al*., 1998), oxidativo (Gónzalez-Párraga *et al*., 2010) e térmico (Hottiger *et al.*, 1987), assim como na resposta de mamíferos a hipóxia (Chen and Haddad, 2004). Em fungos, a hidrólise da trealose é o principal evento durante o início da germinação, e presumivelmente, serve como uma fonte para síntese de carboidratos para obtenção de energia (Thevelein, 1984, Rosseau *et al.,* 1972). A principal via pela qual a trealose é sintetizada em microrganismos envolve a trealose fosfatase (Iordachescu and Imai, 2008). Em *Paracoccidioides*, o transcrito codificante para trealose fosfatase foi induzido, sugerindo que o fungo possa estar produzindo trealose, provavelmente como fonte de energia. A regulação da via de biossíntese desse dissacarídeo é importante para a patogenicidade de diversos fungos (Petzold *et al*., 2006; Maidan *et al*., 2008). Em *C. neoformans* a trealose é importante para a sobrevivência por conferir ao fungo resistência ao estresse térmico e osmótico encontrado no hospedeiro (Himmelreich *et al*., 2002; Steen *et al*., 2003). Em *A. fumigatus* a trealose fosfatase foi descrita como sendo importante para integridade da parede celular, pelo fato de a trealose conferir estabilidade a parede e por estar envolvida na sua biossíntese (Puttikamonkul *et al*., 2010). Este transcrito também foi induzido em *Paracoccidioides* recuperado do fígado de animais infectados (Costa *et al*., 2007), mais uma vez sugerindo a importância da trealose durante o processo infectivo.

Facilitadores de transporte

Houve também um aumento de transcritos de genes codificantes para facilitadores de transporte que participam na obtenção de nutrientes. O transportador succinato-fumarato interconecta a produção de succinato no citosol, pelo ciclo do glioxalato, com o ciclo do ácido tricarboxílico na mitocôndria. O fumarato exportado para o citosol pelo transportador succinato-fumarato é convertido em malato e posteriormente em oxalacetato (Palmieri *et al*., 2000). Em 15 dias de infecção pode-se observar uma alta freqüência do transcrito codificante para uma permease de aminoácidos dicarboxílicos

(*DIP5*) sugerindo um aumento no transporte e captação de aminoácidos neste órgão. Esse resultado foi corroborado pelas análises de qRT-PCR em *Paracoccidioides* derivado diretamente de pulmões infectados. O transcrito codificante para esta permease foi também induzido durante infecção de *C. albicans* em rins de mamíferos (Walker *et al*., 2009). A permease de aminoácido ácido (Dip5p) pode mediar a captação de glutamato e aspartato (Regenberg *et al.,* 1998). O glutamato seria substrato para glutamina sintase e, consequentemente, poderia estar relacionado com a deposição de quitina e a um remodelamento da parede do fungo *Paracoccidioides*. Neste sentido, a alta expressão do gene codificante desta permease estaria relacionada com a captação deste aminoácido no ambiente pulmonar. Este transcrito também foi induzido em *Paracoccidioides* incubado com plasma humano (Bailão *et al*., 2007).

A superfamília de transportadores MFS está envolvida com o transporte ativo de vários substratos e exibem especificidade por açúcares, polióis, drogas, metabólitos do ciclo do ácido tricarboxílico, aminoácidos, sideróforos, nucleosídeos, íons e outros (Pao *et al*., 1998; Paulsen *et al*., 1998). A expressão deste transportador durante a infecção no pulmão pode estar relacionado à captação de nutrientes pelo fungo neste órgão.

Defesa celular/Virulência

Durante os processos de infecção organismos patogênicos são confrontados com diversas condições, que buscam eliminá-los do hospedeiro e controlar o processo infeccioso. Assim, como resposta adaptativa, moléculas de defesa celular relacionadas com a resposta ao estresse oxidativo, nitrosativo, térmico e nutricional apresentam um aumento de expressão em patógenos, sendo caracterizadas como importantes fatores de virulência. Neste trabalho se observou a superexpressão do transcrito codificante da Hsp60 de *Paracoccidioides*. A Hsp60 é uma chaperona mitocondrial, homóloga a chaperona GroEL de *Escherichia coli* (Bukau and Horwich, 1998), que está envolvida na resposta celular a vários tipos de estresses, incluidndo o estresse oxidativo (Cabiscol *et al.,* 2002). Tem sido observado que células que apresentam altos níveis de Hsp60 são mais resistentes a agentes oxidativos como H_2O_2 e menadiona. A indução do transcrito codificante da Hsp60 em *Paracoccidioides* exposto a radicais oxidativos produzidos por macrófagos, pode ter função protetora similar (Tavares *et al.*, 2007). O transcrito codificante para a proteína responsiva ao estresse Ish1 também foi identificado tanto em 7 quanto em 15 dias de infecção. Essa proteína de envelope nuclear, caracterizada principalmente em fungos, mostra-se induzida em condições limitantes de glicose e nitrogênio e durante estresse osmótico (Taricani *et al*., 2002).

Muitas evidências sugerem que proteases são requeridas para o sucesso de invasão nos tecidos do hospedeiro por patógenos e para nutrição destes organismos nestes ambientes hostis. Serina protease de *Bacillus subtilis* facilita a captação de ferro da molécula transferrina através da clivagem da proteína (Park *et al.,* 2006). Complementando, a incubação de *A. fumigatus* em meio contendo soro humano estimula a secreção de proteases, sendo a atividade de serina proteases a classe enzimática com a maior atividade (Gifford *et al.*, 2002). Estudos em *Paracoccidioides* mostraram que uma serina proteinase extracelular cliva, *in vitro*, componentes de membrana basal, sendo, portanto, relevante no processo de disseminação do fungo (Puccia *et al.*, 1999). Também em *Paracoccidioides*, Parente e colaboradores (2010) demonstraram que Pbser foi induzida durante deprivação de nitrogênio e em leveduras do fungo durante infecção de macrófagos. Além disso, foi demonstrado que a proteína serino protease pode estar envolvida no enovelamento e endereçamento de proteínas e na reorganização do citoesqueleto (Parente *et al*., 2010). Nishikaku *et al*., (2009) e Bailão *et al* (2007) demonstraram que metaloproteinases são induzidas durante modelos de paracoccidioidomicose experimental, sendo importantes para disseminação fúngica. Portanto, a identificação de ESTs de genes codificantes para serina proteinases nas análises subtrativas de infecção no pulmão corrobora o papel destas moléculas na progressão do processo infeccioso por *Paracoccidioides*. Este transcrito também foi induzido no fungo derivado diretamente do pulmão infectado. A identificação destas proteases, associadas à presença de transportadores de peptídeos e aminoácidos nesse modelo, sugere que o fungo esteja reorganizando as funções de aquisição e assimilação de moléculas para utilizar os nutrientes disponíveis nesse nicho, característica esta também observada em *C. albicans* durante a fagocitose (Lorenz *et al*., 2004).

Comunicação Celular/Transdução de sinal

Muitos dos processos celulares básicos que permitem a sobrevivência de patógenos em seus hospedeiros são controlados por vias de transdução de sinal. Estes processos são regulados por cascatas, com mecanismos de controle, incluindo várias proteínas ativadoras e inibidoras. Um sincronismo da sinalização celular leva a uma regulação morfológica, favorecendo a sobrevivência de organismos patogênicos no interior de hospedeiros infectados. Durante o processo de infecção foram identificados genes envolvidos em vias de transdução de sinais tais como MAPK e serina/treonina quinase. Esta última foi descrita como estando envolvida no controle do ciclo celular

por regulação da fosfatase Cdc25p em resposta ao estresse em *S. pombe* (López-Avilés *et al*., 2005).

Outro transcrito encontrado induzido durante a infecção foi o codificante para arginina N-metiltranferase. Este gene pode estar relacionado à ligação de *Paracoccidoides* ao colágeno e à fibronecticna, durante a adesão no processo de infecção (Bailão *et al*., 2012).

Um homólogo de gene codificante para proteína da superfamília PAS (Per-Arnt-Sim) que desempenha papéis em processos de sinalização, detecção de estímulos e pode também mediar interações proteína-proteína (Taylor and Zhulin, 1999) foi induzido durante a infecção no pulmão. Tal fato suporta o papel predito destas proteínas como sensores na percepção das diferentes condições encontradas por *Paracoccidioides* durante o processo infectivo.

Divisão celular

A proteína Mpv17p compartilha considerável identidade com uma proteína de membrana peroxissomal de mamíferos (Pmp22p). Em mamíferos a Mpv17p têm a função de regular a produção de ROS (Reuter *et al*., 1998). O transcrito para esta proteína foi induzido durante a infecção no pulmão. Em *S. cerevisae* foi encontrada uma proteína homóloga da Mpv17p inserida na membrana mitocondrial. Nesse organismo ela tem a função de resposta ao estresse por choque térmico e metabolismo de etanol (Trott and Morano, 2004).

4. CONCLUSÕES

Várias vias metabólicas foram induzidas durante o processo infectivo no pulmão, com destaque para metabolismo de lipídios, ácidos graxos e isoprenóides, metabolismo de aminoácidos, resposta ao estresse e virulência e metabolismo de carboidratos. Estas vias são descritas como induzidas em outros patógenos durante a infecção. Isso pode indicar que *Paracoccidioides* está regulando o seu metabolismo em resposta a interação patógeno-hospedeiro e às condições adversas encontradas durante a infecção.

5. PERSPECTIVAS

- Comparação da resposta obtida pela infecção no pulmão com outros sítios no hospedeiro utilizando-se tecnologias de alto desempenho;

- Comparar os perfis transcricionais de células leveduriformes de diferentes membros do complexo *Paracoccidioides,* pós infecção.
- Análise proteômica de células leveduriformes de *Paracoccidioides* derivadas de pulmão de modelos experimentais;
- Avaliação da relação transcrito/proteína de *Paracoccidioides* durante infecção no pulmão.
- Análises bioquímicas de enzimas chave de processos metabólicos encontradas induzidas durante a infecção no pulmão através de ensaios enzimáticos

Capítulo 4

Produção Científica Durante o Doutorado

1. MANUSCRITO

Important Message: You have 45 days remaining to complete the consolidation process. **Click here to consolidate.**

Submissions Being Processed for Author Celia Maria De Almeida Soares

Page: 1 of 1 (1 total submissions) Display 10 results per page.

Action	Manuscript Number	Title	Initial Date Submitted	Status Date	Current Status
View Submission View QC Results Send E-mail		A proteomic view of Paracoccidioides yeast cells during zinc deprivation	05 Dec 2012	05 Dec 2012	Submitted to Journal

Page: 1 of 1 (1 total submissions) Display 10 results per page.

<< Author Main Menu

A proteomic view of *Paracoccidioides* yeast cells during zinc deprivation

Kelly Pacheco de Castro[a,b]; Tereza Cristina Vieira de Rezende[a]; Ana Flávia Alves Parente[a]; Alexandre Melo Bailão[a]; Juliana Alves Parente[a]; Clayton Luiz Borges[a]; Luciano Paulino Silva[c] ; Célia Maria de Almeida Soares[a,*]

[a]Laboratório de Biologia Molecular, Instituto de Ciências Biológicas, Universidade Federal de Goiás, Goiânia, Goiás, Brazil.

[b] Programa de Pós Graduação em Patologia Molecular, Faculdade de Medicina, Universidade de Brasília, Brasília, Distrito Federal, Brazil.

[c] Laboratório de Espectrometria de Massa, Centro Nacional de Pesquisa de Recursos Genéticos e Biotecnologia, Empresa Brasileira de Pesquisa Agropecuária, Brasília, Distrito Federal, Brazil.

* Corresponding author: C. M. A. Soares, Laboratório de Biologia Molecular, ICB II, Campus II, Universidade Federal de Goiás, 74001-970, Goiânia-Goiás, Brazil. Tel/fax: 55-62-3521-1110. e-mail: cmasoares@gmail.com

Abstract

Zinc plays a critical role in a diverse array of biochemical processes. However, excess of zinc is deleterious to cells. Therefore, cells require finely tuned homeostatic mechanisms to balance uptake and storage of zinc. There is increasing evidence for the importance of zinc during infection. In order to better understand how *Paracoccidioides* adapts to zinc deprivation we compared the two-dimensional (2D) gel protein profile of yeast cells during zinc starvation to that of zinc rich condition. Protein spots were selected for comparative analysis based on the protein staining intensity as determined by image analysis. A total of 423 out of 845 protein spots were determined to have changed significantly in abundance due to zinc depletion. A correlation between protein and transcript levels was also discovered using quantitative RT-qPCR analysis from RNA of *Paracoccidioides* under zinc restricting conditions. According to proteomic data, *Paracoccidioides* may experience a stress when in zinc-deficient condition, as suggested by the up regulation of a number of proteins related to stress response, cell rescue and virulence. Other process induced by zinc deprivation seems to be gluconeogenesis. On the other hand the methylcitrate cycle seems to be downregulated. Overall the results indicate a remodeling of *Paracoccidioides* response to a probable oxidative stress induced during zinc deprivation.

Keywords: *Paracoccidioides*, zinc deprivation, proteomic analysis

1. Introduction

Zinc is an essential nutrient because it is a required cofactor for many enzymes and transcription factors and like other metals, it is both vital in trace amounts and toxic at high concentrations (Finney and O'Halloran 2003). Zinc homeostasis is maintained by transcriptional and posttranslational homeostatic regulatory mechanisms (Eide 2003; Lyons *et al*. 2000). In *Saccharomyces cerevisiae*, the best studied organism for zinc homeostasis, the uptake of this micronutrient is mediated by two systems; a high-affinity system, that is active in zinc-limited conditions (Zhao and Eide 1996a) and a lower affinity uptake system, that is not highly regulated by zinc concentrations (Zhao and Eide 1996b). The expression of the high-affinity zinc transporter Zrt1p and the low-affinity zinc transporter Zrt2p is regulated by the transcription factor Zap1p, which plays a central role in zinc homeostasis (Zhao and Eide 1997). *ZAP1* encodes a transcriptional activator with seven carboxy-terminal C_2H_2 zinc finger domains and two amino terminal activation domains. Rutherford and Bird (2004), reported that under conditions of limited zinc in *S. cerevisiae* Zap1p induces the expression of genes coding for the transporters Zrt1p and Zrt2p. A second mechanism in *S. cerevisiae* regulates zinc transporter activity at a post-translational level. In zinc-limited cells, Zrt1p is a stable plasma membrane protein. Exposure to high levels of extracellular zinc triggers a rapid loss of Zrt1p uptake activity and protein. This inactivation occurs through zinc-induced endocytosis of the protein and its subsequent degradation in the vacuole (Gitan *et al*. 1998).

Aspergillus fumigatus presents three genes encoding for zinc transporters, belonging to the ZIP family, whose expression is regulated by both pH and the environmental concentration of zinc (Amich *et al*. 2010). The *ZRFA* and *ZRFB* genes of *A. fumigatus* are transcribed at higher levels and are required for fungal growth under acidic zinc-limiting conditions whereas they are dispensable for growth in neutral or alkaline zinc-limited media (Amich *et al*. 2009; Amich *et al*. 2010). The transporter for the zinc uptake system that functions in *A. fumigatus* growing in neutral or alkaline environments is encoded by *ZRFC* (Amich *et al*. 2010). It seems that ZrfBp represents a high-affinity zinc permease, since the cognate transcript was down regulated in high zinc condition (Vicentefranqueira *et al*. 2005).

Paracoccidioides, a complex of several phylogenetic species (Carrero *et al*. 2008; Matute *et al*. 2006; Teixeira *et al*. 2009), is the causative agent of paracoccidioidomycosis (PCM), a human systemic mycosis, prevalent in South America (Restrepo *et al*. 2001). The fungus is thermo dimorphic, that is, it grows as a yeast-like form in host tissues or when cultured at 35 - 37 ºC, and as mycelium in saprobe condition or when cultured at room temperature (Brummer 1993). After penetrating the host, *Paracoccidioides* differentiates into the yeast form, a fundamental step for the successful establishment of the disease (San-Blas *et al*. 2002). Temperature-dependent cellular differentiation to the parasitic yeast cell takes place in the lungs. From the primary pulmonary infection site, the fungus eventually disseminates to other organs by hematogenic and/or lymphatic routes (Brummer 1993).

Scrutiny of the *Paracoccidioides* genome at (http://www.broad.mit.edu/annotation/genome/*Paracoccidioides*_brasiliensis/MultiHome.html) revealed that it actually has orthologues to zinc transporters described in *S. cerevisiae* that are localized in the plasmatic, vacuolar and endoplasmic reticulum membranes (Silva *et al*. 2011). Importantly, genes encoding to zinc transporters of the ZIP family, with homology to *S. cerevisiae* Zrt1p or Zrt2p, are present in the *Paracoccidioides* genomic database (Silva *et al*. 2011), whose transcripts could be addressed by transcriptional analysis of *Paracoccidioides* yeast cells after incubation in human blood and plasma (Bailão *et al*. 2006, 2007). *Paracoccidioides* isolate Pb01 has two vacuolar membrane zinc transporters, encoded by the *ZRC1* and *COT1* genes, whereas isolates Pb03 and Pb18 contain only the *COT1* homolog. An orthologue to the transcription factor Zap1p of *S. cerevisiae* is also present in the three *Paracoccidioides* isolates. Therefore, zinc assimilation in *Paracoccidioides* may be similar to that of *S. cerevisiae* (Silva *et al*. 2011). The *ZRT2* transcript, but not *ZRT1*, was highly expressed in neutral to alkaline pH during zinc depletion, as observed to the A. *fumigatus ZRFC*, suggesting that expression of this gene may be regulated by both zinc and pH in *Paracoccidioides* (Bailão *et al*. 2012).

Studies have shown that zinc is an essential micronutrient for the proliferation of pathogenic fungi. In this way, it has been demonstrated that zinc deprivation is a host defense mechanism utilized by macrophages during *Histoplasma capsulatum* infection (Winters *et al*. 2010). It was demonstrated that GM-CSF activated macrophages reduce

intracellular zinc concentration upon *H. capsulatum* infection in order to kill the pathogen (Winters *et al*. 2010). A novel zinc acquisition system was described in *Candida albicans* during endothelial cell invasion. Analogous to siderophore-mediated iron acquisition, *C. albicans* utilizes an extracellular zinc scavenger for acquiring this essential metal. The system is composed of a secreted protein encoded by the gene *PRA1* and a transporter encoded by *ZRT*: *C. albicans* secretes the scavenger protein (a ‘‘zincophore’’), Pra1p. This component binds host cellular zinc. Pra1p then reassociates with the fungal cell via a membrane transporter (Zrt1p) to deliver its zinc load. Deletion of *PRA1* prevented utilization of host zinc and damage of host cells in the absence of exogenous zinc (Citiulo *et al*. 2012). In *Cryptococcus gattii* the zinc finger protein Zap1p, induced by zinc deprivation, was functionally characterized. Inactivation of *ZAP1* compromises the growth of the fungus under zinc limited conditions and reduces *C. gattii* virulence in a murine model of cryptococcosis infection (Schneider *et al.* 2012).

Due to the relevance of micronutrients to fungal homeostasis and pathogenesis, our group had previously employed proteomic approaches to study the *Paracoccidioides* response to metals starvation. Parente *et al*. (2011) demonstrated that iron deprivation promotes an increase in the amount of proteins of the glycolytic pathway, while the proteins of the tricarboxylic acid, glyoxylate and methylcitrate cycles, and electron transport chain decreased in abundance under iron limiting conditions. These data suggest a remodeling of *Paracoccidioides* metabolism by prioritizing iron independent pathways. To address the question of what proteins and processes are important for *Paracoccidioides* in a zinc-limited condition, we utilized 2D gel electrophoresis coupled to mass spectrometry to identify proteins sensitive to low zinc levels. We discovered 423 differentially regulated proteins/spots and from those, 157 were identified. From the analyzed proteins 55 were induced and 56 were repressed in response to zinc starvation, rendering an integrated view of metabolic and cellular processes reorganization during zinc deprivation. A view of the metabolic cell shape, as determined by proteomics, reflected a shift in the cells metabolism during zinc deprivation, as suggested by the increase in oxidative stress response, gluconeogenesis and repression of methylcitrate cycle.

2. Materials and methods

2.1. *Paracoccidioides* isolate and growth conditions

Paracoccidioides, *Pb* 01 (ATCC MYA-826), was used in all experiments. The yeast phase was maintained in vitro by subculturing at 36 ^{o}C in Fava Netto's semisolid medium [1% (w/v) peptone, 0.5% (w/v) yeast extract, 0.3% (w/v) proteose peptone, 0.5% (w/v) beef extract, 0.5% (w/v) NaCl, 4% (w/v) glucose, 1.2% (w/v) agar, pH 7.2] every 7 days.

2.2. Zinc depletion experiments

For the experiments of intra and extracellular zinc depletion *Paracoccidioides* yeast cells were incubated in McVeigh/Morton medium (MMcM) (Restrepo and Jiménez 1980) in the presence and absence of zinc, as following. Zinc depleted medium was prepared without the addition of $ZnSO_4$ and supplemented with the zinc chelator N,N,N_,N_-tetrakis (2-pyridyl-methyl) ethylenediamine (TPEN 0.05 mM; Sigma Aldrich, Co., St. Louis, MO). Cultures were allowed to grow at 36 °C, 150 rpm, and the number of viable cells was determined at each specific time interval (1, 2, 3, 4, 6, 8 and 24 h) by counting living cells using trypan blue as vital dye. Viability results were used to determine the time of cells exposure to zinc starvation for proteomic assays.

To obtain protein extracts, yeast cells were prepared by inoculating 50 mL of Fava Netto's liquid medium with 10^8 cells/mL of *Paracoccidioides*. Cultures were maintained at 36 ^{o}C under gentle shaking for 72 h. Thereafter, the culture was centrifuged and the cells washed in sterile phosphate buffered saline solution 1 X (PBS; 1.4 mM KH_2PO_4, 8 mM Na_2HPO_4, 140 mM NaCl, 2.7 mM KCl; pH 7.3), and then resuspended in modified MMcM culture medium (Restrepo and Jiménez 1980) and maintained 18 h at 36 ºC under agitation. Cells were centrifuged at 5000 X *g* for 5 min and washed in PBS 1X. After, 2 x 10^6 cells were introduced into MMcM medium supplemented with zinc chelate-specific TPEN (Sigma Aldrich, Germany) at a concentration of 0.05 mM. The cultures were incubated for 6 and 24 h upon deprivation of zinc under gentle shaking at 36 ° C. For the control, yeast cells of *Paracoccidioides* were incubated in MMcM medium containing 0.03 mM of $ZnSO_4$, for 6 and 24 h. In

order to obtain RNA to quantitative RT-qPCR analysis, cells were incubated as described above for 3, 6 and 24 h.

2.3. Preparation of protein extracts

Yeast cells were collected at 6 and 24 h of zinc deprivation and submitted to total protein extraction. The cells were centrifuged at 10.000 X *g* for 15 min at 4 ºC and disrupted by vigorous mixing with glass beads in a solution containing 20 mM Tris-HCl, pH 8.8, 2 mM $CaCl_2$ (Fonseca CA *et al*. 2001) and a mixture of nuclease and protease inhibitors (serine, cysteine and calpain) (GE Healthcare, Uppsala, Sweden). After centrifugation the supernatant was collected and the protein concentrations were determined using the Bradford reagent (Sigma Aldrich), using bovine serum albumin (BSA) as a standard (Bradford 1976). The samples were stored in aliquots at - 80 ºC.

2.4. Two-dimensional gel electrophoresis

This experimental step was performed as previously described (Parente *et al*. 2011; Rezende *et al*. 2011). Briefly, protein samples (300 µg) were treated with 2-D Clean-up Kit (GE Healthcare) following the procedure recommended by the manufacturer. The precipitate was solubilized in a rehydration buffer {7 M urea, 2 M thiourea, 2% (w/v) [(3-cholamidopropyl)dimethylammonio]-1-propanesulfonate (CHAPS), 65mM dithiothreitol (DTT), 0.5% (v/v) ampholyte-containing buffer (IPG) and 0.001% (w/v) bromophenol blue]. This solution was then applied onto immobiline nonlinear Dry Strips pH 3–11 (13 cm long) (GE Healthcare). Subsequently, the IPG strips were rehydrated for 14 h (30 V) using the Ettan IPGphor III Isoelectric Focusing System (GE Healthcare). The isoelectric focusing was performed with a limiting current of 50 µA/strip under the following steps: 500 V for 1 h; 500–1000 V for 1 h; 1000–8000 V over 12 h and 30 min and 8000 V for 2 h and 30 min. IPG strips were reduced with 0.5% (w/v) DTT for 40 min by gentle agitation and then alkylated with 2.5% (w/v) iodoacetamide for 40 min by gentle agitation in the dark, in equilibration buffer [6 M urea, 0.5 M Tris–HCl, pH 8.8, 30% (v/v) glycerol, 2% (w/v) SDS and 0.001% (w/v) bromophenol blue]. The second dimension electrophoresis was performed in a Hoefer SE 600 electrophoresis (GE Healthcare) system at 15 °C at 100 V for 1 h, followed by 200 V until the indicator reached the bottom of the gel. Proteins were stained using

Coomassie brilliant blue (PlusOne Coomassie Tablets PhastGel Blue R-350, GE Healthcare) according to the manufacturer's instructions.

2.5. 2D-gel image analysis

Gel images were produced using the Image Scanner III (GE Healthcare). The relative determination of the spot volumes was performed with the Image Master Platinum 6.0 software (GE Healthcare). To refine automatic spot matching, mismatched spots were corrected manually. To compare the proteins with multiple isoforms, the sum of the percentage of the volumes, relative to the total protein, of each isoform was first obtained in triplicate. The sum of the percentage of volumes for the proteins was used for statistical analysis, which was performed to determine the significant differences in expression profiles. One-way ANOVA (Statistics software version 7.0 Statsoft Inc. 2005) was used to compare the differences in the mean spot volume. Differentially accumulated proteins with $p \leq 0.05$ were considered statistically significant and were selected to mass spectrometry analysis.

2.6. In-gel digestion

This experimental step was performed as previously described (Parente *et al*. 2011; Rezende *et al*. 2011). Briefly, protein spots were manually excised from the 2D-gel. The gel pieces were dehydrated in acetonitrile (ACN) and dried in a speed vacuum. The gel pieces were then reduced (10 mM DTT) and alkylated (55 mM iodoacetamide). The supernatant was removed, and gel pieces were dehydrated with solution containing 25 mM ammonium bicarbonate/50% (v/v) ACN solution. The gel pieces were dried, and a 10ng/μL trypsin solution (sequencing grade modified trypsin, Promega, Madison, WI, USA) was added, followed by rehydration on ice at 4 °C for 10 min. After the supernatant is removed, 25 mM ammonium bicarbonate solution was added to the gel pieces, followed by incubation at 37 °C for 16 h. After the digestion, the supernatant was placed into a clean tube. A solution containing ACN [50% (v/v)], trifluoroacetic acid (TFA) [5% (v/v)] was added to the gel pieces. The samples were mixed for 10 min, sonicated for 3 min and combined with the aqueous extraction above. The samples were dried in a speed vacuum, and the peptides were solubilized in water. Two microliters of each sample were delivered to a target plate and dried at room temperature.

Subsequently, the peptide mixtures were covered with 2 μL of MALDI matrix solution [10 ng/mL alphacyano-4-hydroxycinammic acid in 50% (v/v) ACN and 5% (v/v) TFA]. Concentration and purification steps were added by using a pipette tip with a bed of chromatographic media (ZipTips® C18 Pipette Tips, Milipore, Bedford, MA, USA) prior to mass spectrometry (MS).

2.7. Mass spectra analysis

MALDI-MS and MALDI- MS/MS were performed using a MALDI Synapt MS™ spectrometer (Waters-Micromass, Manchester, UK) and UltraFlex III MALDI-TOF/TOF mass spectrometer (Bruker, Bremen, Germany). All spectra were obtained in positive reflector mode. Mass spectrometric data analysis was performed using Masslynx 4.0 software (Waters-Micromass, Manchester, UK) and Flex Analysis (Bruker Daltonics version 2.4) softwares. Protein identification was performed as previously described (Rezende *et al*. 2011). Briefly, the monoisotopic peak lists were submitted using an in-house Mascot server (Version 2.1.04, Matrix Sciences, London, UK) to identify candidate proteins. For the MS data the following parameters were selected: only tryptic peptides with up to one missed cleavage site were allowed; carbamidomethylcysteine as a fixed modification and oxidized methionine as a variable modification. For the MS data, a mass tolerance of 25–100 ppm was used and 0.2-0.6 Da for MS/MS fragment ions. For both MS and MS/MS, only proteins with statistical significance ($p \leq 0.05$), as determined by the MASCOT algorithm, were accepted as a protein sequence match. The analysis by MS/MS confirmed the proteins identified on the basis of the PMFs, validating the identifications.

The ORF sequences of identified proteins were analyzed by using the Pedant-Pro Sequence Analysis Suite of Biomax GmbH (http://pedant.gsf.de.) and all identified proteins were categorized according Functional Catalogue (FunCat2).

2.8. RNA extraction, cDNA synthesis and RT-qPCR

These experiments were performed as previously described (Rezende *et al*. 2011). Briefly, the cells were disrupted by vigorous mixing with glass beads for 10 min in the presence of Trizol (GIBCO™Invitrogen Corporation) according to the manufacturer's instructions. The cDNAs were prepared using the high capacity RNA-to-

cDNA kit (Applied Biosystems, Foster City, CA, USA). Quantitative RT-PCR analysis was performed on a StepOnePlus™ real-time PCR system (Applied Biosystems, Foster City, CA, USA). PCR thermal cycling was performed at 40 cycles of 95°C for 15 s followed by 60°C for 1 min. The data were normalized with transcript encoding α-tubulin amplified in each set of qRT-PCR experiments. A nontemplate control was also included to elimate contamination or nonspecific reaction. Samples of each cDNA were pooled and serially diluted 1:5 to generate a relative standard curve. Relative expression levels of the genes of interest were calculated using the standard curve method for relative quantification (Bookout *et al*. 2006). The oligonucleotides used in the real-time PCR analyses are listed in Table S1 (see "Supplementary information").

3. Results

3.1. Expression of *Paracoccidioides* zinc acquisition genes during zinc starvation

To investigate the transcriptional profile of zinc responsive genes in *Paracoccidioides* we used real-time RT-qPCR. The analyzed genes included the *Paracoccidioides* orthologues to zinc transporters *ZRT11*and *ZRT2* (Fig 1 and Table S1, see "Supplementary information"). Although the two orthologues for zinc transporters were induced upon zinc deficiency from 3 h to 24 h treatments, a higher induction in expression was observed for *ZRT2* at 6 h and 24 h of zinc deprivation, with induction values higher than 20 fold (Fig 1). The zinc transporter ZRT1 presented 10 fold induction at 24 h of zinc deprivation. From these results, times of 6 h and 24 h were chosen for protein extraction and proteomic analyzes.

3.2. 2D-gel analysis of *Paracoccidioides* during zinc starvation

Using trypan blue staining it was observed that around 90% of the cells remained viable up to 24 h upon zinc deprivation (data not shown). Two-dimensional gel analysis was used to separate cytosolic fungal proteins while image analysis allowed for the quantification of proteins/isoforms. Three independent experiments generate three replicates which included: 6 h control, 6 h in zinc depletion 24 h control and 24 h in zinc depletion (Fig 2A-D, respectively).Using the gel image software a total of 845 spots were successfully matched between control yeast cells and zinc depletion

conditions (Fig 2 and Fig S1, see "Supplementary information"). Statistical analysis revealed that 127 and 296 proteins/isoforms were differentially accumulated in 6 and 24 h, respectively of zinc deprivation, yielding a total of 423 differentially regulated proteins/isoforms (Fig S1, see "Supplementary information").

3.3. Identification of zinc-regulated proteins

In order to determine the identities of the differentially regulated protein spots in-gel digestion using trypsin was performed followed by MS analysis. Mass spectrometry analysis followed by protein database sequence matching resulted in the identification of 157 differentially expressed proteins/isoforms (Fig 2, Fig S1 and Table S2, see "Supplementary information"). One hundred and twenty proteins/isoforms were identified by peptide mass fingerprinting (PMF) and confirmed by MS/MS analysis while 37 of protein/isoforms spots yielded identification by PMF. All the spots identified are depicted in Table S2 (see "Supplementary information"). GenBank general information identifiers (gi), PMF and MS/MS mascot scores, protein molecular mass, and isoelectric points (*pI*) of each spot are also listed in Table S2 (see "Supplementary information").

3.3.1. Proteins induced in zinc starvation conditions

Some proteins were detected in more than one spot. To further improve the understanding of the differentially regulated proteins and characterize global abundance of the proteins, composite expression profiles were generated by summing percentage of the volumes of all isoforms to each protein.

The categorization of the proteins preferentially expressed upon zinc depletion in comparison to the control condition allowed identifying a total of 55 proteins (Table 1). *Paracoccidioides* induced proteins were mainly those involved in cell rescue, defense and virulence, representing a total of 18 proteins, corresponding to 33% of the identified induced proteins (Fig. S2, see "Supplementary information"). In this functional category of induced proteins figure components of the antioxidant response such as thioredoxin, glutathione reductase, glutathione synthetase , disulfide isomerase, Y20 and mitochondrial peroxiredoxin, all induced upon 24 h of zinc deprivation, ranging in fold change from 1.58 to 3.17. Additionally, eleven proteins, belonging to the

heat shock protein family were over expressed, mainly following zinc limitation upon 24 h (Table 1).

Enzymes of gluconeogenesis including phosphoenolpyruvate carboxykinase, phosphoglycerate kinase, glyceraldehyde-3-phosphate dehydrogenase and fructose-bisphosphate aldolase were up regulated. The increased regulation was mainly at 24 h of zinc deprivation (Table 1). Enzymes of the metabolism of amino acids such as aspartate aminotransferase and delta-1-pyrroline-5-carboxylate dehydrogenase were induced at 24 h of zinc deprivation (Table 1).

It is summarized in Fig 3 some aspects of the metabolism presumed to be induced at 24 h of zinc deprivation, as suggested by proteomic analysis. Proline and arginine can be converted to glutamate by the action of the enzyme delta-1-pyrroline-5-carboxylate dehydrogenase. The formed glutamate can be used for the synthesis of glutathione through the action of the enzyme glutathione synthetase. The peroxiredoxin metabolizes hydrogen peroxide in a reaction in which residues in the enzyme molecule become oxidized, requiring thioredoxin to reduce the molecule back to the active state. Thioredoxin, in turn, requires thioredoxin reductase to be restored to its active, reduced state (Wu *et al*. 2009).

3.3.2. Proteins with decreased expression upon zinc deprivation

The categorization of the proteins repressed during zinc starvation allowed identifying a total of 56 proteins (Table 2), ranging in fold change from 1.17 to 7.93. At 6 h of zinc deprivation, some antioxidant proteins such as glutathione reductase, Y20 and peroxisomal catalase were repressed. It is important to note that glutathione reductase and Y20 were induced at 24 h, as described above. Three *Paracoccidioides* enzymes involved in the methylcitrate cycle were decreased in abundance following zinc restriction. These enzymes were aconitase, 2-methycitrate dehydratase and 2-methylcitrate synthase. Also, the enzyme alcohol dehydrogenase, involved in fermentation, was downregulated in yeast cells upon zinc deprivation (Table 2).

Enzymes of the amino acids metabolism were also decreased in abundance during zinc starvation, mainly those involved with metabolism of valine and isoleucine, such as the acetolactate synthase and methylmalonate-semialdehyde dehydrogenase (Table 2). This regulation occurs at 6 h of zinc deprivation.

The proteins acetyl-coA acetyltransferase, short chain dehydrogenase and peroxisomal multifunctional enzyme, related to lipid metabolism, were decreased in abundance during zinc deprivation.

3.4. The correlation between the proteomic and transcriptional data

In order to validate the significance of our proteomic results we next sought to determine if changes in protein levels could be correlated with changes in transcript levels. We determined that the differences observed in proteomic assay are in agreement with transcriptional findings, using quantitative RT-PCR to measure isocitrate lyase (*ICL*), citrate synthase (*CS*), peroxisomal catalase (*CATP*) and alcohol dehydrogenase (*ADH*), transcripts (Fig 4). Protein and transcript levels of *ADH* and *CATP* decreased during upon zinc limitation, as depicted in Fig 4 and Table 2. The *CS* and *ICL* transcript levels were increased and also correlated with protein levels (Fig 4 and Table 1).

4. Discussion

It is know that a component of the cellular response to zinc deprivation operates through the induction of a number of transcripts (Amich *et al*. 2010; Zhao and Eide 1996a; Zhao and Eide 1996b). Under zinc restriction it was observed the induction of *Paracoccidioides* orthologues for zinc dependent transcripts. The results obtained by RT-qPCR using cDNAs derived from yeast cells of *Paracoccidioides* grown in zinc deprived medium, demonstrated that gene expression of *PbZRT2* was over induced in cells grown upon zinc deprivation, suggesting that Zrt2p behaves as a high-affinity transporter. Bailão *et al*. (2012) demonstrated that the *ZRT2* transcript, but not *ZRT1*, was highly expressed in neutral to alkaline pH during zinc depletion, as observed to the A. *fumigatus ZRFC*, suggesting that expression of this gene may be regulated by both zinc and pH in *Paracoccidioides*.

We analyzed the proteome of *Paracoccidioides* yeast cell upon zinc deprivation. The proteome analysis resulted in the identification of 157 proteins. Out of those, 19 proteins were detected in more than one spot and 9 of them were observed in repressed and induced forms, at different times of zinc deprivation. The descriptions here presented, although not exhaustible, provide the first information of *Paracoccidioides*

behavior during zinc deprivation. Our results demonstrated the over expression of proteins related to stress response in zinc starvation conditions. Reactive oxygen species (ROS), including the superoxide anion, hydrogen peroxide (H_2O_2), and hydroxyl radical, can cause various types of biological damage. Zinc deficiency is associated with high steady-state levels of nitric oxide (NO) and H_2O_2 in rat adrenal medulla PC12 cells, H_2O_2 in human IMR-32 neuroblastoma cells (Mackenzie *et al*. 2006), and NO in the rat glioma C6 cells (Ho and Ames 2002). Additionally, studies both *in vitro* and *in vivo* have established that zinc deficiency leads to increased oxidative stress in mammalian cells (Wu *et al*. 2009). It was also demonstrated that yeast cells of *S. cerevisae* experience oxidative stress when grown under low zinc conditions (Wu *et al*. 2007). The *S. cerevisiae* Zap1p activates expression of the *TSA1* gene, encoding for a cytosolic peroxiredoxin, which metabolizes H_2O_2 (Rhee *et al*., 2005). Cysteine residues in Tsa1p become oxidized during this reaction and require thioredoxin to be reduced back to their active state. Thioredoxin, in turn, requires thioredoxin reductase to be restored to its active, reduced state (Wu *et al*. 2009). According to the proteomic analysis here presented, the proteins thioredoxin, glutathione reductase, peroxiredoxin and thioredoxin reductase were induced upon zinc deprivation strongly suggesting that *Paracoccidioides* experienced oxidative stress induced by zinc deprivation. Genes and proteins have been identified to be related to oxidative stress in *Paracoccidioides*: the activation of the antioxidant defense mediated by the enzymes catalase, superoxide dismutase (SOD), peroxiredoxin, cytochrome C peroxidase, glutathione and thioredoxin have been described, indicating that *Paracoccidioides* uses several antioxidant systems to combat ROS (Campos *et al*. 2005; Chagas *et al*. 2008; Dantas *et al*. 2008).

Molecular chaperones are conserved and abundant proteins that guard the conformational homeostasis of proteins (Hartl 1996). They maintain signaling, regulate proliferation, differentiation and apoptotic pathways (Sõti *et al*. 2005). Chaperones (or stress proteins) confer cytoprotection and assure survival upon various stresses. In this study 15 proteins of *Paracoccidioides*, including isoforms, belonging to the heat shock protein family were altered in abundance following zinc limitation. This result could be an indication of the involvement of chaperones in protecting the fungus of the stress generated by zinc deprivation.

Zinc deficiency leads to increased oxidative stress, as cited above. Under long term oxidative stress the fungi *Aspergillus niger* reduce the glucose uptake (Li *et al*. 2008). In this way, it has been observed that enzymes of the gluconeogenesis pathway, such as phosphoenolpyruvate carboxykinase and phosphoglycerate kinase were induced in response to the probable oxidative stress caused by zinc deprivation in *Paracoccidioides*.

Three *Paracoccidioides* enzymes involved in the methylcitrate cycle were decreased in abundance following zinc restriction. The methylcitrate cycle is a system that provides an alternative source of carbon through pyruvate production (Bramer *et al*. 2002). One of the major pathways for propionyl-CoA metabolism is the methylcitrate pathway. Propionyl-CoA is generated by the breakdown of odd-chain fatty acids and of the amino acids valine and isoleucine (Fleck and Brock 2008). According to the proteomic analysis here presented, it is observed a reduction on the expression of the enzymes involved to metabolism of valine and isoleucine , as well as enzymes of the and lipid metabolism, putatively reducing the production of propionyl-CoA. The data add further support to the overall metabolic adjustment of *Paracoccidioides* under zinc deprivation.

The alcohol dehydrogenase enzyme catalyzes the oxidation of ethanol to acetaldehyde. This enzyme is zinc-dependent and it is highly expressed in zinc-replete cells but is repressed in zinc-deficient cells of *S. cerevisiae* (Bird *et al*. 2006). We have demonstrated that alcohol dehydrogenase is down-regulated during zinc starvation in *Paracoccidioides*, suggesting again that differential gene expression aid in the adaptation of *Paracoccidioides* to zinc deficiency.

Proteomic analysis of *Paracoccidioides* revealed that the major cellular response affected by zinc restriction was related to oxidative stress response. Our data suggest also that cell rescue, defense and virulence, was the most favored pathway during zinc deprivation. Our results provide the first view of *Paracoccidioides* proteome response to zinc starvation

5. Acknowledgments

This work at Universidade Federal de Goiás was supported by grants from Conselho Nacional de Desenvolvimento Científico e Tecnológico- CNPq (process

numbers 558923/2009-7, 563398/2010-5 and 473277/2011-5) and Fundação de Amparo à Pesquisa do Estado de Goiás-FAPEG.

6. References

Amich J, Leal F, Calera JA, 2009. Repression of the acid ZrfA/ZrfB zinc-uptake system of *Aspergillus fumigatus* mediated by PacC under neutral, zinc-limiting conditions. International microbiology: the official journal of the Spanish Society for Microbiology, 12: 39-47.

Amich J, Vicentefranqueira R, Leal F, Calera JA, 2010. *Aspergillus fumigatus* survival in alkaline and extreme zinc-limiting environments relies on the induction of a zinc homeostasis system encoded by the zrfC and aspf2 genes. Eukaryotic cell, 9: 424-37.

Bailão AM, Schrank A, Borges CL, Dutra V, Molinari-Madlum EEWI, Felipe MSS, Mendes-Giannini MJS, Martins WS, Pereira M, Soares CMA, 2006. Differential gene expression by *Paracoccidioides brasiliensis* in host interaction conditions: representational difference analysis identifies candidate genes associated with fungal pathogenesis. Microbes and infection, 8: 2686–2697.

Bailão AM, Shrank A, Borges CL, Parente JA, Dutra V, Felipe MS, Fiuza RB, Pereira M, Soares CMA, 2007. The transcriptional profile of *Paracoccidioides brasiliensis* yeast cells is influenced by human plasma. FEMS immunology and medical microbiology, 51: 43–57.

Bailão EFLC, Parente AF, Parente JA, Silva-Bailão MG, Castro KP, Rosa e Silva LK, Staats CC, Schrank A, Vainstein MH, Borges CL, Bailão AM, Soares CMA, 2012. Metal Acquisition and Homeostasis in Fungi. Current Fungal Infection Reports, 6: 1-10.

Bird AJ, Gordon M, Eide DJ, Winge DR, 2006. Repression of ADH1 and ADH3 during zinc deficiency by Zap1-induced intergenic RNA transcripts. The EMBO journal, 25: 5726–5734.

Bookout AL, Cummins CL, Mangelsdorf DJ, Pesola JM, Kramer MF, 2006. High-throughput real-time quantitative reverse transcription PCR. In: Ausubel FM, Brent R, Kingston RE, Moore DD, Seidman JG, Smith JA (eds), *Current Protocols in Molecular Biology*. Hoboken NJ: John Wiley and Sons, pp. 1581–1628.

Bradford MM, 1976. A dye binding assay for protein. Analytical biochemistry. 72: 248–254.

Bramer CO, Silva LF, Gomez JG, Priefert H, Steinbuchel A, 2002. Identification of the 2-methylcitrate pathway involved in the catabolism of propionate in the polyhydroxyalkanoate-producing strain Burkholderia sacchari IPT101(T) and analysis of a mutant accumulating a copolyester with higher 3-hydroxyvalerate content. Applied and environmental microbiology, 68: 271–279.

Brummer E, Castaneda E, Restrepo A, 1993. Paracoccidioidomycosis: an update. Clinical microbiology reviews, 6: 89-117.

Campos EG, Jesuino RS, Dantas Ada S, Brigido MM, Felipe MS, 2005. Oxidative stress response in *Paracoccidioides brasiliensis*. Genetics and molecular research, 4: 409-429.

Chagas RF, Bailão AM, Pereira M, Winters MS, Smullian AG, Deepe GS Jr, Soares CMA, 2008. The catalases of *Paracoccidioides brasiliensis* are differentially regulated: protein activity and transcript analysis. Fungal genetics and biology, 45: 1470-1478.

Carrero LL, Niño-Vega G, Teixeira MM, Carvalho MJ, Soares CMA, Pereira M, Jesuino RS, McEwen JG, Mendoza L, Taylor JW, Felipe MS and San-Blas G, 2008. New *Paracoccidioides brasiliensis* isolate reveals unexpected genomic variability in this human pathogen. Fungal genetics and biology, 45: 605-612.

Citiulo F, Jacobsen ID, Miramón P, Schild L, Brunke S, Zipfel P, Brock M, Hube B, Wilson D, 2012. *Candida albicans* Scavenges Host Zinc via Pra1 during Endothelial Invasion. PLoS pathogens, 8: e1002777.

Dantas AS, Andrade RV, de Carvalho MJ, Felipe MS, Campos EG, 2008. Oxidative stress response in *Paracoccidioides brasiliensis*: assessing catalase and cytochrome C peroxidase. Mycological research, 112: 747-756.

Eide DJ, 2003. Multiple regulatory mechanisms maintain zinc homeostasis in *Saccharomyces cerevisiae*. The Journal of nutrition, 133: 1532S–1535S.

Finney LA and O'Halloran TV, 2003. Transition metal speciation in the cell: insights from the chemistry of metal ion receptors. Science, 300: 931–936.

Fleck CB, Brock M, 2008. Characterization of an acyl-CoA: carboxylate CoA-transferase from *Aspergillus nidulans* involved in propionyl-CoA detoxification. Molecular microbiology, 68: 642-656.

Fonseca CA, Jesuino RS, Felipe MS, Cunha DA, Brito WA, 2001. Two dimensional electrophoresis and characterization of antigens from *Paracoccidioides brasiliensis*. Microbes and infection, 3: 535–542.

Gitan RS, Luo H, Rodgers J, Broderius M, Eide D, 1998. Zinc-induced inactivation of the yeast ZRT1 zinc transporter occurs through endocytosis and vacuolar degradation. The Journal of biological chemistry, 273: 28617–28624.

Hartl FU, 1996. Molecular chaperones in cellular protein folding. Nature, 381: 571–580.

Ho E and Ames BN, 2002. Low intracellular zinc induces oxidative DNA damage, disrupts p53, NFkappa B, and AP1 DNA binding, and affects DNA repair in a rat glioma cell line. Proceedings of the National Academy of Sciences of the United States of America, 99: 16770–16775.

Li Q, Abrashev R, Harvey LM, McNeil B, 2008. Oxidative stress-associated impairment of glucose and ammonia metabolism in the filamentous fungus, *Aspergillus niger* B1-D. Mycological research, 112: 1049-1055.

Lyons TJ, Gasch AP, Gaither LA, Botstein D, Brown PO, Eide DJ, 2000. Genome-wide characterization of the Zap1p zinc-responsive regulon in yeast. Proceedings of the National Academy of Sciences of the United States of America, 97: 7957–7962.

Mackenzie GG, Zago MP, Erlejman AG, Aimo L, Keen CL, Oteiza PI, 2006. alpha-Lipoic acid and N-acetyl cysteine prevent zinc deficiency-induced activation of NF-kappa B and AP-1 transcription factors in human neuroblastoma IMR-32cells. Free radical research, 40: 75–84.

Matute DR, Sepulveda VE, Quesada LM, Goldman GH, Taylor JW, Restrepo A, McEwen JG, 2006. Microsatellite analysis of three phylogenetic species of *Paracoccidioides brasiliensis*. Journal of clinical microbiology, 44: 2153-2157.

Parente AF, Bailao AM, Borges CL, Parente JA, Magalhães AD, Ricart CA, Soares CMA, 2011. Proteomic analysis reveals that iron availability alters the metabolic status of the pathogenic fungus *Paracoccidioides brasiliensis*. PloS one, 6: e22810.

Restrepo A, McEwen JG, Castañeda E, 2001. The habitat of *Paracoccidioides brasiliensis*: how far from solving the riddle Medical mycology: official publication of the International Society for Human and Animal Mycology, 39: 233-241.

Restrepo A and Jiménez BE, 1980. Growth of *Paracoccidioides brasiliensis* yeast phase in a chemically defined medium. Journal of clinical microbiology, 12: 279-281.

Rezende TCV, Borges CL, Magalhães AD, de Sousa MV, Ricart CAO, Bailão AM, Soares CMA, 2011. A quantitative view of the morphological phases of *Paracoccidioides brasiliensis* using proteomics. Journal of Proteomics, 75: 572-587.

Rhee SG, Chae HZ, Kim K, 2005. Peroxiredoxins: a historical overview and speculative preview of novel mechanisms and emerging concepts in cell signaling. Free radical biology & medicine, 38: 1543-1552.

Rutherford JC and Bird AJ, 2004. Metal-Responsive Transcription Factors That Regulate Iron, Zinc, and Copper Homeostasis in Eukaryotic Cells. Eukaryotic Cell, 3: 1-13.

San-Blas G, Niño-Vega G, Iturriaga T, 2002. *Paracoccidioides brasiliensis* and paracoccidioidomycosis: molecular approaches to morphogenesis, diagnosis, epidemiology, taxonomy and genetics. Medical mycology: official publication of the International Society for Human and Animal Mycology, 40: 225-242.

Schneider RO, Fogaça NS, Kmetzsch L, Schrank A, Vainstein MH, Staats CC, 2012. Zap1 regulates zinc homeostasis and modulates virulence in *Cryptococcus gattii*. PloS One, 7: e43773

Silva MG, Schrank A, Bailão EFLC, Bailão AM, Borges CL, Staats CC, Parente JL, Pereira M, Salem-Izacc SL, Mendes-Giannini MJS, Oliveira RMZ, Lívia Kmetzsch Rosa e Silva LK, Nosanchuk JD, Vainstein MH, Soares CMA, 2011. The homeostasis of iron, copper, and zinc in *Paracoccidioides brasiliensis*, *Cryptococcus neoformans var. grubii*, and *Cryptococcus gattii*: a comparative analysis. Frontiers in microbiology, 2: 1-19.

Sõti C, Pál C, Papp B, Csermely P, 2005. Molecular chaperones as regulatory elements of cellular networks. Current opinion in cell biology, 17: 210–215.

Teixeira MM, Theodoro RC, de Carvalho MJ, Fernandes L, Paes HC, Hahn RC, Mendoza L, Bagagli E, San-Blas G, Felipe MS, 2009. Phylogenetic analysis reveals a

high level of speciation in the *Paracoccidioides* genus. Molecular phylogenetics and evolution, 52: 273-283.

Vicentefranqueira R, Moreno MA, Leal F, Calera JA, 2005. The zrfA and zrfB genes of *Aspergillus fumigatus* encode the zinc transporter proteins of a zinc uptake system induced in an acid, zinc-depleted environment. Eukaryotic Cell, 4: 837-48.

Winters MS, Chan Q, Caruso JA, Deepe GS Jr. 2010, Metallomic analysis of macrophages infected with *Histoplasma capsulatum* reveals a fundamental role for zinc in host defenses. The Journal of infectious diseases, 202: 1136–1145.

Wu CY, Bird AJ, Winge DR, Eide DJ, 2007. Regulation of the yeast TSA1 peroxiredoxin by ZAP1 is an adaptive response to the oxidative stress of zinc deficiency. The Journal of biological chemistry, 282: 2184–2195.

Wu CY, Roje S, Sandoval FJ, Bird AJ, Winge DR, Eide DJ, 2009. Repression of Sulfate Assimilation Is an Adaptive Response of Yeast to the Oxidative Stress of Zinc Deficiency. The Journal of biological chemistry, 284: 27544-27556.

Zhao H and Eide D, 1996a. The yeast ZRT1 gene encodes the zinc transporter protein of a high-affinity uptake system induced by zinc limitation. Proceedings of the National Academy of Sciences of the United States of America, 93:2454–2458.

Zhao H and Eide D, 1996b. The ZRT2 gene encodes the low affinity zinc transporter in *Saccharomyces cerevisiae*. The Journal of biological chemistry, 271: 23203–23210.

Zhao H and Eide DJ, 1997. Zap1p, a metalloregulatory protein involved in zinc-responsive transcriptional regulation in *Saccharomyces cerevisiae*. Molecular and cellular biology, 17: 5044–5052.

Table 1: *Paracoccidioides* proteins with increased expression upon 6 and 24 h of zinc starvation and their predicted biological function-FunCat2[†]

Accession number[a]/Protein description	Time[b]	Number of isoforms in *Paracoccidioides*[c]	Average of amount of isoform abundances in zinc starvation[d]	Average of amount of isoform abundances in control[e]	ANOVA (p-value)[f]	Fold Change[g]
Cell rescue, defense and virulence						
gi|295670221 - Thioredoxin	24 h	1	0.52	**	**	**
gi|295664022 - Glutathione reductase	24 h	1	0.19	0.12	0.033	1.58
gi|295674755 - Glutathione synthetase	24 h	1	0.07	0.04	0.006	1.61
gi|295661107 - Thioredoxin reductase	24 h	1	0.16	**	**	**
gi|295668244 - Mitochondrial peroxiredoxin PRX1	24 h	1	0.08	**	**	**
gi|17980998 - Y20 protein	24 h	1	0.89	0.28	0.001	3.17
gi|295673162 - Disulfide isomerase Pdi1	24 h	1	0.94	0,33	0.003	2.83
gi|295658865 - Heat shock protein	6 h	1	0.14	**	**	**
gi|4164594 - Heat shock protein 70	6 h	1	1.75	1.51	0.044	1.16
gi|14538021 - Heat shock protein 70	24 h	3	2.43	0.94	0.0012	2.58
gi|295659116 - Hsp70-like protein	6 h	1	0.14	**	**	**
gi|295673716 - Hsp70-like protein	24 h	2	1.06	0.53	0.0014	2.00
gi|295659116 - Hsp70-like protein	24 h	3	1.68	1.0	0.0013	1.68
gi|14538021 - Heat shock protein 70	24 h	1	0.63	0.20	0.046	3.19
gi|295671569 - Heat shock protein SSC1	6 h	2	0.20	**	**	**
gi|295659837 - Heat shock protein SSB1	24 h	1	0.11	0.09	0.020	1.81
gi|295659787 - Heat shock protein Hsp88	24 h	2	0.99	0.61	0.0052	1.64
gi|295665077 - Hsp90 binding co-chaperone (Sba1)	24 h	2	0.25	0.11	0.00005	2.32
Protein synthesis and Fate						
gi|295657024 - Puromycin-sensitive aminopeptidase	6 h	1	0.06	**	**	**
gi|295669794 - Elongation factor Tu	6 h	1	0.08	**	**	**
gi|295675019 - Elongation factor 2	24 h	2	0.37	0.28	0.001	1.34
gi|295674319 - Polyadenylate-binding protein	6 h	1	0.05	**	**	**
gi|295660511 - Glycyl-tRNA synthetase	24 h	1	0.07	**	**	**
Glycolysis and Gluconeogenesis						
gi|295671152 - Phosphoglucomutase	24 h	1	0.22	0.04	0.013	5.54
gi|295658119 - Glyceraldehyde-3-phosphate dehydrogenase	24 h	3	3.95	2.14	0.0061	1.85
gi|295669690 - Phosphoglycerate kinase	24 h	1	0.37	0.25	0.032	1.50
gi|295671120 - Fructose-1,6-bisphosphate aldolase	24 h	2	0.33	0.19	0.05	1.73
gi|295658778 - Phosphoenolpyruvate carboxykinase	24 h	1	0.13	0.05	0.000	2.59
Citric acid cycle						
gi|295658897 - Citrate synthase	24 h	3	0.39	0.10	0.0008	3.84
gi|295669416 - 2-oxoglutarate dehydrogenase E1	6 h	1	0.16	**	0.018	1.86

gi|295669416 - 2-oxoglutarate dehydrogenase E1	24 h	4	0.41	0.17	0.003	2.42
gi|295658595 - Pyruvate dehydrogenase E1 component subunit alpha	24 h	1	0.31	0.20	0.002	1.60
Glyoxylate cycle						
gi|295660969 - Isocitrate lyase	24 h	1	0.25	0.11	0.001	2.36
Oxidation of fatty acids						
gi|295665123 - Aldehyde dehydrogenase	24 h	3	1.22	0.15	0.0002	8.25
Carbohydrate metabolism						
gi|295672968 - Phosphomannomutase	24 h	1	0.25	0.05	0.000	4.74
gi|295663567 - 6-phosphogluconolactonase	24 h	1	0.15	0.08	0.016	1.87
gi|295661432 - UTP-glucose-1-phosphate-uridylyltransferase	6 h	1	0.14	**	**	**
Nucleotide metabolism						
gi|295672652 - Bifunctional purine biosynthesis protein ADE17	24 h	2	0.37	0.17	0.004	2.17
Amino acid and nitrogen metabolism						
gi|295669240 - Kynurenine-oxoglutarate transaminase	6 h	1	0.16	**	**	**
gi|295669670 - Adenosylhomocysteinase	6 h	1	0.19	0.07	0.033	2.67
gi|295667902 - Aminomethyltransferase	24 h	1	0.10	0.05	0.014	1.96
gi|226294930 - Ketol-acid reductoisomerase	24 h	1	0.19	**	**	**
gi|295658698 - Fumarylacetoacetase	24 h	1	0.19	0.15	0.028	1.30
gi|295665131 - Delta-1-pyrroline-5-carboxylate dehydrogenase	24 h	1	0.07	**	**	**
gi|295662426 - Aspartate aminotransferase	24 h	1	0.16	**	**	**
Lipid, fatty acid and isoprenoid metabolism						
gi|295657225 - Peroxisomal multifunctional enzyme	6 h	1	0.14	**	**	**
gi|295668707 - Acetyl-CoA acetyltransferase	24 h	1	0.32	0.20	0.002	1.58
gi|295664927 - ATP-citrate-lyase	6 h	1	0.17	0.05	0.003	3.31
gi|295664927 - ATP citrate lyase	24 h	1	0.26	0.17	0.011	1.50
Metabolism of vitamins, cofactors and prosthetic groups						
gi|295657369 - Nicotinate-nucleotide pyrophosphorylase	24 h	1	0.25	0.13	0.011	1.88
gi|295660716 - UDP-galactopyranose mutase	24 h	1	0.18	0.10	0.046	1.69
Protein/peptide degradation						
gi|295666766 - vacuolar aminopeptidase	24 h	1	0.04	**	**	**
Cell growth / morphogenesis						
gi|295657091 - Tropomyosin-1	6 h	1	0.26	**	**	**
gi|295673184 - Actin-interacting protein	24 h	1	0.23	**	**	**
Unclassified Proteins						
gi|295661500 - Conserved hypothetical protein	24 h	1	0.11	0.07	0.016	1.62

**Spots visualized only in zinc-starvation condition;

[a]GenBank general information identifier**;**
[b]Time of exposure to zinc starvation;
[c]Number of identified isoforms of protein in *Paracoccidioides*. Pb01 during zinc starvation
[d,e]The average of amount of values of abundances of all identified isoforms used to statistical test
[f]$p < 0.05$ was used to considerer statistically significant differences
[g]Fold change increase in protein expression in zinc starvation.
[†]Functional classification by FunCat2 (http://pedant.helmholtzmuenchen.de/pedant3htmlview/pedant3view?Method=analysis&Db=p3_r48325_Par_brasi_Pb01)

Table 2: *Paracoccidioides* proteins with decreased expression upon 6 and 24 h of zinc starvation and their predicted biological function-FunCat2[†]

Accession number[a]/Protein description	Time[b]	Number of isoforms in *Paracoccidioides*[c]	Average of amount of isoform abundances in zinc starvation[d]	Average of amount of isoform abundances in control[e]	ANOVA (*p*-value)f	Fold Change[g]
Cell rescue, defense and virulence						
gi|295664022 - Glutathione reductase	6 h	1	0.19	0.34	0.024	1.83
gi|225681400 - Peroxisomal catalase	6 h	1	0.12	0.21	0.027	1.69
gi|295662873 - Mitochondrial co-chaperone GrpE	6 h	1	0.13	0.30	0.003	2.35
gi|295673162 - Disulfide isomerase Pdi1	6 h	1	0.22	0.36	0.013	1.66
gi|17980998 - Y20 protein	6 h	1	0.80	1.31	0.025	1.64
gi|295672932 - 30 kDa heat shock protein	6 h	1	0.29	0.59	0.03	2.02
gi|295672932 - 30 kDa Heat shock protein	24 h	2	0.49	0.88	0.00072	1.80
gi|295658865 - Heat shock protein	24 h	2	0.06	0.13	0.009	2.28
gi|295664909 - 10 kDa heat shock protein. mitochondrial	24 h	1	**	0.52	**	**
Protein synthesis and Fate						
gi|295663887 - 40S ribosomal protein S19	6 h	1	0.45	0.90	0.007	2.01
gi|295663887 - 40S ribosomal protein S19	24 h	1	**	0.47	**	**
gi|295664112 - 40S ribosomal protein S22	24 h	1	**	0.53	**	**
Glycolysis and Gluconeogenesis						
gi|295671120 - Fructose1,6-bisphosphate aldolase	6 h	2	1.56	2.35	0.0054	1.5
gi|295658119 – Glyceraldehyde 3-phosphate dehydrogenase	6 h	1	0.78	2.18	0.001	2.80
Citric acid cycle						
gi|295673937 - Malate dehydrogenase	6 h	1	0.36	0.77	0.004	2.12
gi|295664721 - Aconitase	24 h	3	0.47	1.17	0.005	2.48
gi|295665542 - Osmotic growth protein	24 h	1	0.10	0.28	0.029	2.7
Oxidation of fatty acids						
gi|295665123 - Aldehyde dehydrogenase	6 h	1	0.03	0.07	0.022	2.49
Carbohydrate metabolism						
gi|295662360 - Mannitol-1-phosphate 5-dehydrogenase	6 h	1	0.14	0.20	0.042	1.41
Nucleotide metabolism						
gi|295666938 - Nucleoside diphosphate kinase	6 h	1	0.82	0.52	0.001	3.12
gi|225681397 - Conserved hypotetical protein	24 h	1	**	0.32	**	**
Amino acid and nitrogen metabolism						
gi|295661139 - Methylmalonate-semialdehyde dehydrogenase	6 h	1	0.11	0.23	0.005	2.15
gi|295662426 - Aspartate aminotransferase	6 h	1	0.08	0.15	0.009	1.83

gi|295674273 - Acetolactate synthase	6 h	1	0.04	0.12	0.031	3.17
gi|295658312 - L-PSP endoribonuclease family protein (Hmf1)	6 h	1	0.17	0.34	0.006	2.00
gi|225678712 - Ketol-acid reductoisomerase	6 h	1	0.27	0.38	0.014	1.40
gi|295674767 - 4-aminobutyrate aminotransferase	6 h	1	0.03	0.02	0.047	1.77
gi|295668370 - Aminopeptidase	24 h	1	0.08	0.13	0.025	1.7
gi|225683481 - Cysteinyl-tRNA synthetase	24 h	1	0.02	0.03	0.05	1.17
gi|295672027 - Glycine dehydrogenase	24 h	1	0.05	0.10	0.009	2.2
gi|295668479 - Formamidase	24 h	1	0.75	1.21	0.020	1.6
Lipid, fatty acid and isoprenoid metabolism						
gi|295668707 - Acetyl-coA acetyltransferase	6 h	1	0.09	0.24	0.002	2.65
gi|295665414 - Short chain dehydrogenase family protein	6 h	1	**	0.15	**	**
gi|295666179 - 2-Methylcitrate synthase	6 h	1	0.55	1.10	0.004	1.99
gi|295666197 - 2-Methylcitrate dehydratase	6 h	1	0.52	0.82	0.028	1.58
gi|295657225 - Peroxisomal multifunctional enzyme	24 h	1	**	0.09	**	**
gi|295670601 - 3-hydroxyisobutyryl-CoA hydrolase	24 h	1	0.06	0.11	0.013	1.7
Metabolism of vitamins, cofactors and prosthetic groups						
gi|295661741- 3-demethylubiquinone 9,3-methyltransferase	24 h	1	0.20	0.39	0.019	1.9
gi|295660455 - Pyridoxine biosynthesis protein PDX1	24 h	1	**	0.09	**	**
Protein/peptide degradation						
gi|295657201 - Glutamate carboxypeptidase	6 h	1	0.07	0.11	0.005	1.69
gi|295674421 - Ubiquitin carboxyl-terminalhydrolase	24 h	1	**	0.03	**	**
gi|295660102 - Dipeptidyl- peptidase	24 h	1	0.20	0.28	0.039	1.4
Transcription						
gi|295665468 - Nucleic acid-binding protein	24 h	2	0.33	1.01	0.00073	3.10
Electron transport and membrane-associated energy conservation						
gi|295658821 - ATP synthase subunit beta	6 h	1	0.22	0.32	0.037	1.48
gi|295658923 - Citochrome b-c1 complex subunit 2	6 h	1	0.12	0.16	0.026	1.42
gi|295669073 - 12-oxophytodienoate reductase	24 h	1	0.56	0.96	0.013	1.7
Fermentation						
gi|295674635 - Alcohol dehydrogenase	6 h	1	0.44	0.81	0.002	1.85
gi|295674635 - Alcohol dehydrogenase	24 h	1	0.37	1.0	0.001	2.7
Phosphate Metabolism						
gi|295672504 - Inorganic pyrophosphatase	6 h	1	0.19	0.25	0.044	1.32
gi|295672504 - Inorganic pyrophosphatase	24 h	2	0.041	0.32	0.002	7.93
Signal transduction						
gi|295662102 - Rab GDP-dissociation inhibitor	6 h	1	0.13	0.29	0.002	2.24
Cytoskeleton/structural proteins						
gi|295669061 - Arp2/3 complex subunit Arc16	6 h	1	0.13	0.18	0.003	1.42

gi|295669061 - Arp2/3 complex subunit Arc16	24 h	1	0.11	0.18	0.006	1.7
DNA synthesis and replication						
gi|295660405 - Hypotetical protein	6 h	1	0.41	0.76	0.011	1.8
Unclassified Proteins						
gi|295673506 - Conserved hypothetical protein	24 h	1	0.10	0.21	0.008	2.0
gi|295659253 - Conserved hypothetical protein	24 h	1	**	0.21	**	**

**Spots visualized only in zinc-replete condition;
[a]GenBank general information identifier**;**
[b]Time of exposure to zinc starvation;
[c]Number of identified isoforms of protein in *Paracoccidioides*. Pb01 in zinc replete conditions
[d,e]The average of amount of values of abundances of all identified isoforms used to statistical test
[f]$p < 0.05$ was used to considerer statistically significant differences
[g]Fold change increase in protein expression in zinc availability.
[†]Functional classification by FunCat2 (http://pedant.helmholtzmuenchen.de/pedant3htmlview/pedant3view?Method=analysis&Db=p3_r48325_Par_brasi_Pb01)

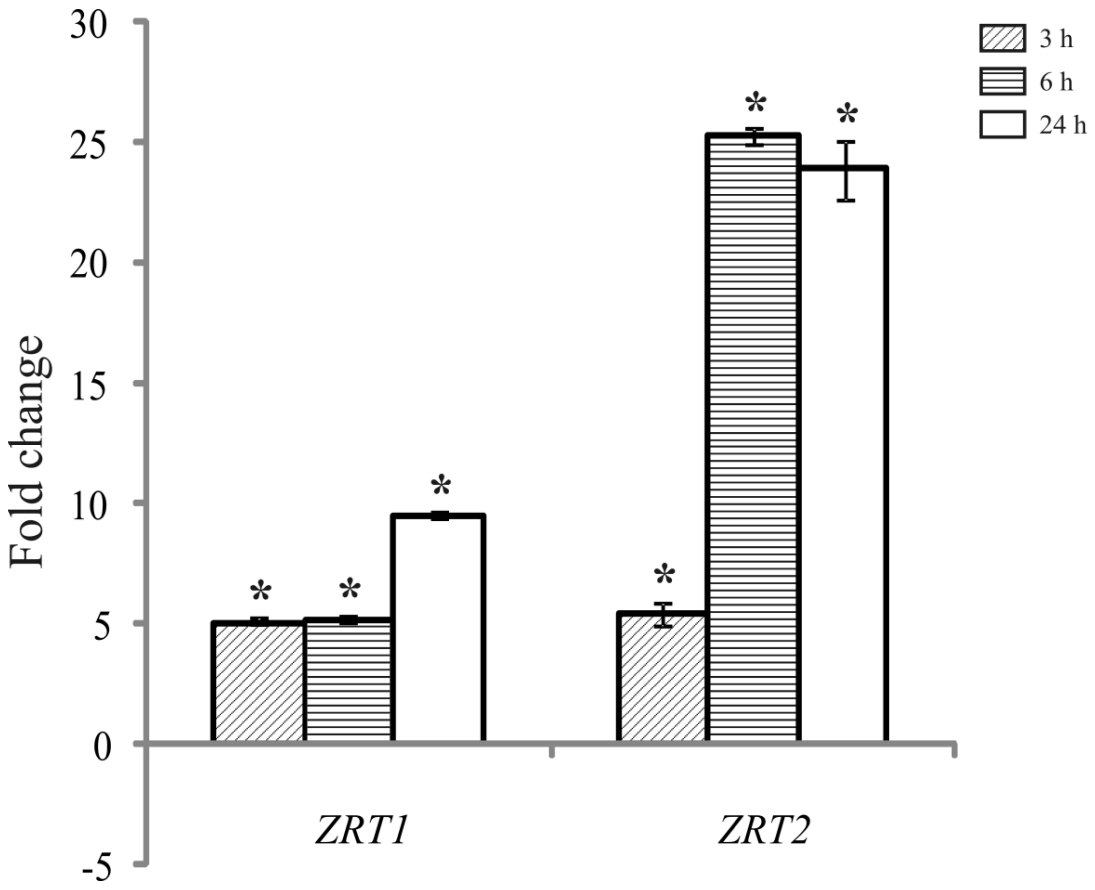

Fig 1. Quantification of the mRNA expression of selected genes of *Paracoccidioides* by quantitative real time RT-PCR. Quantitative RT-PCR determined *Paracoccidioides* transcript levels of *ZRT1* and *ZRT2* during zinc deprivation. Data were normalized to the α-tubulin protein transcript and presented as fold change. Student's *t* test was used for statistical comparisons. Error bars represent standard deviation from three biological replicates while * represents $p \leq 0.05$.

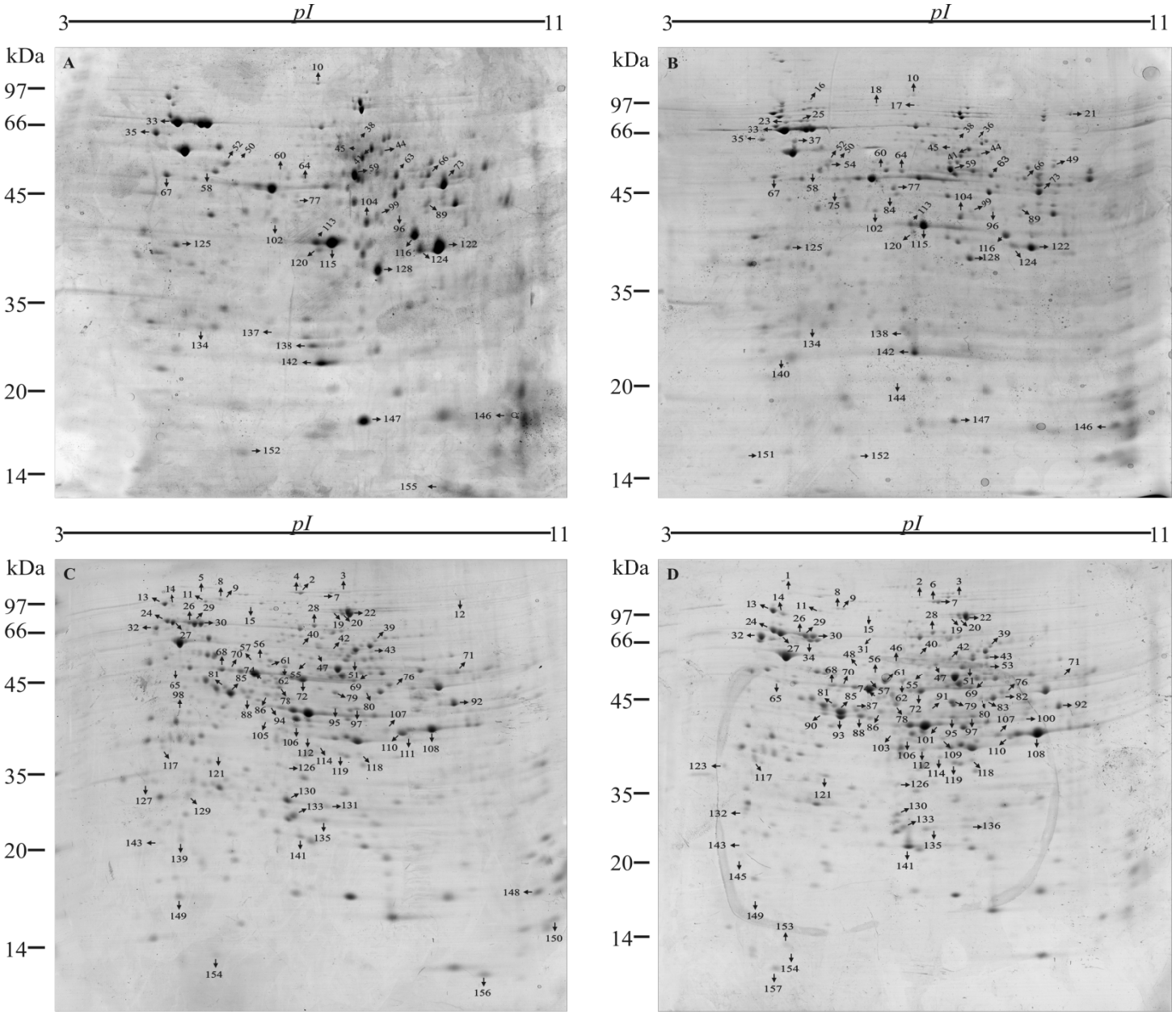

Fig 2. 2D-gel analysis of *Paracoccidioides* proteins extracted from yeast cells grown in zinc depleted media for 6 h (B) and 24 h (D). Gels A and C represent zinc rich conditions. Identified protein spots are numbered and listed in table S2 (see "Supplementary information").

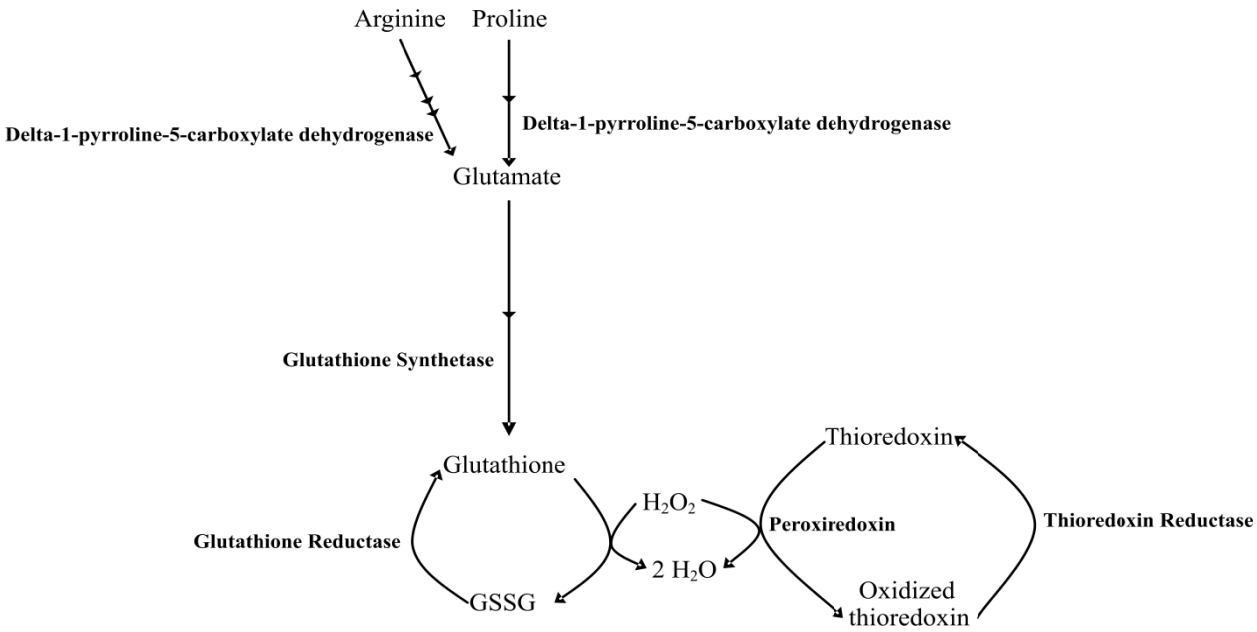

Fig 3. View of *Paracoccidioides* response to stress during zinc starvation revealed by proteomic analysis. Schematic representation of proteins involved in *Paracoccidioides* stress response. GSSG represents glutathione-oxidized.

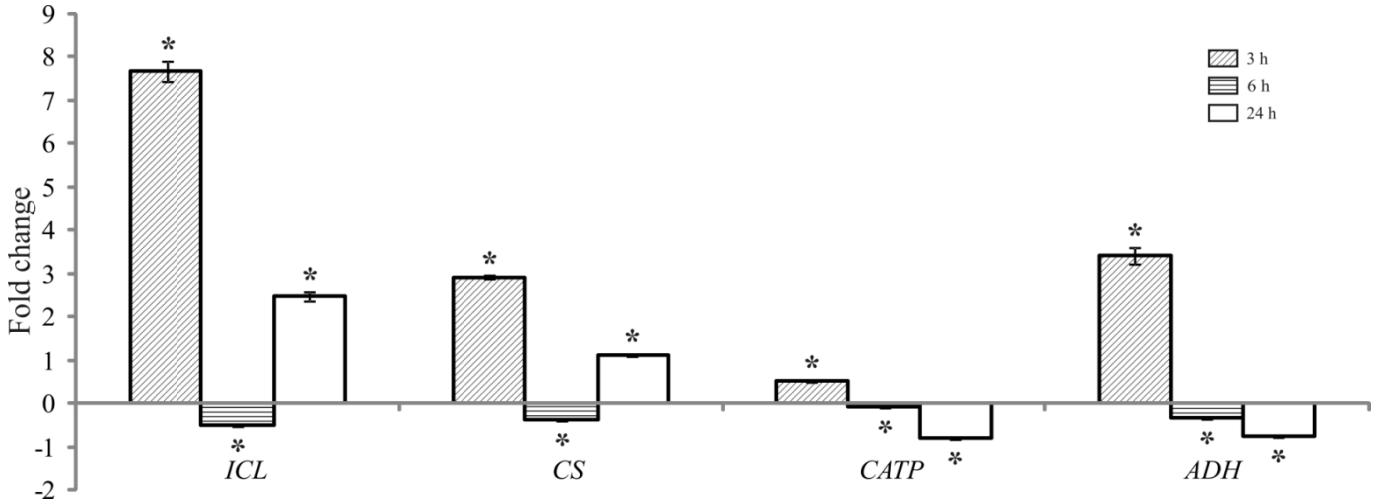

Fig 4. Validation of proteomic data by quantitative real time RT-PCR. *Paracoccidioides* transcript levels of genes encoding isocitrate lyase (*ICL*), citrate synthase (*CS*), peroxisomal catalase (*CATP*) and alcohol dehydrogenase (*ADH*) transcript levels were measured using quantitative RT-qPCR. Data were normalized to the α-tubulin protein transcript and presented as fold change. Student's *t* test was used for statistical comparisons. Error bars represent standard deviation from three biological replicates while * represents $p \leq 0.05$.

Table S1: Oligonucleotides used in RT-qPCR

Oligonucleotide	Sequence	Accession number[a]
Tubulin sense	5' ACAGTGCTTGGGAACTATACC 3'	PAAG_01647.1
Tubulin anti-sense	5' GGGACATATTTGCCACTGCC 3'	PAAG_01647.1
Zrt1 sense	5' CTATCCGCTGTGTTCGTCAT 3'	PAAG_08727.1
Zrt1 anti-sense	5' GGAGATGGATGAAAGCTGTG 3'	PAAG_08727.1
Zrt2 sense	5' GCAAAATCCCCCAATGGTAGT3'	PAAG_03419.1
Zrt2 anti-sense	5' GGGTAAGGCCGATTATGATAG3'	PAAG_03419.1
Alcohol dehydrogenase sense	5' ACCTTGTTGTGCTGGAGTAGA 3'	PAAG_06715.1
Alcohol dehydrogenase anti-sense	5' GGAGTCTGGAATCGGGGTG 3'	PAAG_06715.1
Isocitrate lyase sense	5' ATGGGAACCGACCTCCTGG 3'	PAAG_06951.1
Isocitrate lyase anti-sense	5' CGTTCTTGCCTGCTTGCTCA 3'	PAAG_06951.1
Citrate synthase sense	5' ACTGAGCACGGCAAGACGG 3'	PAAG_08075.1
Citrate synthase anti-sense	5' TTCCCAATGCACGGTCGATAA 3'	PAAG_08075.1
Peroxisomal catalase sense	5' AGGTGCAGGAGCTTACGGTG 3'	PAAG_01454.1
Peroxisomal catalase anti-sense	5' CCCAATTTCCTTGCTCGGTG 3'	PAAG_01454.1

[a]Accession number – accession number of the protein identified in the database Broad Institute of MIT and Harvard: (http://www.broadinstitute.org/annotation/genome/*Paracoccidioides*_brasiliensis/MultiHome.html)

Table S2: *Paracoccidioides* identified protein upon 6 and 24 hours of zinc starvation

Accession number[a]/Protein description	Spot number[b]	Time[c]	PMF		MS/MS	Exp/Theo pI[g]	Exp/Theo MW[h]
			Score[d]	Seq. Cov (%)[e]	Matched Peptides[f]		
gi|295673162 - Disulfide isomerase Pdi1	35	6 h	195	49	14	4.44/4.80	63.67/59.31
gi|295673162 - Disulfide isomerase Pdi1	32	24 h	265	55	4	4.53/4.80	69.67/59.3
gi|295664022 - Glutathione reductase	63	6 h	154	44	15	8.42/6.74	50.83/51.96
gi|295664022 - Glutathione reductase	69	24 h	94	23	2	8.06/6.74	49.67/51.9
gi|295674755 - Glutathione synthetase	55	24 h	158	35	1	7.09/6.14	53.33/56.7
gi|295671569 - Heat shock protein SSC1	30	24 h	239	43	8	5.32/5.92	72.83/73.82
gi|295671569 - Heat shock protein SSC1	26	24 h	168	49	12	5.12/5.92	74.33/73.82
gi|295671569 - Heat shock protein SSC1	29	24 h	175	59	7	5.21/5.92	73.0/73.82
gi|295671569 - Heat shock protein SSC1	16	6 h	173	60	7	5.21/5.92	97.33/73.82
gi|295671569 - Heat shock protein SSC1	25	6 h	98	65	6	4.99/5.92	76.0/73.82
gi|295671569 - Heat shock protein SSC1	34	24 h	104	20	1	5.40/5.92	67.0/73.82
gi|295671569 - Heat shock protein SSC1	81	24 h	86	16	2	5.69/5.92	44.67/73.8
gi|295671569 - Heat shock protein SSC1	87	24 h	108	16	1	6.12/5.92	43.67/73.82
gi|295671569 - Heat shock protein SSC1	86	24 h	**	**	2	6.41/5.92	43.83/73.8
gi|295671569 - Heat shock protein SSC1	117	24 h	**	**	1	4.56/5.92	38.0/73.8
gi|295658865 - Heat shock protein	127	24 h	106	47	**	4.24/5.51	35.0/62.27
gi|295658865 - Heat shock protein	37	6 h	177	52	4	4.87/5.51	63.33/62.27
gi|295658865 - Heat shock protein	1	24 h	**	**	1	5.09/5.51	130.33/62.27
gi|4164594 - Heat shock protein 70	33	6 h	**	**	5	4.82/5.43	68.5/65.3
gi|14538021 - Heat shock protein 70	27	24 h	143	26	5	4.84/5.05	74.0/70.9
gi|14538021 - Heat shock protein 70	95	24 h	100	21	1	7.52/5.05	42.67/70.9

gi|14538021 - Heat shock protein 70	93	24 h	183	25	5	5.92/5.05	42.67/70.9
gi|14538021 - Heat shock protein 70	88	24 h	207	35	**	6.09/5.05	43.17/70.9
gi|295659116 - Hsp70-like protein	23	6 h	182	49	11	4.72/5.08	76.0/70.92
gi|295659116 - Hsp70-like protein	123	24 h	**	**	2	4.05/5.08	36.67/70.9
gi|295659116 - Hsp70-like protein	85	24 h	187	28	3	5.79/5.08	43.83/70.9
gi|295659116 - Hsp70-like protein	90	24 h	148	23	1	5.67/5.08	43.0/70.92
gi|295673716 - Hsp70-like protein	24	24 h	234	36	5	4.73/5.39	76.0/68.8
gi|295673716 - Hsp70-like protein	91	24 h	85	23	1	7.34/5.39	43.0/68.86
gi|295659787 - Heat shock protein Hsp88	13	24 h	201	35	4	4.69/4.92	97.83/80.7
gi|295659787 - Heat shock protein Hsp88	14	24 h	157	30	4	4.85/4.92	95.5/80.7
gi|295665077 - Hsp90 binding co-chaperone (Sba1)	143	24 h	**	**	1	4.49/4.23	22.5/21.3
gi|295665077 - Hsp90 binding co-chaperone (Sba1)	145	24 h	**	**	1	4.38/4.23	20.0/21.3
gi|295659837 - Heat shock protein SSB1	65	24 h	96	22	2	4.85/5.47	50.5/60.6
gi|295672932 - 30 kDa heat shock protein	138	6 h	109	53	11	7.06/9.75	24.83/28.64
gi|295672932 - 30 kDa Heat shock protein	133	24 h	170	48	**	6.80/9.75	27.0/28.64
gi|295672932 - 30 kDa Heat shock protein	135	24 h	120	57	**	7.28/9.75	26.5/28.64
gi|295664909 - 10 kDa heat shock protein, mitochondrial	156	24 h	102	58	1	9.41/8.79	12.67/11.19
gi|295668244 - Mitochondrial peroxiredoxin PRX1	132	24 h	**	**	1	4.45/5.28	28.33/24.9
gi|295668244 - Mitochondrial peroxiredoxin PRX1	132	24 h	**	**	1	4.45/5.28	28.33/24.9
gi|295662873 - Mitochondrial co-chaperone GrpE	134	6 h	**	**	6	5.30/8.89	26.5/28.51
gi|225681400 - Peroxisomal catalase	45	6 h	121	41	**	7.73/6.42	57.0/57.66
gi|295661107 - Thioredoxin reductase	103	24 h	87	29	1	6.77/5.51	41.0/38.19
gi|295670221 - Thioredoxin	153	24 h	77	56	1	5.21/5.24	13.33/12.9
gi|17980998 - Y20 protein	142	6 h	60	33	1	7.19/6.09	22.83/21.64
gi|17980998 - Y20 protein	141	24 h	**	**	2	6.90/6.09	23.0/21.6

gi|295657024 - Puromycin sensitive aminopeptidase	18	6 h	283	58	12	6.31/5.65	90.0/100.71
gi|295669794 - Elongation factor Tu	75	6 h	73	44	3	5.57/6.11	45.67/48.71
gi|295675019 - Elongation factor 2	112	24 h	116	16	2	7.08/6.46	39.17/92.6
gi|295675019 - Elongation factor 2	118	24 h	**	**	2	7.85/6.46	37.83/92.7
gi|295674319 - Polyadenylate binding protein	17	6 h	74	37	**	6.99/6.31	92.0/86.92
gi|295672445 - Alanyl-tRNAsynthetase	9	24 h	121	18	**	5.76/5.52	103.83/108.4
gi|295660511 - Glycyl-tRNAsynthetase	31	24 h	**	**	2	6.40/5.77	70.67/74.9
gi|146762537 - Enolase	70	24 h	89	27	**	5.82/5.67	49.5/47.4
gi|146762537 - Enolase	68	24 h	205	64	6	5.66/5.67	50.17/47.41
gi|295671152 - Phosphoglucomutase	42	24 h	**	**	1	7.48/6.59	58.33/83.6
gi|295669690 - Phosphoglyceratekinase	79	24 h	91	27	2	7.51/6.48	44.83/45.3
gi|295658778 - Phosphoenolpyruvate carboxykinase	40	24 h	128	27	2	6.99/6.10	60.5/63.9
gi|295671120 - Fructose-1,6-bisphosphate aldolase	101	24 h	133	43	1	7.48/6.09	41.67/39.72
gi|295671120 - Fructose-1,6-bisphosphate aldolase	113	6 h	190	69	7	7.08/6.09	38.67/39.72
gi|295671120 - Fructose1,6-bisphosphate aldolase	115	6 h	**	**	1	7.32/6.09	38.5/39.72
gi|295671120 - Fructose1,6-bisphosphate aldolase	94	24 h	153	58	**	6.33/6.09	42.67/39.72
gi|295658119 - Glyceraldehyde-3-phosphate dehydrogenase	122	6 h	286	85	8	9.13/8.26	36.83/36.62
gi|295658119 - Glyceraldehyde-3-phosphate dehydrogenase	111	24 h	88	50	**	8.47/8.26	39.67/36.62
gi|295658119 - Glyceraldehyde-3-phosphate dehydrogenase	108	24 h	140	42	**	8.95/8.26	40.17/36.6
gi|295658119 - Glyceraldehyde-3-phosphate dehydrogenase	107	24 h	193	69	3	8.28/8.26	40.17/36.6
gi|295658897 - Citrate synthase	80	24 h	84	26	2	7.99/8.75	44.83/52.2
gi|295658897 - Citrate synthase	82	24 h	**	**	1	8.51/8.75	44.67/52.20
gi|295658897 - Citrate synthase	83	24 h	**	**	1	8.25/8.75	44.33/52.20
gi|295669416 - 2-oxoglutarate dehydrogenase E1	10	6 h	122	20	1	7.11/6.68	103.5/121.6
gi|295669416 - 2-oxoglutaratedehydrogenase E1	6	24 h	91	13	1	7.36/6.68	110.0/121.63

gi|295669416 - 2-oxoglutarate dehydrogenase E1	7	24 h	221	27	4	7.30/6.68	108.67/121.6
gi|295669416 - 2-oxoglutarate dehydrogenase E1	46	24 h	83	10	**	6.79/6.68	56.33/121.63
gi|295673931 - Pyruvate dehydrogenase protein X complex	54	6 h	98	33	6	5.46/6.45	53.67/52.71
gi|295673931 - Pyruvate dehydrogenase protein X component	58	6 h	79	55	5	5.31/6.45	51.83/52.71
gi|295673937 - Malate dehydrogenase	128	6 h	185	49	10	8.10/8.99	34.17/36.02
gi|295664721 - Aconitase	20	24 h	146	47	13	7.64/6.49	86.5/79.20
gi|295664721 - Aconitase	19	24 h	109	24	12	7.51/6.49	88.17/79.20
gi|295664721 - Aconitase	22	24 h	131	50	13	7.75/6.49	85.5/79.20
gi|295665542 - Osmotic growth protein	71	24 h	159	50	**	9.37/6.90	49.33/68.04
gi|295669416 - 2-oxoglutarate dehydrogenase E1	4	24 h	84	39	**	6.79/6.68	114.0/121.63
gi|295658595 - Pyruvate dehydrogenase E1 component subunit alpha	78	24 h	130	28	2	6.63/8.62	44.83/45.3
gi|295660969 - Isocitrate lyase	36	6 h	215	74	12	8.05/6.79	63.67/60.17
gi|295660969 - Isocitrate lyase	43	24 h	161	27	2	8.10/6.79	57.83/60.2
gi|295660969 - Isocitrate lyase	41	6 h	364	46	13	8.01/6.79	59.67/60.17
gi|295665123 - Aldehyde dehydrogenase	57	24 h	170	41	2	6.19/5.87	52.33/54.5
gi|295665123 - Aldehyde dehydrogenase	60	6 h	106	55	7	6.51/5.87	51.5/54.56
gi|295665123 - Aldehyde dehydrogenase	61	24 h	140	38	3	6.46/5.87	51.17/54.5
gi|295665123 - Aldehyde dehydrogenase	157	24 h	**	**	3	5.08/5.87	12.0/54.5
gi|295672968 - Phosphomannomutase	121	24 h	**	**	2	5.57/5.60	37.17/30.6
gi|295663567 - 6-phosphogluconolactonase	126	24 h	148	40	3	6.70/5.86	36.17/29.3
gi|295661432 - UTP-glucose-1-phosphate uridylyltransferase	49	6 h	93	42	7	9.37/9.11	55.0/58.87
gi|295674635 - Alcohol dehydrogenase	116	6 h	178	84	7	8.72/7.55	38.33/38.00
gi|295674635 - Alcohol dehydrogenase	110	24 h	134	61	6	8.5/7.55	39.83/38.00
gi|295662360 - Mannitol-1-phosphate 5-dehydrogenase	102	6 h	138	26	1	6.44/5.66	41.5/43.12

gi|295666179 - 2- Methylcitrate synthase	73	6 h	127	66	12	9.23/9.02	47.17/51.52
gi|295666197 - 2-Methylcitrate dehydratase	59	6 h	**	**	3	7.72/8.55	51.67/62.26
gi|295672652 - Bifunctional purine biosynthesis protein ADE17	39	24 h	98	20	1	8.15/6.70	62.83/67.2
gi|295672652 - Bifunctional purine biosynthesis protein ADE17	47	24 h	153	29	2	7.26/6.70	56.17/67.2
gi|295665468 - Nucleic acid-binding protein	130	24 h	79	26	**	6.70/9.40	30.0/30.41
gi|295665468 - Nucleic acid-binding protein	131	24 h	101	41	**	7.18/9.40	30.0/30.41
gi|295666938 - Nucleoside diphosphate kinase	147	6 h	187	71	**	7.89/6.84	17.5/16.88
gi|225681397 - Conserved hypotetical protein	129	24 h	78	50	**	4.93/5.25	32.33/23.11
gi|295665131 - Delta-1-pyrroline-5-carboxylate dehydrogenase	53	24 h	**	**	1	8.25/7.68	54.0/62.9
gi|225683481 - Cysteinyl-tRNAsynthetase	15	24 h	81	22	**	6.18/6.09	95.5/89.20
gi|295672027 - Glycine dehydrogenase	3	24 h	106	36	5	7.64/8.84	115.0/129.88
gi|295668479 - Formamidase	72	24 h	**	**	5	7.02/6.06	47.17/46.10
gi|295674273 - Acetolactate synthase	38	6 h	95	35	5	7.81/8.93	62.83/74.16
gi|295674767 - 4-aminobutyrate aminotransferase	66	6 h	75	29	**	8.98/9.21	50.5/32.28
gi|295668370 - Aminopeptidase	11	24 h	158	58	6	5.41/6.20	100.67/73.39
gi|295661139 - Methylmalonate-semialdehyde dehydrogenase	44	6 h	168	51	8	8.17/8.99	57.67/63.11
gi|295658698 - Fumarylacetoacetase	74	24 h	99	26	2	6.36/5.95	45.83/46.7
gi|295667902 - Aminomethyltransferase	76	24 h	110	31	**	8.44/9.59	45.5/53.1
gi|295669670 - Adenosylhomocysteinase	77	6 h	129	26	1	6.76/5.83	45.17/49.0
gi|295669240 - Kynurenine-oxoglutarate transaminase	84	6 h	82	39	6	6.54/7.05	44.0/50.88
gi|295662426 - Aspartate aminotransferase	96	6 h	88	30	5	8.46/8.39	42.5/50.91
gi|295662426 - Aspartate aminotransferase	100	24 h	89	26	**	8.83/8.39	42.0/50.91
gi|295672504 - Inorganic pyrophosphatase	2	24 h	99	59	4	7.0/5.13	115.67/33.55
gi|295672504 - Inorganic pyrophosphatase	98	24 h	121	61	**	4.82/5.13	42.0/33.55
gi|295672504 - Inorganic pyrophosphatase	125	6 h	187	63	11	4.84/5.13	36.5/33.55
gi|225678712 - Ketol-acid reductoisomerase	104	6 h	192	60	10	7.92/9.12	40.83/44.86

gi|226294930 - Ketol-acidreductoisomerase	136	24 h	**	**	1	7.92/9.12	26.0/44.8
gi|295658312 - L-PSP endoribonuclease family protein (Hmf1)	152	6 h	77	46	1	5.98/8.96	15.17/18.72
gi|295670601 - 3-hydroxyisobutyryl-CoA hydrolase	56	24 h	80	62	**	6.30/7.09	53.17/57.35
gi|295657225 - Peroxisomal multifunctional enzyme	12	24 h	93	38	**	9.37/8.98	100.33/97.15
gi|295657225 - Peroxisomal multifunctional enzyme	21	6 h	**	**	2	9.59/8.98	86.33/97.15
gi|295665414 - Short chain dehydrogenase family protein	137	6 h	63	18	**	6.62/6.77	25.67/32.09
gi|295666416 - Short-chain-fatty-acid-CoA ligase	124	6 h	51	11	**	8.82/7.09	36.67/55.37
gi|295666416 - Short-chain-fatty-acid-CoA ligase	144	6 h	51	11	**	6.55/7.09	20.33/55.37
gi|295666416 - Short-chain-fatty-acid-CoA ligase	151	6 h	46	11	**	3.96/7.09	15.33/55.37
gi|295668707 - Acetyl-CoA acetyltransferase	97	24 h	**	**	1	7.85/8.98	42.33/46.6
gi|295668707 - Acetyl-coA acetyltransferase	99	6 h	**	**	4	8.09/8.98	42.0/46.65
gi|295664927 - ATP-citrate-lyase	64	6 h	**	**	3	6.91/5.99	50.67/52.9
gi|295664927 - ATP citrate lyase	62	24 h	**	**	1	6.73/5.99	51.17/52.9
gi|295658821 - ATP synthase subunit beta	67	6 h	233	57	18	4.54/5.28	50.33/55.18
gi|295658923 - Citochrome b-c1 complex subunit 2	89	6 h	138	45	5	8.92/9.10	43.17/49.01
gi|295669073 - 12-oxophytodienoate reductase	92	24 h	250	71	13	9.31/8.69	42.83/43.25
gi|295657369 - Nicotinate-nucleotide pyrophosphorylase	119	24 h	101	33	1	7.56/6.55	37.67/33.7
gi|295660716 - UDP-galactopyranose mutase	51	24 h	100	22	**	7.82/6.81	54.5/58.3
gi|295661741 - 3- demethylubiquinone 9,3-methyltransferase	149	24 h	96	40	**	4.74/4.93	17.0/22.42
gi|295660455 - Pyridoxine biosynthesis protein PDX1	105	24 h	94	70	**	6.26/6.04	40.67/34.41
gi|295663887 - 40S ribosomal protein S19	146	6 h	129	80	5	10.45/9.69	17.67/16.41
gi|295663887 - 40S ribosomal protein S19	148	24 h	121	77	**	10.32/9.69	17.33/16.41
gi|295664112 - 40S ribosomal protein S22	150	24 h	94	92	**	10.50/9.99	16.0/14.73
gi|295672445 - Alanyl-tRNA synthetase	8	24	242	50	10	5.67/5.52	104.33/108.48
gi|295666766 - Vacuolar aminopeptidase	48	24 h	62	18	**	6.17/5.75	55.33/56.65
gi|295657201 - Glutamate carboxypeptidase	50	6 h	**	**	5	5.81/6.23	54.83/64.62

gi|295674421 - Ubiquitin carboxyl-terminal hydrolase	5	24 h	154	46	4	5.21/5.33	111.67/88.03
gi|295660102 - Dipeptidyl- peptidase	28	24 h	226	66	**	7.21/7.99	73.50/86.55
gi|295662102 - Rab GDP-dissociation inhibitor	52	6 h	158	64	9	5.64/5.44	54.33/52.54
gi|295657091 - Tropomyosin-1	140	6 h	80	50	1	4.52/4.99	23.0/18.83
gi|295673184 - Actin-interacting protein	109	24 h	93	23	1	7.53/6.48	40.0/65.9
gi|295669061 - Arp2/3 complex subunit Arc16	120	6 h	**	**	5	7.13/5.87	37.5/36.15
gi|295669061 - Arp2/3 complex subunit Arc16	106	24 h	**	**	2	6.87/5.87	40.5/36.15
gi|295660405 - Hypotetical protein	155	6 h	152	64	7	9.26/10.06	13.33/14.97
gi|295661500 - Conserved hypothetical protein	114	24 h	**	**	2	7.28/6.36	38.5/33.1
gi|295673506 - Conserved hypothetical protein	154	24 h	113	95	6	5.3/5.36	13.33/13.55
gi|295659253 - Conserved hypothetical protein	139	24 h	86	61	**	4.81/5.15	23.67/17.35

**Spots visualized only in zinc-depleted or zinc replete conditions;
[a]GenBank general information identifier**;**
[b]Spot numbers as depicted in Fig 2;
[c] Time of exposure to zinc starvation;
[d]Mascot score;
[e]Amino acid sequence coverage for the identified protein;
[f]Number of matched peptides on MS/MS searching;
[g]Experimental/theoretical isoelectric point;
[h]Experimental/theoretical molecular weight;

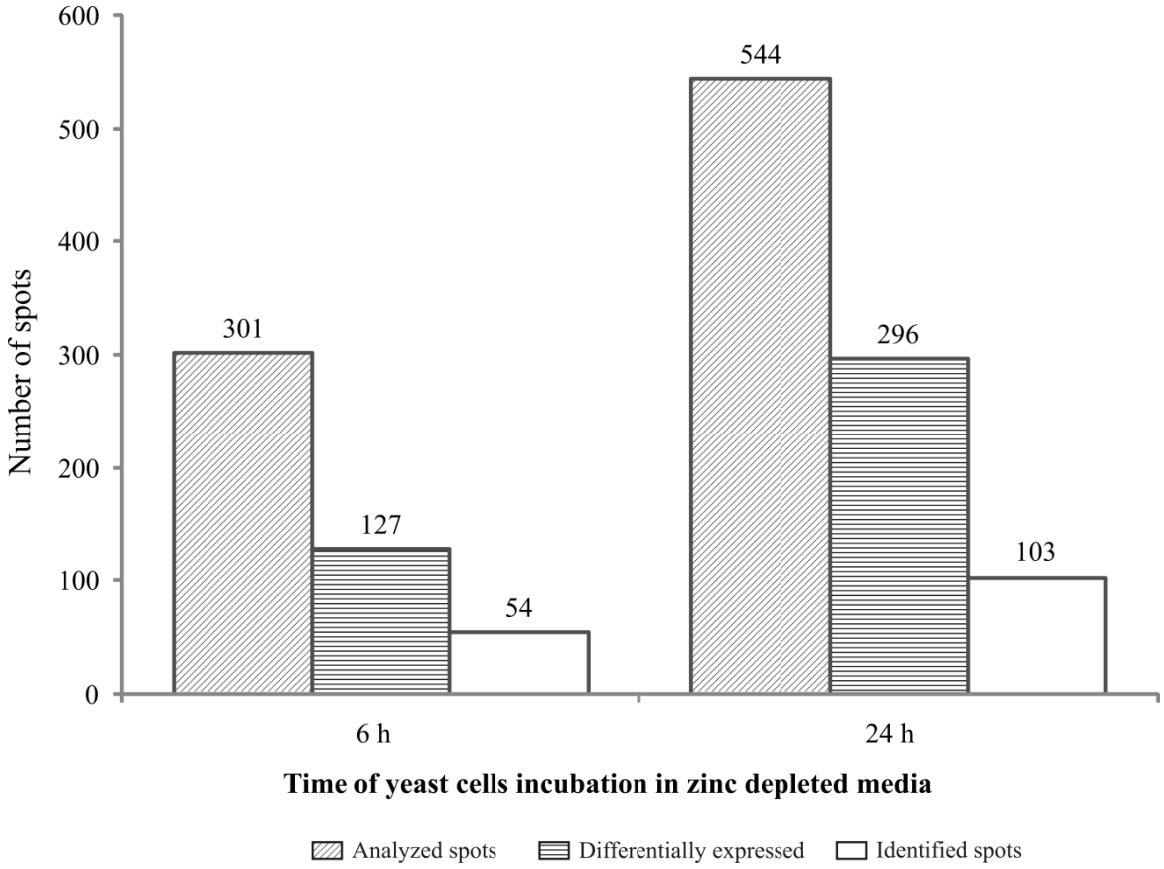

Fig S1. Graphic summation of *Paracoccidioides* zinc restriction proteomic analysis. Number of spots differentially expressed was determined using 2D-gel image analysis software. Statistical analyses of the matched proteins/spots were performed using ANOVA.

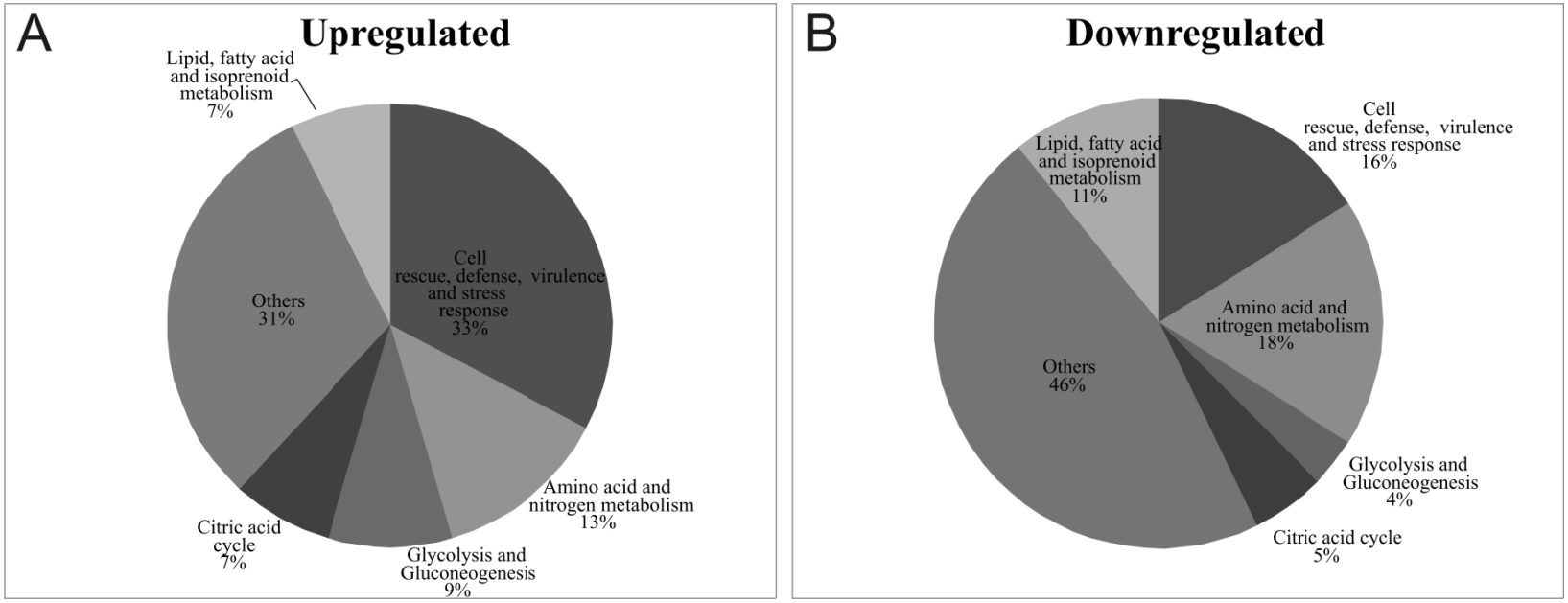

Fig S2.Categorical representation of regulated *Paracoccidioides* proteins following zinc starvation. Identified proteins were classified according FunCat2. Classification of proteins with induced (A) and repressed expression (B) in zinc limiting condition.

2. ARTIGOS EM COLABORAÇÃO

RESEARCH ARTICLE

Characterization and functional analysis of the β-1,3-glucanosyltransferase 3 of the human pathogenic fungus *Paracoccidioides brasiliensis*

Nadya da Silva Castro[1], Kelly Pacheco de Castro[1], Ivan Orlandi[2], Luciano dos Santos Feitosa[3], Lívia Kmetzsch Rosa e Silva[4], Marilene Henning Vainstein[4], Sônia Nair Báo[5], Marina Vai[2] & Célia Maria de Almeida Soares[1]

[1]Laboratório de Biologia Molecular, Instituto de Ciências Biológicas, Universidade Federal de Goiás, Goiânia, Goiás, Brazil; [2]Dipartimento di Biotecnologie e Bioscienze, Università degli Studi di Milano-Bicocca, Milan, Italy; [3]Disciplina de Microbiologia, Imunologia e Parasitologia, Universidade Federal de São Paulo, São Paulo, Brazil; [4]Centro de Biotecnologia, Universidade Federal do Rio Grande do Sul, Porto Alegre, Brazil; and [5]Laboratório de Microscopia Eletrônica, Universidade de Brasília, Brasília, Brazil

Correspondence: Célia Maria de Almeida Soares, Laboratório de Biologia Molecular, Instituto de Ciências Biológicas 2, Campus 2, Universidade Federal de Goiás, 74001-970 Goiânia, Goiás, Brazil. Tel.:/fax: +55 62 3521 1110; e-mail: celia@icb.ufg.br

Received 17 April 2008; revised 30 September 2008; accepted 17 October 2008.
First published online 8 December 2008.

DOI:10.1111/j.1567-1364.2008.00463.x

Editor: José Ruiz-Herrera

Keywords
Paracoccidioides brasiliensis; β-1,3-glucanosyltransferase; glycosylphosphatidylinositol anchored; cell wall biosynthesis.

Abstract

The fungus *Paracoccidioides brasiliensis* causes paracoccidioidomycosis, a systemic granulomatous mycosis prevalent in Latin America. In an effort to elucidate the molecular mechanisms involved in fungus cell wall assembly and morphogenesis, β-1,3-glucanosyltransferase 3 (*Pb*Gel3p) is presented here. *Pb*Gel3p presented functional similarity to the glucan-elongating/glycophospholipid-anchored surface/pH-regulated /essential for pseudohyphal development protein families, which are involved in fungal cell wall biosynthesis and morphogenesis. The full-length cDNA and gene were obtained. Southern blot and *in silico* analysis suggested that there is one copy of the gene in *P. brasiliensis*. The recombinant *Pb*Gel3p was overexpressed in *Escherichia coli*, and a polyclonal antibody was obtained. The *PbGEL3* mRNA, as well as the protein, was detected at the highest level in the mycelium phase. The protein was immunolocalized at the surface in both the mycelium and the yeast phases. We addressed the potential role of *Pb*Gel3p in cell wall biosynthesis and morphogenesis by assessing its ability to rescue the phenotype of the *Saccharomyces cerevisiae gas1*Δ mutant. The results indicated that *Pb*Gel3p is a cell wall-associated protein that probably works as a β-1,3-glucan elongase capable of mediating fungal cell wall integrity.

Introduction

Paracoccidioides brasiliensis is a thermally dimorphic fungus that causes paracoccidioidomycosis, a systemic mycosis with a broad distribution in Latin America. Mycelia airbone propagules are inhaled and converted to the yeast form in the host lung, establishing the infection. The disease presents diverse clinical forms, ranging from asymptomatic pulmonary to severely disseminated and lethal infection (Restrepo *et al*., 2001).

The cell wall plays an essential role in the pathobiology of *P. brasiliensis*, because it is directly linked to the morphogenetic changes during phase transition. The fungal growth requires continuous remodeling of the cell wall polysaccharide network. Mycelium to yeast transition is characterized by a threefold increase in chitin content, as well as by a change of glucose polymer glucoside bonds, arranged only as β-1,3-glucan in the mycelium and mainly as α-1,3-glucan in the pathogenic yeast form (San-Blas & San-Blas, 1977). In this respect, studies on the fungal cell wall as well as the enzymes involved in cell wall biosynthesis and recycling provide excellent information for the design of antifungal drugs and for new preventive approaches.

Despite all the information accumulated about the cell wall structure, the enzymes responsible for its remodeling are still largely unknown, especially for *P. brasiliensis*. Several evidences suggest that for glucan-elongating protein (Gel), through its β-1,3-glucanosyltransferase activity, plays a role in the cross-linking of cell wall components in fungi (Popolo & Vai, 1999; Mouyna *et al*., 2000a). Gel1p of *Aspergillus fumigatus* (*Af*Gel1p) catalyzes *in vitro* a two-step β-1,3-glucanosyltransferase reaction: (1) first, an internal

glycosidic linkage of a donor β-1,3-glucan chain is cleaved and the reducing portion is released, (2) then the new reducing end is transferred to the nonreducing end of an acceptor β-1,3-glucan chain. Therefore, the generation of a new β-1,3-linkage between the acceptor and the donor molecule results in the elongation of β-1,3-glucan on branching points of other glucans, creating multiple anchoring sites for mannoproteins, chitin or for galactomannans. Thus, β-1,3-glucanosyltransferases act in a manner similar to glycoside hydrolases (GHs) in the first step, but a carbohydrate is preferred over a water molecule in the second one (Mouyna *et al.*, 2000a, b, 2005; Ragni *et al.*, 2007b). Despite the role of *Af*Gel1p in the cell wall architecture, as mentioned above, no descriptions are found for Gel3p.

Gelp(s) are homologous to the glycophospholipid-anchored surface (Gas)/pH-regulated (Phr)/essential for pseudohyphal development (Epd), which are present in yeast species, fungi and human fungal pathogens (Saporito-Irwin *et al.*, 1995; Mühlschlegel & Fonzi, 1997; Nakazawa *et al.*, 1998, 2000; Mouyna *et al.*, 2005; Ragni *et al.*, 2007b), but not in mammalian cells (Klis, 1994). All these members are clustered in the GH72 family in the carbohydrate active enzymes database (CAZy) of GHs (http://www.cazy.org/fam/GH72.html).

The *Sc*Gas1, *Ca*Phr1 and *Ca*Phr2 proteins of *Saccharomyces cerevisiae* and *Candida albicans*, respectively, and more recently *Af*Gel2p, a paralogue of *Af*Gel1p, share the same catalytic residues and exhibit the same *in vitro* activity (Mouyna *et al.*, 2000a, b, 2005). Moreover, *Af*Gel1, *Af*Gel2 and *Ca*Phr1 restore the defective phenotype of an *S. cerevisiae gas1* null mutant, indicating that these homologues are not only structurally but also functionally similar (Vai *et al.*, 1996; Mouyna *et al.*, 2000a, 2005). These proteins not only play an active role in the biosynthesis and morphogenesis by the correct incorporation of glucan molecules into the cell wall but are also required for virulence in *C. albicans* and *A. fumigatus* in a murine model of infection (Ghannoum *et al.*, 1995; Mouyna *et al.*, 2005), as well as in *Fusarium oxysporum* during plant infection (Caracuel *et al.*, 2005).

In this paper, we described the first functional study of a Gel3p in pathogenic fungi. Our results indicated that *Pb*Gel3p is more abundant in the mycelium phase and is associated with the fungus cellular surface. Genetic complementation studies with the *S. cerevisiae gas1* mutant demonstrated that *Pb*Gel3p is able to participate in the maintenance of fungal cell wall integrity by its ability to restore the Gas1p activity.

Materials and methods

Fungal strains and growth conditions

Paracoccidioides brasiliensis, isolate *Pb*01 (ATCC-MYA-826), which is standard to the studies in our laboratory (Bastos *et al.*, 2007), and isolate from armadillo (*Pb*Ar) previously identified by Bagagli *et al.* (2003) were used in this work. It was grown in semisolid Sabouraud medium as mycelium or yeast at 22 and 36 °C, respectively. The cells were maintained in liquid Sabouraud medium for 18 h before varying the culture temperature from 22 to 36 °C for the mycelium to yeast transition, which was maintained for 24 h.

The *S. cerevisiae* null mutant WB2d (*gas1*Δ::*LEU2*), a derivative of W303-1B (*MAT*α *ade2-1 his3-11,15 leu2-3,112 trp1-1 ura3-1 can1-100*), was constructed in a previous study (Vai *et al.*, 1996) and was the host strain for complementation experiments. Yeast cells were grown in batches at 30 °C in Difco yeast nitrogen base medium without amino acids (YNB − aa, 6.7 g L^{-1}) containing glucose or galactose at 2% (w/v) and the required supplements. Buffered media were prepared by adding MES (10 g L^{-1}) to YNB medium, followed by pH adjustment to 5.5 or 6.5. During growth, the pH was monitored and never varied by more than 0.1. Cell number was determined on mildly sonicated and diluted samples using a Coulter counter particle count and size analyser, model Z2, as described previously (Vanoni *et al.*, 1983). Specific growth rates and duplication times (T_d) were obtained by fitting the cell number against time.

Recombinant DNA procedures and plasmids

Paracoccidioides brasiliensis yeast cells were harvested, washed and frozen in liquid nitrogen. Grinding with a mortar and pestle broke the cells, and the genomic DNA was prepared by the cationic hexadecyl trimethyl ammonium bromide method according to Del Sal *et al.* (1989). *Paracoccidioides brasiliensis* genomic DNA was used as a template for the PCR amplification of a partial fragment encoding the *Pb*Gel3p. The Gel3-S-1 (5′-CATCGATACCCTTG CCCCTTAC-3′) and Gel3-AS-1 (5′-CATAGATATTTGTT TGGGGTTGG-3′) oligonucleotide primers were designed based on the partial *PbGEL3* sequence found in the *P. brasiliensis* ESTs available at the GenBank database (Felipe *et al.*, 2003). The PCR reaction was conducted in a total volume of 25 μL containing 20 ng of DNA as a template. The resulting 752-bp product was subcloned into pGEM-T-Easy (Promega) and sequenced.

Southern blot analysis was performed on total DNA (25 μg) digested with the restriction enzymes XhoI, DraI, EcoRV, HindIII and SalI. Standard conditions for electrophoresis were used (Sambrook & Russell, 2001). The blot was probed to the 752-bp *PbGEL3* genomic fragment labeled using the Gene Images Random Prime labeling module (GE Healthcare) and washed under high-stringency conditions according to the manufacturer's instructions. Hybridization was detected by a Gene Image CDP-Star detection module (GE Healthcare).

Cloning of the cDNA and genomic sequences encoding *Pb*Gel3p

A *P. brasiliensis* yeast phase cDNA library was constructed into EcoRI/XhoI sites of λ Zap II (Stratagene, LaJolla, CA) (Felipe *et al.*, 2003). The screening of this library was performed using the 752-bp PCR fragment radiolabeled with [α-^{32}P]dCTP. Plating 5×10^6 PFU, DNA transfer to membranes and hybridization were performed as described in standard procedures (Sambrook & Russell, 2001). Three positive clones were obtained and phage particles were released from the plaques. The *in vivo* excision of pBluescript phagemids (Stratagene) in *Escherichia coli* XL1 blue Minus Restriction (MRFs) was performed.

The *PbGEL3* complete genomic sequence was obtained by PCR amplification of the total DNA of *P. brasiliensis*. The Gel3-S-2 (5′-CTCTCCAACCTCTCCAACCTCTCTC-3′) and Gel3-AS-2 (5′-ACACAATCACATCCCCTCCATCTCAC-3′) primers were constructed based on the cDNA sequence. The PCR reaction was performed with 20 ng of total DNA of *P. brasiliensis*. An amplified PCR product of 2199 bp was gel purified, subcloned into pGEM-T-Easy vector (Promega) and sequenced.

DNA sequencing and sequence analysis

The nucleotide sequences were determined on both strands by the dideoxy chain terminator method using a MegaBace® 1000 sequencer (GE Healthcare). The obtained sequences were translated and compared with all nonredundant polypeptides in the translated GenBank (http://www.ncbi.nlm.nih.gov) database. Amino acid analyses were performed using the PROSITE (http://us.expasy.org/prosite), PSORT II (http://www.psort.org/) databases and the big-PI fungal predictor (http://mendel.imp.univie.ac.at/gpi/fungi/gpi_fungi.html) (Eisenhaber *et al.*, 2004) algorithm. The GenBank/EMBL/DDBJ accession numbers for the *PbGEL3* sequences reported in this paper are AY324033 (cDNA) and DQ534494 (genomic).

Quantitative real-time PCR (QRT-PCR)

Total RNA of *P. brasiliensis* mycelium, mycelium during transition to yeast and yeast cells of *Pb*01 and *P. brasiliensis* isolated from armadillo (*Pb*Ar) was obtained. The fungal cells were harvested and frozen in liquid nitrogen, followed by grinding with a mortar and pestle. After addition of glass beads, the RNAs were extracted using Trizol (Invitrogen) according to the manufacturer's instructions. The quality of RNA was assessed using the $A_{260\,nm}/A280_{\,nm}$ ratio, and by visualization of rRNA on 1.2% (w/v) agarose gel electrophoresis. In this case, a densitometric analysis of the ethidium bromide-stained bands of the different rRNA species was performed and the rRNA was calculated. The larger species was more intense than the 18S species, as described by Uppuluri *et al.* (2007). The RNAs were used to construct single-stranded cDNAs using a reverse transcription system (Promega) following the recommendations of the manufacturer. As a control for genomic contamination, the same reactions were performed in the absence or presence of reverse transcriptase.

RNAs from *P. brasiliensis* were extracted and first-strand cDNAs were synthesized as described above. QRT-PCR reactions were performed in an ABI PRISM 7500 Sequence Detection System. The PCR thermal cycling conditions were as follows: an initial step at 50 °C for 2 min, followed by 5 min at 95 °C, and 40 cycles at 95 °C for 15 s, 60 °C for 10 s and 72 °C for 15 s. The Platinum SYBR Green qPCR Supermix (Invitrogen) was used as a reaction mixture, with addition of 10 pmol of each primer and 1 μL of template cDNA, in a final volume of 25 μL. Each cDNA sample was analyzed in triplicate with each primer pair. A melting curve analysis was performed at the end of the reaction to confirm a single PCR product. The data were normalized with ribosomal protein L34 (Andrade *et al.*, 2006; Bastos *et al.*, 2007) and ribosomal protein S30 cDNAs amplified in each set of QRT-PCR experiments. No statistical difference between these two normalizers was observed. Accordingly, the calibrator gene considered for the expression experiments was the one encoding L34 protein. The relative expression data were obtained using the $2^{-\Delta\Delta C_T}$ method (Livak & Schmittgen, 2001). A nontemplate control with no genetic material was included to eliminate contamination or nonspecific reactions. The QRT-PCR primers for each gene were as follows: Gel3, 5′-CGTTGTCAGCGGAGGTATCG TC-3′ and 5′-AGGGCAGGTTCGGAGTTCAGTG-3′; L34, 5′- CGGCAACCTCAGATACCTTC-3′ and 5′-GGAGACCT GGGAGTATTCACG-3′.

Expression and purification of recombinant *Pb*Gel3p

The cDNA of *PbGEL3* that encodes amino acids 19–529 (predicted mature protein; see Fig. 1) was subcloned into the pGEX-4T-3 (GE Healthcare). EcoRI/XhoI restriction sites (underlined) were introduced into the Gel3-S-3 (5′-GA ATTCCGCTGACCTGGATCCTATTGTC-3′) and Gel3-AS-3 (5′-CTCGAGTTACAACAACAAAATACTCATC-3′) oligonucleotides for the DNA synthesis. The obtained plasmid was sequenced in both strands and used to transform *E. coli* BL21 pLysS. The recombinant *P. brasiliensis* Gel3 protein (r*Pb*Gel3p) was induced with 0.1 mM IPTG and purified by affinity chromatography, as reported previously (Castro *et al.*, 2008).

Antibody production

Polyacrylamide gel containing 100 μg of the r*Pb*Gel3p was injected into rabbit three times at 10-day intervals

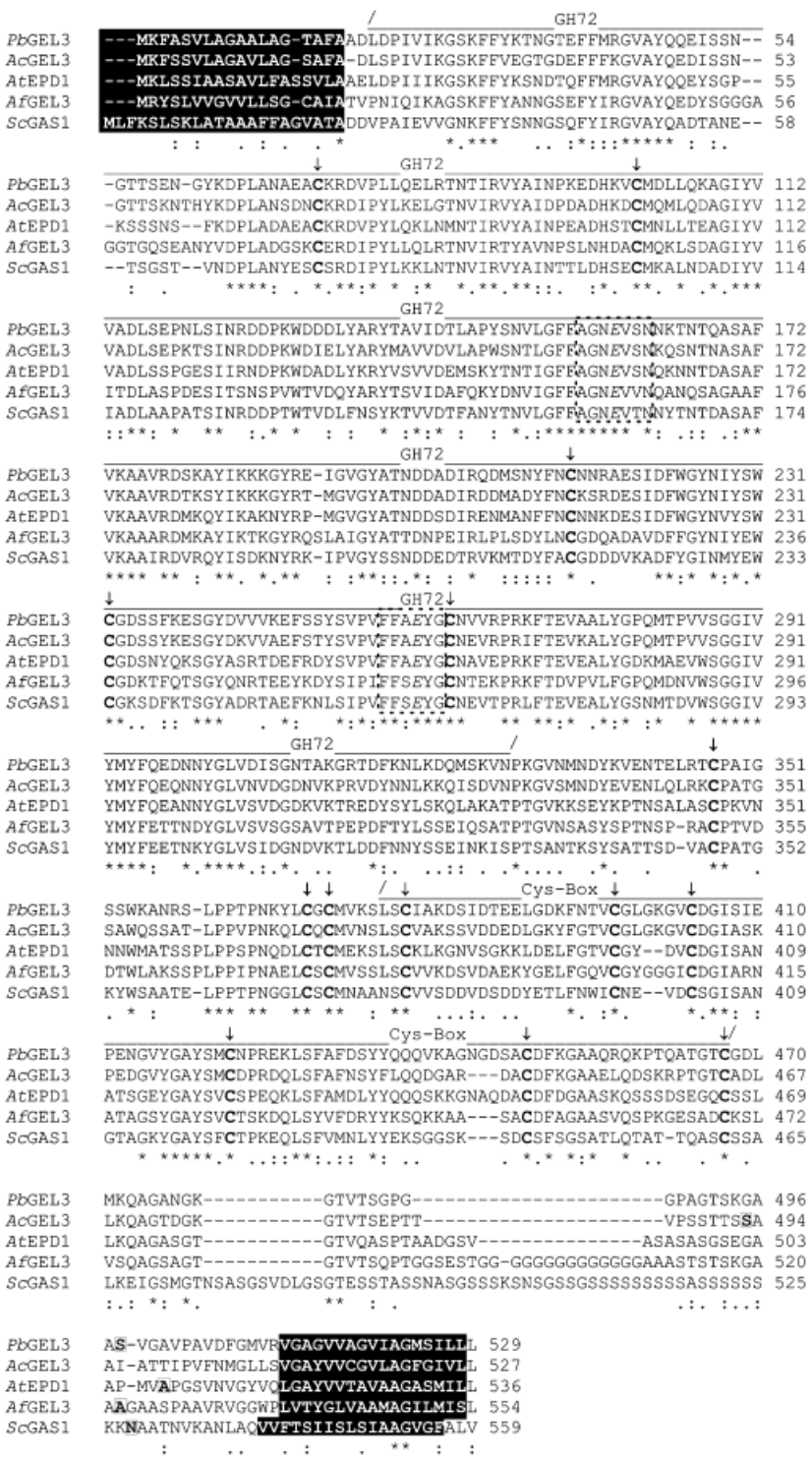

Fig. 1. Comparison of the deduced amino acid sequence of *Pb*Gel3p with those of β-1,3-glucanosyltransferases from fungi. Asterisks indicate amino acid identity and dots represent conserved substitutions. The hydrophobic amino and carboxy termini are indicated by white letters and black blocks. Conserved catalytic motifs are boxed (dotted lines) and the conserved glutamate residue into the catalytic site is detached by italic letters. Fourteen aligned cysteine residues are indicated by arrows and bold letters. Predicted glycosylphosphatidylinositol anchor sites in the C-terminal regions are boxed (solid lines). The GH72 and Cys-Box domains are indicated above the amino acid sequences. Accession numbers were as follows: *Ajellomyces capsulatus* (*Ac*Gel3, XP_001539818); *Aspergillus terreus* (*At*Epd1, XP_001212455); *Aspergillus fumigatus* (*Af*Gel3, AAF40140); and *Saccharomyces cerevisiae* (*Sc*Gas1, CAA89140).

to generate specific rabbit polyclonal serum. Both rabbit preimmune and immune serum (containing anti-r*Pb*Gel3p polyclonal antibody) were sampled and stored at $-20\,^{\circ}C$.

Western blotting analysis

Paracoccidioides brasiliensis protein extracts were obtained by disruption of frozen cells in the presence of protease

inhibitors. The mixture was centrifuged at 12 000 ***g*** at 4 °C for 15 min, and the supernatant was used. Sodium dodecyl sulfate polyacrylamide gel electrophoresis (SDS-PAGE) was carried out and the proteins (30 μg) were electrophoretically transferred to a nylon membrane, according to standard protocols. *Pb*Gel3p was detected with the polyclonal antibody (1 : 1000 diluted). The reaction was revealed with 5-bromo-4-chloro-3-indolylphosphate/nitroblue tetrazolium. Negative controls were obtained with rabbit preimmune serum.

Protein extracts from *S. cerevisiae* cells, prepared as described in (Mouyna *et al*., 2005), were resolved by SDS-PAGE on 8% polyacrylamide gels. After blotting, filters were stained for total protein with Ponceau Red (Sigma) before immunolabeling, which was performed using anti-*Pb*Gel3p antibody (1 : 1000 diluted). Binding was visualized with the ECL Western Blotting Detection Reagents (GE Healthcare).

Confocal analysis

The cellular localization of the *Pb*Gel3p was performed as described by Batista *et al*. (2006). Images of diamidino-2-phenylindole-stained cells were observed in a Bio-Rad 1024 UV confocal system attached to a Zeiss Axiovert 100 microscope, using a × 40 numerical aperture, a 1.2 plan-apochromatic differential interference contrast water immersion objective. All images were collected by Kalman averaging at least every eight frames (512 × 512 pixels), using an aperture (pinhole) of 2 mm.

Transmission electron microscopy of *P. brasiliensis* yeast cells and immunocytochemistry of the Gel3p

For the ultrastructural and immunocytochemistry studies, we used the protocols described previously in Barbosa *et al*. (2006). The ultrathin sections were incubated with the polyclonal antibody to the r*Pb*Gel3p (diluted 1 : 100), washed and then incubated with the labeled secondary antibody (anti-mouse IgG, Au conjugated, 10 nm average size; 1 : 20 diluted). The grids were observed with a Jeol 1011 transmission electron microscope (Jeol, Tokyo, Japan). Controls were incubated with mouse preimmune serum (1 : 100 diluted).

Saccharomyces cerevisiae genetic procedures

For ectopic expression of *P. brasiliensis PbGEL3* in *S. cerevisiae*, a 2-kb HindIII/XhoI fragment containing the *PbGEL3* cDNA and its 5′ and 3′ untranslated regions was cloned into HindIII/XhoI-digested pYES2 (Invitrogen) under the control of the *GAL1* promoter. The resulting plasmid was used to transform the WB2d strain. The transformed strain is indicated throughout the text as YGEL3. For ectopic expression of *S. cerevisiae GAS4*, the whole coding sequence of *GAS4* plus 203 bases downstream was PCR-amplified from yeast chromosomal DNA and fused with the PCR-amplified promoter region of *S. cerevisiae GAS1* to obtain expression in vegetative growth. PCR amplifications were carried out using specific primers where appropriate restriction sites were introduced at the extremes to facilitate fusion and cloning. PCR products were first subcloned into the pGEM-7Zf(+) (Promega), generating the pG4 plasmid, and then into the high-copy YEp24 vector. The latter resulting vector was introduced into WB2d, generating the YGAS4 strain. PCR products were routinely checked by sequence analysis. The sequences of all the oligonucleotide primers used for PCR are available upon request. Standard methods were used for DNA manipulation and yeast transformation (Hill *et al*., 1991; Sambrook & Russell, 2001).

Light and fluorescence microscopy

Saccharomyces cerevisiae cellular morphology was examined by Nomarski phase-contrast microscopy. Chitin was visualized after staining with calcofluor white (CW; Fluorescent Brightener 28, Sigma-Aldrich) as reported (Cipollina *et al*., 2007) under a Nikon Eclipse E600 fluorescence microscope equipped with a Leica DC 350F ccd camera.

Statistical analysis

Duplication time values are presented as means ± SDs. Pairwise comparisons between duplication times were made for mean values of the different strains using Student's *t*-test. The level of statistical significance was set at a P value of ≤ 0.01.

Sensitivity assay

To determine the sensitivity of the different strains to SDS and to CW, yeast cells exponentially growing in galactose medium (pH 6.5) were dropped (5 μL from a concentrated suspension of 10^7 cell mL^{-1} and from serial 10-fold dilutions) onto galactose (pH 6.5) medium plates supplemented with 0.01% (w/v) SDS or 50 μg mL^{-1} of CW. Plates were incubated at 30 °C for 3 days. Cells were also dropped onto plates without SDS and CW to monitor cell growth.

Results

Isolation and sequence analysis of *PbGEL3*

A BLASTX search of the partial *P. brasiliensis* EST available in the GenBank database (Castro *et al*., 2005) revealed an 812-bp ORF that showed a high sequence homology (51% identity, 66% similarity) to *Aspergillus nidulans* β-1,3-glucanosyltransferase 3 (Mouyna *et al*., 2000b). In order to isolate the complete cDNA encoding *Pb*Gel3p, we initially

obtained a genomic PCR product corresponding to the described ORF and used it as a probe to screen a yeast *P. brasiliensis* cDNA library. The entire cDNA consisted of 2057 bp and encoded a 529-amino-acid polypeptide with a theoretical molecular mass of 57.1 kDa and a p*I* of 6.1. The complete genomic sequence was obtained by PCR amplification using oligonucleotide primers complementary to the cDNA sequence. The *PbGEL3* included four introns of 79, 133, 78 and 68 bp (data not shown).

The deduced amino acid sequence of *PbGEL3* showed significant homology to Gel3p and all four homologues, Gel/Gas/Phr/Epd, belonging to the GH72 family. The highest sequence similarity and identity were among the Gel3 proteins of *P. brasiliensis*, *Ajellomyces capsulatus*, *Aspergillus terreus* and *A. fumigatus* (Fig. 1) and were most evident within the region of the first 300 amino acids. The PSORT analysis revealed a putative N-terminal signal peptide, with a predicted cleavage site between amino acids 18 and 19 (Fig. 1). The position of the 14 cysteine residues was conserved among the Gel3 proteins shown in Fig. 1. A domain named Cys-Box, which contained six conserved cysteine residues and is present in some members of the GH72 family, was also found in *Pb*Gel3p near the carboxy-terminal region. Two glutamic residues (E^{159} and E^{260}), essential for the enzymatic activity, were conserved in the catalytic domain. The potential glycosylphosphatidylinositol anchor site at S^{498} and a hydrophobic region encompassing residues 512–528 (VGAGVVAGVIAGMSILL) were found at the carboxy terminus (Fig. 1).

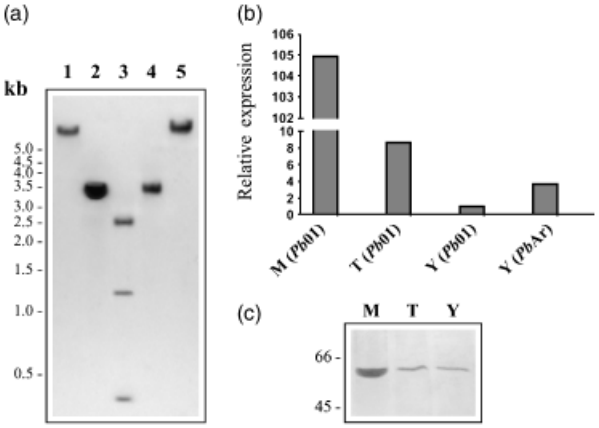

Fig. 2. Analysis of the *Paracoccidioides brasiliensis GEL3* gene organization and evaluation of the expression levels. (a) Southern blot analysis of *PbGEL3*. Total DNA (25 μg) was digested with restriction enzymes XhoI, DraI, EcoRV, HindIII and SalI (lanes 1–5, respectively). The blot was hybridized to a 752-bp *PbGEL3* labeled PCR fragment. (b) QRT-PCR plot of *PbGEL3* expression levels in different phases and isolates. cDNAs derived from mycelium (M), mycelium during 24 h of transition to yeast (T) and yeast (Y) cells of two *P. brasiliensis* isolates, *Pb*01 and *Pb*Ar, are shown. The $\Delta\Delta C_T$ method was used to calculate the relative amount of specific RNA present in each sample relative to the yeast phase of the *Pb*01 isolate (set as 1.0). The *L34* gene was used to normalize each reaction. (c) Western blot analysis of the native *Pb*Gel3p in a cellular extract during the dimorphic transition. The samples from mycelium (M), mycelium during 24 h of transition (T) and yeast (Y) cells were fractionated (12% SDS-PAGE) and transferred to a membrane. The blots were reacted to the rabbit polyclonal anti-r*Pb*Gel3p antibody and developed with 5-bromo-4-chloro-3-indolylphosphate/nitroblue tetrazolium. Molecular size markers are indicated.

Hybridization analysis

Southern blot analysis using a 752-bp *PbGEL3* probe under high-stringency conditions was able to detect a single DNA fragment in the *P. brasiliensis* DNA digested with the restriction enzymes XhoI, DraI, EcoRV, HindIII and SalI (Fig. 2a, lanes 1, 2, 4 and 5, respectively). EcoRV digestion produced fragments consistent, in number and size, with the single restriction site presumed to occur in *PbGEL3* (Fig. 2a, lane 3). The obtained restriction profiles indicated that the *P. brasiliensis* genome contained a single copy of the *PbGEL3* gene. Confirming this suggestion, one copy of the *PbGEL3* gene was detected by *in silico* analysis at the genome project developed by BROAD Institute (http://www.broad.mit.edu/annotation/genome/paracoccidioides_brasiliensis/MultiHome.html).

Transcript analysis by QRT-PCR

Template cDNAs derived from mycelium (M), mycelium during transition to yeast (T) and yeast (Y) cells of the *Pb*01 isolate and of *Pb*Ar isolate were used to estimate the relative transcript levels of the *PbGEL3* by QRT-PCR analysis. The L34 mRNA was chosen as a reference transcript, because the expression of the *L34* gene does not fluctuate significantly during the differentiation of *P. brasiliensis* (Andrade *et al.*, 2006; Bastos *et al.*, 2007). As shown in Fig. 2b, a peak of expression occurred in the mycelium (M) phase, which decreased considerably during 24 h of transition (T), reaching a faint expression in the yeast (Y) phase in the *Pb*01 isolate. The mycelium and transition cells revealed an increase in the transcript level of 104.9- and 8.6-fold, respectively, compared with yeast cells (Fig. 2b). The transcript was also present at low levels in the yeast phase of the *Pb*Ar isolate (Fig. 2b).

Expression, purification and detection of Gel3p in *P. brasiliensis*

The cDNA encoding the *P. brasiliensis* Gel3p was subcloned into the expression vector pGEX-4T-3 to obtain the recombinant fusion protein that was purified by affinity chromatography and cleaved by addition of thrombin (data not shown). Protein extracts from mycelium (M), mycelium during 24 h of transition to the yeast phase (T) and yeast (Y) cells were blotted onto nitrocellulose membranes and

reacted to the polyclonal antibody (Fig. 2c). As demonstrated, a single band of 58 kDa was detected in all extracts. The protein is strongly accumulated in the mycelia phase (Fig. 2c) and its expression is decreased during the transition to yeast (Fig. 2c). No cross-reactivity to the rabbit preimmune serum was evidenced with the samples (data not shown).

Determination of *Pb*Gel3p cellular localization by confocal and immunoelectron microscopy analysis

Representative confocal microscopy images of mycelium (Fig. 3a–d) and yeast (Fig. 3e–h) cells of *P. brasiliensis* showed that anti-r*Pb*Gel3p reacted with the surface and cytoplasmatic components of both phases (Fig. 3d and h). The cell surface fluorescence was clearer in yeast cells (Fig. 3h) due to their definite rounding format and larger size. No cross-reaction was observed with the preimmune serum (Fig. 3b and f).

In order to detail the cellular localization of *Pb*Gel3p, we further performed immunocytochemistry experiments in yeast cells. The cell surface and organelle structures were preserved and free of label when incubated with the rabbit preimmune serum (Fig. 4a). In yeast cells processed by the postembedding method, gold particles were predominantly associated with the cell wall (Fig. 4b and c). The number of gold-labeled particles, counted in five immunocytochemistry assays, was significantly higher in the cell wall ($P < 0.05$) than in the cytoplasmic compartment (data not shown).

PbGEL3 completely suppresses the *S. cerevisiae gas1* disruptant phenotype at pH values above 5

The *PbGEL3* cDNA was expressed, under the control of the *GAL1* promoter, in the *gas1*Δ background and the resulting phenotype was analyzed in galactose-containing medium (inducing condition). Total proteins from the transformed strain were analyzed by immunoblot using the antibody against *Pb*Gel3p. In these cells, a unique band of about 58 kDa was detected that was absent in untranformed cells (Fig. 5a). Moreover, as shown in Table 1, *PbGEL3* partially suppressed the slow growth of *gas1*Δ cells. In fact, cells expressing the *PbGEL3* cDNA (YGEL3 strain) had a T_d of about 2.31 h, an intermediate value between those determined for W303-1B and *gas1*Δ-empty vector strains (T_d of 1.83 and 3.02 h, respectively). A partial reversion was also observed for other phenotypic traits such as abnormal morphology and CW sensitivity (data not shown).

We considered that the partial rescue of the *gas1*Δ mutant phenotype could be ascribed to nonoptimal environmental conditions for *Pb*Gel3p activity as reported recently for Gas2 and Gas4 proteins of *S. cerevisiae*, two redundant versions of Gas1p that are specialized to function at pH values close to neutrality (Ragni *et al.*, 2007a). Thus, we analyzed the YGEL3 phenotype in galactose media buffered to pH 5.5 and 6.5 to avoid acidification that usually takes place following yeast cells' growth (Sigler & Höfer, 1991). At pH 6.5, in theYGEL3 strain, the protein of about 58–60 kDa showed levels comparable to those detected in the unbuffered growth medium (Fig. 5a). The same results were obtained for cells grown at pH 5.5 (data not shown). Interestingly, in both buffered media, the YGEL3 strain behaved in a manner similar to *gas1*Δ cells expressing *GAS4* (YGAS4 strain). In fact, under these two growth conditions, *PbGEL3*, like *ScGAS4*, completely rescued growth rate defects of *gas1*Δ cells (Table 1), whose T_d increased along with the increase in pH. In addition, YGEL3 cells reassumed the ellipsoidal shape and cells carrying two or more buds (pluribudded cells) that are distinctive of *gas1*Δ were absent (Fig. 5b). Moreover, after CW staining for chitin, YGEL3 cells showed definite fluorescence in the bud scars and at the mother–daughter junction. Chitin in cells deprived of Gas1p activity increased and was delocalized (Fig. 5b) as expected. In the *gas1* null mutant, the increase of chitin level determined a hypersensitivity to growth in the presence of CW. Thus, cells exponentially growing in galactose medium (pH

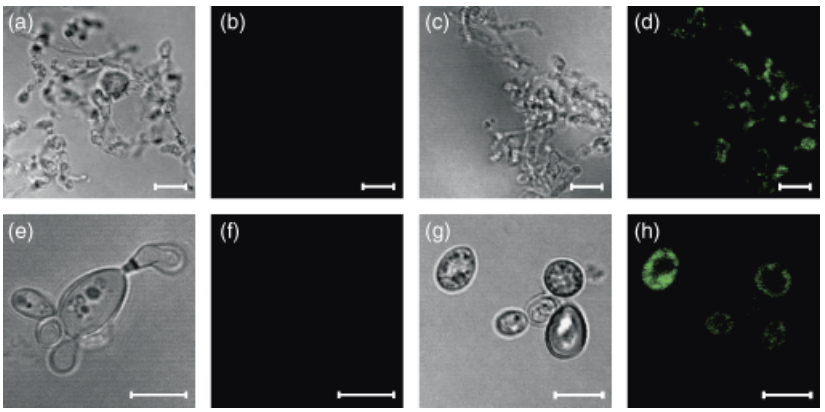

Fig. 3. Distribution of Gel3p in *Paracoccidioides brasiliensis*. (a, c) Mycelium and (e, g) yeast cells using differential interferential contrast microscopy. (b, f) Control systems, without polyclonal antibodies before incubation with fluorescein isothiocyanate-labeled rabbit anti-IgG. Confocal microscopy with antibodies generated against the recombinant GST-*Pb*Gel3p in (d) mycelium and (h) yeast cells. Labeling of *P. brasiliensis* was obtained by anti-r*Pb*Gel3p polyclonal antibodies (green). Scale bar = 10 μm.

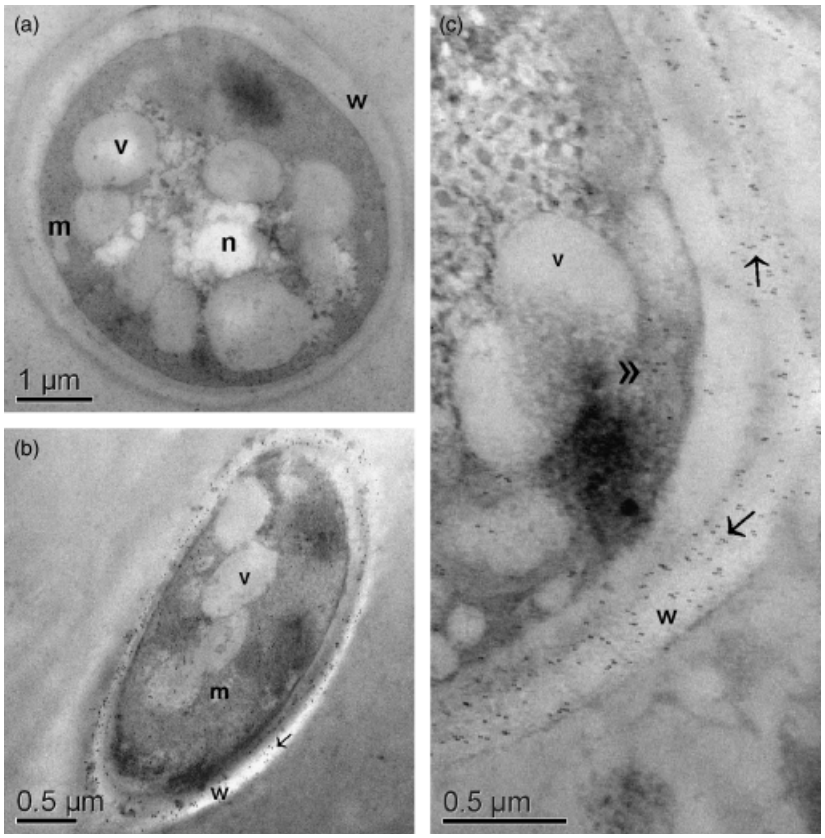

Fig. 4. Immunoelectron microscopy detection of Gel3p in *Paracoccidioides brasiliensis* yeast cells by postembedding methods. (a) Negative control exposed to the rabbit preimmune serum in transmission electron microscopy of *P. brasiliensis* yeast cells. (b and c) Gold particles are observed at the fungus cell wall (arrow) and in the cytoplasm (double arrowheads). n, nucleus; v, intracytoplasmic vacuoles; m, mitochondria; w, cell wall.

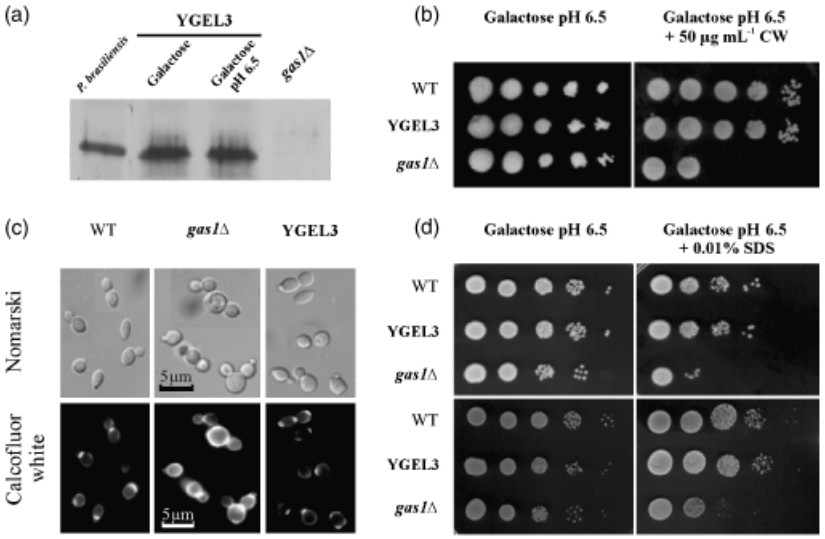

Fig. 5. *Paracoccidioides brasiliensis* Gel3p restores the phenotypic defects of the *Saccharomyces cerevisiae gas1*Δ mutant at pH 6.5. (a) Total extracts from *S. cerevisiae* cells exponentially growing in unbuffered and buffered media were analyzed by immunoblotting with anti-*Pb*Gel3p antibodies. The same amount of proteins (70 µg) was loaded on each lane. A sample from mycelium of *P. brasiliensis* was also loaded as a control. (b) Cellular morphology visualized by Nomarsky (upper panel) and CW staining (lower panel) of exponentially growing yeast cells in galactose medium, pH 6.5. Five microliters from a concentrated suspension (10^7 mL^{-1}) of yeast cells grown as in (b) and from serial 10-fold dilutions were spotted onto galactose medium plates, pH 6.5, with or without CW (c) and with or without SDS (d). WT, wild type.

6.5) were spotted onto plates of the same medium containing 50 µg mL^{-1} of CW or onto plates without it to monitor cell growth. *PbGEL3* completely abolished the CW hypersensitivity of *gas1*Δ cells (Fig. 5c). Similar results were obtained for YGEL4 (data not shown). Finally, we tested the sensitivity to SDS. In fact, *gas1*Δ cells are also hypersensitive to growth in the presence of such an anionic destabilizing detergent, as a consequence of a weakened cell wall (Vai *et al.*, 1996). As shown in Fig. 5d, YGEL3 displayed the same sensitivity to SDS as YGAS4 and the reference wild-type strains.

Table 1. *Paracoccidioides brasiliensis GEL3* abrogates the slow growth phenotype of *Saccharomyces cerevisiae gas1*Δ mutant according to the pH of the growth medium

Growth condition	Strain	T_d (h)*
Galactose medium (unbuffered)	W303-1B	1.83 ± 0.08
	*gas1*Δ	3.02 ± 0.1
	YGEL3	2.31 ± 0.06
	YGAS4	2.33 ± 0.07
Galactose medium (pH 5.5)	W303-1B	2.33 ± 0.11
	*gas1*Δ	4.12 ± 0.12
	YGEL3	2.37 ± 0.09
	YGAS4	2.40 ± 0.12
Galactose medium (pH 6.5)	W303-1B	2.46 ± 0.07
	*gas1*Δ	4.15 ± 0.09
	YGEL3	2.42 ± 0.11
	YGAS4	2.43 ± 0.14

Student's *t*-test was applied for their comparison setting a *P* value of ≤ 0.01.

*The T_d was calculated as ln2/*k*, where *k* is the constant rate of exponential growth. Data represent the average of three independent experiments; SDs are indicated.

Discussion

The mechanisms through which the cell wall proteins of *P. brasiliensis* respond to different environmental conditions remain largely unknown. In an effort to understand the mechanisms that are involved in this fungus cell wall assembly and integrity maintenance, we initially searched for cDNAs encoding homologues of cell wall-associated proteins (Castro *et al.*, 2005). We identified an 812-pb fragment ORF that encodes a homologue of Gel3p of *A. nidulans* (Mouyna *et al.*, 2000b). The full-length cDNA and gene were obtained. The complete *Pb*Gel3p deduced amino acid sequence presented homology to glycosylphosphatidylinositol-anchored Gas/Gel/Phr/Epd proteins, which are plasma membrane and cell wall-associated enzymes, responsible for the elongation of β-1,3-glucan chains and are required for correct morphogenesis in yeast (Mouyna *et al.*, 2000a). All these proteins belong to the GH72 family (CAZy database), whose conformation of the catalytic domain is predicted to assume a TIM-barrel shape (Mouyna *et al.*, 1998; Papaleo *et al.*, 2006). These enzymes, which are organized in characteristic domains, contained basically: (1) a signal peptide and an N-terminal catalytic domain with two conserved glutamate residues identified as essential for catalysis and (2) a hydrophobic attachment signal characteristic of glycosylphosphatidylinositol-anchored proteins in the C-terminus region (Mouyna *et al.*, 2000a, b; Carotti *et al.*, 2004; Ragni *et al.*, 2007b). Nevertheless, in some members of the GH72 family (subfamily 72+), including *Pb*Gel3p, a Cys-box domain can be found that contain six conserved cysteine residues presumably involved in the formation of three disulfide bridges (Palomares *et al.*, 2003; Carotti *et al.*, 2004). This domain is present in some β-1,3-glucanases of plants and it is associated with enzyme activity (Palomares *et al.*, 2003; Barral *et al.*, 2005). Moreover, a previous study revealed that the removal of this domain in *S. cerevisiae* Gas1p totally abolished the enzymatic activity, showing, therefore, that it is essential for the function and stability of the protein (Carotti *et al.*, 2006).

QRT-PCR and Western blot analysis demonstrated the *Pb*Gel3p expression. The transcript and protein levels were more abundant in the mycelium phase. A drastic reduction in both the transcript and the protein was observed during the first 24 h of temperature shift from 22 to 36 °C, reaching low levels in the yeast phase. The mycelium cell wall of *P. brasiliensis* is composed mainly of β-1,3-glucan. In agreement, the *PbGEL3* transcript and protein expression levels described here predominate largely in the mycelium phase. The decrease in expression as the fungus triggers the differentiation to yeast is consistent with transforming to α-glucan when the yeast phase is reached (San-Blas & San-Blas, 1994). The data also suggest a putative role of *Pb*Gel3p in cell wall maintenance and fungal morphology. In fact, this protein family has been described in the plasma membrane (Popolo *et al.*, 1988; Fankhauser & Conzelmann, 1991), as well as covalently linked to the cell wall via a glycosylphosphatidylinositol remnant (De Sampaïo *et al.*, 1999; Yin *et al.*, 2005). The confocal and immunoelectron microscopy analysis confirmed the preferential surface localization of *Pb*Gel3p.

Although the absence of an efficient molecular toolbox for gene disruption in *P. brasiliensis* has limited the functional studies in the organism itself, we addressed the potential role of *Pb*Gel3p in cell wall biosynthesis and morphogenesis by investigating whether it could rescue *in vivo* the *S. cerevisiae gas1*Δ mutant phenotype. In fact, in *S. cerevisiae* the lack of Gas1 β-1,3-glucanosyltransferase activity drastically affects the correct relative proportion and the degree of cross-linking of cell wall constituents (Popolo *et al.*, 1997; Ram *et al.*, 1998). This leads to a detectable mutant phenotype characterized by reduced growth, round-cell morphologies, sensitivity to CW, increased cell wall permeability and secretion (Popolo & Vai, 1999; Vai *et al.*, 2000). We observed that *PbGEL3* was able to partially complement the mutant phenotype of *gas1*Δ in unbuffered medium and fully at higher pH values. Similar results were found for *GAS4* of *S. cerevisiae*, a paralogue of *GAS1*, encoding a protein specialized to function at a pH value close to neutrality (Ragni *et al.*, 2007a). In this growth condition, *PbGEL3* was able to correct the alterations of cell wall constituents due to *GAS1* inactivation, as observed by the ellipsoidal morphology and the T_d similar to that of wild-type cells displayed by YGEL3 cells, by their ability to grow in the presence of CW and SDS and by the quantity

and localization of chitin molecules. This indicates that *PbGEL3* expression abrogates *gas1*Δ structural defects that depend on altered connections between glucans and mannoproteins, which are required to form a selective barrier at the outer surface of the cell wall. On the whole, our results show that *Pb*Gel3p is functional in *S. cerevisiae* and it suppresses both the morphological defects and the compensatory responses induced by the lack of Gas1p. The complete functionality of *Pb*Gel3p is detected at extracellular pH values above 5. This requirement could reflect both the environmental growth conditions of *P. brasiliensis* and the pH of the niches colonized by this dimorphic pathogen. In fact, yeast forms did not grow below pH 3.6; most of the clinical isolate strains require a pH of culture medium above 5.6 and the establishment of yeast infection takes place in host tissues at pH values close to neutrality (Franco, 1986; Sano *et al.*, 1997; Restrepo *et al.*, 2001).

Thus, our results suggest that, similar to Gas1p of *S. cerevisiae*, *Pb*Gel3p can play an active role in biosynthesis and morphogenesis of the *P. brasiliensis* cell wall, especially in mycelium cells, the fungus infective phase. Elucidation of these molecular mechanisms involved in the cell wall assembly of *P. brasiliensis* is important and necessary once the pathogenicity of this fungus appears to be correlated with changes in the cell wall composition, organization and structure that occur during the morphogenetic transition from the mycelium to the yeast form.

Acknowledgements

This investigation at Universidade Federal de Goiás was financially supported by CNPq (Grant no. 505658/2004-6), FINEP (Grant no. 0104077500 and 0106121200), FAPEG and SECTEC-GO. K.P.C. and N.S.C. have a fellowship from CAPES. We thank Gustavo A. Niño-Vega, IVIC, Venezuela, for providing the plasmid pYES2.

References

Andrade RV, Paes HC, Nicola AM *et al.* (2006) Cell organization, sulphur metabolism and ion transport-related genes are differentially expressed in *Paracoccidioides brasiliensis* mycelium and yeast cells. *BMC Genomics* **7**: 208–220.

Bagagli E, Franco M, Bosco SM, Hebeler-Barbosa F, Trinca LA & Montenegro MR (2003) High frequency of *Paracoccidioides brasiliensis* infection in armadillos (*Dasypus novemcinctus*): an ecological study. *Med Mycol* **41**: 217–223.

Barbosa MS, Báo SN, Andreotti PF, Faria FP, Felipe MSS, Feitosa LS, Mendes-Giannini MJ & Soares CMA (2006) Glyceraldehyde-3-phosphate dehydrogenase of *Paracoccidioides brasiliensis* is a cell surface protein involved in fungal adhesion to extracellular matrix proteins and interaction with cells. *Infect Immun* **74**: 382–389.

Barral P, Suárez C, Batanero E, Alfonso C, Alché JD, Rodríguez-García MI, Villalba M, Rivas G & Rodríguez R (2005) An olive pollen protein with allergenic activity, Ole e 10, defines a novel family of carbohydrate-binding modules and is potentially implicated in pollen germination. *Biochem J* **390**: 77–84.

Bastos KP, Bailão AM, Borges CL, Faria FP, Felipe MSS, Silva MG, Martins WS, Fiúza RB, Pereira M & Soares CMA (2007) The transcriptome analysis of early morphogenesis in *Paracoccidioides brasiliensis* mycelium reveals novel and induced genes potentially associated to the dimorphic process. *BMC Microbiol* **7**: 29.

Batista WL, Matsuo AL, Ganiko L, Barros TF, Veiga TR, Freymüller E & Puccia R (2006) The *PbMDJ1* gene belongs to a conserved *MDJ1*/*LON* locus in thermodimorphic pathogenic fungi and encodes a heat shock protein that localizes to both the mitochondria and cell wall of *Paracoccidioides brasiliensis*. *Eukaryot Cell* **5**: 379–390.

Caracuel Z, Martínez-Rocha AL, Di Pietro A, Madrid MP & Roncero MIG (2005) *Fusarium oxysporum gas1* encodes a putative beta-1,3-glucanosyltransferase required for virulence on tomato plants. *Mol Plant Microbe In* **18**: 1140–1147.

Carotti C, Ragni E, Palomares O, Fontaine T, Tedeschi G, Rodriguez R, Latge JP, Vai M & Popolo L (2004) Characterization of recombinant forms of the yeast Gas1 protein and identification of residues essential for glucanosyltransferase activity and folding. *Eur J Biochem* **271**: 3635–3645.

Carotti C, Ragni E, Palomares O, Gissi C, Latgé J, Fontaine T & Popolo L (2006) A Cys-enriched domain related to a novel plant carbohydrate-binding module is essential for the glucantransferase activity of a Phr/Gel/Gas protein subfamily. *8th ASM Conference on Candida and Candidiasis*, p. 94. ASM Press, Washington, DC.

Castro NS, Maia ZA, Pereira M & Soares CMA (2005) Screening for glycosylphosphatidylinositol-anchored proteins in the *Paracoccidioides brasiliensis* transcriptome. *Genet Mol Res* **4**: 326–345.

Castro NS, Barbosa MS, Maia ZA, Báo SN, Felipe MS, Santana JM, Mendes-Giannini MJS, Pereira M & Soares CMA (2008) Characterization of *Paracoccidioides brasiliensis Pb*Dfg5p, a cell-wall protein implicated in filamentous growth. *Yeast* **25**: 141–154.

Cipollina C, Vai M, Porro D & Hatzis C (2007) Towards understanding of the complex structure of growing yeast populations. *J Biotechnol* **128**: 393–402.

Del Sal G, Manfioletti G & Schneider C (1989) The CTAB-DNA precipitation method: a common mini-scale preparation of template DNA from phagemids, phages or plasmids suitable for sequencing. *Biotechniques* **7**: 514–520.

De Sampaïo G, Bourdineaud JP & Lauquin GJ (1999) A constitutive role for GPI anchors in *Saccharomyces cerevisiae*: cell wall targeting. *Mol Microbiol* **34**: 247–256.

Eisenhaber B, Schneider G, Wildpaner M & Eisenhaber F (2004) A sensitive predictor for potential GPI lipid modification sites in fungal protein sequences and its application to genome-

wide studies for *Aspergillus nidulans*, *Candida albicans*, *Neurospora crassa*, *Saccharomyces cerevisiae* and *Schizosaccharomyces pombe*. *J Mol Biol* **337**: 243–253.

Fankhauser C & Conzelmann A (1991) Purification, biosynthesis and cellular localization of a major 125-kDa glycophosphatidylinositol-anchored membrane glycoprotein of *Saccharomyces cerevisiae*. *Eur J Biochem* **195**: 439–448.

Felipe MSS, Andrade RV, Petrofeza SS *et al*. (2003) Transcriptome characterization of the dimorphic and pathogenic fungus *Paracoccidioides brasiliensis* by EST analysis. *Yeast* **20**: 263–271.

Franco M (1986) Host-parasite relationships in paracoccidioidomycosis. *J Med Vet Mycol* **25**: 5–18.

Ghannoum MA, Spellberg B, Saporito-Irwin SM & Fonzi WA (1995) Reduced virulence of *Candida albicans PHR1* mutants. *Infect Immun* **63**: 4528–4530.

Hill J, Jan KA, Donald G & Griffiths E (1991) DMSO-enhanced whole cell yeast transformation. *Nucleic Acids Res* **19**: 5791.

Klis FM (1994) Review: cell wall assembly in yeast. *Yeast* **10**: 851–869.

Livak KJ & Schmittgen TD (2001) Analysis of relative gene expression data using real-time quantitative PCR and the 2(-Delta Delta C(T)) method. *Methods* **25**: 402–408.

Mouyna I, Hartland RP, Fontaine T, Diaquin M, Simenel C, Delepierre M, Henrissat B & Latgé JP (1998) A 1,3-beta-glucanosyltransferase isolated from the cell wall of *Aspergillus fumigatus* is a homologue of the yeast Bgl2p. *Microbiology* **144**: 3171–3180.

Mouyna I, Fontaine T, Vai M, Monod M, Fonzi WA, Diaquin M, Popolo L, Hartland RP & Latge JP (2000a) Glycosylphosphatidylinositol-anchored glucanosyltransferases play an active role in the biosynthesis of the fungal cell wall. *J Biol Chem* **275**: 14882–14889.

Mouyna I, Monod M, Fontaine T, Henrissat B, Lechenne B & Latge JP (2000b) Identification of the catalytic residues of the first family of beta(1-3)glucanosyltransferases identified in fungi. *Biochem J* **347**: 741–747.

Mouyna I, Morelle W, Vai M *et al*. (2005) Deletion of *GEL2* encoding for a beta(1-3)glucanosyltransferase affects morphogenesis and virulence in *Aspergillus fumigatus*. *Mol Microbiol* **56**: 1675–1688.

Mühlschlegel FA & Fonzi WA (1997) *PHR2* of *Candida albicans* encodes a functional homolog of the pH-regulated gene *PHR1* with an inverted pattern of pH-dependent expression. *Mol Cell Biol* **17**: 5960–5967.

Nakazawa T, Horiuchi H, Ohta A & Takagi M (1998) Isolation and characterization of *EPD1*, an essential gene for pseudohyphal growth of a dimorphic yeast, *Candida maltosa*. *J Bacteriol* **180**: 2079–2086.

Nakazawa T, Takahashi M, Horiuchi H, Ohta A & Takagi M (2000) Cloning and characterization of *EPD2*, a gene required for efficient pseudohyphal formation of a dimorphic yeast, *Candida maltosa*. *Biosci Biotechnol Bioch* **64**: 369–377.

Palomares O, Villalba M & Rodríguez R (2003) The C-terminal segment of the 1,3-beta-glucanase Ole e 9 from olive (*Olea europaea*) pollen is an independent domain with allergenic activity: expression in *Pichia pastoris* and characterization. *Biochem J* **369**: 593–601.

Papaleo E, Fantucci P, Vai M & De Gioia L (2006) Three-dimensional structure of the catalytic domain of the yeast beta-(1,3)-glucan transferase Gas1: a molecular modeling investigation. *J Mol Model* **12**: 237–248.

Popolo L & Vai M (1999) The Gas1 glycoprotein, a putative wall polymer cross-linker. *Biochim Biophys Acta* **1426**: 385–400.

Popolo L, Grandori R, Vai M, Lacanà E & Alberghina L (1988) Immunochemical characterization of gp115, a yeast glycoprotein modulated by the cell cycle. *Eur J Cell Biol* **47**: 173–180.

Popolo L, Gilardelli D, Bonfante P & Vai M (1997) Increase in chitin as an essential response to defects in assembly of cell wall polymers in the *ggp1*Δ mutant of *Saccharomyces cerevisiae*. *J Bacteriol* **179**: 463–469.

Ragni E, Coluccio A, Rolli E, Rodriguez-Peña JM, Colasante G, Arroyo J, Neiman AM & Popolo L (2007a) *GAS2* and *GAS4*, a pair of developmentally regulated genes required for spore wall assembly in *Saccharomyces cerevisiae*. *Eukaryot Cell* **6**: 302–316.

Ragni E, Fontaine T, Gissi C, Latge JP & Popolo L (2007b) The gas family of proteins of *Saccharomyces cerevisiae*: characterization and evolutionary analysis. *Yeast* **24**: 297–308.

Ram AF, Kapteyn JC, Montijn RC, Caro LH, Douves JE, Baginsky W, Mazur P, Van Den Ende H & Klis FM (1998) Loss of the plasma membrane-bound protein Gas1p in *Saccharomyces cerevisiae* results in the release of beta-1,3-glucan into the medium and induces a compensation mechanism to ensure cell wall integrity. *J Bacteriol* **180**: 1418–1424.

Restrepo AM, McEwen JG & Castaneda E (2001) The habitat of *Paracoccidioides brasiliensis*: how far from solving the riddle? *Med Mycol* **39**: 233–241.

Sambrook J & Russell DW (2001) *Molecular Cloning: A Laboratory Manual*, 3rd edn. Cold Spring Harbor Laboratory Press, Cold Spring Harbour, New York.

San-Blas G & San-Blas F (1977) *Paracoccidioides brasiliensis*: cell wall structure and virulence. A review. *Mycopathologia* **62**: 77–86.

San-Blas G & San-Blas F (1994) Biochemistry of *Paracoccidioides brasiliensis* dimorphism. *Paracoccidioidomycosis* (Franco MF, Lacaz CS, Restrepo-Moreno A & Del Negro A, eds), pp. 49–66. CRC Press, Boca Raton, FL.

Sano A, Tanaka R, Nishimura K, Kurokawa CS, Coelho KIR, Franco M, Montenegro MR & Miyaji M (1997) Characteristics of 17 *Paracoccidioides brasiliensis* isolates. *Mycoscience* **38**: 117–122.

Saporito-Irwin SM, Birse CE, Sypherd PS & Fonzi WA (1995) *PHR1*, a pH-regulated gene of *Candida albicans*, is required for morphogenesis. *Mol Cell Biol* **15**: 601–613.

Sigler K & Höfer M (1991) Mechanisms of acid extrusion in yeast. *Biochim Biophys Acta* **1071**: 375–391.

Uppuluri P, Perumal P & Chaffin WL (2007) Analysis of RNA species of various sizes from stationary-phase planktonic yeast cells of *Candida albicans*. *FEMS Yeast Res* **7**: 110–117.

Vai M, Orlandi I, Cavadini P, Alberghina L & Popolo L (1996) *Candida albicans* homologue of *GGP1*/*GAS1* gene is functional in *Saccharomyces cerevisiae* and contains the determinants for glycosylphosphatidylinositol attachment. *Yeast* **12**: 361–368.

Vai M, Brambilla L, Orlandi I, Rota N, Ranzi BM, Alberghina L & Porro D (2000) Improved secretion of native human insulin-like growth factor 1 from *gas1* mutant *Saccharomyces cerevisiae* cells. *Appl Environ Microbiol* **66**: 5477–5479.

Vanoni M, Vai M, Popolo L & Alberghina L (1983) Structural heterogeneity in populations of the budding yeast *Saccharomyces cerevisiae*. *J Bacteriol* **156**: 1282–1291.

Yin QY, de Groot PW, Dekker HL, de Jong L, Klis FM & de Koster CG (2005) Comprehensive proteomic analysis of *Saccharomyces cerevisiae* cell walls: identification of proteins covalently attached via glycosylphosphatidylinositol remnants or mild alkali-sensitive linkages. *J Biol Chem* **280**: 20894–20901.

INSTITUT PASTEUR

Microbes and Infection 11 (2009) 895–903

www.elsevier.com/locate/micinf

Original article

Identification and characterization of antigenic proteins potentially expressed during the infectious process of *Paracoccidioides brasiliensis*

Sabrina Fonseca Ingênito Moreira Dantas [a], Tereza Cristina Vieira de Rezende [a], Alexandre Melo Bailão [a], Carlos Pelleschi Taborda [b], Rodrigo da Silva Santos [a], Kelly Pacheco de Castro [a], Célia Maria de Almeida Soares [a,*]

[a] *Laboratório de Biologia Molecular, Instituto de Ciências Biológicas, Universidade Federal de Goiás, 74001-970 Goiânia, GO, Brazil*
[b] *Instituto de Ciências Biomédicas, Departamento de Microbiologia, Universidade de São Paulo, 05508-900 São Paulo, SP, Brazil*

Received 19 March 2009; accepted 24 May 2009
Available online 13 June 2009

Abstract

Paracoccidioides brasiliensis causes paracoccidioidomycosis (PCM), a systemic mycosis presenting clinical manifestations ranging from mild to severe forms. A *P. brasiliensis* cDNA expression library was produced and screened with pooled sera from PCM patients adsorbed against antigens derived from in vitro-grown *P. brasiliensis* yeast cells. Sequencing DNA inserts from clones reactive with PCM patients sera indicated 35 open reading frames presenting homology to genes involved in metabolic pathways, transport, among other predicted functions. The complete cDNAs encoding aromatic-L-amino-acid decarboxylase (*Pbddc*), lumazine synthase (*Pbls*) and a homologue of the high affinity copper transporter (*Pbctr*3) were obtained. Recombinant proteins *Pb*DDC and *Pb*LS were obtained; a peptide was synthesized for *Pb*CTR3. The proteins and the synthetic peptide were recognized by sera of patients with confirmed PCM and not by sera of healthy patients. Using the in vivo-induced antigen technology (IVIAT), we identified immunogenic proteins expressed at high levels during infection. Quantitative real time RT-PCR demonstrated high transcript levels of *Pbddc*, *Pbls* and *Pbctr*3 in yeast cells infecting macrophages. Transcripts in yeast cells derived from spleen and liver of infected mice were also measured by qRT-PCR. Our results suggest a putative role for the immunogenic proteins in the infectious process of *P. brasiliensis*.

Keywords: *Paracoccidioides brasiliensis*; Immunogenic proteins; Infectious process; DOPA Decarboxylase; Lumazine synthase; High affinity copper transporter

1. Introduction

Paracoccidioides brasiliensis causes paracoccidioidomycosis (PCM), a human systemic granulomatous disease, prevalent in South America [1]. The fungus is thermo dimorphic and causes by inhalation of airborne propagules of the mycelia phase, which reach the lungs and differentiates into the yeast phase [2].

Although the disease process is well characterized, the fungal expression of genes in vivo is poorly explored. During disease, *P. brasiliensis* must adapt to a range of environments and survival in any one niche should require the differential expression of genes. The in vivo gene expression pattern of *P. brasiliensis* has been examined by our laboratory by transcriptome analysis [3–5]. A wide array of genes involved in nutrient acquisition, melanin synthesis, adhesion, stress response, general metabolism were induced and have been identified.

Abbreviations: BCIP, 5-bromo-4-chloro-3-indolyl phosphate; CTR3, high affinity copper transporter; DDC, aromatic-L-amino acid decarboxylase IPTG, Isopropyl-β-D-thiogalactopyranoside; IVIAT, in vivo-induced antigen technology; LS, lumazine synthase; NBT, nitroblue tetrazolium; Pb, *Paracoccidioides brasiliensis*; PCM, Paracoccidioidomycosis; TPI, triosephosphate isomerase.

* Corresponding author. Laboratório de Biologia Molecular, Instituto de Ciências Biológicas, ICBII, Campus II, Universidade Federal de Goiás, 74001-970 Goiânia, Goiás, Brazil. Tel./fax: +55 62 3521 1110.
E-mail address: celia@icb.ufg.br (C. Maria de Almeida Soares).

1286-4579/$ - see front matter © 2009 Elsevier Masson SAS. All rights reserved.
doi:10.1016/j.micinf.2009.05.009

With the purpose of identifying antigenic proteins potentially expressed during the fungal infectious process, here we applied the in vivo-induced antigen technology (IVIAT). IVIAT has been used to identify genes expressed during human infection by several microorganisms [6–11]. A *P. brasiliensis* cDNA expression library was screened in order to identify clones reactive with sera of PCM patients. Specifically, we hypothesized that by using the IVIAT immunological screening, we could identify proteins that play a role during fungal infection.

Screening of the cDNA library resulted in the identification of 29 genes, putatively playing a role in the fungus-host interaction. The cDNAs, encoding aromatic-L-amino acid decarboxylase (DDC, EC 4. 1. 1. 28), lumazine synthase (LS, EC 2. 5. 1. 9) and high affinity copper tansporter (CTR3) orthologues of *P. brasiliensis* were selected for further analysis. The recombinant proteins (*Pb*DDC and *Pb*LS) and a synthetic peptide (*Pb*CTR3) were obtained and showed strong reactivity with sera of PCM patients. The predictable expression of those transcripts was evaluated by quantitative real time RT-PCR (qRT-PCR) in models of infection. The results suggest a role in the pathogen-host interaction. Due to the relevance of melanin in pathogenesis of microorganisms, we investigated the involvement of *Pb*DDC in this pathway; results demonstrated correlation between the increase of melanin and the enzyme expression in fungal yeast cells.

2. Materials and methods

2.1. P. brasiliensis *isolate growth conditions and differentiation assays*

*P. brasiliensis Pb*01 isolate (ATCC-MYA-826) was cultivated in semi-solid Fava Netto's medium [1% (w/v) peptone, 0.5% (w/v) yeast extract, 0.3% (w/v) proteose peptone, 0.5% (w/v) beef extract, 0.5% (w/v) NaCl, 1% (w/v) agar, pH 7.2] at 36 °C in the yeast form and at 22 °C, for its mycelia phase.

2.2. *Adsorbing PCM patients sera to* P. brasiliensis *grown in vitro*

Human sera were collected from 11 patients with well-documented PCM in chronic disease phase and pooled. The serum samples were selected at the time of diagnosis from patients with mycological confirmed disease. Human control sera obtained from 11 healthy individuals were pooled.

A mixture of equal volumes of sera of PCM patients was diluted with *Escherichia coli* cells lysate and the same volume of PBS 1X. The mixture was incubated at 37 °C for 1 h, and centrifuged at 10,000 × g, 4 °C during 20 min. In the second stage, the supernatant was incubated during 1 h at 37 °C, with the same volume of a mixture containing protein extract of *P. brasiliensis* yeast cells (100 μg/mL) and whole yeast cells. This mixture was centrifuged at 10,000 × g, 4 °C for 20 min; the supernatant was collected. The efficiency of the incubation was monitored by two-dimensional polyacrylamide gel electrophoresis (SDS-PAGE) and Western blotting.

2.3. *Infection of mice with* P. brasiliensis *and RNA extraction*

Female BALB/c mice, 8–12 weeks old, were inoculated with 1×10^7 yeast cells of *P. brasiliensis*. In brief, yeast cells suspension at the 7th day of in vitro growth were washed in PBS 1X and inoculated intraperitoneally in mice. Matched groups of four animals were injected with sterile PBS and used as uninfected controls. The animals were killed on the 15th day after infection. The livers and spleens were removed. Serial dilutions of the lysate were plated in infusion brain and heart (BHI) medium supplemented with 4% (v/v) of fetal bovine serum (FBS) and the plates were incubated at 36 °C for 7 days. The recovered cells were submitted to total RNA extraction by using Trizol reagent (Invitrogen™, Life Technologies), according to the manufacturer's instructions. Total RNA from *P. brasiliensis* yeast cells and mycelium grown in vitro, in the same medium, was also obtained.

2.4. *Construction of a cDNA expression library of* P. brasiliensis

For the construction of a cDNA expression library, the RNA of yeast cells recovered from mice liver on the 15th day after infection was purified by using the Poly (A) Quick® mRNA isolation kit (Stratagene, La Jola, CA). The cDNA library was constructed by using the SUPERSCRIPT™ plasmid system with GATEWAY® technology for cDNA synthesis and cloning.

2.5. *Immunological screening of the cDNA library, identification of inserts and prediction of function of the identified antigens*

The pooled sera were used in the screening of the cDNA library. An aliquot of the cDNA library was diluted and spread onto LB medium plates containing ampicillin (100 μg/ml) to produce 300–600 colonies per plate. The bacterial colonies were grown at 37 °C overnight. The colonies were held up by using nitrocellulose membranes, replica plated onto LB containing ampicillin and 1 mM of isopropyl-β-D-thiogalactopyranoside (IPTG), and incubated overnight at 37 °C. The colonies grown onto membrane were exposed to chloroform for 20 min. Following washing and blocking of membranes, they were incubated with the adsorbed sera (1:1000 diluted) in PBS 1X, 0.1% (v/v) Tween 20, at 4 °C for 18 h. The induced proteins reacting with antibodies in the sera were detected by using peroxidase-conjugated goat, anti-human IgG (1:2000 diluted) and revealed with the ECL Advance™ Western blotting detection kit (GE Healthcare, Amersham Biosciences). Reactive cDNAs were identified by their position on the master plate; each positive cDNA was isolated at least by two additional plating and reaction to the pooled sera.

We recovered plasmid DNA from 35 positive clones and sequenced the inserts from their 5′ end by employing the standard fluorescence labeling DYEnamic™ ET dye terminator kit

(GE Healthcare). An automated DNA sequence analysis was performed in a MegaBACE 1000 DNA sequencer (GE Healthcare). The proteins encoded in the cloned cDNAs were compared against the GenBank non-redundant (nr) database from the National Center for Biotechnology Information (http://www.ncbi.nlm.nih.gov/) using the BLAST × algorithm and against *P. brasiliensis* genome database (http://www.broad.mit.edu/annotation/genome/paracoccidioides_brasiliensis/MultiHome.html).

2.6. Cloning of P. brasiliensis aromatic-L-amino-acid decarboxylase (Pbddc) and lumazine synthase (Pbls) cDNAs, expression and purification of the recombinant proteins

Oligonucleotide primers were designed to amplify the 1.6 kb and 525 bp cDNAs containing the complete coding regions of *Pbddc* and *Pbls*, respectively. The 1.6 kb and 525 bp amplicons were gel-excised and cloned into pGEX-4T-3 (GE Healthcare) to yield the constructs pGEX-4T3-*ddc* and pGEX-4T-3-*ls*. The recombinant plasmids were used to transform *E. coli*, according to standard procedures [12]. The cells were grown to an absorbance of 0.6 at 600 nm and 0.5 mM IPTG was added to the growing cultures. After 16 h incubation, at 15 °C, the bacterial cells were harvested, ressuspended in PBS 1X, lysed by sonication and the recombinant fusion proteins were cleaved by thrombin addition (10 U/mg fusion protein).

2.7. Production of polyclonal antibody anti-PbDDC

The recombinant *Pb*DDC was used to generate specific rabbit polyclonal serum. Rabbit pre immune serum was obtained. The purified protein (300 μg) was injected into rabbit with Freund's adjuvant three times at 2-week intervals.

2.8. Western blotting of the recombinant proteins with sera of PCM patients

The recombinant proteins were fractionated by SDS-PAGE [13]. The gels were either stained with Coomassie blue or blotted onto nitrocellulose membranes that were blocked with 5% non-fat skim milk and reacted with sera from PCM patients or from healthy individuals (1:1000 diluted). The secondary antibody was alkaline phosphatase coupled anti-human IgG. The reactions were developed with 5-bromo-4-chloro-3-indolyl phosphate and nitroblue tetrazolium (BCIP/NBT).

2.9. Preparation and infection of mice macrophages by P. brasiliensis yeast cells

Bone marrow-derived macrophages were obtained by flushing the femurs of 4–12 weeks old female C57BL/6 mice [14]. The prepared cells were cultured at 37 °C under 6% CO_2 in RPMI 1640 medium (Biowhittaker, Walkersville, Md.) supplemented with 10% (v/v) FBS, 1% (w/v) l-glutamine, 5×10^{-5} M 2-mercaptoethanol, 100 ng/mL granulocyte macrophage colony stimulating factor (GM-CSF), and 10 μg/mL of gentamicin. After 8 days, the non-adherent cells were discarded and the remaining cells were washed twice with 10 mL of Hank's Balanced Salt Solution (HBSS). The cells were treated with 10 μg/mL of dispase in HBSS at 37 °C for 5 min. Further, macrophages were removed using a cell scraper and washed in HBSS. Cells were centrifuged at 500 × g for 5 min, and resuspended in RPMI 1640 medium (supplemented as described above, minus GM-CSF) at a concentration of 1×10^6 cells/mL. *P. brasiliensis* yeast cells (5×10^6) were added to 2 mL of macrophage suspension plated on 6 well plates. After 24 h of co-cultivation at 37 °C, the non-phagocyted yeast cells were discarded and the bottom cells were washed twice. The RNA of infected mice macrophages and control macrophages were extracted using Trizol.

2.10. Quantitative analysis of RNA transcripts encoding Pbddc, Pbls and Pbctr3 by reverse transcription real-time PCR (qRT-PCR)

The RNA of yeast cells, mycelium, infected macrophages and yeast cells derived from infection of mice liver and spleen after 15 days were used in this analysis. Total RNAs treated with DNAse were reverse transcribed using Superscript II reverse transcriptase (Invitrogen) and oligo$(dT)_{15}$ primer. qRT-PCR was performed in triplicate, with samples from three independent experiments in the StepOnePlus™ real-time PCR system (Applied Biosystems, Foster City, CA). The PCR thermal cycling was 40 cycles of 95 °C for 15 s; 60 °C for 1 min. The SYBR green PCR master mix (Applied Biosystems) was used as reaction mixture, added of 10 pmol of each primer and 40 ng of template cDNA, in a final volume of 25 μl. A melting curve analysis was performed to confirm a single PCR product. The data were normalized with the ribosomal protein L34 amplified in each set of qRT-PCR experiments. A non-template control was included. A cDNA for a relative standard curve was generated by pooling an aliquot of cDNA from each sample. The standard cDNA was serially diluted 1:5, and a standard curve was generated using four samples from the pooled cDNA. Relative expression levels of genes of interest were calculated using the standard curve method for relative quantification [15].

2.11. Dot blot analysis

To analyze the melanin and DDC accumulation in yeast forms of *P. brasiliensis*, the cells (1.5 g) were sub cultured in Mc Veigh-Morton liquid minimal medium (MMcMi) [16] supplemented or not with 1.0 mM L-Dopa (Sigma) for 15 days at 36 °C. All cultures were incubated in the dark to avoid photo polymerization of L-Dopa into melanin. The viability of fungal suspensions was determined by staining with 0.01% (w/v) Trypan blue in PBS 1X. The cells were collected by centrifugation at 5000 × g for 5 min, frozen in liquid nitrogen and disrupted by maceration. The cellular

powder was centrifuged at 12,000 × g for 20 min. The cellular extracts were vacuum spotted onto nitrocellulose membranes that were blocked and reacted with the anti-melanin antibody of *Sporothrix schenckii* (1:1000 diluted, kindly provided by Dr Joshua D. Nosanchuck, Albert Einstein College of Medicine, New York) and antibody anti-DDC (1:500 diluted). The anti-melanin secondary antibody was biotin anti-mouse IgM (1:500 diluted) plus streptavidin-HRP (1:1000 diluted) and the reactive bands were developed with hydrogen peroxide and diaminebenzidine. The anti-DDC secondary antibody was alkaline phosphatase coupled anti-rabbit IgG (1:2000 diluted), and the reaction was developed with BCIP/NBT. Dot blot analysis was also performed to assay the reactivity of a peptide synthesized on basis on the deduced sequence of *Pb*CTR3 (Supplementary Fig. S3) to the serum of PCM patients. Reactions were performed as described above.

3. Results

3.1. Identification of P. brasiliensis antigens by IVIAT

We immuno-screened approximately 6000 clones inducible in the *P. brasiliensis* expression library. We identified 35 immuno-reactive clones representing 29 distinct *P. brasiliensis* genes encoding proteins that were persistently reactive after at least three rounds of screening. The predicted proteins encoded by the cDNAs are shown in Table 1. They are implicated in cell metabolism, biogenesis of cellular components, transport, energy, transcription, protein fate and signal transduction.

Table 1
Predicted proteins of *Paracoccidioides brasiliensis* encoded by the cDNAs identified by IVIAT.

Functional category	Gene Product-description, function (reference)	Best Hit/GenBank accession number* or *P. brasiliensis* genome locus†	e-value	EC number	Number of positive cDNAs obtained through IVIAT
Metabolism	Acyl-CoA dehydrogenase	*P. brasiliensis*/CA581965*	5e-101	1.3.1.8	1
	Aromatic-L-amino acid decarboxylase	*P. brasiliensis Pb*01/PAAG_01563.1†	0.0	4.1.1.28	1
	Ubiquinone (COQ9)	*P. brasiliensis Pb*01/PAAG_05083.1†	1e-25	–	1
	Lumazine synthase	*P. brasiliensis*/DQ081183*	4e-78	2.5.1.9	1
	Alfa-1,2-galactosyl transferase	*P. brasiliensis Pb*01/PAAG_02629.1†	1e-8	2.4.1.	1
	Pyridine nucleotide-disulphide oxidoreductase	*P. brasiliensis Pb01*/PAAG_01677.1†	6e-19	1.-	1
Biogenesis of cellular components	Lipopolysaccharide biosynthesis protein	*Trichophyton rubrum*/DW709722*	3e-33	–	1
	Cofilin	*P. brasiliensis Pb*03/PABG_07299.1†	8e-32	–	1
Transport	Coatomer zeta subunit	*Schizosaccharomyces pombe*/AA21186.1*	1e-67	–	1
	High affinity copper transporter	*P. brasiliensis*/ABF93409.1*	2e-59	–	1
	Outer membrane ferric siderophore receptor	*Phakopsora pachyrhizi*/DN739539*	1e-63	–	1
	Carboxylate/amino acid/amine transporter	*Trichophyton rubrum*/DW701041*	1e-29	–	1
	ABC transporter	*P. brasiliensis Pb03*/PABG_07206.1†	1e-7	–	3
Energy	ATP synthase F0 F1 subunit 9	*P. brasiliensis*/YP_537116.1*	7e-15	3.6.3.14	1
	Alcohol dehydrogenase	*P. brasiliensis Pb*01/PAAG_02965.1†	2e-9	1.1.1.1	1
	Mitochondrial cytochrome c oxidase subunit VIIa	*P. brasiliensis*/ABU46290.1*	1e-86	1.9.3.1	1
Transcription	C2H2 finger domain protein	*P. brasiliensis Pb*01/PAAG_04481.1†	0.0	–	1
	Nitrogen regulation protein	*P. brasiliensis*/EH041264.1*	5e-52	–	2
Protein fate	Ubiquitin	*P. brasiliensis Pb*01/PAAG_06536.1†	3e-29	–	1
	Midasin	*P. brasiliensis Pb*01/PAAG_00114.1†	0.0	–	3
Signal Transduction	Protein kinase domain	*P. brasiliensis Pb*01/PAAG_00114.1†	0.0	2.7.1.37	1
	WD repeat protein	*P. brasiliensis Pb*01/PAAG_02429.1†	0.0	–	2
	Diguanylate cyclase	*Trichophyton rubrum*/DW692821*	3e-15	4.6.1.-	1
Unclassified	Conserved hypothetical protein	*P. brasiliensis*/YP_537116*	5e-15	–	1
	Conserved hypothetical protein	*P. brasiliensis*/CN244805*	1e-23	–	1
	Conserved hypothetical protein	*P. brasiliensis Pb*01/PAAG_08269.1†	4e-24	–	1
	Conserved hypothetical protein	*Ajellomyces capsulatus*/XP_001537205.1*	2e-12	–	1
	Hypothetical protein	No hits found	–	–	1
	Hypothetical protein	*Neurospora crassa*/XP_001728522.1*	1e-10	–	1
Total					35

3.2. Nucleotide and deduced amino acid sequences of aromatic-L-amino-acid decarboxylase (Pb*DDC*), lumazine synthase (Pb*LS*) and high affinity copper transporter (Pb*CTR3*)

We selected the cDNAs encoding *Pbddc*, *Pbls* and *Pbctr*3 for further analysis. The entire cDNA encoding *Pbddc* consisted of 2371 bp and encoded a protein of 545 amino acids, predicted molecular mass of 60 kDa and p*I* of 6.5. The cDNA sequence encoding *Pb*DDC had been deposited on GenBank under accession number ABH03461. The deduced amino acid sequence displayed strong identity to DDCs of fungal origin. The alignment of *Pb*DDC with pathogenic fungi orthologues is presented in Supplementary Fig. S1.

The analysis of *Pbls* showed a single open reading frame (ORF) with 174 amino acids with a molecular mass prediction of 19 kDa and p*I* of 6.6. The cDNA and genomic sequences encoding *Pbls* had been deposited on GenBank under accession numbers DQ081183 and DQ186604, respectively. The sequence of amino acid encoding *Pb*LS was compared with orthologues of fungi (Supplementary Fig. S2).

The analysis of *Pbctr*3 demonstrated a single ORF with 193 amino acids, with a predicted molecular mass of 21 kDa and p*I* of 8.6 (Supplementary Fig. S3). The cDNA encoding *Pbctr*3 had been deposited on GenBank under accession number DQ534496.

3.3. Reactivity of Pb*DDC*, Pb*LS* and Pb*CTR3* to sera of PCM patients

The expression of the recombinant *Pb*DDC and *Pb*LS was obtained. SDS-PAGE was used to verify the composition of

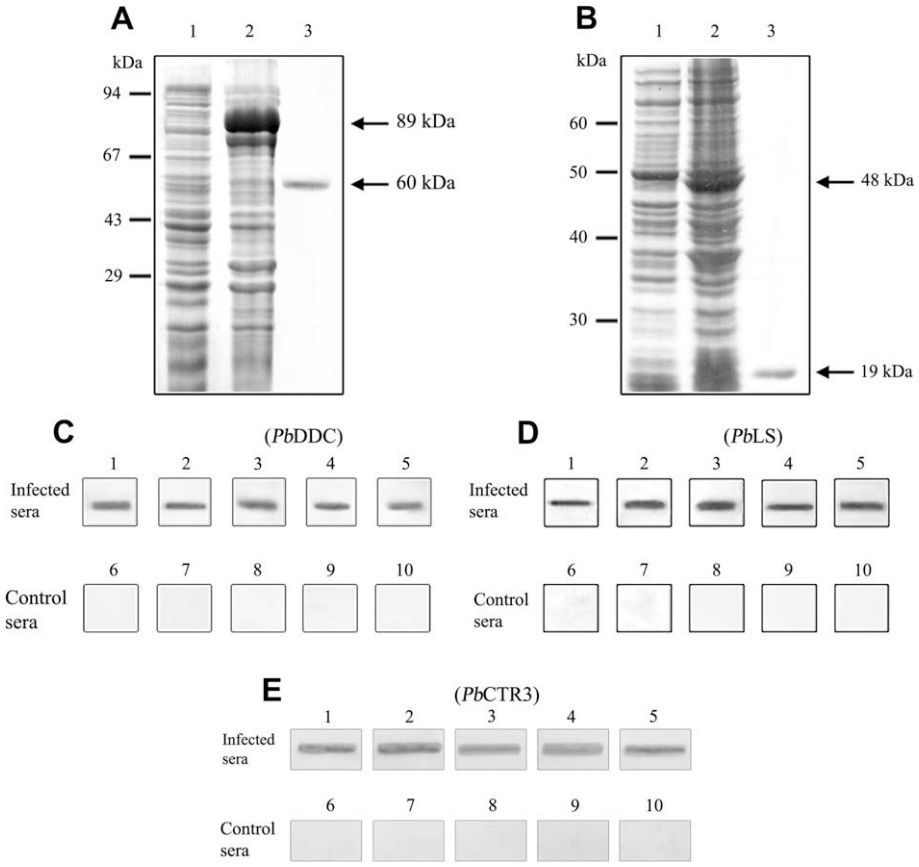

Fig. 1. Reactivity of the recombinant *Pb*DDC and *Pb*LS and of the synthetic peptide of *Pb*CTR3 with sera of PCM patients. The nucleotide sequences of the *Pbddc* oligonucleotide primers were sense 5′-*GGATCC*ATGGACCAGGAAGAATTCAG-3′ and antisense 5′-*CTCGAG*CTAGTTTTTCACAGCCCTGC-3′, which contained engineered *Bam*HI and *Xho*I restriction sites (italicized), respectively. The oligonucleotide primers for *Pbls* were sense 5′-TGGT*GAATTC*CATGGCTACTCTCAAAGG-3′, and antisense 5′-GGTGGT*CTCGAG*CTACGAAAACTTCCCCATTG-3′, which contained engineered *Eco*RI and *Xho*I restriction sites (italicized), respectively. The PCR products were digested with the cited restriction enzymes, electrophoresed on agarose gel cloned into pGEX-4T-3, and used to transform *E. coli* cells. (A) SDS-PAGE analysis of *P. brasiliensis* recombinant DDC. The *E. coli* cells harboring the pGEX-4T-3-*ddc* plasmid were grown to an A_{600} of 0.6 and harvested before (lane1), and after 16 h (lane 2) incubation with 0.5 mM IPTG at 15 °C; the affinity-isolated recombinant *Pb*DDC after thrombin addition and protein purification by affinity chromatography (lane 3). (B) Induced bacterial cells of *E. coli* harboring the pGEX-4T-3-*ls* plasmid were grown at 15 °C to an A_{600} of 0.6 and harvested before (lane 1) and after 16 h incubation with IPTG, at 15 °C (lane 2). The purified recombinant protein was obtained after thrombin digestion and affinity chromatography (lane 3). (C and D) Immunoblot analyses of the recombinant proteins. The recombinant *Pb*DDC and *Pb*LS (1.0 μg) were reacted with sera of five PCM patients (1:1000 diluted), (lanes 1−5) and to control sera (1:1000 diluted), (lanes 6−10). (E) Reactivityof the synthetic peptide from *Pb*CTR3 with the same sera as in C and D. A peptide was synthesized from amino acids 90−130 in the deduced *Pb*CTR3 (Invitrogen, life technologies). One hundred ηg of the synthetic peptide was blotted onto nitrocellulose membrane and reacted with sera from PCM patients and with control sera. After reaction with anti-human IgG alkaline phosphatase coupled antibody (1:2000 diluted), the reaction was developed with BCIP/NBT. Molecular mass of the proteins and standards (kDa) are indicated.

the cells lysates obtained from *E. coli* cells which had been transformed with the plasmid constructs, as shown in Fig. 1A and B, lane 1. After induction with IPTG, 89-kDa and 48-kDa recombinant proteins were detected in the bacterial lysates (Fig.1A and B, lane 2), respectively, for *Pb*DDC and *Pb*LS, which included the vector-encoded fusion protein at its N-terminus. The fusion proteins were cleaved by the addition of thrombin protease (Fig. 1A and B, lane 3). As observed, highly purified proteins were obtained, that migrated on SDS-PAGE as a single species of 60 kDa and 19 kDa, for *Pb*DDC and *Pb*LS, respectively. A peptide was synthesized toward amino acids 90–130 of the deduced *Pb*CTR3 (Supplementary Fig. S3).

Five sera samples from PCM patients and five control sera samples were reacted with the recombinant proteins *Pb*DDC and *Pb*LS and with the synthetic peptide of *Pb*CTR3 in immunoblot assays (Fig. 1C–E, respectively). Strong reactivity was observed with sera of PCM patients (Fig. 1C–E, lanes 1–5) and no cross-reactivity was observed with control sera (Fig. 1C–E, lanes 6–10).

3.4. *Assessment of the expression of* Pbddc, Pbls *and* Pbctr3 *by reverse transcription real-time PCR in models of infection*

The expression of the genes in a macrophage model of infection is shown in Fig. 2A. In our study, the genes are induced in yeast cells, when compared to mycelia. During macrophage infection, it was detected overexpression of *Pbddc* and *Pbctr*3, when compared to the expression in the mycelium and yeast cells after in vitro growth. Although expressed during macrophage infection, *Pbls* was not upregulated in vivo relative to the highest level of expression in vitro (Fig. 2A).

The expression of the genes was also evaluated by qRT-PCR analysis in yeast cells of *P. brasiliensis* derived from infected mice liver and spleen (Fig. 2B). We have shown that *Pbddc* is upregulated in vivo, with the expression occurring at 15 days post inoculation in spleen, but not in liver (Fig. 2B). We have also shown that *Pbctr*3 is upregulated in liver and spleen (Fig. 2B). Of the genes characterized by qRT-PCR, *Pbls* was not overexpressed in vivo relative to the highest level of expression in vitro (Fig. 2B).

3.5. *Melanin accumulation in yeast cells of* P. brasiliensis

We directed our experiments toward the analysis of melanin accumulation in *P. brasiliensis*. The fungus was grown on a chemically defined medium supplemented or not with L-Dopa (Fig. 3). The viability was of 62.5% and 75.7%, respectively, for yeast cells grown in media enriched or not with L-Dopa (data not shown). Light microscopy (400× magnification) shows darkly pigmented yeast cells in the presence of L-Dopa (Fig. 3A, panel 2). The accumulation of melanin and DDC were higher when the fungus was grown in medium supplemented with L-Dopa (Fig. 3B and C, respectively). Loading control was performed with the antibody to the recombinant triosephosphate isomerase [17].

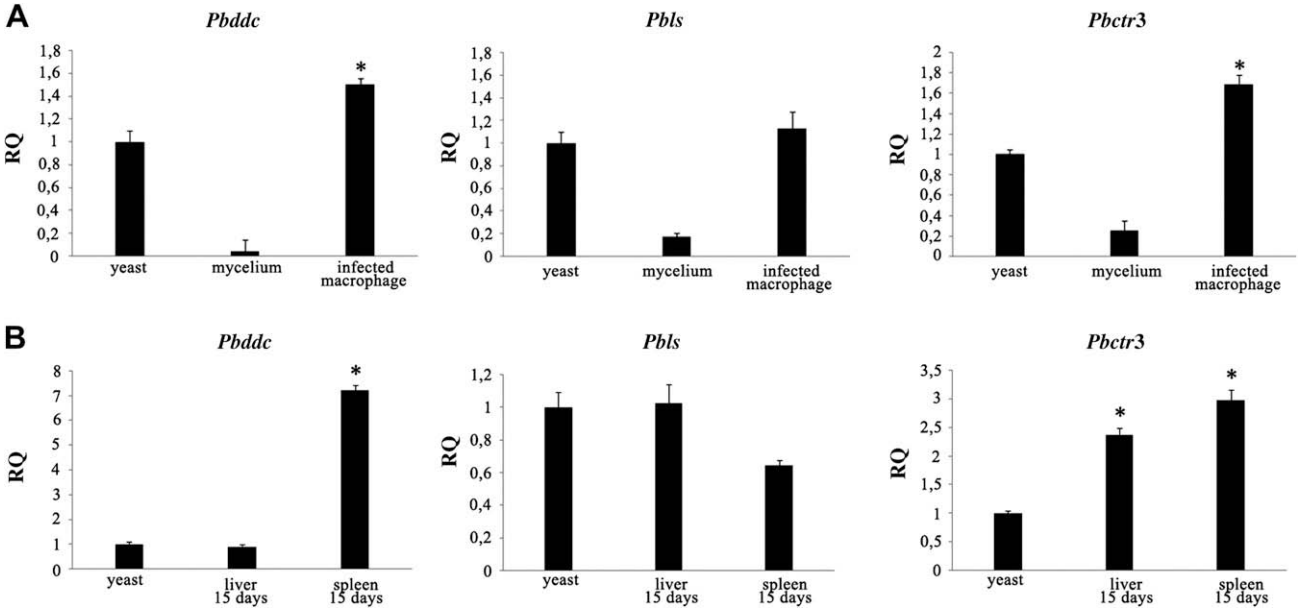

Fig. 2. Average of gene expression of *Pbddc* , *Pbls* and *Pbctr*3 as determined by quantitative real time RT-PCR. (A) qRT-PCR plot of *Pbddc*, *Pbls* and *Pbctr*3 expression levels in mycelium, yeast cells and in a macrophage model of infection. (B) qRT-PCR plot of *Pbddc*, *Pbls* and *Pbctr*3 expression in yeast cells derived from infected tissues of mice. The primers were as following: *Pbddc*, sense 5′-GTACCTTCGTCCTCTTCTTC-3′, antisense 5′-GGGTAAGTCACACAAGAGGG-3′; *Pbls,* sense, 5′-GCCTATTGCTATGGAGAGAATA-3′, antisense, 5′-GTTGACGGTGTTGAATGAGG-3′; *Pbctr*3 sense, 5′-ATGTGAAGC AGCGAGCGG-3′, antisense 5′-CATGGAATGCACGGCGGC-3′ *Pbl34*, sense, 5′-CGGCAACCTCAGATACCTTC-3′, antisense 5′-GGAGACCTGGGAGTATTCAC-3′. The values of expression of the *Pbddc*, *Pbls* and *Pbctr3* were standardized using the values of expression of the constitutive gene encoding to the ribosomal protein L34. The expression level was calculated by relative standard curve method. The standard deviations are presented from three independent experiments. *Significantly increased expression ($P \leq 0.05$).

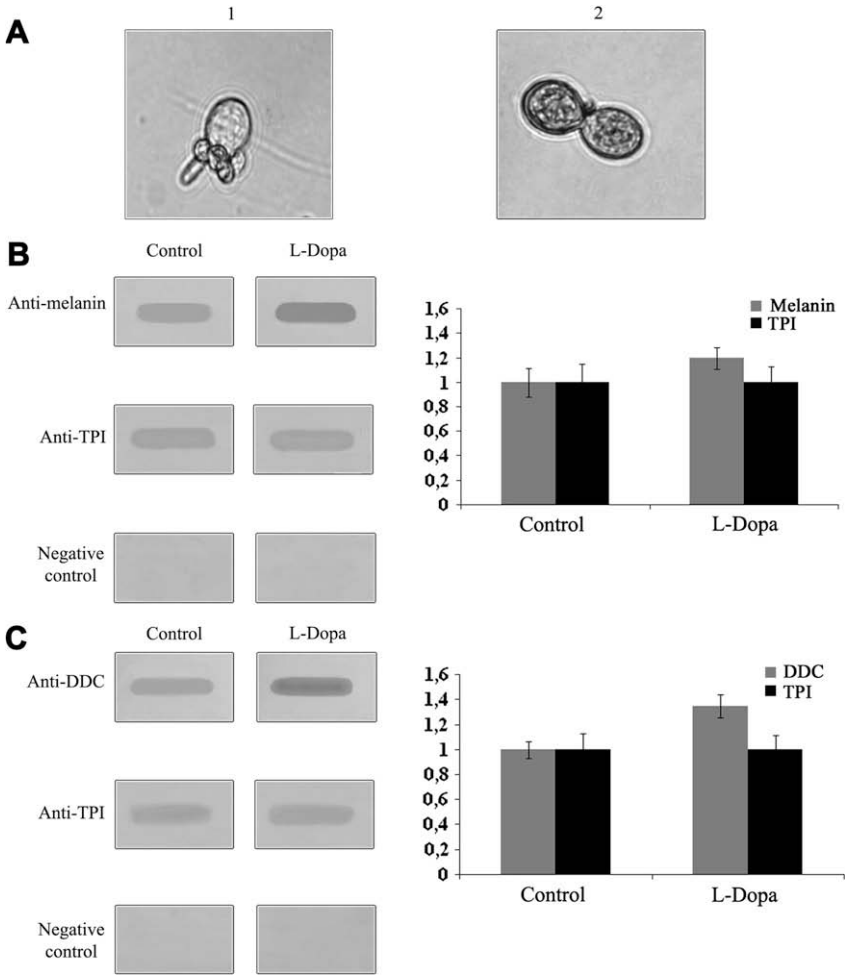

Fig. 3. Analysis of melanization of *P. brasiliensis* yeast cells. A – Light microscopy (400× magnification) of *P. brasiliensis* yeast cells grown in chemically defined liquid medium (1) or the same medium supplemented with L-Dopa (2). B – Dot blot analysis of cellular extracts of *P. brasiliensis* grown in same conditions and reacted with antibody anti-melanin of *S. schenckii* (B) or (C) anti-*Pb*DDC. The antibody to the antigen triosephosphate isomerase (*Pb*TPI), was used as the loading control. The analysis of relative differences were performed by using the Scion Image Beta 4,03 program. In the graphics, the black bars represent the reaction to the antibody anti-*Pb*TPI and the gray bars represent the reaction with the antibodies anti-melanin or anti-*Pb*DDC. The standard deviations are presented from three independent experiments.

4. Discussion

Our objective in the present work was uncovering antigenic proteins that could be expressed during infection with *P. brasiliensis*. Sera from PCM patients were polled and reacted with in vitro-grown *P. brasiliensis*. Antibodies that remain in these sera should be reactive with proteins expressed by the pathogen during the natural infection, as described in other organisms [6–11].

Screening of the *P. brasiliensis* cDNA library with sera from individuals with active PCM resulted in the identification of 35 clones encoding putative immunogenic proteins. Sequence analysis of the reactive clones in the present study identified genes varying from cell metabolism, transport, energy, transcription, protein fate, signal transduction and control of cellular organization, as well as unknown functions. Among the identified transcripts, some encoded molecules presumably present at the fungal cell wall such as high affinity copper transporter, siderophore receptor, carboxylate/amino acid/amine transporter and ABC transporter. Interestingly, some of the identified cDNAs encoded proteins described as immunogenic in organisms, such as DDC [18], acetyl-CoA acetyltransferase [19], LS [20], alcohol dehydrogenase [21]. LS is an enzyme of the family 6,7-dimethyl-8-ribityllumazine synthase, which catalyzes the penultimate step of synthesis of vitamin B_2 (riboflavin). Plants, bacteria and fungi are vulnerable to inhibitors of the synthesis of riboflavin. The lack of such a homologue in humans suggests that *Pb*LS may serve as antifungal drug target, as described [22].

To further confirm the validity of the screening strategy in identifying *P. brasiliensis* antigens potentially relevant to the fungal infection, we selected *Pb*DDC, *Pb*LS and *Pb*CTR3 for further analysis. The recombinant proteins *Pb*DDC and *Pb*LS, as well as the synthetic peptide of *Pb*CTR3 were recognized by sera of PCM patients, validating the IVIAT strategy here employed. LS is an immunogenic molecule and an useful marker in the serological diagnosis of brucellosis in human beings and animals [23].

We selected *Pbddc*, *Pbls* and *Pbctr*3 to follow with experiments concerning to gene expression in models of infection. The

transcripts encoding *Pbddc* and *Pbctr*3 were overexpressed in fungal yeast cells infecting macrophages and in cells derived from tissues of infected mice. We detected overexpression of the transcript encoding *Pbddc* in yeast cells derived from spleen and not in liver at 15 days postinoculation, which could reflect niche regulation of genes in *P. brasiliensis* microenvironments, as described to fungi [24,25]. Noteworthy, *Pbctr*3 was overexpressed in all analyzed conditions corroborating previous transcriptome analysis from our laboratory [3]. This may not be surprising considering the obvious necessity for upregulating copper acquision during infection [26]. It has long been established that invading pathogens must compete favorably for limited nutrients to both establish and maintain a successful host infection. Studies indicate that copper modulates critical virulence determinants. Genetic analysis in *Cryptococcus neoformans* has demonstrated that a high affinity copper transporter and its corresponding transcriptional regulator are required for infection of the brain [27]. Although expressed in liver and spleen at 15 days postinoculation, *Pbls* was not upregulated in vivo relative to the highest level of expression in vitro. There are possible explanations for this result. The gene expression could be induced earlier or later during the infectious process and we could have missed the time at which the expression increased relative to the in vitro growth. Additionally, the amount of RNA could not reflect the amount of protein if the gene regulation occurs at posttranscriptional level. Further investigation will be required.

The fungus *P. brasiliensis* is known to make Dopa-melanin from L-Dopa [28,29]. The production of melanin-like pigments by *P. brasiliensis* protects the fungus from phagocytosis and increases its resistance to antifungal drugs [29]. We verified in this work a correlation between increase in melanin accumulation and *Pb*DDC in yeast cells incubated in the presence of L-Dopa, which resulted in the presence of dark pigment by yeast cells. The results suggest that *Pb*DDC could be involved in the melanin biosynthesis pathway.

In conclusion, the present study has shown the successful application of IVIAT in the identification of *P. brasiliensis* genes expressed during fungal infection. The identified genes ranged from those involved in metabolic pathways to those with unknown function. The study of the identified genes could improve our understanding of the adaptative mechanisms used by *P. brasiliensis* in the infectious process.

Acknowledgments

This work at Universidade Federal de Goiás was supported by grants from FINEP, CNPq, and SECTEC-GO, FAPEG.

Appendix. Supplementary data

Supplementary data associated with this article can be found, in the online version, at doi:10.1016/j.micinf.2009.05.009.

References

[1] A. Restrepo, J.G. Mc Eween, E. Castaneda, The habitat of *Paracoccidioides brasiliensis*: how far from solving the riddle? Med. Mycol. 39 (2001) 233–241.
[2] E. Brummer, E. Castañeda, A. Restrepo, Paracoccidioidomycosis: an update, Clin. Microbiol. Rev. 6 (1993) 89–117.
[3] A.M. Bailão, A. Schrank, C.L. Borges, V. Dutra, E.E.W.I. Molinari-Madlum, M.S.S. Felipe, M.J.S. Mendes-Giannini, W.S. Martins, M. Pereira, C.M.A. Soares, Differential gene expression by *Paracoccidioides brasiliensis* in host interaction conditions: representational difference analysis identifies candidate genes associated with fungal pathogenesis, Microbes Infect. 8 (2006) 2686–2697.
[4] A.M. Bailão, A. Shrank, C.L. Borges, J.A. Parente, V. Dutra, M.S.S. Felipe, R.B. Fiúza, M. Pereira, C.M.A. Soares, The transcriptional profile of *Paracoccidioides brasiliensis* yeast cells is infuenced by human plasma, FEMS Immunol. Med. Microbiol. 51 (2007) 43–57.
[5] M. Costa, C.L. Borges, A.M. Bailão, G.V. Meirelles, Y.A. Mendonça, S.F.I.M. Dantas, F.P. Faria, M.S.S. Felipe, E.E.W.I. Molinari-Madlum, M.J.S.M. Giannini, R.B. Fiúza, W.S. Martins, M. Pereira, C.M.A. Soares, Transcriptome profiling of *Paracoccidioides brasiliensis* yeast-phase cells recovered from infected mice brings new insights into fungal response upon host interaction, Microbiology 153 (2007) 4194–4207.
[6] S. Cheng, C.J. Clancy, M.A. Checkley, M. Handfield, J.D. Hillman, A. Progulske-Fox, A.S. Lewin, P.L. Fidel, M.H. Nguyen, Identification of *Candida albicans* genes induced during thrush offers insight into pathogenesis, Mol. Microbiol. 48 (2003) 1275–1288.
[7] L. Hang, M. John, M. Asaduzzaman, E.A. Bridges, C. Vanderspurt, T.J. Kirn, R.K. Taylor, D.J. Hillman, A. Progulske-Fox, M. Handfield, E.T. Ryan, S.B. Calderwood, Use of in vivo-induced antigen technology (IVIAT) to identify genes uniquely expressed during human infection with *Vibrio cholerae*, Proc. Natl. Acad. Sci. USA 100 (2003) 8508–8513.
[8] J. Richardson, J.C. Craighead, S.L. Cao, M. Handfield, Concurrence between the gene expression pattern of *Actinobacillus actinomycetemcomitans* in localized aggressive periodontitis and in human epithelial cells, J. Med. Microbiol. 54 (2005) 497–504.
[9] M. John, I.T. Kudva, R.W. Griffin, A.W. Dodson, B. McManus, B. Krastins, D. Sarracino, A. Progulske-Fox, J.D. Hillman, M. Handfield, P.I. Tarr, S.B. Calderwood, Use of in vivo-induced antigen technology for identification of *Escherichia coli* O157:H7 proteins expressed during human infection, Infect. Immun. 73 (2005) 2665–2679.
[10] K.Y. Salim, D.G. Cvitkovitch, P. Chang, D.J. Bast, M. Handfield, J.D. Hillman, J.C. Azavedo, Identification of group A *Streptococcus* antigenic determinants upregulated in vivo, Infect. Immun. 73 (2005) 6026–6038.
[11] J.B. Harris, A. Baresch-Bernal, S.M. Rollins, A. Alam, R.C. LaRocque, M. Bikowski, A.F. Peppercorn, M. Handfield, J.D. Hillman, F. Qadri, S.B. Calderwood, E. Hohmann, R.F. Breiman, W.A. Brooks, E.T. Ryan, Identification of in vivo-induced bacterial protein antigens during human infection with *Salmonella enterica serovar Typhi*, Infect. Immun. 74 (2006) 5161–5168.
[12] J. Sambrook, D.W. Russel (Eds.), Molecular Cloning: A Laboratory Manual, Cold Spring Harbor, New York, 2001.
[13] U.K. Laemmli, Cleavage of structural proteins during the assembly of head of bacteriophage T_4, Nature 2227 (1970) 680–685.
[14] A.H. Fortier, L.A. Falk, Isolation of mice macrophages, in: J.E. Coligan, B.E. Bierer, D.H. Margulies, E.M. Shevach, W. Strober, P. Brown (Eds.), Current Protocols in Immunology, John Wiley & Sons, 2007, pp. 14.1.1–14.1.9.
[15] A.L. Bookout, C.L. Cummins, D.J. Mangelsdorf, J.M. Pesola, M.F. Kramer, High-throughput real-time quantitative reverse transcription PCR, in: F.M. Ausubel, R. Brent, R.E. Kingston, D.D. Moore, J.G. Seidman, J.A. Smith, K. Struhl (Eds.), Current Protocols in Molecular Biology, John Wiley & Sons, 2006, pp. 15.8.1–15.8.28.
[16] A. Restrepo, B. Jiménez, Growth of *Paracoccidioides brasiliensis* yeast phase in a chemically defined culture medium, J. Clin. Microbiol. 12 (1980) 279–281.

[17] L.A. Pereira, S.N. Báo, M.S. Barbosa, J.L.M. Silva, M.S.S. Felipe, J.M. Santana, M.J.S. Mendes-Giannini, C.M.A. Soares, Analysis of the *Paracoccidioides brasiliensis* triosephosphate isomerase suggests the potential for adhesion function, FEMS Yeast Res. 8 (2007) 1381–1388.

[18] E. Bratland, A.S.B. Wolff, J. Haavik, O. Kämpe, F. Sköldberg, J. Perheentupa, G. Bredholt, P.M. Knappskog, E.S. Husebye, Epitope mapping of human aromatic L-amino acid decarboxylase, Biochem. Biophys. Res. Commun. 353 (2007) 692–698.

[19] Y. Sakolvaree, S. Maneewatch, S. Jiemsup, B. Klavysing, P. Tongtawe, P. Srimanote, P. Saengjaruk, S. Banven, P. Tapchaisri, M. Chonsa-nguan, W. Chaicumpa, Proteome and immunome of pathogenic *Leptospira* spp. revealed by 2DE and 2DE-immunoblotting with immune serum, Asian. Pac. J. Allergy. Immunol. 25 (2007) 53–73.

[20] D. Bellido, P.O. Craig, M.V. Mozgovoj, D.D. Gonzales, A. Wigdorovitz, F.A. Goldbaum, M.J. Dus Santos, *Brucella* spp. lumazine synthase as a bovine rotavirus antigen delivery system, Vaccine 27 (2009) 136–145.

[21] A. Pitarch, J. Abian, M. Carrascal, M. Sánchez, C. Nombela, C. Gil, Proteomics-based identification of novel *Candida albicans* antigens for diagnosis of systemic candidiasis in patients with underlying hematological malignancies, Proteomics 4 (2004) 3084–3106.

[22] E. Morgunova, W. Meining, B. Illarionov, I. Haase, G. Jin, A. Bacher, M. Cushman, M. Fischer, R. Landenstein, Crystal structure of lumazine synthase from *Mycobacterium tuberculosis* as a target for drug design: binding mode of a new class of purinetrione inhibitors, Biochemistry 44 (2005) 2746–2758.

[23] P.C. Baldi, M.M. Wanke, M.E. Loza, N. Monachesi, C.A. Fossati, Diagnosis of canine brucellosis by detection of IgG antibodies against an 18 kDa cytoplasmic protein of *Brucella* spp., Vet. Microbiol. 57 (1997) 273–281.

[24] C.J. Barelle, C.J. Priest, D.M. Mac-Calum, N.A. Gow, F.C. Odds, A.J. Brown, Niche-specific regulation of central metabolic pathways in a fungal pathogen, Cell. Microbiol. 8 (2006) 961–971.

[25] B. Enjalbert, D.M. Mac-Calum, F.C. Odds, A.J. Brown, Niche-specific activation of the oxidative stress response by the pathogenic fungus *Candida albicans*, Infect. Immun. 745 (2007) 2143–2151.

[26] A.M. Prentice, H. Ghattas, S.E. Cox, Host-pathogen interactions: can micronutrients tip the balance? J. Nutr. 137 (2007) 1334–1337.

[27] S.R. Waterman, M. Hacham, G.X. Hu, Y.D. Park, S. Shin, J. Panepinto, T. Valyi-Nagy, C. Beam, S. Husain, N. Singh, P.R. Williamson, Role of CUF1/CTR4 copper regulatory axis in the virulence of *Cryptococcus neoformans*, J. Clin. Invest. 117 (2007) 794–802.

[28] B.L. Gomez, J.D. Nosanchuk, S. Diez, S. Youngchim, P. Aisen, L.E. Cano, A. Restrepo, A. Casadevall, A.J. Hamilton, Detection of melanin-like pigments in the dimorphic fungal pathogen *Paracoccidioides brasiliensis* in vitro and during infection, Infect. Immun. 69 (2001) 5760–5767.

[29] M.B. Silva, A.F. Marques, J.D. Nosanchuk, A. Casadevall, L.R. Travassos, C.P. Taborda, Melanin in the dimorphic fungal pathogen *Paracoccidioides brasiliensis*: effects on phagocytosis, intracellular resistance and drug susceptibility, Microbes Infect. 8 (2006) 197–205.

Institut Pasteur
Research in Microbiology 163 (2012) 182–191
www.elsevier.com/locate/resmic

Comparative transcriptome analysis of *Paracoccidioides brasiliensis* during in vitro adhesion to type I collagen and fibronectin: identification of potential adhesins

Alexandre Melo Bailão [a], Sarah Veloso Nogueira [a], Sheyla Maria Rondon Caixeta Bonfim [a], Kelly Pacheco de Castro [a], Julhiany de Fátima da Silva [b], Maria José Soares Mendes Giannini [b], Maristela Pereira [a], Célia Maria de Almeida Soares [a,*]

[a] *Laboratório de Biologia Molecular, Instituto de Ciências Biológicas, Universidade Federal de Goiás, 74001-970 Goiânia, GO, Brazil*
[b] *Departamento de Análises Clínicas, Faculdade de Ciências Farmacêuticas, UNESP, Araraquara, SP 14801-902, Brazil*

Received 9 September 2011; accepted 12 January 2012
Available online 23 January 2012

Abstract

Paracoccidioidomycosis is caused by the dimorphic fungus *Paracoccidioides brasiliensis*. The extracellular matrix (ECM) plays an important role in regulation of cell adhesion, differentiation, migration and proliferation of cells. An in vitro binding assay of *P. brasiliensis* yeast cells adhering to type I collagen and fibronectin was performed in order to identify novel adhesins. Representational difference analysis (RDA) was employed to identify genes upregulated under adhesion-inducing conditions. Expressed sequence tags (ESTs) from cDNA libraries generated by the RDA technique were analyzed. Genes related to functional categories, such as metabolism, transcription, energy, protein synthesis and fate, cellular transport and biogenesis of cellular components were upregulated. Transcripts encoding the *P. brasiliensis* protein enolase (*Pb*Eno) and the high-affinity cooper transporter (*Pb*Ctr3) were identified and further characterized. The recombinant enolase (r*Pb*Eno) and a synthetic peptide designed for *Pb*Ctr3 were obtained and demonstrated to be able to bind ECM components. Immunofluorescence assays demonstrated that r*Pb*Eno specifically binds to the macrophage surface, reinforcing the role of this molecule in the *P. brasiliensis* interaction with host cells. In addition, upregulation of selected genes was demonstrated by qRT-PCR. In synthesis, the strategy can be useful in characterization of potential *P. brasiliensis* adhesins.

Keywords: *Paracoccidioides brasiliensis*; Adhesin; RDA; Enolase; Cooper transporter

1. Introduction

Paracoccidioides brasiliensis is the causative agent of paracoccidioidomycosis (PCM), a human systemic mycosis prevalent in South America (Restrepo et al., 2001). In the soil, the fungus grows as a saprobic mycelium, resulting in formation of propagules. After reaching the host, the fungus must convert to the yeast form, a fundamental step in successful establishment of the infection (San-Blas et al., 2002). The mycelial propagules adhere to and invade alveolar cells and the basal lamina, the latter of which is composed of a specialized extracellular matrix (ECM) in which laminin, collagen and fibronectin can be found (Dunsmore and Rannels, 1996; Gonzaléz et al., 2008; Hanna et al., 2000).

Adherence of the pathogens to host cells is considered an essential step in the establishment of infection (Carneiro et al., 2004; Marchais et al., 2005). *P. brasiliensis* has been shown to adhere to ECM proteins. Several studies have established the role of certain *P. brasiliensis* proteins in the adherence process. An antigenic component of *P. brasiliensis*, glycoprotein gp43,

* Corresponding author.
E-mail addresses: alexandre.bailao@gmail.com (A.M. Bailão), shvnogueira@gmail.com (S.V. Nogueira), sheylabonfim@gmail.com (S.M. Rondon Caixeta Bonfim), kellypcastro@gmail.com (K.P. de Castro), julhiany.silva@gmail.com (J. de Fátima da Silva), giannini@fcfar.unesp.br (M.J.S. Mendes Giannini), maristelaufg@gmail.com (M. Pereira), celia@icb.ufg.br (C.M. de Almeida Soares).

0923-2508/$ - see front matter © 2012 Institut Pasteur. Published by Elsevier Masson SAS. All rights reserved.
doi:10.1016/j.resmic.2012.01.004

binds laminin, thereby increasing the pathogenicity of the yeast cells (Vicentini et al., 1994). Proteins with molecular masses of 19 and 32 kDa are present on the fungal surface and interact with laminin, fibronectin and fibrinogen (Gonzaléz et al., 2005). The 32 kDa protein (*Pb*Had32p) was characterized as a hydrolase that influences *P. brasiliensis* pathogenicity (Hernández et al., 2010). In addition, Andreotti et al. (2005) demonstrated that a *P. brasiliensis* 30 kDa protein is able to bind laminin. We characterized several *P. brasiliensis* adhesins such as *Pb*Dfg5p (defective for filamentous growth protein Dfg5p), which was detected by electron microscopy in the cell wall of the fungus and binds laminin, fibronectin and types I and IV collagen (Castro et al., 2008). In addition, triosephosphate isomerase (*Pb*TPI) which binds laminin and fibronectin (Pereira et al., 2007), and glyceraldehyde-3-phosphate dehydrogenase (*Pb*GAPDH), which binds fibronectin, type I collagen and laminin (Barbosa et al., 2006), were found in the *P. brasiliensis* cell wall mediating fungal adherence to in vitro cultured cells. Malate synthase (*Pb*MLS) binds fibronectin and types I and IV collagen and is present in the *P. brasiliensis* cell wall (Neto et al., 2009). In addition, *P. brasiliensis* enolase is a fibronectin and plasminogen binding protein (Donofrio et al., 2009; Nogueira et al., 2010). Therefore, *P. brasiliensis* seems to possess several proteins involved in adhesion, and knowledge of these proteins could advance our understanding of the first steps in establishment of the infection.

To obtain and characterize new molecules involved in the adhesion process in *P. brasiliensis*, we used cDNA representational difference analysis (cDNA-RDA) to identify genes induced during incubation of *P. brasiliensis* yeast cells with ECM components. Fibronectin, a multifunctional extracellular matrix and plasma protein that plays a central role in cell adhesion (Ruoslahti, 1988), and collagens, as the most common matrix molecules (Lyons and Jones, 2007), represent targets for microorganism adherence. Therefore, in this study, we investigated involvement of type I collagen and fibronectin in the adherence process of *P. brasiliensis* and described several putative novel adhesins.

2. Materials and methods

2.1. P. brasiliensis *growth conditions*

P. brasiliensis Pb 01 (ATCC MYA-826) is being studied at our laboratory (Bailão et al., 2006; Barbosa et al., 2006). This isolate was cultivated at 36 °C in Fava-Netto's medium [1% (w/v) peptone; 0.5% (w/v) yeast extract; 0.3% (w/v) proteose peptone; 0.5% (w/v) beef extract; 0.5% (w/v) NaCl; 4% (w/v) glucose; 1% (w/v) agar; pH 7.2] for 4 days.

2.2. *Adherence assay on polystyrene flasks*

The adherence assays were performed as described by Penalver et al. (1996) with several modifications. Briefly, polystyrene flasks (Corning Ultra-Low Attachment 75 cm^2 rectangular canted-neck cell-culture flask) were coated with type I collagen or fibronectin at 50 μg/ml in coating buffer ($NaHCO_3$, Na_2CO_3, [pH 9.6]) and incubated for 1 h at 37 °C and overnight at 4 °C. The plates were blocked by adding PBS (1 mM $Na_2HPO_4.2H_2O$, 1 mM $NaH_2PO_4.H_2O$, 50 mM NaCl, pH 7.4)−1% (w/v) BSA and washed three times with PBS−0.1% (v/v) Tween 20 before a yeast cell suspension (10^8/ml) in PBS was added. The control yeast cells were incubated in PBS−1% (w/v) BSA. The plates were incubated for 1 h at 37 °C and washed three times with PBS−0.1% (v/v) Tween 20 following RNA isolation.

2.3. *RNA isolation*

Total RNAs from *P. brasiliensis* were obtained by the Trizol method according to the manufacturer's instructions (GIBCO, Invitrogen, Carlsbard, CA, USA). DNA contamination was extinguished by treating total RNA with RNAse free DNAse (Promega Corporation®). The RNAs were used to construct double-stranded cDNAs.

2.4. *Subtractive hybridization and generation of subtracted libraries*

Subtractive hybridization was performed as previously described by Bailão et al. (2006). Briefly, 1.0 μg of total RNA was used to produce cDNA. The synthesis of the first strand was performed with SuperScript II reverse transcriptase (Invitrogen Life Technologies); this product was then used as a template to synthesize double-stranded cDNA. The resulting cDNAs were digested with restriction enzyme *Sau3*AI. The subtracted cDNA libraries were constructed using driver cDNAs (from RNAs extracted from the control) and tester cDNAs (synthesized from RNAs extracted from *P. brasiliensis* adhered to type I collagen or fibronectin). The resulting products were purified using a GFX kit (GE Healthcare, Chalfont St. Giles, UK). The tester-digested cDNA was ligated to adapters (a 24-mer annealed to a 12-mer) and amplified by PCR. The amplicons were digested with *Sau3*AI to remove the adapters that had been incorporated into the cDNAs and, after spin-column purification, a new 24-mer adapter was ligated onto the cDNA tester and a different DNA molecule was ligated onto the cDNA driver. The cDNA driver was PCR-amplified and, after cleavage to remove the adapters, it was purified and quantified.

For generation of the differential products, tester and driver cDNAs were mixed, hybridized at 67 °C for 18 h and amplified by PCR with the 24-mer adapter. Two successive rounds of subtraction and PCR amplification using hybridization tester-driver ratios 1:10 and 1:100 were performed. The adapters used for subtractive hybridizations are listed in Table 1 in supplementary material.

After the second subtractive reaction, the final amplified cDNAs were cloned into a pGEM-T Easy vector (Promega, Madison, USA). *Escherichia coli* XL1 Blue competent cells were transformed with the ligation products. Selected colonies were picked and grown in microliter plates and plasmid DNA was prepared. To generate expressed sequence tags (ESTs),

single-pass, 5′-end sequencing of cDNAs by standard fluorescence labeling dye-terminator protocols with T7 flanking vector primer was performed. The samples were loaded onto a MegaBACE 1000 DNA sequencer (GE Healthcare) for automated sequencing analysis.

2.5. EST processing pipeline, annotation and sequence analysis

EST sequences were preprocessed using Phred (Ewing and Green, 1998) and Crossmatch programs (http://www.genome.washington.edu/UWGC/analysistools/Swat.cfm) and were assembled into contigs using CAP3 (Huang and Madan, 1999). All of these tools were integrated in a specific pipeline (http://www.lbm.icb.ufg.br/pipelineUFG/). Only sequences with at least 75 nucleotides and PHRED quality greater than or equal to 20 were considered. ESTs were screened for vector sequences against UniVec data. The clustered sequences were compared using Blast X against the GenBank non-redundant (nr) database from the National Center for Biotechnology Information (NCBI) and the nucleotide database generated from the *P. brasiliensis* structural genome (http://www.broad.mit.edu/annotation/genome/paracoccidioides_brasiliensis/MultiHome.html). The database sequence matches were considered significant at E-values $\leq 10^{-10}$.

The search for functional categories was performed using the bioinformatic tool Blast2GO that combines, in one application, GO annotation based on similarity searches with statistical analysis and highlight visualization on directed acyclic graphs (Conesa et al., 2005). The Blast2GO annotation algorithm takes multiple parameters into account, such as sequence similarity, BLAST HSP (highest scoring pair) length and e-values, the GO hierarchical structure and GO term evidence codes (Conesa et al., 2005; Götz et al., 2008). The sequences were grouped into functional categories according to the classification of the MIPS functional catalog (Munich Center for Protein Sequences; http://mips.gst.de/).

The in silico prediction of adhesins was performed using the tool Faapred (Fungal adhesin and adhesin-like proteins prediction) hosted at http://bioinfo.icgeb.res.in/faap (Ramana and Gupta, 2010). The protein sequences encoded by RDA products were obtained from the *P. brasiliensis* database (http://www.broad.mit.edu/annotation/genome/paracoccidioides_brasiliensis/MultiHome.html) and then loaded onto the software above for predictions.

2.6. Analysis of RNA transcripts by quantitative reverse-transcription PCR (qRT-PCR)

This assay was performed to confirm RDA results and the reliability of our approaches. Total RNAs from *P. brasiliensis* control yeast cells and from yeast cells adhered to type I collagen or fibronectin were obtained as previously described in independent experiments from those used in the RDA. Total RNAs treated with DNAse were reverse-transcribed using Superscript II reverse transcriptase (Invitrogen) and oligo $(dT)_{15}$ primer. The qRT-PCR was performed in triplicate with samples from three independent experiments in the StepOnePlus™ real-time PCR system (Applied Biosystems, Foster City, CA). The PCR thermal cycling was 40 cycles of 95 °C for 15 s and 60 °C for 1 min. SYBR Green PCR master mix (Applied Biosystems) was used as the reaction mixture to which were added 10 pmol of each specific primer and 40 ng of template cDNA in a final volume of 20 µl. Melting curve analysis was performed to confirm a single PCR product. The data were normalized with the transcript for α-tubulin amplified in each set of qRT-PCR experiments. A non-template control was included. A cDNA for a relative standard curve was generated by pooling an aliquot from each cDNA sample. The standard curve was serially diluted 1:5 and a standard curve was generated using five samples from the pooled cDNA. Relative expression levels of genes of interest were calculated using the standard curve method for relative quantification (Bookout et al., 2006). The specific primers, both sense and antisense, are described in Table 1 in supplementary material.

2.7. Cloning the cDNA encoding enolase into an expression vector and purification of the recombinant protein

The procedures for obtaining the recombinant protein enolase were performed as previously described (Nogueira et al., 2010). The complete enolase cDNA (GenBank accession number EF558735.1), obtained from a library from yeast cells of *P. brasiliensis* (Costa et al., 2007), was amplified by PCR employing primers, as described in Table 1 of the supplementary material. The PCR product was cloned in-frame with the glutathione S-transferase (GST) coding region of the pGEX-4T3 vector to yield the GST-*Pb*Eno construct. The procedures for obtaining the recombinant protein were performed as previously described (Nogueira et al., 2010).

Bacteria of the *E. coli* strain BL21 pLys, transformed with the GST-*Pb*Eno construct, were grown in Luria Bertani (LB) medium supplemented with ampicillin (100 µg/ml) and glucose (20 mM) at 37 °C, 200 rpm. At an A_{600} of 0.6, protein production was induced by the addition of isopropyl-β-D-thiogalactopyranoside (IPTG) to a final concentration of 0.1 mM. After centrifugation, *E. coli* bacterial pellets were resuspended in PBS, incubated on ice for 30 min and sonicated on ice 15 times for 60 s each. The GST-*Pb*Eno protein was affinity-purified using glutathione Sepharose 4B (GE Healthcare) according to the manufacturer's protocol, and *Pb*Eno was released from GST-*Pb*Eno by the addition of thrombin (Sigma Aldrich). The cleavage reaction was stopped by freezing the sample at −20 °C. The purity and integrity of the protein were verified by sodium dodecyl sulfate-polyacrylamide gel electrophoresis (SDS-PAGE), followed by Coomassie Blue staining.

2.8. Affinity ligand assays and dot blot analysis

Far-western assays were carried out as previously described (Barbosa et al., 2006; Castro et al., 2008). The recombinant

enolase (r*Pb*Eno) was submitted to SDS-PAGE and blotted onto nitrocellulose membranes. The blotted protein was assayed for laminin, fibronectin, type I and type IV collagen binding, as follows. The blotted membranes were blocked for 4 h with PBS–1% (w/v) BSA and 5% (w/v) milk, incubated with laminin (30 μg/ml), fibronectin (30 μg/ml), type I collagen (20 μg/ml) or type IV collagen (20 μg/ml) diluted in PBS–1% (w/v) BSA for 90 min and washed three times with PBS–0.1% (v/v) Tween 20. The membranes were incubated overnight with the rabbit antibodies anti-laminin, anti-fibronectin, anti-type I collagen or anti-type IV collagen (diluted 1:100). The blots were washed with PBS–0.1% (v/v) Tween 20 and incubated with peroxidase-labeled goat anti-rabbit immunoglobulin (diluted 1:1000) for 2 h. The blots were washed with PBS–0.1% (v/v) Tween 20 and the reactive bands were developed with hydrogen peroxide diaminobenzidine as the chromogenic reagent. As a negative control, r*Pb*Eno was incubated only with peroxidase-labeled goat anti-rabbit immunoglobulin in the absence of the ECM proteins (laminin, fibronectin and type I and IV collagen). An additional control was obtained by incubating r*Pb*Eno with BSA.

A peptide was synthesized based on the deduced sequence of *Pb*Ctr3 (GenBank accession number DQ534496) toward amino acids 90–130 (Dantas et al., 2009), and dot blot analysis was performed to assay the reactivity of this peptide to the ECM proteins. The reactions were performed as described above for the affinity ligand assay.

2.9. Immunofluorescence

J774 A.1 macrophage cells purchased from Banco de Células do Rio de Janeiro (Rio de Janeiro Brazil) were cultured over coverslips in 6-well plates and subjected to an enolase binding assay. Mammalian cells were cultured in RPMI supplemented with interferon gamma (1 U/ml). The medium was removed and the cells were washed 3 times with PBS, fixed for 30 min with cold methanol and air-dried. Either recombinant enolase (350 μg/ml) or 1% BSA (w/v, negative control) in PBS was added and incubated with fixed J774 cells at room temperature for 1 h. After cells were washed 3 times with PBS, mouse enolase antiserum (1:100 dilution) was added. The system was incubated for 1 h at 37 °C and washed 3 times with PBS. The cells were incubated with anti-rabbit IgG coupled to fluorescein isothiocyanate (FITC; 1:100 dilution) for 1 h. The cells were incubated with 50 μM 4′,6-diamidino-2-phenylindole (DAPI) for nuclear staining.

2.10. Statistical analysis

The experiments were performed in triplicate with samples in triplicate. The results were presented as means ± standard deviation. The statistical comparisons were performed using Student's *t*-test. Statistical significance was accepted for $P < 0.05$.

3. Results

3.1. Expression profile of P. brasiliensis yeast cells adhering to type I collagen and fibronectin

The RDA approach was performed with RNAs obtained under three conditions: (a) *P. brasiliensis* yeast cells adhering to type I collagen; (b) *P. brasiliensis* yeast cells adhering to fibronectin; and (c) control *P. brasiliensis* yeast cells. The first and second conditions were used independently as tester cDNA populations and the third was used as the driver cDNA population. Subtraction hybridization was performed by incubating the driver with each tester. Selection of the cDNAs was achieved by construction of subtracted libraries.

For comparative analysis, the 535 ESTs from the cells adhering to type I collagen were grouped into 65 clusters, represented by 30 contigs and 35 singlets. Most of the annotated ESTs (34%) corresponded to energy production. A high proportion of the ESTs found under type I collagen conditions (55%) exhibited sequence similarity to genes of unknown function or encoding hypothetical proteins (Table 1). A broad view of the nature of adaptations made by *P. brasiliensis* during adherence to type I collagen was obtained by classifying the ESTs into seven groups of functionally related genes (Table 1).

ESTs from cells adhering to fibronectin were grouped in 62 clusters, as represented by 25 contigs and 37 singlets. The analysis of 583 ESTs revealed that most of the annotated ESTs (42%) corresponded to transcripts related to cell rescue, defense and virulence (Table 2), while 31% of the ESTs found under fibronectin-binding conditions did not show similarity to known *P. brasiliensis* genes. The annotated ESTs comprised nine different MIPS categories, indicating a wide range of processes probably involved in *P. brasiliensis* adhesion to fibronectin (Table 2).

The Faapred bioinformatics tool used for identification of fungal adhesins is trained software with different compositional features: namely, amino acid, dipeptide, multiplet fractions, charge and hydrophobic compositions, as well as PSI-Blast (Ramana and Gupta, 2010). In silico adhesin prediction analysis using the Faapred tool returned 16 out of 30 upregulated genes and 27 out from 44 upregulated genes from collagen and fibronectin conditions, respectively (Tables 1 and 2).

3.2. qRT-PCR assays in analysis of gene expression

For further confirmatory data on the expression level from EST redundancy analysis, an assessment of *P. brasiliensis* alcohol dehydrogenase (*Pbadh*), enolase (*Pbeno*), arginine N-methyltransferase (*Pbskb1*), enoyl-CoA hydratase (*Pbenoyl-CoA*), copper transporter (*Pb*ctr3) and heat-shock protein 70 (*Pbhsp70*) was provided by qRT-PCR analysis. *Pbadh*, *Pbeno* and *Pbskb1* were induced in yeast cells adhering to type I collagen and fibronectin (Fig. 1A), as demonstrated in the RDA. *Pbenoyl-CoA* was induced in yeast

cells adhering to collagen (Fig. 1B), and *Pb*ctr3 and *Pbhsp70* were induced in yeast cells adhering to fibronectin (Fig. 1C), confirming RDA.

3.3. *r*Pb*Eno and* Pb*Ctr3 bind to matrix proteins*

We selected the transcripts encoding enolase (*Pb*eno) and the high-affinity cooper transporter (*Pb*ctr3) for testing the ability of the cognate proteins to adhere to ECM components in vitro. The criterion for selection was the predicted cell wall localization of both proteins, as previously described (Dantas et al., 2009; Nogueira et al., 2010). For that, the full-length cDNA encoding enolase consisted of 1684 bp with an open reading frame encoding 438 amino acids with a calculated molecular mass of 47 kDa. cDNA encoding *P. brasiliensis* enolase was cloned into the expression vector pGEX-4T-3 to obtain the recombinant fusion protein in *E. coli*. After induction with IPTG, a recombinant protein was detected in bacterial lysates (Fig. 2A, lane 2). The fusion protein was affinity-purified and r*Pb*Eno was obtained by digestion with thrombin (Fig. 2A, lane 3).

The ability of r*Pb*Eno to bind laminin, fibronectin and type I and IV collagens was determined by far-western blotting assays, as shown in Fig. 2B. r*Pb*Eno exhibited the ability to bind to laminin (lane 3), fibronectin (lane 4) and type I collagen (lane 5). There was no detectable reaction with type IV collagen (lane 6). Negative controls were obtained by incubating r*Pb*Eno in the absence of the ECM proteins (lane 1), and by using BSA (lane 2).

In addition, the synthetic peptide (*Pb*Ctr3) (Fig. 2C), reacted with type I collagen (lane 2), type IV collagen (lane 3) and fibronectin (lane 4). There was no reactivity with BSA (negative control) (lane 1) or laminin (lane 5).

Table 1
Annotated ESTs with high abundance in yeast cells during adhesion to collagen versus control yeast cells.

Functional category	Gene product	Best hit/GenBank accession number* or *P. brasiliensis* genome locus**	e-Value	Number of occurrences
Metabolism	Acetamidase[b]	*P. brasiliensis*/PAAG_03626.1**	1e−55	12
	Transketolase	*P. brasiliensis*/PAAG_04444.1**	1e−55	5
	Enoyl-CoA hydratase	*P. brasiliensis*/PABG_02862.1**	1e−38	2
	Mitochondrial protein potentially involved in regulation of respiratory metabolism	*Saccharomyces cerevisiae*/NP_690845.1*	3e−11	8
	Alcohol dehydrogenase[a]	*P. brasiliensis*/PAAG_04541.1**	1e−51	1
Energy	NADH dehydrogenase[b]	*P. brasiliensis*/PAAG_04760.1**	1e−26	176
	Enolase[a,b]	*P. brasiliensis*/PAAG_00771.1**	1e−56	3
Transcription	Transcription factor MetR	*P. brasiliensis*/PAAG_04371.1**	1e−14	5
	Endoribonuclease ysh1 (Bzip)	*P. brasiliensis*/PAAG_08788.1**	1e−76	6
	SWI/SNF transcription activation complex subunit	*P. brasiliensis*/PAAG_06542.1**	1e−52	1
	Protein Kruppel[b]	*P. brasiliensis*/PAAG_06709.1**	1e−27	1
	Pre mRNA splicing factor prp1	*P. brasiliensis*/PAAG_00995.1**	1e−26	1
Protein binding	FAD-linked sulfhydryl oxidase	*P. brasiliensis*/PAAG_06132.1**	1e−35	2
	Cytosolic Fe-S cluster assembling factor NBP35[b]	*P. brasiliensis*/PAAG_03944.1**	1e−112	1
Cell cycle and DNA processing	DNA polymerase epsilon subunit c[b]	*P. brasiliensis*/PAAG_00002.1**	1e−10	4
Cell rescue virulence	Hsp98/Hsp104	*P. brasiliensis*/PAAG_02130.1**	1e−49	2
Protein fate	Arginine N-methyltransferase skb1[a,b]	*P. brasiliensis*/PAAG_02402.1**	1e−85	3
Unclassified proteins	Conserved hypothetical protein[b]	*P. brasiliensis*/PADG_08537.1**	5e−41	32
	Conserved hypothetical protein[b]	*P. brasiliensis*/PAAG_08039.1**	1e−19	2
	Conserved hypothetical protein[b]	*P. brasiliensis*/PABG_01516.1**	1e−13	1
	Conserved hypothetical protein	*P. brasiliensis*/PAAG_04760.1**	1e−26	1
	Conserved hypothetical protein	*P. brasiliensis*/PAAG_01303.1**	1e−34	1
	Conserved hypothetical protein	*P. brasiliensis*/PAAG_07033.1**	1e−13	16
	Conserved hypothetical protein[b]	*P. brasiliensis*/PABG_03557.1**	1e−34	2
	Conserved hypothetical protein[b]	*P. brasiliensis*/PABG_07127.1**	1e−18	6
	Hypothetical protein[b]	*P. brasiliensis*/PABG_06807.1**	1e−27	167
	Hypothetical protein[b]	*P. brasiliensis*/PAAG_07288.1**	1e−36	49
	Hypothetical protein	*P. brasiliensis*/PABG_01874.1**	1e−64	4
	Hypothetical protein[b]	*P. brasiliensis*/PAAG_03580.1**	1e−49	3
	Hypothetical protein[b]	*P. brasiliensis*/PAAG_02061.1**	1e−19	2
No significant similarity found				2

[a] Transcripts overexpressed in the presence of type I collagen and fibronectin.
[b] Putative adhesins predicted by Faadpred in silico analysis.

Table 2
Annotated ESTs with high abundance in yeast cells during adhesion to fibronectin versus control yeast cells.

Functional category	Gene product	Best hit/GenBank accession number* or *P. brasiliensis* genome locus**	e-Value	Number of occurrences
Metabolism	Alanine-glyoxylate aminotransferase	*P. brasiliensis*/PAAG_03138.1**	1e−105	5
	Betaine aldehyde dehydrogenase[b]	*P. brasiliensis*/PAAG_05392.1**	1e−63	7
	Mitochondrial NADP-specific isocitrate dehydrogenase[b]	*P. brasiliensis*/PAAG_08351.1**	1e−57	1
	Alcohol dehydrogenase[a]	*P. brasiliensis*/PAAG_00403.1**	1e−59	1
	C-5 sterol desaturase	*P. brasiliensis*/PAAG_03651.1**	1e−68	1
Energy	Enolase[a,b]	*P. brasiliensis*/PAAG_00771.1**	1e−43	10
	Hexokinase-1[b]	*P. brasiliensis*/PAAG_01377.1**	1e−15	1
Transcription	C2H2 transcription factor (Seb1)[b]	*P. brasiliensis*/EEH47059.1*	1e−21	4
	Sexual development transcription factor NsdD[b]	*P. brasiliensis*/PAAG_05818.1**	1e−47	74
	C2H2 transcription factor (Con7)[b]	*Ajellomyces dermatitidis*/EEQ91999.1*	1e−52	1
	C6 transcription factor (Ctf1B)[b]	*P. brasiliensis*/PAAG_01359.1**	1e−12	2
	NF-X1 finger transcription factor	*Ajellomyces dermatitidis*/EEQ87210.1*	7e−89	15
	APSES transcription factor[b]	*Aspergillus fumigatus*/EDP51876.1*	1e−41	1
	Forkhead box protein D1	*P. brasiliensis*/PAAG_07388.1**	1e−14	1
	Transcription factor atf1[b]	*P. brasiliensis*/PAAG_01945.1**	1e−22	2
Protein binding	SCP-like extracellular[b]	*P. brasiliensis*/XP_752604.1*	1e−50	1
	Ribosomal protein mrp4[b]	*P. brasiliensis*/PAAG_07873.1**	1e−70	1
	Hsp90 binding co-chaperone (Sba1)	*P. brasiliensis*/PAAG_05226.1**	1e−16	1
Cell cycle and DNA processing	Cell cycle inhibitor Nif1[b]	*Ajellomyces capsulatus*/EER43226.1*	1e−15	1
Cell rescue and virulence	Heat-shock protein 70 Hsp70[b]	*P. brasiliensis*/PAAG_08003.1**	1e−37	231
	Heat-shock protein 60 Hsp60	*P. brasiliensis*/PAAG_08059.1**	1e−56	7
	Heat-shock protein 30 Hsp30	*P. brasiliensis*/PAAG_00871.1**	1e−62	5
	DnaJ domain protein Psi	*P. brasiliensis* /PAAG_00478.1**	1e−24	1
Cellular transport	*Pb*Ctr 3-high-affinity copper transporter	*P. brasiliensis*/PAAG_05251.1**	1e−92	15
	Mechanosensitive ion channel family	*P. brasiliensis*/PAAG_01645.1**	1e−84	2
	Golgi membrane protein (Coy1)	*P. brasiliensis*/PAAG_05425.1**	1e−53	1
	Benomyl/methotrexate resistance protein[b]	*P. brasiliensis*/PAAG_07478.1**	1e−84	2
Protein fate	Galactosyltransferase[b]	*P. brasiliensis*/PADG_00117.1**	1e−66	1
	Arginine N-methyltransferase Skb1[a,b]	*P. brasiliensis*/PAAG_02402.1**	1e−61	1
Protein synthesis	CAP20[b]	*P. brasiliensis*/PAAG_06538.1**	1e−79	7
Unclassified proteins	Urg3	*P. brasiliensis*/PABG_03978.1**	1e−89	3
	Conserved hypothetical protein[b]	*P. brasiliensis*/PAAG_08906.1**	1e−23	103
	Conserved hypothetical protein[b]	*P. brasiliensis*/PADG_08537.1**	8e−45	40
	Conserved hypothetical protein[b]	*P. brasiliensis*/PAAG_05634.1**	0.0	1
	Conserved hypothetical protein[b]	*P. brasiliensis*/PAAG_03559.1**	0.0	2
	Conserved hypothetical protein[b]	*P. brasiliensis*/PAAG_07480.1**	0.0	1
	Conserved hypothetical protein[b]	*P. brasiliensis*/PAAG_00128.1**	0.0	1
	Hypothetical protein[b]	*P. brasiliensis*/PAAG_01169.1**	6e−26	8
	Hypothetical protein	*P. brasiliensis*/PAAG_00089.1**	0.0	3
	Hypothetical protein[b]	*P. brasiliensis*/PAAG_08515.1**	1e−33	3
	Hypothetical protein[b]	*P. brasiliensis*/XP_002484510.1*	1e−44	1
	Hypothetical protein	*Shewanella oneidensis*/NP_717361.1*	3e−11	3
	Hypothetical protein	*P. brasiliensis*/PAAG_03092.1**	0.0	1
	Hypothetical protein	Gibberella zeae/XP_382291.1*	1e−11	1
No significant similarity found				7

[a] Transcripts overexpressed in the presence of type I collagen and fibronectin.
[b] Putative adhesins predicted by Faadpred *in silico* analysis.

3.4. *r*Pb*Eno attaches to the macrophage surface*

Immunofluorescence assays were also conducted to visualize whether *P. brasiliensis* enolase can specifically adhere to the surface of J774 A.1 cells (Fig. 3). Evidence of enolase binding to the macrophage cells was found. The immunomicroscopy showed that enolase specifically bound to the macrophage the surface (Fig. 3B). No binding was observed with BSA as a control (Fig. 3A). This observation reinforces previous findings suggesting the role of this molecule in the

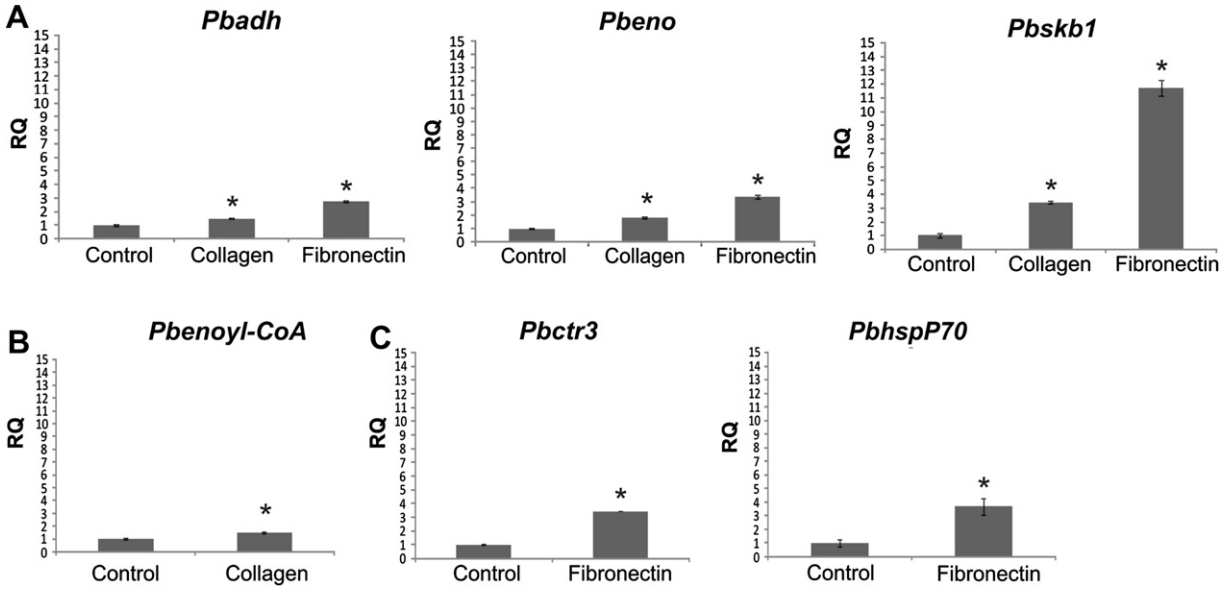

Fig. 1. Average gene expression of *Pbadh*, *Pbeno*, *Pbskb*1, *Pbenoyl-CoA*, *Pbctr3* and *Pbhsp70*, as determined by quantitative real-time RT-PCR. (A) qRT-PCR plot of *Pbadh*, *Pbeno* and *Pbskb*1 expression levels in yeast cells adhering to type I collagen and fibronectin. (B) qRT-PCR plot of *Pbenoyl-CoA* expression levels in yeast cells adhering to type I collagen. (C) qRT-PCR plot of *Pbctr3* and *Pbhsp70* expression levels in yeast cells adhering to fibronectin. The values of expression were standardized using values of expression of the constitutive gene encoding α-tubulin. The expression level was calculated by the relative standard curve method. The standard deviations are presented from three independent experiments. *, Significantly different from the control, at a *P*-value of <0.05.

attaching process between *P. brasiliensis* and host cells (Nogueira et al., 2010).

4. Discussion

Our objective in the present work was to uncover potential adhesins that could be expressed during the adhesion process of *P. brasiliensis*. For this purpose, in vitro adherence assays to extracellular matrix proteins were performed. The RDA assays allowed identification of 69 upregulated genes during fibronectin and collagen adhering conditions. Three genes were found in both conditions. Among the identified transcripts, several were identified as coding for previously characterized adhesins such as alcohol dehydrogenase (ADH), Hsp60 and Hsp70. Many differentially expressed transcripts detected in this work, such as C-5 sterol desaturase, cap20 protein, high-affinity copper transporter, hexokinase and transketolase, had already been described as upregulated genes in yeast cells derived from models of infection (Bailão et al., 2006; Costa et al., 2007). The induced expression of putative virulence factors indicates that the presence of ECM components may be a stimulus to trigger mechanisms to adapt to the host milieu. Among the RDA differential products, many transcripts encoding hypothetical proteins were isolated. Bioinformatics-based analysis confirmed that most RDA products are predicted to be adhesin-like molecules and many of them are proteins with unknown function.

By screening a cDNA expression library of *Candida albicans* yeast cells with polyclonal antiserum to human fibronectin, Klotz et al. (2001) isolated cDNA clones that encode ADH, suggesting that this protein is found on the cell surface of this fungus and could be a receptor for fibronectin. Also, Crowe et al. (2003), in an attempt to identify *C. albicans* proteins involved in plasminogen binding, identified ADH in cell wall protein extracts of this fungus. Upregulation of transcripts encoding *P. brasiliensis* ADH during contact with ECM components suggests the role of this protein in adhesion of yeast cells to host tissues.

The transcript-encoding enolase was induced under both studied conditions. Several studies had demonstrated the role of enolase as an ECM binding protein. This molecule is a cell surface protein in *Staphylococcus aureus* and mediates binding of this microorganism to laminin, potentially playing a critical role in its pathogenesis (Carneiro et al., 2004). In addition, previous works showed the surface localization of *Streptococcus suis* enolase and its ability to bind to fibronectin (Esgleas et al., 2008) and to Hep-2 cell surface (Feng et al., 2009). Using a proteomic approach, Chen et al. (2011) showed that *S. suis* enolase is a protein that binds to macrophage surface molecules. Moreover, Castaldo et al. (2009), using immune electron microscopy also demonstrated the cell surface localization of *Lactobacillus plantarum* enolase, where it can bind fibronectin and mediate adhesion of this commensal bacterium to human intestinal cells. Regarding *P. brasiliensis*, *Pb*Eno was previously described as a fibronectin-binding protein that mediates the interaction between the fungus and pulmonary epithelial cells, A549 (Donofrio et al., 2009). Our recent studies demonstrated the potential contribution of *Pb*Eno as a virulence factor for *P. brasiliensis*. In fact, in *P. brasiliensis*, surface-associated enolase was documented and shown to bind host plasminogen. Moreover, plasminogen-coated *P. brasiliensis* yeast cells are capable of degrading purified fibronectin, providing in vitro evidence for the generation of plasmin on the fungus surface. In addition,

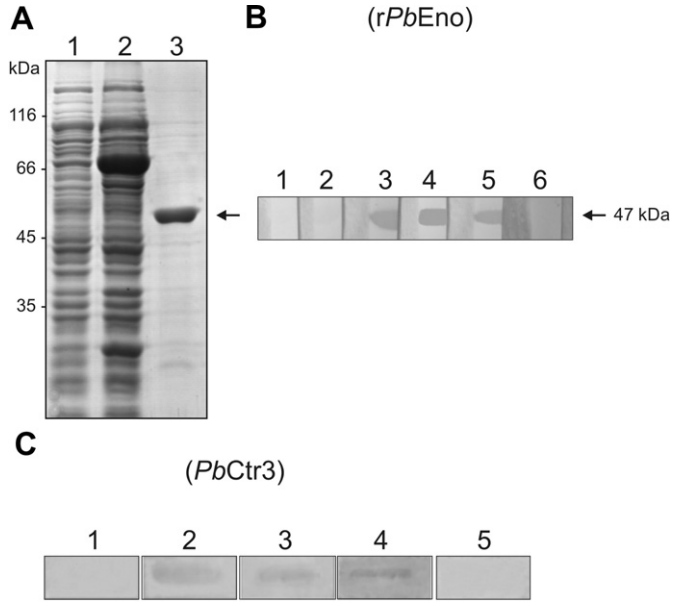

Fig. 2. Binding of *Pb*Eno and *Pb*Ctr3 to extracellular matrix components. (A) SDS-PAGE analysis of *P. brasiliensis* recombinant enolase (r*Pb*Eno). *E. coli* cells harboring the pGEX-4T-3-enolase plasmid were grown at 37 °C to an A_{600} of 0.6 and harvested before (lane 1) and after (lane 2) 16 h incubation at 15 °C with 0.1 mM IPTG. The cells were lysed by extensive sonication. Lane 3, purified r*Pb*Eno (after cleavage with thrombin). The protein extracts were fractionated by one-dimensional gel electrophoresis and stained by Coomassie Blue. (B) Recombinant enolase (0.5 μg) was subjected to SDS-PAGE and electroblotted. The membranes were reacted with laminin (lane 3), fibronectin (lane 4), type I collagen (lane 5) and type IV collagen (lane 6) and were subsequently incubated with rabbit IgG anti-laminin, anti-fibronectin, anti-type I collagen and anti-type IV collagen antibodies, respectively. The use of peroxidase-conjugated anti-rabbit IgG revealed the reactions. The negative controls were obtained by incubating the r*Pb*Eno with no ECM component (lane 1) and using BSA (lane 2). (C) Reactivity of the synthetic peptide from *Pb*Ctr3 with type I collagen (lane 2), type IV collagen (lane 3), fibronectin (lane 4) or laminin (lane 5). The negative control was obtained by using BSA (lane 1).

recombinant enolase promoted an increase in the association of *P. brasiliensis* with host cells in ex vivo models of infection (Nogueira et al., 2010). The ability of *Pb*Eno to bind to ECM components and to the macrophage surface, as demonstrated by far-western and immunofluorescence in the present work, may account for the molecule's effect in promoting *P. brasiliensis* adhesion to host cells. Although these results point to a contribution by *Pb*Eno to *P. brasiliensis* pathogenesis, studies have been hampered by the lack of a standardized protocol for generation of *P. brasiliensis* knockout mutants and by the fact that the enolase gene is essential.

Molecular chaperones were upregulated during *P. brasiliensis* in vitro adhesion to fibronectin. Chaperones had been detected at the surface of microorganisms, supporting their potential role in adhesion. Specifically, Batista et al. (2006) reported the presence of a member of the J-domain protein family, Mdj1, at the cell surface of *P. brasiliensis*. Hsp60, which has been detected in small clusters at discrete points on the *Histoplasma capsulatum* cell wall, has been shown to mediate attachment of the fungus to macrophages via CD11/CD18 receptors (Long et al., 2003). *Helicobacter pylori* Hsp70 was found at the cell surface and mediates adhesion of the bacteria to glycolipids found in the stomach tissue (Huesca et al., 1998). Likewise, Hsp30, Hsp60 and Hsp70 were found in secretory vesicles in *H. capsulatum* (Albuquerque et al., 2008), suggesting a secretory route for such molecules.

The high-affinity copper transporter is a key molecule related to homeostasis of copper to fungal pathogens. The capacity for copper uptake by pathogenic microorganisms is considered to be a virulence factor because the availability of this metal is low in host tissues (Silva et al., 2011). The impairment of copper uptake in *Cryptococcus neoformans* led to diminished fungal burden in a mouse model of infection (Waterman et al., 2007). The *Pb*ctr3 transcript was induced in *P. brasiliensis* yeast cells derived from infected tissues (Bailão et al., 2006) and was also recognized by sera from PCM patients (Dantas et al., 2009), suggesting its role in the infectious process. The transcript encoding *Pb*Ctr3 was induced in yeast cells in contact with fibronectin. In addition, *Pb*Ctr3 synthetic peptide was able to bind to fibronectin, type I collagen and type II collagen. Taken together, these results suggest that adhesion could be a secondary function of Ctr3, although further investigations are necessary to elucidate this new function. Although this molecule has not been described before as an ECM binding

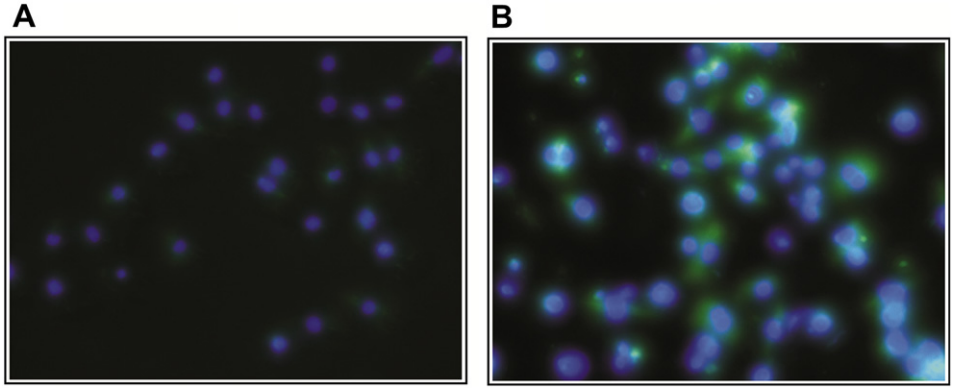

Fig. 3. Binding of r*Pb*Eno to the macrophage surface. Immunofluorescence analysis showing binding of the recombinant enolase to J774 A.1 mouse macrophage cells. (B) Blue indicates the macrophage nucleus and green indicates enolase bound to the surface of the macrophage. (A) The negative control was performed with an unrelated protein (BSA). (For interpretation of the references to color in this figure legend, the reader is referred to the web version of this article.)

component, its probable localization at the cell surface should enable its binding capacity.

Extracellular matrix in the host tissues provides structural support, compartmentalizes tissues, serves as a physical barrier and is permeable to many compounds. Fibronectin and collagen are major components of the protein content of ECM (Dunsmore and Rannels, 1996). These proteins are the main targets enabling pathogenic microorganisms to attach and invade host tissues by means of adhesins. RDA products obtained from *P. brasiliensis* incubated with fibronectin and collagen revealed many specifically upregulated transcripts. Those findings likely indicate that different ECM components elicit specific pathways that permit a *P. brasiliensis* adaptation mechanism in host tissues. Studies had demonstrated that *C. albicans* is able to respond to very subtle differences in the environment during adhesion to various growth substrates (Sohn et al., 2006; Zakikhany et al., 2007).

In conclusion, this study enabled identification of proteins that may be involved in the adhesion process of *P. brasiliensis*. Indeed, a number of these proteins have already been described in the pathogenesis of this and other microorganisms and elucidation of the role of hypothetical proteins could reveal more information regarding molecules involved in adherence and pathogenesis.

Acknowledgments

This work at the Universidade Federal de Goiás was supported by grants from Financiadora de Estudos e Projetos (FINEP-0107055200 and 0106121200) and Conselho Nacional de Desenvolvimento Científico e Tecnológico (CNPq-471808/2006-7 and 472947/2007-9). We wish to thank Nadya da Silva Castro and Juliana Alves Parente for their helpful suggestions.

Appendix. Supplementary material

Supplementary data associated with this article can be found, in the online version, at doi:10.1016/j.resmic.2012.01.004.

References

Albuquerque, P.C., Nakayasu, E.S., Rodrigues, M.L., Frases, S., Casadevall, A., Zancope-Oliveira, R.M., Almeida, I.C., Nosanchuk, J.D., 2008. Vesicular transport in *Histoplasma capsulatum*: an effective mechanism for trans-cell wall transfer of proteins and lipids in ascomycetes. Cell. Microbiol. 10, 1695–1710.

Andreotti, P.F., da Silva, J.L.M., Bailão, A.M., Soares, C.M.A., Bernard, G., Soares, C.P., Mendes-Giannini, M.J., 2005. Isolation and partial characterization of a 30 kDa adhesin from *Paracoccidioides brasiliensis*. Microbes Infect. 7, 875–881.

Bailão, A.M., Schrank, A., Borges, C.L., Dutra, V., Molinari-Madlum, E.E.W.I., Felipe, M.S.S., Mendes-Giannini, M.J.S., Martins, W.S., Pereira, M., Soares, C.M.A., 2006. Differential gene expression by *Paracoccidioides brasiliensis* in host interaction conditions: representational difference analysis identifies candidate gene associated with fungal pathogenesis. Microbes Infect. 8, 2686–2697.

Barbosa, M.S., Báo, S.N., Andreotti, P.F., Faria, F.P., Felipe, M.S., Feitosa, L.S., Mendes-Giannini, M.J.S., Soares, C.M.A., 2006. Glyceraldehyde-3-phosphate dehydrogenase of *Paracoccidioides brasiliensis* is a cell surface protein involved in fungal adhesion to extracellular matrix proteins and interaction with cells. Infect. Immun. 74, 382–389.

Batista, W.L., Matsuo, A.L., Ganiko, L., Barros, T.F., Veiga, T.R., Freymuller, E., Puccia, R., 2006. The PbMDJ1 gene belongs to a conserved MDJ1/LON locus in thermodimorphic pathogenic fungi and encodes a heat shock protein that localizes to both the mitochondria and cell wall of *Paracoccidioides brasiliensis*. Eukaryot. Cell 5, 379–390.

Bookout, A.L., Cummins, C.L., Mangelsdorf, D.J., Pesola, J.M., Kramer, M.F., 2006. High-throughput real-time quantitative reverse transcription PCR. Curr. Protoc. Mol. Biol. 15. 15.8.

Carneiro, C.R.W., Postol, E., Nomizo, R., Reis, L.F.L., Brentani, R.R., 2004. Identification of enolase as a laminin-binding protein on the surface of *Staphylococcus aureus*. Microbes Infect 6, 604–608.

Castaldo, C., Vastano, V., Siciliano, R.A., Candela, M., Vici, M., Muscariello, L., Marasco, R., Sacco, M., 2009. Surface displaced alpha-enolase of *Lactobacillus plantarum* is a fibronectin binding protein. Microb. Cell Fact. 16, 8–14.

Castro, N.S., Barbosa, M.S., Maia, Z.A., Bao, S.N., Felipe, M.S.S., Santana, J.M., Mendes-Giannini, M.J.S., Pereira, M., Soares, C.M.A., 2008. Characterization of *Paracoccidioides brasiliensis* PbDfg5p, a cell-wall protein implicated in filamentous growth. Yeast 25, 141–154.

Chen, B., Zhang, A., Xu, Z., Li, R., Chen, H., Jin, M., 2011. Large-scale identification of bacteria-host crosstalk by affinity chromatography: capturing the interactions of *Streptococcus suis* proteins with host cells. J. Proteome Res. 10, 5163–5174.

Conesa, A., Göts, S., García-Gómez, J.M., Terol, J., Talón, M., Robles, M., 2005. Blast2GO: a universal tool for annotation, visualization and analysis in functional genomics research. Bioinformatics 21, 3674–3676.

Costa, M., Borges, C.L., Bailão, A.M., Meirelles, G.V., Mendonça, Y.A., Dantas, S.F.M., de Faria, F.P., Felipe, M.S.S., Molinari-Madlun, E.E.W.I., Mendes-Giannini, M.J.S., Fiúza, R.B., Martins, W.S., Pereira, M., Soares, C.M.A., 2007. Transcriptome profiling of *Paracoccidioides brasiliensis* yeast-phase cells recovered from infected mice brings new insights into fungal response upon host interaction. Microbiology 153, 4194–4207.

Crowe, J.D., Sievwright, I.K., Auld, G.C., Moore, N.R., Gow, N.A., Booth, N.A., 2003. *Candida albicans* binds human plasminogen: identification of eight plasminogen-binding proteins. Mol. Microbiol. 47, 1637–1651.

Dantas, S.F., Vieira de Rezende, T.C., Bailão, A.M., Taborda, C.P., Santos, R.S., Pacheco, K.C., Soares, C.M.A., 2009. Identification and characterization of antigenic proteins potentially expressed during the infectious process of *Paracoccidioides brasiliensis*. Microbes Infect. 11, 895–903.

Donofrio, F.C., Calil, A.C., Miranda, E.T., Almeida, A.M., Bernard, G., Soares, C.P., Nogueira, S.V., Soares, C.M.A., Mendes-Giannini, M.J., 2009. Enolase from *Paracoccidioides brasiliensis*: isolation and identification as a fibronectin-binding protein. J. Med. Microbiol. 58, 706–713.

Dunsmore, S.E., Rannels, D.E., 1996. Extracellular matrix biology in the lung. Am. J. Physiol. 270, L3–27.

Esgleas, M., Li, Y., Handock, M.A., Harel, J., Dubreuil, J.D., Gottschalk, M., 2008. Isolation and characterization of alpha-enolase, a novel fibronectin-binding protein from *Streptococcus suis*. Microbiology 154, 2668–2679.

Ewing, B., Green, P., 1998. Base-calling of automated sequencer traces using phred II. Error probabilities. Genome Res. 8, 186–194.

Feng, Y., Pan, X., Sun, W., Wang, C., Zhang, H., Li, X., Ma, Y., Shao, Z., Ge, J., Zheng, F., Gao, G.F., Tang, J., 2009. *Streptococcus suis* enolase functions as a protective antigen displayed on the bacterial cell surface. J. Infect. Dis. 200, 1583–1592.

Gonzaléz, A., Goméz, B.L., Diez, S., Hernández, O., Restrepo, A., Hamilton, A.J., Cano, L.E., 2005. Purification and partial characterization of a *Paracoccidioides brasiliensis* protein with capacity to bind to extracellular matrix proteins. Infect. Immun. 73, 2486–2495.

Gonzaléz, A., Caro, E., Muñoz, C., Hamilton, A.J., Cano, L.E., 2008. *Paracoccidioides brasiliensis* conidia recognize fibronectin and fibrinogen

which subsequently participate in adherence to human type II alveolar cells: involvement of a specific adhesin. Microb. Pathog. 44, 389−401.

Götz, S., García-Gómez, J.M., Terol, J., Williams, T.D., Nagaraj, S.H., Nueda, M.J., Robles, M., Talón, M., Dopazo, J., Conesa, A., 2008. High-throughput functional annotation and data mining with the Blast2GO suite. Nucleic Acids Res. 36, 3420−3435.

Hanna, S.A., Monteiro da Silva, J.L., Giannini, M.J., 2000. Adherence and intracellular parasitism of *Paracoccidioides brasiliensis* in Vero cells. Microbes Infect. 2, 877−884.

Hernández, O., Almeida, A.J., Gonzalez, A., Garcia, A.M., Tamayo, D., Cano, L.E., Restrepo, A., McEwen, J.G., 2010. A 32-kilodalton hydrolase plays an important role in *Paracoccidioides brasiliensis* adherence to host cells and influences pathogenicity. Infect. Immun. 78, 5280−5286.

Huang, X., Madan, A., 1999. CAP3: a DNA sequence assembly program. Genome Res. 9, 868−877.

Huesca, M., Goodwin, A., Bhagwansingh, A., Hoffman, P., Lingwood, C.A., 1998. Characterization of an acidic-pH-inducible stress protein (hsp70), a putative sulfatide binding adhesin, from *Helicobacter pylori*. Infect. Immun. 66, 4061−4067.

Klotz, S.A., Pendrak, M.L., Hein, R.C., 2001. Antibodies to alpha5beta1 and alpha(v)beta3 integrins react with *Candida albicans* alcohol dehydrogenase. Microbiology 147, 3159−3164.

Long, K.H., Gomez, F.J., Morris, R.E., Newman, S.L., 2003. Identification of heat shock protein 60 as the ligand on *Histoplasma capsulatum* that mediates binding to CD18 receptors on human macrophages. J. Immunol. 170, 487−494.

Lyons, A.J., Jones, J., 2007. Cell adhesion molecules, the extracellular matrix and oral squamous carcinoma. Int. J. Oral Maxillofac. Surg. 36, 671−679.

Marchais, V., Kempf, M., Licznar, P., Lefrançois, C., Bouchara, J.P., Robert, R., Cottin, J., 2005. DNA array analysis of *Candida albicans* gene expression in response to adherence to polystyrene. FEMS Microbiol. Lett. 245, 25−32.

Neto, B.R.S., Silva, J.F., Mendes-Giannini, M.J., Lenzi, H.L., Soares, C.M.A., Pereira, M., 2009. The malate synthase of *Paracoccidioides brasiliensis* is a linked surface protein that behaves as an anchorless adhesin. BMC Microbiol. 9, 272.

Nogueira, S.V., Fonseca, F.L., Rodrigues, M.L., Mundodi, V., Abi-Chacra, E.A., Winters, M.S., Alderete, J.F., Soares, C.M.A., 2010. *Paracoccidioides brasiliensis* enolase is a surface protein that binds plasminogen and mediates interaction of yeast forms with host cells. Infect. Immun. 78, 4040−4050.

Penalver, M.C., O'Connor, J.E., Martinez, J.P., Gil, M.L., 1996. Binding of human fibronectin to *Aspergillus fumigatus* conidia. Infect. Immun. 64, 1146−1153.

Pereira, L.A., Báo, S.N., Barbosa, M.S., Silva, J.L., Felipe, M.S., Santana, J.M., Mendes-Giannini, M.J.S., Soares, C.M.A., 2007. Analysis of the *Paracoccidioides brasiliensis* triosephosphate isomerase suggests the potential for adhesin function. FEMS Yeast Res. 7, 1381−1388.

Ramana, J., Gupta, D., 2010. FaaPred: a SVM-based prediction method for fungal adhesins and adhesin-like proteins. PLoS One 5, e9695.

Restrepo, A., McEwen, J.G., Castaneda, E., 2001. The habitat of *Paracoccidioides brasiliensis*: how far from solving the riddle? Med. Mycol. 39, 233−241.

Ruoslahti, E., 1988. Fibronectin and its receptors. Annu. Rev. Biochem. 57, 375−413.

San-Blas, G., Niño-Vega, G., Iturriaga, T., 2002. *Paracoccidioides brasiliensis* and paracoccidioidomycosis: molecular approaches to morphogenesis, diagnosis, epidemiology, taxonomy and genetics. Med. Mycol. 40, 225−242.

Silva, M.G., Schrank, A., Bailao, E.F.L.C., Bailao, A.M., Borges, C.L., Staats, C.C., Parente, J.A., Pereira, M., et al., 2011. The homeostasis of iron, copper and zinc in *Paracoccidioides brasiliensis*, *Cryptococcus neoformans* var. grubi, and *Cryptococcus gatii*: a comparative analysis. Front. Microbiol. 2, 1−12.

Sohn, K., Senyurek, I., Fertey, J., Konigsdorfer, A., Joffroy, C., Hauser, N., Zelt, G., Brunner, H., Rupp, S., 2006. An in vitro assay to study the transcriptional response during adherence of *Candida albicans* to different human epithelia. FEMS Yeast Res. 6, 1085−1093.

Vicentini, A.P., Gesztesi, J.L., Franco, M.F., Souza, W., Moraes, J.Z., Travassos, L.R., Lopes, J.D., 1994. Binding of *Paracoccidioides brasiliensis* to laminin through surface glycoprotein gp43 leads to enhancement of fungal pathogenesis. Infect. Immun. 4, 1465−1469.

Waterman, S.R., Hacham, M., Hu, G., Zhu, X., Park, Y.D., Shin, S., Panepinto, J., Valyi-Nagy, T., Beam, C., Husain, S., Singh, N., Williamson, P.R., 2007. Role of a CUF1/CTR4 copper-regulatory axis in the virulence of *Cryptococcus neoformans*. J. Clin. Invest. 117, 794−802.

Zakikhany, K., Naglik, J.R., Schmidt-Westhausen, A., Holland, G., Schaller, M., Hube, B., 2007. In vivo transcript profiling of *Candida albicans* identifies a gene essential for interepithelial dissemination. Cell. Microbiol. 9, 2938−2954.

Photochemistry and Photobiology, 2012, 88: 992–1000

Cell Survival and Altered Gene Expression Following Photodynamic Inactivation of *Paracoccidioides brasiliensis*

Luciane M. Almeida*[1,2], Fabiana F. Zanoelo[2,3], Kelly P. Castro[2], Iouri E. Borissevitch[4], Célia M. A. Soares[2] and Pablo J. Gonçalves[5]

[1]Universidade Estadual de Goiás (UEG), UnU-Ipameri, GO, Brazil
[2]Laboratório de Biologia Molecular, Instituto de Ciências Biológicas-Universidade Federal de Goiás (UFG), Goiânia, GO, Brazil
[3]Laboratório de Bioquímica, Centro de Ciências Biológicas e da Saúde (CCBS), Universidade Federal de Mato Grosso do Sul (UFMS), Campo Grande, MS, Brazil
[4]Departamento de Física e Matemática (FFCLRP/USP), Ribeirão Preto, SP, Brazil
[5]Instituto de Física, Universidad Federal de Goiás (UFG), Goiânia, GO, Brazil

Received 25 September 2011, accepted 03 February 2012, DOI: 10.1111/j.1751-1097.2012.01112.x

ABSTRACT

Paracoccidioidomycosis (PCM) is a systemic mycosis caused by *Paracoccidioides brasiliensis*. Currently, the treatment approach involves the use of antifungal drugs and requires years of medical therapy, which can induce nephrotoxicity and lead to resistance in yeast strains. Photodynamic inactivation (PDI) is a new therapy capable of killing microorganisms *via* the combination of a nontoxic dye with visible light to generate toxic reactive oxygen species (ROS). We investigated the phototoxic effect of 5,10,15,20-*tetrakis*(1-methyl-4-pyridinio)porphyrin (TMPyP), a cationic porphyrin, on the survival of *P. brasiliensis* following exposure to light. Phototoxicity was found to depend on both the fluence and concentration of the photosensitizer (PS). Although the biological effects of PDI are known, the molecular mechanisms underlying the resultant damage to cells are poorly defined. Therefore, we evaluated the molecular response to PDI-induced oxidative stress by gene transcription analysis. We selected genes associated with the high-osmolarity glycerol (HOG)-mitogen-activated protein kinase (MAPK) pathway and antioxidant enzymes. The genes analyzed were all overexpressed after PDI treatment, suggesting that the oxidative stress generated in our experimental conditions induces antioxidant activity. In addition to PDI-induced gene expression, there was high cell mortality, suggesting that the antioxidant response was not sufficient to avoid fungal mortality.

INTRODUCTION

Paracoccidioides brasiliensis, a dimorphic fungus found in Central and South America, is responsible for paracoccidioidomycosis (PCM), a form of systemic mycosis that affects at least 10 million people in Latin America (1). In Brazil, PCM is one of the most common causes of death due to chronic/recurrent infection and parasitic disease (2). Infection is thought to occur *via* the inhalation of conidia that subsequently transform into yeast forms within the lungs. There are two forms of PCM: the acute, juvenile form and the chronic, adult form. The former has a faster course, and is more severe than the latter (3). However, in the absence of effective treatment, cell-mediated immune functions are abnormal, and mortality is high in both forms (4).

Although effective treatment regimes are available to control the infection process, most patients develop fibrotic sequelae (5). Treatment with antifungal drugs, such as sulfonamides, ketoconazole, itraconazole, fluconazole and amphotericin B requires many years to be efficacious, and is nephrotoxic in nature (6). In addition, the use of antifungal drugs encourages the selection of tolerant pathogens, and is, therefore, detrimental to the entire population (7).

Photodynamic inactivation (PDI) is a promising new option for killing pathogenic microorganisms. In the last few years, some studies have shown the efficacy of PDI in human pathogenic yeast species, such as *Candida albicans* (8,9), *Cryptococcus neoformans* (10) and *Cryptococcus gattii* (11), and in filamentous fungi such as *Aspergillus fumigatus* (12) and *Trichophyton rubrum* (13). PDI provides significant advantages over existing antimicrobial therapies, as it acts faster against microorganisms, and there is no evidence of PDI resistance to date (14).

Photodynamic inactivation involves the use of nontoxic photosensitizers (PSs), which are excited by exposure to visible light, and can generate a high number of reactive oxygen species (ROS; 15). ROS are byproducts of the normal metabolism of oxygen, and play important roles in cell signaling and homeostasis. However, high levels of ROS may result in significant damage to cellular structures, inducing cell death.

Two possible oxidative mechanisms can be observed after light activation of the PS. In the Type 1 mechanism, the excited PS reacts with the surrounding molecules to yield radical species and hydrogen peroxide (H_2O_2). In the Type 2 mechanism, the excited PS transfers its energy to molecular oxygen ($^3O_2$) to produce the highly toxic singlet oxygen ($^1O_2$). Both types of PDI cause cell death; however, the main photodynamic effect occurs *via* the Type 2 mechanism (16).

*Corresponding author email: almeidalm@hotmail.com (Luciane Madureira de Almeida)

Many studies have been performed to evaluate the effectiveness of these new therapies (8–14), understand the photophysical characteristics of the PSs (15–20), develop new techniques for characterization (19,21), as well as to develop more efficient PS molecules (22–24). In addition to these studies, a better understanding of the molecular mechanics associated with PDI could facilitate further development of this therapy. Photodynamic therapy (PDT) induces a cascade of molecular events in human tumors, including activation of transcription factors, heat shock proteins, antioxidant enzymes, and apoptotic pathways, as well as altered cell attachment and protein transport, which can lead to cell death (25–27). Currently, the underlying molecular events involved in cell death after PDI are poorly defined in pathogenic fungus (28–30). However, it is known that transcriptional activation in *P. brasiliensis* plays an important role in the molecular response to PDI, and therefore, further study of this fungus will help broaden our knowledge of PDT. Analysis of transcriptional regulation does not permit determination of the importance of gene expression in response to PDI, but does improve the understanding of the underlying molecular process.

The objective of this study was to evaluate the efficacy of PDI based on cell viability of *P. brasiliensis* exposed to the PS TMPyP. Moreover, we evaluated the differential expression of genes associated with antioxidant enzymes and the high-osmolarity glycerol (HOG)-mitogen-activated protein kinase (MAPK) pathway.

MATERIALS AND METHODS

P. brasiliensis *yeast cells*. *Paracoccidioides brasiliensis* Pb01 (ATCC MYA-826) yeast cells were grown in Fava-Netto solid medium (1% [wt/vol] peptone; 0.5% [wt/vol] yeast extract; 0.3% [wt/vol] proteose peptone; 0.5% [wt/vol] beef extract; 0.5% [wt/vol] NaCl; 1.2% [wt/vol] agar; pH 7.2) for 7 days at 36°C (31). For PDI experiments, *P. brasiliensis* cells were grown in liquid Fava-Netto medium for 72 h. The fungal culture was then centrifuged at $1\ 000 \times \boldsymbol{g}$ for 10 min, and the supernatant was discarded. This procedure was repeated, and the sediment was resuspended in 50 mL of phosphate buffered saline (PBS; pH 7.4). The number of viable cells in the suspension was determined by Trypan blue exclusion in a Neubauer counting chamber. A cell density of 10^9 cells mL^{-1} was used in the PDI experiments.

PS. 5,10,15,20-*tetrakis*(1-methyl-4-pyridinio)porphyrin was purchased from Sigma–Aldrich. TMPyP is a water-soluble porphyrin that shows a Soret band at 424 nm and Q-bands at 519, 558, 585 and 638 nm. Its fluorescence emission spectrum shows two bands at 675 and 706 nm (18). Moreover, on irradiation with visible light, this porphyrin produces a high number of triplet and singlet oxygen (O_2) radicals (17,18,21).

The stock solution was prepared in Milli-Q water to a final concentration of 200 μM, filtered using a 0.22 μm membrane (Millipore), and kept in the dark at 10°C. The absorption spectra and concentrations were determined using a Beckman DU 940 spectrometer, and the fluorescence spectra were measured using a Fluorolog-3 spectrofluorometer (Horiba Jobin Yvon Inc.).

PS binding to yeast cells. Cell suspensions of *P. brasiliensis* (1 mL of 10^6 cells mL^{-1}) prepared in PBS were incubated in the dark at 36°C with 50 μM TMPyP for 0, 10, 60 and 180 min. The cell suspensions were centrifuged ($16\ 800 \times \boldsymbol{g}$ for 2 min), and the pellets were resuspended in 1 mL of 2% sodium dodecyl sulfate (SDS), incubated overnight at 4°C, and sonicated for 30 min. The PS concentration in the supernatant was measured using a spectrofluorometer with an excitation wavelength (λ_{ex}) of 585 nm and an emission wavelength (λ_{em}) of 656 nm in PBS solutions containing 2% SDS. Fluorescence values were obtained for each sample with reference to the total number of cells in the suspension. The concentration of TMPyP in these samples was estimated by comparison to a calibration curve of standard TMPyP solutions in 2% SDS.

Light source. A visible light source (Br. Patent: PI 0802369-7 A2, 2008) equipped with a 500 W halogen lamp was used for illumination. To prevent heating of the sample, the light was passed through a thick water filter, and the sample temperature, which varied by < 2°C, was measured during the irradiation. The irradiance during the treatment was 120 mW cm^{-2}, and the fluence ranging from 0 to 432 J cm^{-2}.

PDI experiments. Two methods, each performed in three independent experiments, were utilized to determine *P. brasiliensis* cell survival rates after PDI treatment. In the first experiment, the *P. brasiliensis* cell suspension (10^9 cells mL^{-1}) was divided into four aliquots (8 mL) and incubated with TMPyP (0, 10, 25 or 50 μM) in the dark for 1 h at 36°C. After incubation, the *P. brasiliensis* cell suspensions were transferred to sterile polystyrene culture dishes (3 cm diameter) and irradiated at 120 mW cm^{-2} for 0, 15, 30 or 60 min with fluence ranging from 0 to 432 J cm^{-2}, respectively. After exposure, aliquots (100 μL) of the suspensions were diluted in PBS to 10^9, 10^8, 10^7 and 10^6 cells mL^{-1}, and grown in Fava-Netto solid medium (1% [wt/vol] peptone; 0.5% [wt/vol] yeast extract; 0.3% [wt/vol] proteose peptone; 0.5% [wt/vol] beef extract; 0.5% [wt/vol] NaCl; 1% [wt/vol] agar; pH 7.2) for 1 month to assess delayed growth (24).

In the second experiment, we evaluated the *P. brasiliensis* survival rate after PDI treatment by measuring the number of colony-forming units (CFUs). The *P. brasiliensis* cell suspension (10^6 cells mL^{-1}) was divided into aliquots (8 mL) and subjected to two different conditions. PS was not added to the control group (group A), whereas the other aliquot was incubated for 60 min with 50 μM TMPyP (group B). After incubation, the *P. brasiliensis* cultures were transferred to sterile polystyrene culture dishes (3 cm diameter) and exposed for different fluences (0, 108, 216 and 432 J cm^{-2}). Next, 100 μL aliquots of the suspensions were diluted 10-fold, and distributed into five sterile polystyrene culture dishes. The number of CFUs was determined after 5 days of cell growth. After additional 30 days, the growth of the fungal culture was also assessed for delayed growth.

Statistical analysis. The survival values, obtained using the CFU count, are expressed in terms of mean (standard deviation [SD]). The differences in the mean values of multiple groups were analyzed using the Student's *t*-test. $P < 0.01$ was considered significant. Pearson correlation coefficients were calculated to compare the survival rate and gene transcription level.

RNA extraction. *Paracoccidioides brasiliensis* cultures (10^6 cells mL^{-1}) were exposed to three independent PDI treatments, and 5 mL aliquots were snap frozen in liquid nitrogen. Four samples were collected after 60 min of light irradiation: without TMPyP (control), with 10 μM TMPyP, 25 μM TMPyP and 50 μM TMPyP. The total RNA was extracted from each sample using the TRIzol reagent. RNA quality was analyzed by agarose gel electrophoresis and ethidium bromide staining, and the total RNA concentration was measured using a NanoDrop 2000 (Uniscience).

Transcriptional analysis using quantitative real-time polymerase chain reaction. Total RNA obtained from the yeast cells subjected to three independent PDI treatments was used in the transcriptional analyses. First, the RNA samples were reverse transcribed using the High Capacity RNA-to-cDNA kit (Applied Biosystems, Foster City, CA). The cDNA samples were diluted 1:2 in water, and quantitative real-time polymerase chain reaction (qRT-PCR) was performed using the SYBR Green PCR master mix (Applied Biosystems) in the Applied Biosystems Step One Plus PCR System (Applied Biosystems Inc.). Each cDNA sample was analyzed in triplicate with each primer pair, and a melting curve analysis was performed to confirm a single PCR product. Gene sequences were obtained from the Broad Institute and the NCBI database; and the PRIMER EXPRESS 3.0 software (Applied Biosystems) was used to design the primers. The primers and sequences used in our analyses are provided in Table 1. The data were normalized to the α-tubulin transcript. A nontemplate control, containing no genetic material, was included to eliminate confounding results due to contamination or nonspecific reactions. The PCR thermal cycling conditions were as follows: 40 cycles at 95°C for 15 s and 60°C for 1 min. The standard cDNA sample for the relative standard curve was generated by pooling cDNA aliquots from each sample. The standard cDNA was serially diluted (1:5), and a standard curve was generated using four samples from the pooled cDNA. The relative expression levels of the genes of interest were calculated using the standard curve method for relative quantification (32). Statistical analysis was performed using the Student's *t*-test. $P < 0.05$ was considered statistically significant.

Table 1. Oligonucleotides used in qRT-PCR.

Gene	Nucleotide sequence (5′–3′)	Accession number
Cytochrome c peroxidase (*ccp*)	F: GGTAGCTATGGACCGGGTTCT R: CTCTCGCAGCTTTCAAACCA	PAAG_03292.1
Peroxiredoxin (*hyr1*)	F: CCAGCCGCTAGACAAAAAGG R: CCAGGGTAGGTAGTCGAGAGG	PAAG_04424.1
Superoxide dismutase (*sod*)	F: ACTGCGCAAGTTATGATGGAA R: CACGGGAAGGGTCCATTTTC	PAAG_02926
Catalase A (*cat*)	F: CGCCTGCTCCTTTCACCACC R: GCACCTGTTCCTCGAGCATG	AY494834.2
Mitogen-activated protein kinase HOG1 (*hog1*)	F: CTCTTGCCATCAGCCTCCTC R: CAACTGGTAAGTCGGCATCG	PAAG_00535
Mitogen-activated protein kinase response regulator (*ssk1*)	F: CGCATATGGTGTTGTCTGCT R: TGATCGAACGGGGTTATCTT	PAAG_05033
α-Tubulin	F: ACAGTGCTTGGGAACTATACC R: GGGACATATTTGCCACTGCC	AAR87484
Alcohol dehydrogenase (*adh*)	F: ACCTTGTTGTGCTGGAGTAGA R: GGAGTCTGGAATCGGGGTG	PAAG_06715
Chitin synthase (*cs1*)	F: GTTATGCTGGCAAGAAGGTGG R: AGGTGGTTGTAGTTGATGGTC	PABG_07036.1
Aqualysin 1 (*aqs*)	R: GGCCTCTCCACACGTTGCTG F: GTTCCAGATAAGAACGTTAGC	XP. 002793896.1
Lumazine (*luz*)	F: CCTCATTCAACACCGTCAAC R: GCCTATTGCTATGGAGAGAATA	PGAA_00851

qRT-PCR, quantitative real-time polymerase chain reaction; F, forward primer; R, reverse primer. Primers were designed using the PRIMER EXPRESS 3.0 software of Applied Biosystems. The gene sequences were obtained from the Broad Institute and NCBI database.

RESULTS AND DISCUSSION

Binding of TMPyP to *P. brasiliensis* cells

An association between the cell wall and PS is essential for PDI efficiency (33). The fungal cell wall provides structure and protection to the cell (34), and is primarily composed of α-glucans, β-glucans, *N*-acetylglucosamine and mannoproteins, resulting in an overall negative charge (35). We used the tetracationic porphyrin TMPyP as the PS in this study because it is nontoxic to *C. albicans* in the dark (9,36), and its positive charge allows effective binding to the negatively charged *P. brasiliensis* yeast wall.

The first step of our analysis was to determine the ability of TMPyP to bind to *P. brasiliensis* cells. The fluorescence spectrum of TMPyP in PBS has a maximum at 656 nm and a shoulder around 705 nm, whereas in the presence of *P. brasiliensis* cells or SDS, the fluorescence spectra has two separate peaks at around 654 and 715 nm (Fig. 1). Although the TMPyP concentration was the same (50 μM) in all the experiments, the fluorescence intensities obtained were different. This increased intensity in the presence of SDS is due to the interaction between the porphyrin and the surfactant molecules (18,36).

5,10,15,20-*tetrakis*(1-methyl-4-pyridinio)porphyrin was recovered from *P. brasiliensis* cells after washing with PBS (Fig. 2). In the absence of a washing step, the normalized fluorescence intensity was initially 0.50, but increased to 0.82 after a 10 min incubation with TMPyP, and reached the maximum intensity after a 60 min incubation. No increase in the amount of TMPyP bound to the cell wall was observed when the incubation time was extended beyond 60 min.

Fluorescence analysis showed that the amount of cell-bound TMPyP decreased in response to the number of washings with PBS. Therefore, the porphyrin molecules removed by washing were probably weakly bound to *P. brasiliensis* cells. The reduction in fluorescence intensity, when compared to the unwashed samples, was only 24% and 28% after the first and second wash, respectively. This result suggests that TMPyP has a high-binding affinity for *P. brasiliensis* cells, which is supported by a recent PDI study involving *C. albicans*, which showed that TMPyP has high-binding affinity for the fungal cell wall (9).

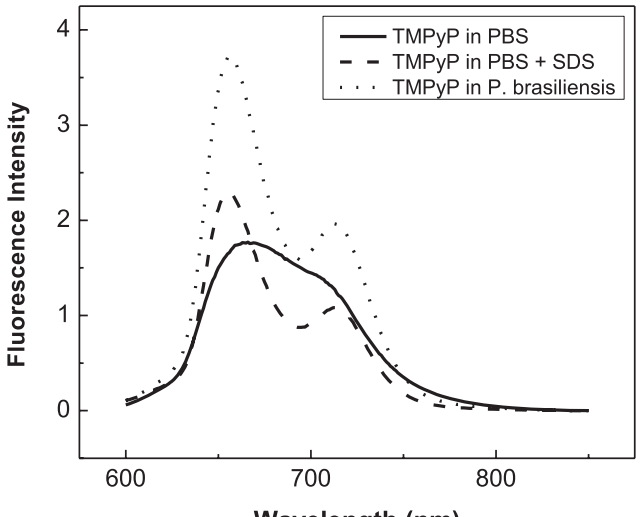

Figure 1. Fluorescence spectra of TMPyP: in PBS (solid line), in PBS with 2% SDS (dashed line) and PBS with *P. brasiliensis* cells (dotted line). The excitation wavelength for all spectra was 585 nm.

Photodynamic inactivation efficacy is also associated with the capability of the PS to penetrate into the cell (10). A recent study in *C. albicans* showed that some PSs such as methylene blue (MB) and toluidine blue (TBO) directly influence cellular

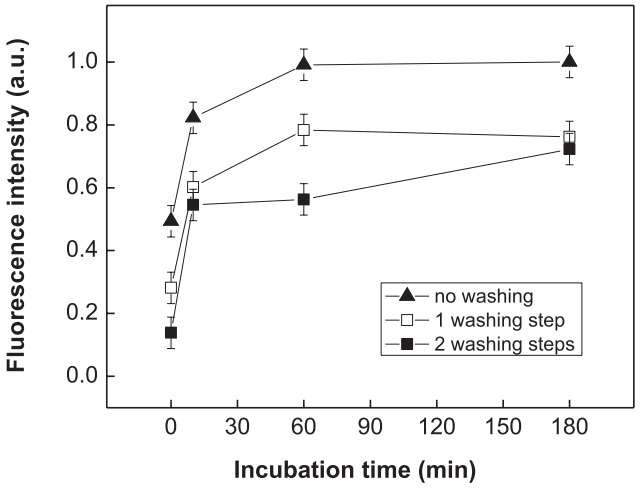

Figure 2. Amount of TMPyP recovered from *P. brasiliensis* yeast cells (10^6 cells mL^{-1}) Samples were incubated (0, 10, 60 and 180 min) with 50 μM TMPyP at 36°C in the dark and subjected to different washing protocols with PBS buffer (no washing, 1 washing step or 2 washing steps). Data are represented as the mean values from three independent experiments with SD (bars).

influx and efflux *via* the pumps of the fungal multidrug efflux systems (37). Some studies using porphyrin as the PS in other microorganisms have shown that porphyrins can cause initial limited alterations to the cytoplasmic membrane only after irradiation. These modifications to the cytoplasmic membrane allow the PS to penetrate into the cell, enabling translocation to the inner membrane, and upon continued irradiation, photodynamic damage of intracellular targets (10,38). However, currently, there is no information regarding porphyrin uptake in *P. brasiliensis*.

PDI treatment

We sought to determine the susceptibility of the fungal pathogen *P. brasiliensis* to PDI. Figure 3 shows the *in vitro* effect of varied TMPyP concentrations and exposure times on yeast cell suspensions. Increased PDI-induced cell death correlated with increased fluence and PS concentration. Specifically, significant cell mortality was observed when ≥25 μM of PS and ≥216 J cm^{-2} of fluence (≥30 min light irradiation) were used.

Therefore, we utilized a TMPyP concentration of 50 μM and fluence ranging from 0 to 432 J cm^{-2} to evaluate the survival of *P. brasiliensis* cells after PDI. We determined the number of CFUs in two groups: A, received only light; B, received light and 50 μM PS. The numbers of CFUs after treatment are shown in Fig. 4A,B. The Student's *t*-test analysis showed a significant difference in the cell survival rates of the control (A) and treated (B) groups. The light exposure times were varied, and the *P*-value between A15 (control group with 15 min exposure) and B15 (treated group with 15 min exposure) was 2.2×10^{-10}, between A30 and B30 was 3.3×10^{-14}, and between A60 and B60 was 1.0×10^{-14}. Intra-group comparisons showed no differences in the control groups, with A0, A15, A30 and A60 showing similar CFU counts. Comparatively, group B showed significant differences with respect to survival; and a comparison between B0 and the longer exposure experiments, B15, B30 and B60, demonstrated *P*-values of 2.1×10^{-11}, 7.7×10^{-11} and 8.1×10^{-13}, respectively.

Cell viability of *P. brasiliensis* was not affected by exposure to light in the absence of TMPyP (group A). Furthermore, there was no significant difference in cell survival in the presence of TMPyP and absence of light (group B0; Fig. 4), which confirms that TMPyP is not toxic to *P. brasiliensis* cells. In the presence of TMPyP, 15 min of light exposure or fluence rate of 108 J cm^{-2} was sufficient to kill almost 95% of the cells. The survival rate after 30 min (216 J cm^{-2}) and 60 min (432 J cm^{-2}) of exposure was 2.5% and 0.5%, respectively.

These results suggest that *P. brasiliensis* is highly sensitive to PDI treatment *in vitro*, as shown by the major reduction in the CFU values after treatment. In addition, our results showed that longer exposure times and higher porphyrin concentrations increased the efficacy against *P. brasiliensis*. To the best of our knowledge, this is the first study demonstrating the antimicrobial photoinactivation of *P. brasiliensis*. Importantly, we have shown that the phototoxic effect of TMPyP depends on the fluence as well as the PS concentration. These results are supported by previous studies, which have shown that other PSs, such as MB, photoditazine, photofrin and TBO also function in a concentration-dependent manner (39–41). Our results showed that the TMPyP concentration required to effectively kill *P. brasiliensis* cells (50 μM) was 10-fold higher than that required to kill *C. albicans* (5 μM; 9). The higher concentration of porphyrin needed could be related to the cell size of *P. brasiliensis* (40–50 μm), which is larger than the cell size of *C. albicans* (10–12 μm). Furthermore, the thicker *P. brasiliensis* cell wall (200–600 nm), compared with *C. albicans* (200–270 nm), may influence the amount of PS required to induce oxidative damage to the cell (42,43).

Transcriptional analysis using quantitative real-time PCR

At the biochemical level, PDT involves the production of $^1O_2$ and ROS, which are responsible for the cytotoxic effect

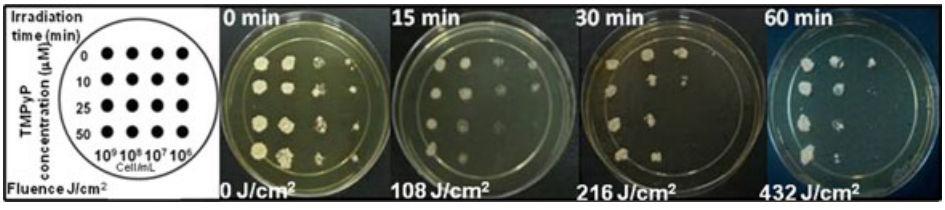

Figure 3. *Left*: diagram showing the parameters utilized in this study. The lines represent different sensitizer concentrations (0, 10, 25 and 50 μM), whereas the columns represent 10-fold serial dilutions of the *P. brasiliensis* cells (10^9, 10^8, 10^7 and 10^6 cells mL^{-1}) after PDI treatment. *Right:* results of four irradiation times (0, 15, 30 and 60 min) at an irradiance of 120 mW cm^{-2}, and their respective fluence rates (0, 108, 216 and 432 J cm^{-2}).

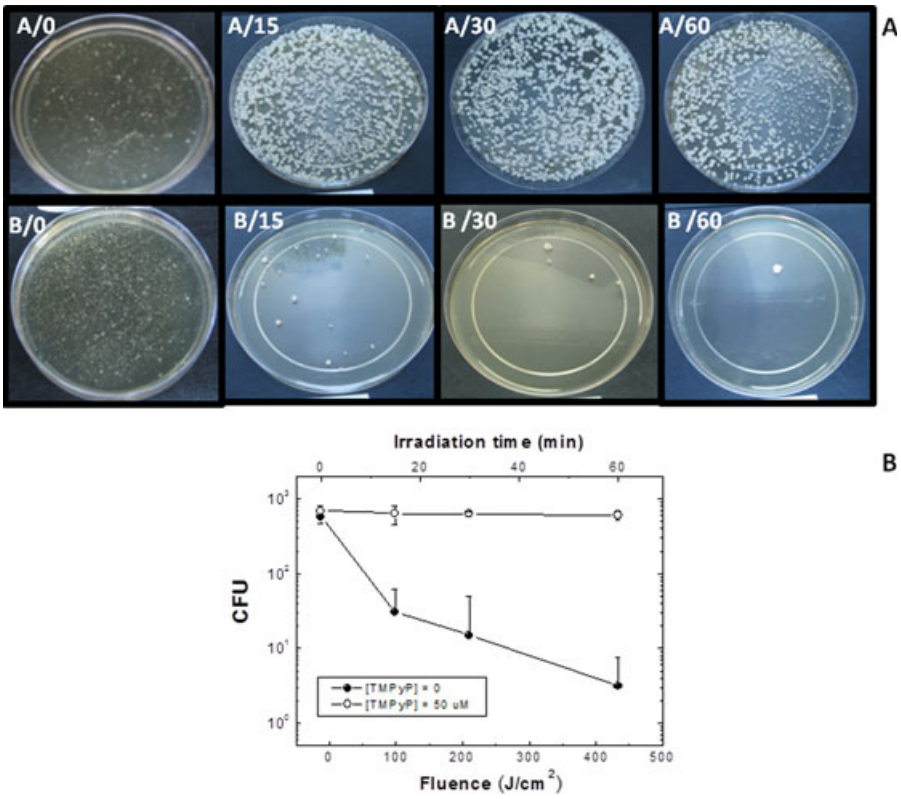

Figure 4. (A) PDI of *P. brasiliensis* cells with 50 μM PS, irradiated with different fluences (0, 108, 216 and 432 J cm^{-2}) during the respective time of irradiation (0, 15, 30 or 60 min) at an irradiance of 120 mW cm^{-2}. After irradiation, the yeast suspensions were grown on solid Fava-Netto medium. The CFU counts were obtained after 5 days. After subsequent 30 days, the fungal development was assessed for delayed growth. (B) Survival curves of *P. brasiliensis* irradiated with different fluences. Data are represented as the mean values from three independent experiments with SD (bars).

observed in yeast cells, such as peroxidation of lipids, photodegradation of unsaturated sterols and inactivation of cell wall proteins (38).

To protect cells from the damage caused by free radicals and related reactants, organisms have evolved several defense mechanisms that rapidly and efficiently remove ROS from the intracellular environment. Antioxidant enzymes, as the first line of defense, metabolize these toxic reactants into innocuous byproducts. To understand the response of *P. brasiliensis* cells to PDI treatment, we used qRT-PCR to analyze the transcript levels of antioxidant enzymes, before and after PDI treatment (Fig. 5). The expression levels of four genes were analyzed: *cytochrome c peroxidase* (*ccp*), *peroxiredoxin* (*hyr1*), *superoxide dismutase* (*sod*) and *catalase A* (*cat*).

Cytochrome *c* peroxidase is a key enzyme in the control of H_2O_2 concentrations (44). Classic peroxidases oxidize various substrates, including aromatic amines, phenols and lignin, whereas CCP is a specific peroxidase that shows low affinity for these substrates (44). CCP is localized to the mitochondrial intermembrane space, where it protects the organism from the damage caused by high concentrations of H_2O_2. As expected, the *ccp* expression in *P. brasiliensis* cells subjected to the PDI treatment was statistically different from that of the control ($P < 0.05$). Our results showed that *ccp* was overexpressed in the *P. brasiliensis* cells after PDI treatment with 25 μM TMPyP ($P = 0.04$) and 50 μM TMPyP ($P = 0.004$; Fig. 5).

Peroxiredoxin, also called thioredoxin peroxidase or thiol-specific antioxidant, reduces H_2O_2, peroxynitrite and a wide range of organic alkyl hydroperoxides (ROOH) to water and the corresponding alcohol (45). This abundant antioxidant enzyme has a highly conserved primary sequence, and is present in a wide variety of organisms (46). Interestingly, it differs from other peroxidases in that it does not require redox cofactors such as metals and prosthetic groups (45). Transcriptional analysis showed that *hyr1* was overexpressed in the *P. brasiliensis* cells after PDI treatment with 25 μM TMPyP ($P = 3 \times 10^{-5}$) and 50 μM TMPyP ($P = 0.001$), but was underexpressed following treatment with 10 μM TMPyP ($P = 4 \times 10^{-4}$).

Superoxide dismutase converts the superoxide anion (O_2^-) into H_2O_2, a less potent biological oxidant that is further decomposed by CAT into water and ground-state oxygen (47). Our results showed that *sod* and *cat* were overexpressed in *P. brasiliensis* cells after PDI treatment with 25 μM TMPyP ($P = 0.008$ and $P = 0.01$, respectively) and 50 μM TMPyP ($P = 0.004$ and $P = 0.003$, respectively), but *cat* was underexpressed following treatment with 10 μM TMPyP ($P = 0.004$).

These results suggest that the oxidative stress generated under our experimental conditions induces the expression of antioxidant genes in *P. brasiliensis* cells at 25 and 50 μM TMPyP (Fig. 5). However, it is important to note that there

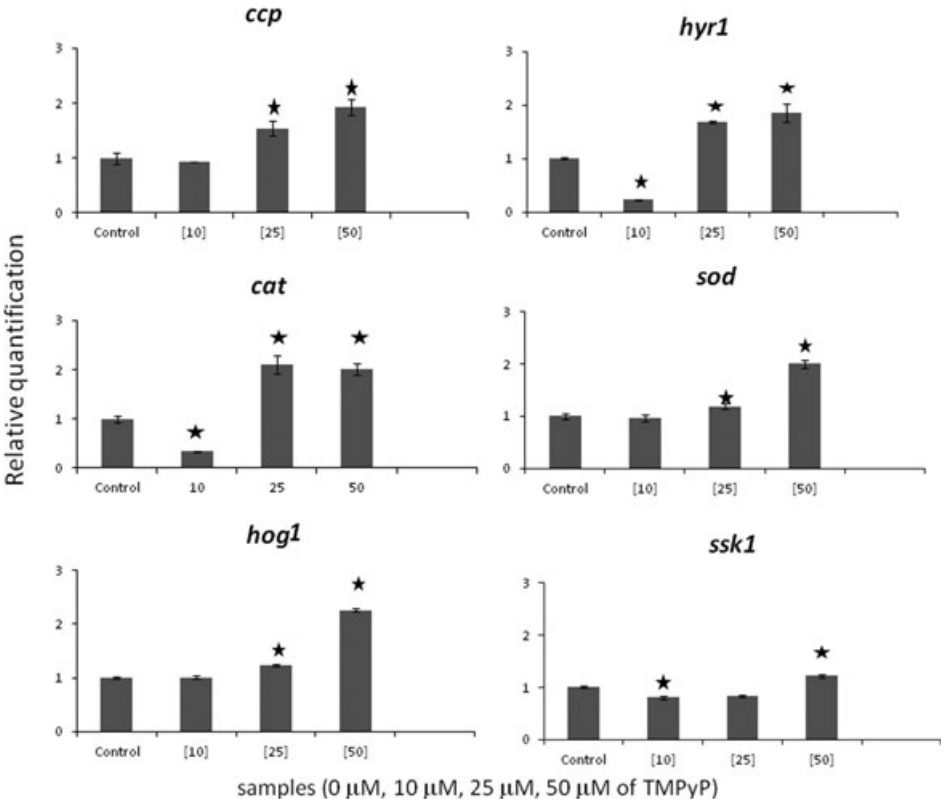

Figure 5. qRT-PCR analysis of differentially expressed (DE) genes of *P. brasiliensis* after PDI treatment with different concentrations of PS (10, 25 and 50 μM) and fluence of 432 J cm^{-2}. DE genes associated with the antioxidant enzymes: cytochrome *c* peroxidase (*ccp*), peroxiredoxin (*hyr1*), superoxide dismutase (*sod*) and catalase A (*cat*). DE genes of the MAPK pathway: mitogen-activated protein kinase (*hog1*) and mitogen-activated protein kinase response regulator (*ssk1*). The asterisks denote values statistically different from the control ($P \leq 0.05$).

are post-transcriptional and post-translational processes capable of regulating the level of antioxidant enzymes after gene transcription. In addition to the increased transcription of antioxidant enzymes, a high mortality of *P. brasiliensis* cells was noted after 60 min (432 J cm^{-2}) of PDI treatment, thereby suggesting the increased transcription levels were inadequate to protect against oxidative stress (Fig. 4). Similar to the results obtained using *Staphylococcus aureus* (48), *sod* expression in our study did not directly affect fungal vulnerability after PDI treatment with porphyrin. However, *P. brasiliensis* cells in the presence of 10 μM TMPyP did not show altered expression levels of the *ccp* and *sod* genes and underexpressed the *hyr1* and *cat* genes, suggesting that this concentration is not sufficient to activate the oxidative stress response. This result is in agreement with the survival experiment, in which lower mortality was observed in the presence of 10 μM TMPyP than 25 and 50 μM. The correlation between the survival rate and the transcription level of antioxidant enzymes was analyzed using the Pearson correlation. The values obtained were *ccp*, −0.52; *hyr1*, −0.21; *sod*, −0.43 and *cat*, −0.32, which represent moderately negative correlations. This result indicates increased transcriptional levels moderately correlate with decreased survival as a function of PDI exposure time.

Previous studies have shown that antioxidant enzymes in fungi have evolved mechanisms to perceive and eliminate ROS (49). Those studies identified three major modules that control the response to oxidative stress: the stress-responsive MAPK cascade, a histidine kinase system and activating protein (AP)-1 like transcription factors (49). In this study, we focused our analyses on the genes of the MAPK cascade. Signal transduction pathways mediated by MAPKs are essential mechanisms used by all living cells to sense and transmit information from the external environment into the cell. In particular, the HOG-MAPK pathway has evolved to respond and adapt to the stresses frequently encountered by the organism (50). The Hog1 MAPK belongs to a subgroup of the large family of MAPKs that protects yeast cells from osmotic and oxidative stresses (50). We analyzed two genes from the HOG-MAPK pathway to evaluate the oxidative response of *P. brasiliensis* to PDI treatment (Fig. 5). Our results showed that *hog1* was overexpressed in *P. brasiliensis* cells after PDI treatment with 25 μM PS ($P = 1 \times 10^{-4}$) and 50 μM PS ($P = 0.004$). The *Ssk1* gene, which encodes a putative response regulator protein associated with *hog 1*, was also analyzed (25). *Ssk1* gene expression analysis showed that this gene is also overexpressed at 50 μM PS ($P = 0.009$), but underexpressed at 10 μM. These results suggest that oxidative stress was generated under our experimental conditions, and that the yeast cells responded to these stress conditions by activating the MAPK pathway; however, lower PS concentrations (10 μM TMPyP) did not seem to be sufficient to induce *hog1* and *ssk1* overexpression. The correlation between survival and transcriptional levels was negatively moderated by the *hog1*gene (−0.44), and close to neutral with respect to the *ssk1* gene (−0.10), indicating a weak correlation.

In a previous study, gene expression analysis following PDI treatment in *Saccharomyces cerevisiae* showed the overexpression of various genes involved in the oxidative stress response, such as *glutamylcysteine synthetase, thioredoxin peroxidase, thioredoxin* and *thioredoxin reductase*. The expression of these genes is coordinated by two transcriptional regulators, *Yap1p* and *Skn7p*, either alone or in concert (51). *Skn7* of *S. cerevisiae* is homologous to *Ssk1* of *P. brasiliensis,* and therefore, *Ssk1* may play an important role in coordinating the stress response in this organism.

Our results have shown that PS concentration and fluence affect the induction of genes involved in antioxidant enzyme production and the oxidative stress response pathway (Fig. 5). The qRT-PCR results showed that higher PS concentrations (50 μM TMPyP) stimulated increased expression of all the genes analyzed. However, the onset of this response did not appear to protect the organism from TMPyP-induced phototoxicity (Fig. 4).

To evaluate whether the response of *P. brasiliensis* cells to PDI treatment is specifically associated with the antioxidant enzymes and the oxidative stress pathway, we analyzed the expression of four genes that are not directly associated with this pathway (Fig. 6). The genes selected were *alcohol dehydrogenase* (*adh*), *chitin synthase* (*cs1*), *aqualysin* (*aqs*) and *lumazine* (*luz*). ADH catalyzes the oxidation of primary and secondary alcohols into aldehydes and ketones; CS1 synthesizes chitin; AQS is a serine protease that cuts peptide bonds; and LUZ is involved in the biosynthesis of flavin (http://fungicyc.broadinstitute). All these genes were overexpressed after PDI treatment (Fig. 6). Activation of genes unrelated to oxidative stress could be coincidental or functionally connected to the networks affected by PDI treatment. Unfortunately, meaningful conclusions about gene expression after PDI cannot be drawn without a global gene expression analysis, and very few of these have been completed in fungi (28,30). One of these studies showed that *S. cerevisiae* cells exposed to 8-methoxypsoralen and UVA initiate a cascade of events leading to a cytotoxic, mutagenic and carcinogenic response (28). The microarray technique identified 128 genes that were overexpressed and 29 genes that were underexpressed after PDI treatment. Genes associated with the following pathways were differentially expressed following PDI treatment: DNA metabolism, cellular functions, maintenance of cellular structures and general metabolism (28). In addition, recent human studies have confirmed the diverse range of cellular functions affected by photodynamic treatment, such as the activation of transcription factors, heat shock proteins and antioxidant enzymes, as well as gene expression alterations in the apoptotic and MAPK signaling pathways, and in cell proliferation and protein transport processes (25–27). The simultaneous activation of all of these pathways may lead to several options for the cell, including repair and cell death, depending on many critical factors and the interaction of different pathways. Our qRT-PCR results showed that PDI treatment greatly enhances antioxidant activity and alters the gene expression levels of other unrelated oxidative stress genes, thereby suggesting that PDI treatment elicits a diverse range of cellular responses, as was demonstrated in previous studies (25–30).

CONCLUSION

Currently, treatment with antifungal drugs often promotes the development of resistant strains (52). Therefore, interest in

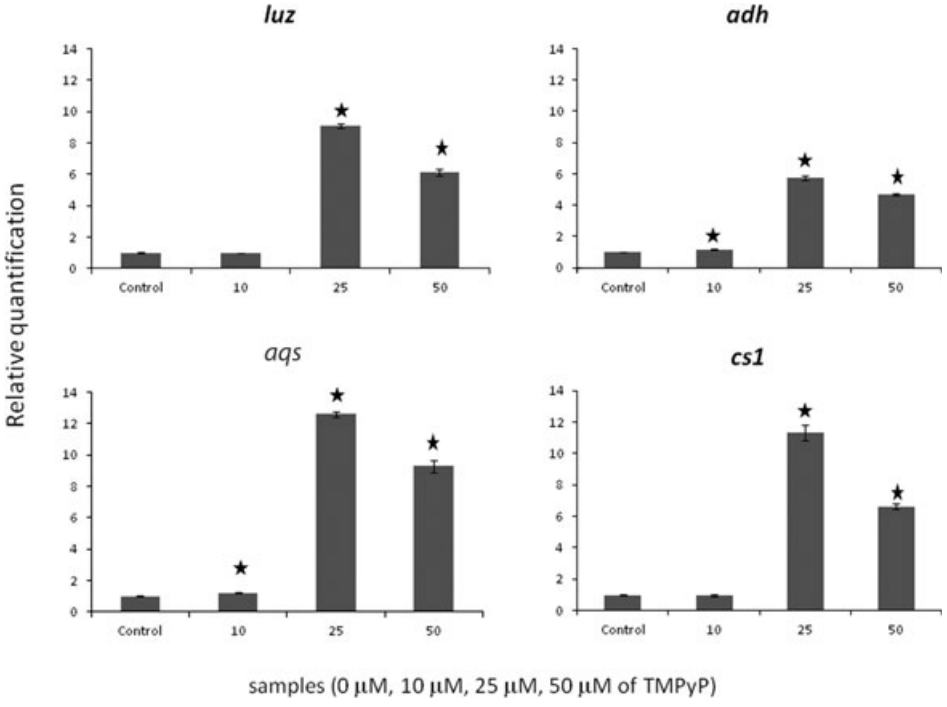

Figure 6. Transcriptional analysis of DE genes not related to the oxidative stress response pathway. Cells were subjected to PDI treatment with different concentrations of PS (10, 25 and 50 μM) and fluence of 432 J cm^{-2}. Genes analyzed were *alcohol dehydrogenase* (*adh*), *chitin synthase* (*cs1*), *aqualysin* (*aqs*) and *lumazine* (*luz*). The asterisks denote values statistically different from the control ($P \leq 0.05$).

PDI is growing, as this treatment effectively inhibits microorganisms without causing human cell toxicity or microbial resistance. PDI is a promising therapy, but the data available regarding its function in fungi is currently limited. Extension of the photosensitization studies to new fungal species and identification of PSs for use as fungicides are important issues concerning the further development of PDI.

Currently, PDI treatment is chiefly used to treat superficial malignances or localized infections (53). Although the disease caused by *P. brasiliensis* is mainly systemic, and PDI is mostly used as a topical therapy, this *in vitro* study may be considered as the first step for further development of strategies aimed at the systemic application of PDI treatment. Indeed, previous studies have shown that PCM secondary lesions frequently appear in mucous membranes (oral, nasal, pharyngeal and anal) and on skin (54), which could be treated using PDI.

To date, most PDI studies on human pathogenic yeast species have been completed *in vitro*, and the majority has shown that PDI can efficiently kill the pathogen (9,11,13). This *in vitro* analysis is the first step in determining pathogenic fungus susceptibility and establishing the best conditions for further *in vivo* PDI applications. To date, some PDI experiments have been performed using animal models and patients (55–60).

This study has established a method for testing the effect of PDI treatment on the pathogen *P. brasiliensis*. The results show that the phototoxic effect of TMPyP depends on the fluence and PS concentration. Exposure to light irradiation, as performed in PDI treatments, can affect cell growth and influence transcription levels. Our results show that transcription was induced in all the genes analyzed; suggesting that PDI activates multiple cellular mechanisms involved in the control of oxidant species levels. Studies using global gene expression analysis and *in vivo* experiments are necessary to verify the susceptibility of *P. brasiliensis* to PDI and the possible application of this new therapy in PCM.

Acknowledgements—This research was supported by the Conselho Nacional de Desenvolvimento Científico e Tecnológico (CNPq grant 477635/2010-5), Coordenação de Aperfeiçoamento de Ensino Superior (CAPES), and Fundação de Amparo à Pesquisa do Estado de Goiás (FAPEG). We also thank the Grupo de Física dos Materiais (IF/UFG) for allowing access to their spectrofluorometer (Fluorolog FL3-221; Horiba Jobin Yvon Inc.).

REFERENCES

1. Brummer, E., E. Castañeda and A. Restrepo (1993) Paracoccidioidomycosis: an update. *Clin. Microbiol. Rev.* **6**, 89–117.
2. Prado, M., M. B. Silva, R. Laurenti, L. R. Travassos and C. P. Taborda (2009) Mortality due to systemic mycoses as a primary cause of death or in association with AIDS in Brazil: a review from 1996 to 2006. *Mem. Inst. Oswaldo Cruz* **104**, 513–521.
3. Franco, M., M. R. Montenegro, R. P. Mendes, S. A. Marques, N. L. Dillon and N. G. Mota (1987) Paracoccidioidomycosis: a recently proposed classification of its clinical forms. *Rev. Soc. Bras. Med. Trop.* **20**, 129–132.
4. Johann, S., N. P. Sá, L. A. R. S. Lima, P. S. Cisalpino, B. B. Cota, T. M. A. Alves, E. P. Siqueira and C. L. Zani (2010) Antifungal activity of schinol and a new biphenyl compound isolated from *Schinus terebinthifolius* against *Paracoccidioides brasiliensis*. *Ann. Clin. Microbiol. Antimicrob.* **9**, 30.
5. Cock, A. M., L. E. Cano, D. Vélez, B. H. Aristizábal, J. Trujillo and A. Restrepo (2000) Fibrotic sequelae in pulmonary paracoccidioidomycosis: histopathologicalaspects in BALB/c mice infected with viable and non-viable *Paracoccidioides brasiliensis* propagules. *Rev. Inst. Med. Trop. São Paulo* **42**, 59–66.
6. Amaral, A. C., L. Fernandes, A. S. Galdino, M. S. Felipe, C. M. Soares and M. Pereira (2005) Therapeutic targets in *Paracoccidioides brasiliensis:* post-transcriptome perspectives. *Genet. Mol. Res.* **30**, 430–449.
7. Abadio, A. K. R., E. S. Kioshima, M. M. Teixeira, N. F. Martins, B. Maigret and M. S. S Felipe (2011) Comparative genomics allowed the identification of drug targets against human fungal pathogens. *BMC Genomics* **12**, 1–10.
8. Donnely, R. F., P. A. McCarron and M. M. Tunney (2008) Antifungal photodynamic therapy. *Microbiol. Res.* **163**, 1–12.
9. Quiroga, E. D., M. G. Alvarez and E. N. Durantini (2010) Susceptibility of *Candida albicans* to photodynamic action of 5,10,15,20-tetra(4-*N* methylpyridyl) porphyrin in different media. *FEMS Immunol. Med. Microbiol.* **60**, 123–131.
10. Fuchs, B. B., G. P. Tegos, M. R. Hamblin and E. Mylonakis (2007) Susceptibility of *Cryptococcus neoformans* to photodynamic inactivation is associated with cell wall integrity. *Antimicrob. Agents Chemother.* **51**, 2929–2936.
11. Soares, M. B., O. A. Alves, M. V. L. Ferreira, J. C. F. Amorim, G. R. Sousa, L. B. Silveira, R. A. Prates, T. V. Ávila, L. M Baltazar, D. G. Souza, D. A. Santos, L. V. Modolo, P. S. Cisalpino and M. Pinotti (2011) *Cryptococcus gattii*: *in vitro* susceptibility to photodynamic inactivation. *Photochem. Photobiol.* **87**, 357–364.
12. Friedberg, J. S., C. Skema, E. D. Baum, J. Burdick, S. A. Vinogradov, D. F. Wilson, A. D. Horan and I. Nachamkin (2001) *In vitro* effects of photodynamic therapy on *Aspergillus fumigatus*. *J. Antimicrob. Chemother.* **48**, 105–107.
13. Smijs, T. G., J. A. Bouwstra, M. Talebi and S. Pravel (2007) Investigation of conditions involved in the susceptibility of the dermatophyte *Trichophyton rubrum* to photodynamic treatment. *J. Antimicrob. Chemother.* **60**, 750–759.
14. Dai, T., Y. Y. Huang and M. R. Hamblin (2009) Photodynamic therapy for localized infections—state of the art. *Photodiagnosis Photodyn. Ther.* **6**, 170–188.
15. Ochsner, M. (1997) Photophysical and photobiological processes in photodynamic therapy of tumors. *J. Photochem. Photobiol. B* **39**, 1–18.
16. Weishaupt, K. R., C. J. Gomer and T. J. Doughert (1976) Identification of singlet oxygen as the cytotoxic agent in photoinactivation of a murine tumor. *Cancer Res.* **36**, 2326–2329.
17. Praseuth, D., A. Gaudener, J. B. Verlhac, I. Kraljic, I. Sissoëff and E. Gullé (1986) Photocleavage of DNA in the presence of synthetic water soluble porphyrins. *Photochem. Photobiol.* **44**, 717–724.
18. Gonçalves, P. J., P. L. Franzen, D. S. Correa, L. M. Almeida, M. Takara, A. S. Ito, S. C. Zílio and I. E. Borissevitch (2011) Effects of environment on the photophysical characteristics of mesotetrakis methylpyridiniumyl porphyrin (TMPyP). *Spectrochim. Acta A Mol. Biomol. Spectrosc.* **79**, 1532–1539.
19. Gonçalves, P. J., I. E. Borissevitch and S. C. Zílio (2009) Effect of protonation on the singlet-singlet excited-state absorption of meso-tetrakis(*p*-sulphonatophenyl) porphyrin. *Chem. Phys. Lett.* **469**, 270–273.
20. Gonçalves, P. J., N. M. Barbosa Neto, G. G. Parra, L. de Boni, L. P. F. Aggarwal, J. P. Siqueira, L. Misoguti, I. E. Borissevitch and S. C. Zílio (2012) Excited-state dynamics of meso-tetrakis(sulfonatophenyl) porphyrin J-aggregates. *Opt. Mater.* **34**, 741–747.
21. De Boni, L., P. L. Franzen, P. J. Gonçalves, I. E. Borissevitch, L. Misoguti, C. R. Mendonça and S. C. Zilio (2011) Pulse train fluorescence technique for measuring triplet state dynamics. *Opt. Express* **19**, 10813–10823.
22. De Boni, L., D. S. Correa, D. L. Silva, P. J. Gonçalves, S. C. Zilio, G. G. Parra, I. E. Borissevitch, S. Canuto and C. R. Mendonca (2011) Experimental and theoretical study of two-photon absorption in nitrofuran derivatives: promising compounds for photochemotherapy. *J. Chem. Phys.* **134**, 014509.
23. Dabrowski, J. M., M. M. Pereira, L. G. Arnaut, C. J. P. Monteiro, A. F. Peixoto, A. Karocki, K. Urbanska and G. Stochel (2007) Synthesis, photophysical studies and anticancer activity of a new halogenated water-soluble porphyrin. *Photochem. Photobiol.* **83**, 897–903.

24. Maximiano, R. V., E. Piovesan, S. C. Zílio, A. E. H. Machado, R. de Paula, J. A. S. Cavaleiro, I. E. Borissevitch, A. S. Ito, P. J. Gonçalves and N. M. Barbosa Neto (2010) Excited-state absorption investigation of a cationic porphyrin derivative. *J. Photochem. Photobiol., A* **214**, 115–120.
25. Chan, W. H. (2011) Photodynamic treatment induces an apoptotic pathway involving calcium, nitric oxide, p53, p21-activated kinase 2, and c-Jun N-terminal kinase and inactivates survival signal in human umbilical vein endothelial cells. *Int. J. Mol. Sci.* **12**, 1041–1059.
26. Sanovic, R., B. Krammer, S. Grumboeck and T. Verwanger (2009) Time-resolved gene expression profiling of human squamous cell carcinoma cells during the apoptosis process induced by photodynamic treatment with hypericin. *Int. J. Oncol.* **35**, 921–939.
27. Cekaite, L., Q. Peng, A. Reiner, S. Shahzidi, S. Tveito, I. E. Furre and E. Hovig (2007) Mapping of oxidative stress responses of human tumor cells following photodynamic using hexaminolevulinate. *BMC Genomics* **8**, 273.
28. Dardahon, M., W. Lin, A. Nicolas and D. Averbeck (2007) Specific transcriptional responses induced by 8-methoxypsoralen and UVA in yeast. *FEMS Yeast Res.* **7**, 866–878.
29. Dardahon, M., B. Agoutin, M. Watzinger and D. Averbeck (2009) Slt2 (Mpk1) MAP kinase is involved in the response of *Saccharomyces cerevisiae* to 8-methoxypsoralen plus UVA. *J. Photochem. Photobiol. B: Biol.* **95**, 148–155.
30. Skjølberg, H. C., Ø. Fensgård, H. Nilsen, B. Grallert and E. Boye (2009) Global transcriptional response after exposure of fission yeast cells to ultraviolet light. *BMC Cell Biol.* **10**, 87.
31. Fava-Netto, C. (1955) Estudos quantitativos sobre a fixação do complemento na blastomicose sul-americana com antígeno polissacarídeo. *Arq. Cir. Clin. Exp.* **18**, 197–253.
32. Bookout, A. L., C. L. Cummins, D. J. Mangelsdorf, J. M. Pesola and M. F. Kramer (2006) High throughput real-time quantitative reverse transcription PCR. *Current Protocols in Molecular Biology* 15.8.1–15.8.28.
33. Lambrechts, S. A. G., M. C. G. Aalders and J. Van Marle (2005) Mechanistic study of the photodynamic inactivation of *Candida albicans* by a cationic porphirin. *Antimicrob. Agents Chemother.* **49**, 2026–2034.
34. Osumi, M. (1998) The ultrastructure of yeast: cell wall structure and formation. *Micron* **29**, 207–233.
35. De Groot, P. W., A. F. Ram and F. M. Klis (2005) Features and functions of covalently linked proteins in fungal cell walls. *Fungal Genet. Biol.* **42**, 657–675.
36. Gonçalves, P. J., L. P. F. Aggarwal, C. A. Marquezin, A. S. Ito, L. De Boni, N. M. Barbosa Neto, J. J. Rodrigues Jr, S. C. Zílio and I. E. Borissevitch (2006) Effects of interaction with CTAB micelles on photophysical characteristics of *meso*-tetrakis (sulfonatophenyl) porphyrin. *J. Photochem. Photobiol., A* **181**, 378–384.
37. Prates, R., I. T. Kato, M. S. Ribeiro, G. P. Tegos and M. R. Hamblin (2011) Influence of multidrug efflux systems on methylene blue-mediated photodynamic inactivation of *Candida albicans*. *J. Antimicrob. Chemother.* **66**, 1525–1532.
38. Bertoloni, G., F. Zambotto, L. Conventi, E. Reddi and G. Jori (1987) Role of specific cellular targets in the hematoporphyrin-sensitized photoinactivation of microbial cells. *Photochem. Photobiol.* **46**, 695–698.
39. Demidova, T. N. and M. R. Hamblin (2005) Effect of cell-photosensitizer binding and cell density on microbial photoinactivation. *Antimicrob. Agents Chemother.* **49**, 2329–2335.
40. Monfrecola, G., E. M. Procaccini, M. Bevilacqua, A. Manco, G. Calabro and P. Santoianni (2004) *In vitro* effect of 5-aminolaevulinic acid plus visible light on *Candida albicans*. *Photochem. Photobiol. Sci.* **3**, 419–422.
41. Zeina, B., J. Greenman, W. M. Purcell and B. Das (2001) Killing of cutaneous microbial species by photodynamic therapy. *Br. J. Dermatol.* **144**, 274–278.
42. Franco, M., C. S. Lacaz, A. Restrepo-Moreno and G. Del Negro (1994) *Paracoccidioides brasiliensis* ultrastructural findings. *Paracoccidioidomycosis* **36**, 27–44.
43. Cassone, A., N. Simonetti and V. Stripoli (1973) Ultrastructural changes in the wall during germ-tube formation from blastospores of *Candida albicans*. *J. Gen. Microbiol.* **77**, 417–426.
44. Erman, J. E. and L. B. Vitello (2002) Yeast cytochrome *c* peroxidase: mechanistic studies *via* protein engineering. *Biochem. Biophys. Acta* **1597**, 193–220.
45. Wood, Z. A., E. Schröder, J. R. Harris and L. B. Poole (2003) Structure, mechanism and regulation of peroxiredoxin. *Trends Biochem. Sci.* **28**, 32–40.
46. Campos, E. G., R. S. Jesuíno, A. S. Dantas, M. M. Brígido and M. S. S. Felipe (2005) Oxidative stress response in *Paracoccidioides brasiliensis*. *Genet. Mol. Res.* **4**, 409–429.
47. Ahn, J., S. Nowell, S. E. McCann, J. Yu, N. P. Lang, F. F. Kadlubar, L. D. Ratnasinghe and C. B. Ambrosone (2006) Associations between catalase phenotype and genotype: modification by epidemiologic factor. *Cancer Epidemiol. Biomarkers Prev.* **15**, 1217–1222.
48. Nakonieczna, J., E. Michta, M. Rybicka, M. Grinholc, A. Gwizdek-Wisniewska and K. P. Bielawski (2010) Superoxide dismutase is upregulated in *Staphylococcus aureus* following protoporphyrin-mediated photodynamic inactivation and does not directly influence the response to photodynamic treatment. *BMC Microbiol.* **10**, 323.
49. San-Blas, G. and R. A. Calderone (2008) Pathogenic fungi: insights in molecular biology. In Chapter 3: *Regulatory Networks in Host-fungal Pathogen Interactions* (Edited by L. Fernandes, A. L. Bocca, A. M. Ribeiro, S. S. Silva, H. C. Paes, A. C. Amaral, V. L. P. Polez, N. F. Martins, C. M. A. Soares and M. S. S. Felipe), pp. 77–110. Caister Academic Press, Wymondham.
50. Arana, D. M., R. Alonso-Monge, C. Du, R. Calderone and J. Pla (2007) Differential susceptibility of mitogen-activated protein kinase pathway mutants to oxidative-mediated killing by phagocytes in the fungal pathogen *Candida albicans*. *Cell. Microbiol.* **9**, 1647–1659.
51. Brombacher, K., B. F. Fischer, K. Rüfenacht and R. I. L. Eggen (2006) The role of YapIp and Skn7p-mediated oxidative stress response in the defence of *Sccharomyces cerevisae* against singlet oxygen. *Yeast* **23**, 741–750.
52. San-Blas, G., G. Nino-Vega and T. Iturriaga (2002) *Paracoccidioides brasiliensis* and paracoccidioidomycosis: molecular approaches to morphogenesis, diagnosis, epidemiology, taxonomy and genetics. *Med. Mycol.* **40**, 225–242.
53. Lopez, R. F., N. Lange, R. Guy and M. V. Bentley (2004) Photodynamic therapy of skin cancer: controlled drug delivery of 5-ALA and its esters. *Adv. Drug Deliv. Rev.* **56**, 77–94.
54. Marques, S. A., D. B. Cortes, J. C. Lastoria, R. M. P. Camargo and M. E. A. Marques (2007) Paracoccidioidomycosis: frequency, morphology and pathogenesis of tegumentary lesion. *An. Bras. Dematol.* **82**, 411–417.
55. Komerik, N. and A. J. McRobert (2006) Photodynamic therapy as an alternative antimicrobial modality for oral infections. *J. Environ. Pathol. Toxicol. Oncol.* **25**, 487–504.
56. Dai, T., V. J. Bil de Arce, G. P. Tegos and M. R. Hamblin (2011) Blue dye and red light: a dynamic combination for prophylaxis and treatment of cutaneous *Candida albicans* infections in mice. *Antimicrob. Agents Chemother.* **12**, 5710–5717.
57. Dai, T., G. P. Tegos, T. Zhiyentayev, E. Mylonakis and M. R. Hamblin (2011) Photodynamic therapy for methicillin-resistant *Staphylococcus aureus* infection in a mouse skin abrasion model. *Lasers Surg. Med.*, **42**, 38–44.
58. Ragàs, X., T. Dai, G. P. Tegos, M. Agut, S. Nomell and M. R. Hamblin (2010) Photodynamic inactivation of *Acinetobacter baumanii* using phenothiazinium dyes: *in vitro* and *in vivo* studies. *Lasers Surg. Med.* **42**, 384–390.
59. Mima, E. G., A. C. Pavarina, L. N. Dovigo, C. E. Vergani, C. A. Costa, C. Kurachi and V. S. Bagnato (2010) Susceptibility of *Candida albicans* photodynamic therapy in a murine model of oral candidosis. *Oral Surg. Oral Med. Oral Pathol. Oral Radiol. Endod.* **109**, 392–401.
60. Mima, E. G., A. C. Pavarina, M. M. Silva, D. G. Ribeiro, C. E. Vergani, C. Kurachi and V. S. Bagnato (2011) Denture stomatitis treated with photodynamic therapy: five cases. *Oral Surg. Oral Med. Oral Pathol. Oral Radiol. Endod.* **112**, 602–608.

Curr Fungal Infect Rep
DOI 10.1007/s12281-012-0108-8

GENOMICS AND PATHOGENESIS (S SHOHAM, SECTION EDITOR)

Metal Acquisition and Homeostasis in Fungi

Elisa Flávia Luiz Cardoso Bailão · Ana Flávia Alves Parente · Juliana Alves Parente · Mirelle Garcia Silva-Bailão · Kelly Pacheco de Castro · Lívia Kmetzsch · Charley Christian Staats · Augusto Schrank · Marilene Henning Vainstein · Clayton Luiz Borges · Alexandre Melo Bailão · Célia Maria de Almeida Soares

Abstract Transition metals, particularly iron, zinc and copper, have multiple biological roles and are essential elements in biological processes. Among other micronutrients, these metals are frequently available to cells in only limited amounts, thus organisms have evolved highly regulated mechanisms to cope and to compete with their scarcity. The homeostasis of such metals within the animal hosts requires the integration of multiple signals producing depleted environments that restrict the growth of microorganisms, acting as a barrier to infection. As the hosts sequester the necessary transition metals from invading pathogens, some, as is the case of fungi, have evolved elaborate mechanisms to allow their survival and development to establish infection. Metalloregulatory factors allow fungal cells to sense and to adapt to the scarce metal availability in the environment, such as in host tissues. Here we review recent advances in the identification and function of molecules that drive the acquisition and homeostasis of iron, copper and zinc in pathogenic fungi.

E. F. L. C. Bailão · A. F. A. Parente · J. A. Parente · M. G. Silva-Bailão · K. P. de Castro · C. L. Borges · A. M. Bailão · C. M. de Almeida Soares (✉)
Laboratório de Biologia Molecular, Instituto de Ciências Biológicas II, Campus Samambaia,
Universidade Federal de Goiás,
74690-900, Goiânia, Goiás, Brazil
e-mail: cmasoares@gmail.com

E. F. L. C. Bailão
Unidade Universitária de Iporá, Universidade Estadual de Goiás,
Iporá, Goiás, Brazil

L. Kmetzsch · C. C. Staats · A. Schrank · M. H. Vainstein
Laboratório de Biologia Molecular, Centro de Biotecnologia,
Universidade Federal do Rio Grande do Sul,
Porto Alegre, Rio Grande do Sul, Brazil

Published online: 22 September 2012

Keywords Iron · Copper · Zinc · Fungal pathogens

Introduction

Metals such as iron, copper and zinc have numerous biological roles and play a central role at the host–pathogen interface. Mammalian and microbial cells have an essential demand for these metals, which act as both structural and catalytic cofactors for proteins, and are therefore required for biological processes. During infection, the competing demands for these nutrients culminate in a struggle for metal acquisition/utilization at the microbe–host interface [1•, 2•]. In the complex interactions between pathogens and their mammalian hosts, metal homeostasis plays an essential role in both virulence and host defense [3, 4].

Iron and copper participate in several oxidation–reduction reactions because of their ability to lose and gain electrons. This same property permits iron and copper to generate reactive oxygen species (ROS) [5, 6]. Zinc is also an essential cofactor of many enzymes, but in excess, may be toxic to cells [7]. For metal balance, cells usually regulate uptake, storage and consumption. Our understanding of the mechanisms involved in metal excretion is incomplete. This review summarizes the current knowledge regarding the most studied metals that contribute to virulence of fungal pathogens: iron, copper and zinc. We focus on the fungal pathogens *Candida albicans*, *Histoplasma capsulatum*, *Aspergillus fumigatus*, *Cryptococcus neoformans* and *Paracoccidioides*. Specifically we discuss the struggle for control of transition metals during infection, the molecular mechanisms involved in iron, copper and zinc uptake and the regulation of metal homeostasis in those pathogens. Additionally we review the preferential host iron sources

and fungal genes related to iron acquisition/homeostasis directly involved in infection.

Host Metal Homeostasis During Infectious Processes

Among metals involved in fungal infection, the functions of iron are well characterized. Hosts have evolved mechanisms to efficiently acquire iron and at the same time decrease its availability to pathogens [2•]. Physiological conditions that lead to metal overload contribute to increased infections. For example, administration of exogenous iron results in exacerbation of cryptococcosis [8] and increases in free iron also results in higher fungal load in mouse tissues infected with *Paracoccidioides* [9]. At the interface between iron and immunity, macrophages appear as a cellular factory that manage metal homeostasis [3]. Upon infection, the iron efflux from macrophages is suppressed resulting in 70 % reduction in plasma iron, thus restricting the amount of the metal available to extracellular pathogens. Infected macrophages, conversely, restrict the amount of iron available to intracellular microbes by pumping out iron via the ferroportin transporter route. Mutation-impaired ferroportin function compromises the ability of macrophages to clear pathogens [10].

Lactoferrin is produced by neutrophils and epithelial cells to chelate iron in extracellular compartments resulting in impairment of proliferation of fungal invaders [11]. Induction of ferritin production to facilitate withholding of intracellular iron diminishes the amount of the metal available to intracellular pathogens [2•, 12]. Iron also influences immune functions mediated by macrophages, and cytokines affect systemic iron homeostasis and cellular iron efflux [13]. Reduced iron levels have been found in macrophages activated by exposure to interferon gamma (IFN-γ) or granulocyte macrophage colony-stimulating factor (GM-CSF) [14]. Transferrin can be used by pathogens as an iron source in host tissues. To counteract this process IFN-γ decreases the expression of transferrin receptor in macrophages. Moreover, the production of the cellular iron storage molecule ferritin can be regulated by proinflammatory signals [15]. So, in the complex host–pathogen interaction, the control of iron homeostasis is a battlefield where the host must withdraw the micronutrient from microbes and at the same time uses iron to elaborate an efficient oxidative burst, since this metal is required for generation of ROS.

Since copper is essential, it is not unexpected that both humans and pathogens share the requirement for acquiring sufficient levels of copper [6]. In response to fungal infection, macrophages phagocytose the fungal cells and initiate cellular events that culminate in the oxidative burst [6]. Studies suggest that fungal pathogens must obtain copper to develop an efficient survival mechanism in host tissues, since genes related to copper acquisition/homeostasis are upregulated during infection [16, 17]. *C. neoformans* fights the host defenses to acquire copper, which promotes melanin synthesis, a virulence factor for this fungus [18]. The dependence of fungi upon copper for survival under the host conditions can be related to their response to ROS generation by the host since superoxide dismutase is a copper-dependent enzyme.

Zinc levels are modulated during infectious processes. During inflammation, the liver sequesters zinc, likely limiting zinc bioavailability to pathogenic microbes [19]. Neutrophils display an antimicrobial mechanism based on competition for zinc. This zinc-chelating system, found in neutrophil cytoplasm and abscess fluid, exerts fungistatic activity based on the calcium- and zinc-binding protein calprotectin [20]. Abscess fluid inhibits the growth of several fungi and the addition of zinc results in fungal growth in this fluid [7], reinforcing the view that zinc sequestration is a strategy used by the host to combat fungal infections. A metallomic study has demonstrated that GM-CSF-activated macrophages reduce intracellular zinc concentrations upon *H. capsulatum* infection in order to kill the pathogen [14].

Molecular Mechanisms of Iron, Copper and Zinc Uptake

Iron uptake mechanisms are highly regulated in fungi since excess iron is toxic and iron excretion systems have not yet been described in fungi [21]. Fungi have evolved different mechanisms for iron acquisition [21]. A low-affinity iron uptake system characterized only in *Saccharomyces cerevisiae* involves permeases that transport not only iron, but also other metals. In the reductive high-affinity ferrous uptake, ferrireductases reduce ferric iron (Fe^{3+}) to its soluble ferrous form (Fe^{2+}). Fe^{2+} is then reoxidized by plasma membrane ferroxidases and Fe^{3+} is promptly internalized by a high-affinity permease [5]. Another high-affinity mechanism for iron uptake is mediated by siderophores, small molecules with high affinity for Fe^{3+}, that allow specific recognition and uptake of iron at the cell surface [22]. Most fungi produce and secrete hydroxamate-type siderophores under low-iron growth conditions [23]. Some fungi, such as *C. neoformans*, do not produce siderophores, but can transport molecules produced by other organisms (xenosiderophores) [24].

The *C. albicans* genome contains genes that encode 18 putative ferrireductases and five ferroxidase homologues [1•, 25]. The ferroxidase Fet34 localizes to the plasma membrane and possibly associates with the permease Ftr1 early in the secretory pathway, promoting the high-affinity iron uptake [26•]. *C. albicans* produces a siderophore transporter [27] that displays broad substrate specificity, transporting various hydroxamate-type siderophores [28].

Under iron-limiting conditions, *H. capsulatum* produces three different reductants: a secreted glutathione dependent γ-glutamyltransferase (Ggt1) [29], non-enzymatic reductants with low molecular weight, and cell surface ferric reducing agents [30]. The *H. capsulatum* genome contains genes that encode seven putative ferrireductases [31]. Although a high-affinity acquisition mechanism has not been described for *H. capsulatum*, genomic analysis of the strain G186AR revealed genes coding iron permease (ftr1) and ferroxidase (Fet3) homologues [32]. *H. capsulatum* is also able to produce multiple hydroxamate siderophores under conditions of low iron availability [33]. In addition, *H. capsulatum* can utilize xenosiderophores [34].

In *A. fumigatus*, the ferrireductase FreB has been characterized. After reduction, iron is internalized by the ferroxidase-permease complex FetC–FtrA [35]. *A. fumigatus* synthesizes three types of siderophores, two of which are responsible for iron storage [36–38]. The iron-loaded siderophore is internalized by specific transporters [39] and the ester bonds of triacetylfusarinine C are then hydrolyzed by an esterase [40]. The cleavage products (fusarinines) are excreted, and the free iron can either be used in cell metabolism or bind to intracellular siderophore desferri-ferricrocin for storage [37, 38, 41•].

Uptake of iron is probably mediated by two large groups of transporters in *C. neoformans*: high- and low-affinity systems [42]. Cft1 is a high-affinity iron permease associated with the reductive system. On the other hand *cft2* possibly encodes for a low-affinity uptake system, since no clear iron-related phenotypes could be detected in *cft2* null mutants [43]. Cfo1 and Cfo2 ferroxidases have also been described in *C. neoformans* [44]. Cfo1 is required for high-affinity and reductive iron transport, since mutants lacking the coding gene show reduced growth under low iron conditions and cannot use ferric iron for growth. Moreover, under low iron conditions, Cfo1 expression is increased and localized mainly in the cell surface [44]. Studies have shown the inability of *Cryptococcus* species to produce siderophores. This is supported by genomic analysis, which has revealed the absence of genes involved in steps of siderophore biosynthesis [24, 45]. Despite the inability to synthesize siderophores, *Cryptococcus* species are presumably able to transport xenosiderophores [43].

Molecular mechanisms for reductive iron uptake in the genus *Paracoccidioides* are coming to light. In silico analysis has revealed that the genome of this fungus contains genes that encode redundant ferrireductase homologues [45]. Experiments have demonstrated a significant increase in the expression of genes coding the ferrireductases *fre3*, *fre7*, *frp1* and *ggt1* upon iron restriction (Fig. 1a). *Paracoccidioides* has glutathione-dependent ferrireductase activity [46], an aspect that is corroborated by the presence of a *ggt1* homologue in the fungus genome [45]. Since iron permease homologues were not detected in the *Paracoccidioides* genome, it has been proposed that a zinc permease could function additionally as an iron permease to acquire this metal [45]. The importance of iron acquisition by siderophores in the *Paracoccidioides* genus have been noted and studies on siderophore production and uptake are in

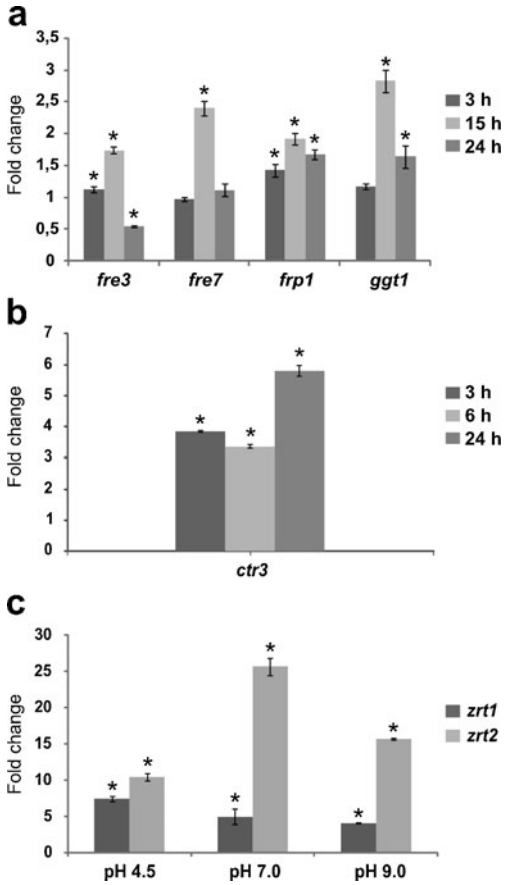

Fig. 1 Expression profile of *Paracoccidioides* (*Pb*01) genes during iron, copper and zinc starvation. *Pb*01 yeast cells were incubated in chemically defined medium containing different concentrations of iron, copper or zinc. Cells were harvested and total RNA was extracted using Trizol and mechanical cell rupture. After in vitro reverse transcription, the cDNAs were submitted to quantitative RT-PCR. The expression values were calculated using the transcripts alpha tubulin or l34 as endogenous controls [9, 82]. Data are presented as fold change relative to experimental controls. **a** Expression of ferrireductases encoding transcripts *fre3*, *fre7*, *frp1*, and *ggt1* evaluated in yeast cells in medium containing 3.5 μM iron (experimental control) or no iron for 3 h, 15 h and 24 h. **b** Expression of copper transporter encoding transcript *ctr3* evaluated in yeast cells in medium containing 50 μM copper (experimental control) or under conditions of copper starvation produced by adding the copper chelator bathocuproine disulphonate (BCS) for 3 h, 6 h and 24 h. **c** Expression level of zinc transporters encoding transcripts *zrt1* and *zrt2* evaluated in yeast cells in medium containing 30 μM zinc (experimental control) or under conditions of zinc depletion produced by adding the zinc chelator *N*,*N*,*N*,*N*-tetrakis(2-pyridylmethyl)ethylenediamine (TPEN) at different pH values (4.5, 7.0 and 9.0) for 6 h. Data are presented as means ± SD from triplicate determinations. *$p \leq 0.05$, *t* test, in relation to the data obtained from the experimental controls

progress. The major evidence of iron capture by siderophores is supported by the stimulation of fungal growth in the presence of coprogen B and dimerum acid [47]. In silico analysis ha revealed the presence of genes putatively involved in hydroxamate-type siderophore biosynthesis and transport [45]. Corroborating these data, it has been demonstrated by chrome azurol S assays that *Paracoccidioides* is a hydroxamate producer (Silva et al., personal communication).

In fungi, copper and iron homeostasis must be intrinsically linked since iron uptake requires ferroxidases, which are members of the multicopper oxidase family. Copper is first reduced by plasma membrane ferrireductases and then Cu^{1+} is internalized via a high-affinity permease [48]. In *C. albicans*, the ferrireductase c*fl1*/*fre1* is transcriptionally regulated in response to both iron and copper availability [49], indicating that this ferrireductase is also important in copper uptake. Furthermore, the mutant for the *ctr1* copper transporter displays deficient growth in medium low in copper and iron indicating that in *C. albicans* iron and copper homeostasis are linked [50].

As observed for iron, copper plays fundamental roles in several aspects of *C. neoformans* biology. For instance, the production of melanin pigment is dependent on a copper oxidase [51] and the copper-containing ferroxidases are necessary for iron uptake [44]. Copper is probably reduced in *C. neoformans* by the same enzymes that reduce iron at the cell surface [52]. Two copper transporters have been described in *C. neoformans*. The *ctr1* null mutant shows reduced growth in copper-depleted medium. Ctr4, by contrast, is not essential for cryptococcal development in low-copper medium. However, mutant cells lacking both *ctr1* and *ctr4* transporters display severe growth defects in copper-deprived environments [53•].

The *Paracoccidioides* genome contains genes that encode redundant ferrireductases [45] as cited above, suggesting that these enzymes could function as iron and copper reductases. Furthermore a high-affinity copper transporter, *ctr3*, is present at increased levels during copper shortage (Fig. 1b), reinforcing the view that Ctr3 could be involved in copper uptake in *Paracoccidioides* [45].

The zinc uptake system in most fungi comprises just high-affinity and low-affinity permeases belonging to the ZIP family [54, 55], since this metal does not need to be reduced before internalization. Eight genes encoding proteins of the ZIP family of zinc transporters have been described in *A. fumigatus* [56]. Expression of *zrfA*, *zrfB* and *zrfC* is regulated by both zinc and pH [56, 57]. ZrfA and ZrfB function under acidic, zinc-limiting conditions. It seems that ZrfB is a high-affinity zinc permease, since a *zrfB* transcript was downregulated under high zinc conditions [58]. ZrfC participates in zinc uptake in a neutral or alkaline, zinc-poor environment [56]. Aspf2 putatively contributes to zinc uptake as a zinc-binding protein localized in the fungal periplasm [56].

Paracoccidioides possesses two zinc permease homologues (*zrt1* and *zrt2*), indicating a specific zinc uptake system [45]. The transcriptional response of *zrt* homologues to zinc starvation has been demonstrated by quantitative RT-PCR (Fig. 1c). The *zrt2* transcript, but not *zrt1* transcript, is highly expressed at neutral to alkaline pH during zinc depletion (Fig. 1c), as observed to *A. fumigatus* ZrfC.

Host Iron Sources

A high proportion of circulating iron in humans exists as heme in hemoglobin and hemin, iron-containing porphyrins. *C. albicans* shows hemolytic activity, and membrane proteins capable of binding hemin/hemoglobin have been identified [1•]. *C. albicans* Rbt5, a glycosylphosphatidylinositol-anchored protein, is the major hemoglobin receptor [59]. *hmx1* encodes an intracellular heme oxygenase that breaks down iron-protoporphyrin IX to α-biliverdin and is required for heme-iron utilization [60]. In silico analysis has revealed that *Paracoccidioides* genome contains genes that encode *hmx1* and *rbt5* homologues, suggesting effective hemoglobin iron acquisition by this fungus [45].

Intracellular iron in humans is bound to ferritin. *C. albicans* hyphae are able to obtain iron from ferritin using Als3 protein as a receptor. Als3 is a multifunctional protein since it can also function as an adhesin and an invasin [1•]. Transferrin is a glycoprotein that transports iron in serum. *C. albicans* is able to take up iron from transferrin by the reductive pathway using the ferrous permease Ftr1 and ferrireductase Fre10 [61]. In *H. capsulatum*, ferrireductase activity is higher in the presence of hemin and transferrin, suggesting that this fungus uses the ferrireductases to obtain iron during infection [34]. *Paracoccidioides* is likely to be able to take up iron from transferrin since the fungus has five genes encoding ferrireductases in the genome [45].

Regulation of Iron, Copper and Zinc Homeostasis in Pathogenic Fungi

Fungi have evolved sophisticated control mechanisms for maintenance of optimal levels of iron, copper and zinc. These mechanisms include the regulation of genes involved in metal ion uptake, utilization and storage. In fungi, metal ion homeostasis is mainly achieved by transcriptional regulation of gene expression. A group of iron-responsive GATA-type transcription factors mediates repression of iron acquisition genes in response to iron

sufficiency [62]. These regulators have a cysteine-rich central domain located between two zinc fingers, which directly interact with iron [63].

A range of genes and regulators involved in the response of *C. albicans* to iron starvation have been described [64]. During iron sufficiency, the GATA-type regulator Sfu1 downregulates expression of *arn1* and *hap43* genes encoding a siderophore transporter and a transcription factor, respectively [64, 65]. Under iron-limited conditions, the Cap2 protein represses the expression of Sfu1, activating genes of iron uptake pathways [66•]. Sef1 and Rim101 were also identified as positive regulators of iron acquisition in *C. albicans* [67, 68].

A GATA-type factor, Sre1, has been described in *H. capsulatum*. Sre1 acts as a negative regulator of siderophore biosynthesis genes in response to iron excess [69]. Sre1 also regulates cellular processes other than iron acquisition, such as optimal filamentous growth [70]. The same occurs with the Sre1 homologue SreB in *Blastomyces dermatitidis*. SreB regulates siderophore biosynthesis and also governs phase transition and cell growth at 22 °C in *B. dermatitidis* [71].

During iron sufficiency, high-affinity iron uptake systems (reductive pathway and siderophore production) are repressed by SreA in *A. fumigatus* [72]. During iron starvation, the *A. fumigatus* bZIP-type regulator HapX represses iron-dependent pathways, such as respiration, TCA cycle and heme biosynthesis, to save iron, and activates iron uptake by siderophores [73•]. Thus the transcription factors SreA and HapX act in opposite ways within the cell depending on the environmental iron status. During iron excess, SreA is activated and represses HapX expression, while during iron paucity, HapX represses the expression of SreA. In *A. fumigatus* the transcription factor AcuM stimulates iron acquisition via HapX induction and SreA repression [74].

C. neoformans Cir1 possesses a cysteine-rich domain, but unlike other fungal GATA-type iron regulators, it has only a zinc finger motif [75]. Cir1 is a global transcription factor which senses iron levels and regulates positively and negatively the transcriptional response [75, 76]. The expression of *C. neoformans* virulence attributes, such as capsule formation, growth at host temperature and melanin production, are also controlled by Cir1 [75]. A post-translational mechanism for the control of the amount of Cir1 suggests that under conditions of iron starvation Cir1 protein levels decrease. In contrast, iron availability promotes Cir1 stabilization and consequent repression of iron acquisition genes [77]. The transcriptional response to iron in *C. neoformans* is also regulated by HapX. As well as Cir1, HapX has both a positive and negative influence in the regulation of gene expression. However, unlike Cir1, HapX plays a modest role during infection and probably is important during environmental iron acquisition [78].

Proteomic analysis has revealed that during iron starvation the metabolic status of the pathogenic fungus *Paracoccidioides* is altered. Glycolysis is upregulated while iron-consuming pathways, such as tricarboxylic and glyoxylate cycles, are repressed. It has been demonstrated that under iron-limited conditions the transcript level of the HapX increases [9]. However, the regulatory mechanisms that orchestrate the global changes in response to iron availability in this fungus have not been described and are the subject of current investigation.

Regulatory mechanisms that respond to copper availability among pathogenic fungi have been best studied in *C. neoformans*. The copper-dependent transcription factor, Cuf1, has a cysteine-rich sequence, which contains a putative copper binding motif [79]. Under conditions of copper limitation, Cuf1 induces the expression of the copper transporter encoding genes *ctr1* and *ctr4*. During copper excess, the metallothionein (copper binding and detoxifying protein) genes *cmt1* and *cmt2* are induced by Cuf1 [53•]. A copper-dependent transcriptional regulator, Mac1, found in *C. albicans*, is transcriptionally autoregulated and activates the expression of *ctr1* and *fre7* genes during copper paucity [80].

Although regulation of copper homeostasis has not yet been described in *Paracoccidioides*, studies have revealed that the high-affinity copper transporter, Ctr3, is upregulated under infection conditions [16, 81] and is also a potential adhesin [82]. Analysis of genes potentially involved in copper regulation has demonstrated the presence of a copper metalloregulatory transcription factor, Mac1, in *Paracoccidioides* [45], thus prompting further investigation.

As for copper, the regulation of zinc homeostasis in pathogenic fungi is poorly understood. A zinc-responsive transcription factor has been described in *C. albicans* [83]. The Zap1/Csr1 factor induces expression of the plasma membrane zinc transporters, Zrt1 and Zrt2, and is also involved in the control of efficient hyphae and biofilm matrix formation and production of quorum sensing molecules [83–86].

In *A. fumigatus* the expression of *zrfA* and *zrfB* is induced by the ZafA zinc-responsive transcriptional activator under zinc-limited conditions [87]. However, under neutral zinc-limited conditions, the expression of these transporters is repressed by the transcriptional regulator PacC [57]. Additionally, the expression of *zrfC* is upregulated by ZafA under zinc-limited conditions regardless of the environmental pH and downregulated by PacC under acidic growth conditions [56].

Although zinc metabolism regulation is not well understood in *Paracoccidioides* and *Cryptococcus* pathogens, a homologue of Zap1 zinc-regulated transcription factor has been found in their genomes [45]. Studies focusing on this potential transcriptional regulator are in progress.

Virulence

Despite the close correlation between metal availability and virulence, the fungal genes related to iron acquisition/homeostasis directly involved in host infection are poorly described [88, 89]. Table 1 lists metal acquisition/homeostasis genes and provides information on their role in virulence.

In *C. albicans,* mutants lacking the iron permease coding gene *ftr1* lose virulence [90]. The involvement of genes related to siderophore uptake in virulence was not observed [27, 28]. Moreover virulence attenuation was observed in *C. albicans* mutants lacking the iron-responsive transcriptional regulators *hap43*, *aft2*, *sef1* and *cap2* and the heme oxygenase coding gene *hmx1* [65, 66•, 91, 92, 93•], indicating that all these genes are important during *C. albicans* infection.

Table 1 Roles of genes involved in metal homeostasis and virulence of pathogenic fungi

Gene	Protein function	Role in virulence	Reference
Candida albicans			
ftr1	High-affinity iron permease	The *ftr1Δ* mutatation results in complete loss of the capacity to damage epithelial cells in vitro. Moreover mutants lacking *ftr1* are avirulent in mice infected with *C. albicans* during the early stationary phase	[90]
hap43	Transcriptional regulator	Deletion of *hap43* attenuates the virulence of *C. albicans* in a mouse model of disseminated infection	[65]
cap2	Transcriptional regulator	The *cap2Δ* mutant shows delayed virulence in a mouse model of *C. albicans* infection	[66•]
aft2	Transcriptional regulator	The *aft2Δ*/*aft2Δ* strain shows attenuated virulence in mice with disseminated infection	[91]
hmx1	Heme oxygenase	The homozygous mutant *hmx1Δ*/*hmx1Δ* shows reduced virulence in mice with disseminated infection	[93•]
sef1	Transcriptional regulator	The *sef1Δ* mutant shows significantly decreased virulence compared to wild-type strain in BALB/c mice with disseminated infection	[92]
Aspergillus			
sidA	Involved in siderophore biosynthesis	The *sidAΔ* mutant shows completely attenuated virulence in mice	[37, 94]
sidD	Involved in siderophore biosynthesis	The *sidDΔ* mutant shows severely attenuated virulence in neutropenic mice	[95]
sidF	Involved in siderophore biosynthesis	The *sidFΔ* mutant shows attenuated virulence in neutropenic mice infected intranasally	[95]
hapX	Transcriptional regulator	The *hapXΔ* mutant shows attenuated virulence in immunosuppressed mice	[73•]
acuM	Transcriptional regulator	The *acuMΔ* mutant shows attenuated virulence in neutropenic mice with disseminated infection and invasive pulmonary aspergillosis, resulting in significantly delayed mortality	[74]
zafA	Transcriptional regulator	The *zafAΔ* mutant shows reduced virulence in immunosuppressed mice infected intranasally	[87]
pacC	Transcriptional regulator	The *Aspergillus nidulans pacCΔ* mutant shows attenuated virulence in immunosuppressed mice	[99]
Histoplasma capsulatum			
sid1	Involved in siderophore biosynthesis	The *sid1Δ* strain shows a significant defect in pulmonary colonization compared to wild-type cells in mice infected intranasally	[31]
Cryptococcus neoformans			
cft1	High-affinity iron permease	The *cft1Δ* mutant shows attenuated virulence and reduced fungal burden	[43]
cfo1	Ferroxidase	The *cfo1Δ* mutant shows significantly attenuated virulence in mice	[44]
cir1	Transcriptional regulator	The *cir1Δ* mutant is avirulent in mice	[75]
ctr4	Copper transporter	The *ctr4Δ* null mutant shows reduced spread to tissues and is completely avirulent in infected mice	[79]
ctr1	Copper transporter	*ctr1Δ* mutant presented reduced melanization, reduced capsule and enhanced phagocytosis index	[97]
clc	Chloride channel	The *clc-A* mutant shows attenuated virulence in a mouse cryptococcosis model, since *clc-A* plays a role in capsule and laccase expression, important virulence factors	[98]
ccc2	Copper transporter	*ccc2* mutation results in absence of melanization, an important virulence factor	[18]
cuf1	Transcriptional regulator	The deletion of *cuf1* results in attenuated virulence in a mouse model of cryptococcosis	[79]

In *Aspergillus*, mutants lacking genes involved in siderophore biosynthesis (*sid*) have pointed to the relevance of this iron uptake pathway to virulence. *sidA* deletion in *A. fumigatus* abolishes siderophore biosynthesis and completely attenuates virulence [37, 94]. A similar effect was observed in mutants lacking the *sidA* homologue, *sid1*, in *H. capsulatum* [31]. Genes related to fusarinine C and triacetylfusarinine C production, *sidD* and *sidF,* significantly affect *A. fumigatus* virulence [95]. Furthermore, the deletion of the transcriptional regulators *hapX* and *acuM* causes significant attenuation of virulence in a murine model of infection [73•, 74].

The role of iron acquisition in *Cryptococcus* virulence has been extensively studied in recent years. Almost all *C. neoformans* genes involved in iron homeostasis that have been analyzed are related to cryptococcal virulence, as evaluated in murine models of cryptococcosis using null gene mutants [44, 75–78]. When considering the iron permeases Cft1 and Cft2, virulence attenuation and reduced fungal burden are observed in the *cft1* gene null mutant and in the *cft1*/*cft2* double mutant, but not in the *cft2* knockout strain [76]. The ferroxidase Cfo1 also plays a role in virulence, since null mutants are also attenuated in virulence [44]. In addition, *C. neoformans cir1* null mutants are completely avirulent in murine models of cryptococcosis, which is consistent with the hypocapsular phenotype and its reduced ability to proliferate at 37 °C [75].

Regarding copper, a pivotal biological role of this metal has been already described for *C. neoformans*, since two proteins involved in virulence, Cu/Zn-Sod1 and laccase, require copper as a cofactor for activity [51, 96]. The *ctr4* gene is expressed during infection and is directly associated with virulence, since null mutants show reduced spread to tissues and are completely avirulent in infected mice [79]. The *ctr1* gene also is associated with virulence, as mutants show reduced melanization, a reduced capsule, and an enhanced phagocytosis index [97]. Moreover, *C. neoformans* strains with mutation in genes encoding copper distribution transporters, such as the *clc* chloride channel and the *ccc2* secretory transporter, show reduced virulence or reduced expression of virulence factors [18, 98]. Furthermore, in a mouse model of cryptococcosis, transcriptional regulator *cuf1* null mutants display disruption of several virulence-linked characteristics, such as reduced laccase activity, severe growth defects in low-copper medium, and reduced virulence [79]. Cuf1 is required for infection of the brain but not of the lung in mouse models of cryptococcosis, suggesting that copper is limiting in neurological infections [79].

Studies investigating the role of zinc during pathogenesis are sparse. Investigations are restricted to the importance of zinc-responsive transcription factors during pathogenesis, such as *zaf*A. In *A. fumigatus,* ZafA regulates zinc homeostasis, and mutants lacking this gene show reduced virulence in mice [87]. A similar result was found for the pH-responsive transcriptional factor *pac*C, that plays an essential role in pulmonary infection by *A. fumigatus* [56, 99].

Conclusions

Iron, copper and zinc acquisition is a critical determinant in fungal pathogenesis. To circumvent metal sequestration by the host during infection, pathogenic fungi have evolved mechanisms of metal acquisition. Understanding of the roles of iron, copper and zinc in fungal pathogenicity has advanced in recent years. As discussed above, fungi demonstrate remarkable flexibility in gaining access to and utilizing the transition metals iron, copper and zinc. The sophisticated acquisition and regulation of homeostasis of these metals are surely an efficient weapon facilitating fungal survival within the human host, and represent an important component of virulence.

Acknowledgments Work at Universidade Federal de Goiás and Universidade Federal do Rio Grande do Sul was supported by grants from Financiadora de Estudos e Projetos (FINEP- 01.07.0552.00) and Conselho Nacional de Desenvolvimento Científico e Tecnológico (CNPq-558923/2009-7 and 478591/2010-1). E.F.L.C.B. and M.G.S.B. are supported by doctoral fellowships from Fundação Coordenação de Aperfeiçoamento de Pessoal de Nível Superior (CAPES). A.F.A.P. and L.K. are supported by postdoctoral fellowships from CAPES. We apologize to colleagues whose work we were not able to cite due to space limitations.

Disclosure E.F. Bailão: grants from Capes, CNPq and FINEP; A.F.A. Parente: grants from CNPq, CAPES and FINEP; J.A. Parente: none; M. Garcia Silva-Bailão: grant from CAPES; K. Castro: grants from FINEP and CNPq; L. Kmetzsch: grants from CAPES, CNPq and FINEP; C. Staats: grants from CNPq and FINEP; A. Schrank: grants from CNPq and FINEP; M. Vainstein: grants from CNPq and FINEP; C. Borges: grants from CNPq and FINEP; A. Bailão: grant from CNPq; C.M. Soares: grants from FINEP and CNPq.

References

Papers of particular interest, published recently, have been highlighted as:
- • Of importance

1. • Almeida RS, Wilson D, Hube B. Candida albicans iron acquisition within the host. FEMS Yeast Res. 2009;9:1000–12. *This article reviews the iron sources used by* C. albicans *during infection in the human host, that are xenosiderophores, hemoglobin, transferrin and ferritin*.
2. • Nairz M, Schroll A, Sonnweber T, Weiss G. The struggle for iron – a metal at the host-pathogen interface. Cell Microbiol. 2010;12:1691–702. *This article reviews the iron functions at the host–pathogen interface since mammalian and microbial cells have an essential demand for the metal. Microbial iron acquisition pathways are attractive targets for the development of new antimicrobial drugs*.

3. Theurl I, Fritsche G, Ludwiczek S, et al. The macrophage: a cellular factory at the interphase between iron and immunity for the control of infections. Biometals. 2005;18:359–67.
4. Ibrahim AS, Gebermariam T, Fu Y, et al. The iron chelator deferasirox protects mice from mucormycosis through iron starvation. J Clin Invest. 2007;117:2649–57.
5. Kaplan CD, Kaplan J. Iron acquisition and transcriptional regulation. Chem Rev. 2009;109:4536–52.
6. Kim BE, Nevitt T, Thiele DJ. Mechanisms for copper acquisition, distribution and regulation. Nat Chem Biol. 2008;4:176–85.
7. Lulloff SJ, Hahn BL, Sohnle PG. Fungal susceptibility to zinc deprivation. J Lab Clin Med. 2004;144:208–14.
8. Barluzzi R, Saleppico S, Nocentini A, et al. Iron overload exacerbates experimental meningoencephalitis by Cryptococcus neoformans. J Neuroimmunol. 2002;132:140–6.
9. Parente AF, Bailão AM, Borges CL, et al. Proteomic analysis reveals that iron availability alters the metabolic status of the pathogenic fungus Paracoccidioides brasiliensis. PLoS One. 2011;6:e22810.
10. Nevitt T. War-Fe-re: iron at the core of fungal virulence and host immunity. Biometals. 2011;24:547–58.
11. Al-Sheikh H. Effect of lactoferrin and iron on the growth of human pathogenic Candida species. Pak J Biol Sci. 2009;12:91–4.
12. Weinberg ED. Iron loading and disease surveillance. Emerg Infect Dis. 1999;5:346–52.
13. Weiss G. Modification of iron regulation by the inflammatory response. Best Pract Res Clin Haematol. 2005;18:183–201.
14. Winters MS, Chan Q, Caruso JA, Deepe Jr GS. Metallomic analysis of macrophages infected with Histoplasma capsulatum reveals a fundamental role for zinc in host defenses. J Infect Dis. 2010;202:1136–45.
15. Byrd TF, Horwitz MA. Regulation of transferrin receptor expression and ferritin content in human mononuclear phagocytes. Coordinate upregulation by iron transferrin and downregulation by interferon gamma. J Clin Invest. 1993;91:969–76.
16. Bailão AM, Schrank A, Borges CL, et al. Differential gene expression by Paracoccidioides brasiliensis in host interaction conditions: representational difference analysis identifies candidate genes associated with fungal pathogenesis. Microbes Infect. 2006;8:2686–97.
17. Samanovic MI, Ding C, Thiele DJ, Darwin KH. Copper in microbial pathogenesis: meddling with the metal. Cell Host Microbe. 2012;11:106–15.
18. Walton FJ, Idnurm A, Heitman J. Novel gene functions required for melanization of the human pathogen Cryptococcus neoformans. Mol Microbiol. 2005;57:1381–96.
19. Beisel WR. Herman Award Lecture, 1995: infection-induced malnutrition – from cholera to cytokines. Am J Clin Nutr. 1995;62:813–9.
20. Sohnle PG, Collins-Lech C, Wiessner JH. The zinc-reversible antimicrobial activity of neutrophil lysates and abscess fluid supernatants. J Infect Dis. 1991;164:137–42.
21. Haas H, Eisendle M, Turgeon BG. Siderophores in fungal physiology and virulence. Annu Rev Phytopathol. 2008;46:149–87.
22. Harrington JM, Crumbliss AL. The redox hypothesis in siderophore-mediated iron uptake. Biometals. 2009;22:679–89.
23. Renshaw JC, Robson GD, Trinci APJ, et al. Fungal siderophores: structures, functions and applications. Mycol Res. 2002;106:1123–42.
24. Jacobson ES, Petro MJ. Extracellular iron chelation in Cryptococcus neoformans. J Med Vet Mycol. 1987;25:415–8.
25. Jeeves RE, Mason RP, Woodacre A, Cashmore AM. Ferric reductase genes involved in high-affinity iron uptake are differentially regulated in yeast and hyphae of Candida albicans. Yeast. 2011;28:629–44.
26. • Ziegler L, Terzulli A, Gaur R, et al. Functional characterization of the ferroxidase, permease high-affinity iron transport complex from Candida albicans. Mol Microbiol. 2011;81:473–85. *This article demonstrates that Fe trafficking in* C. albicans *involves a complex Fet34-Ftr1 using* S. cerevisiae *as host for the functional expression of the* C. albicans *Fe-uptake proteins*.
27. Heymann P, Gerads M, Schaller M, et al. The siderophore iron transporter of Candida albicans (Sit1p/Arn1p) mediates uptake of ferrichrome-type siderophores and is required for epithelial invasion. Infect Immun. 2002;70:5246–55.
28. Hu CJ, Bai C, Zheng XD, et al. Characterization and functional analysis of the siderophore-iron transporter CaArn1p in Candida albicans. J Biol Chem. 2002;277:30598–605.
29. Zarnowski R, Cooper KG, Brunold LS, et al. Histoplasma capsulatum secreted gamma-glutamyltransferase reduces iron by generating an efficient ferric reductant. Mol Microbiol. 2008;70:352–68.
30. Timmerman MM, Woods JP. Ferric reduction is a potential iron acquisition mechanism for Histoplasma capsulatum. Infect Immun. 1999;67:6403–8.
31. Hwang LH, Mayfield JA, Rine J, Sil A. Histoplasma requires SID1, a member of an iron-regulated siderophore gene cluster, for host colonization. PLoS Pathog. 2008;4:e1000044.
32. Hilty J, George Smulian A, Newman SL. Histoplasma capsulatum utilizes siderophores for intracellular iron acquisition in macrophages. Med Mycol. 2011;49:633–42.
33. Howard DH, Rafie R, Tiwari A, Faull KF. Hydroxamate siderophores of Histoplasma capsulatum. Infect Immun. 2000;68:2338–43.
34. Timmerman MM, Woods JP. Potential role for extracellular glutathione-dependent ferric reductase in utilization of environmental and host ferric compounds by Histoplasma capsulatum. Infect Immun. 2001;69:7671–8.
35. Blatzer M, Binder U, Haas H. The metalloreductase FreB is involved in adaptation of Aspergillus fumigatus to iron starvation. Fungal Genet Biol. 2011;48:1027–33.
36. Charlang G, Ng B, Horowitz NH, Horowitz RM. Cellular and extracellular siderophores of Aspergillus nidulans and Penicillium chrysogenum. Mol Cell Biol. 1981;1:94–100.
37. Schrettl M, Bignell E, Kragl C, et al. Siderophore biosynthesis but not reductive iron assimilation is essential for Aspergillus fumigatus virulence. J Exp Med. 2004;200:1213–9.
38. Eisendle M, Schrettl M, Kragl C, et al. The intracellular siderophore ferricrocin is involved in iron storage, oxidative-stress resistance, germination, and sexual development in Aspergillus nidulans. Eukaryot Cell. 2006;5:1596–603.
39. Haas H. Molecular genetics of fungal siderophore biosynthesis and uptake: the role of siderophores in iron uptake and storage. Appl Microbiol Biotechnol. 2003;62:316–30.
40. Kragl C, Schrettl M, Abt B, et al. EstB-mediated hydrolysis of the siderophore triacetylfusarinine C optimizes iron uptake of Aspergillus fumigatus. Eukaryot Cell. 2007;6:1278–85.
41. • Haas H. Iron – a key nexus in the virulence of Aspergillus fumigatus. Front Microbiol. 2012;3:28. *This article reviews iron homeostasis and its participation in virulence in* Aspergillus *genus. The knowledge of the iron handling between host and fungus might improve therapy and diagnosis of fungal infections*.
42. Jacobson ES, Goodner AP, Nyhus KJ. Ferrous iron uptake in Cryptococcus neoformans. Infect Immun. 1998;66:4169–75.
43. Jung WH, Kronstad JW. Iron and fungal pathogenesis: a case study with Cryptococcus neoformans. Cell Microbiol. 2008;10:277–84.
44. Jung WH, Hu G, Kuo W, Kronstad JW. Role of ferroxidases in iron uptake and virulence of Cryptococcus neoformans. Eukaryot Cell. 2009;8:1511–20.
45. Silva MG, Schrank A, Bailão EF, et al. The homeostasis of iron, copper, and zinc in Paracoccidioides brasiliensis, Cryptococcus neoformans var. grubii, and Cryptococcus gattii: a comparative analysis. Front Microbiol. 2011;2:49.
46. Zarnowski R, Woods JP. Glutathione-dependent extracellular ferric reductase activities in dimorphic zoopathogenic fungi. Microbiology. 2005;151:2233–40.

47. Castaneda E, Brummer E, Perlman AM, et al. A culture medium for Paracoccidioides brasiliensis with high plating efficiency, and the effect of siderophores. J Med Vet Mycol. 1988;26:351–8.
48. Knight SA, Labbe S, Kwon LF, et al. A widespread transposable element masks expression of a yeast copper transport gene. Genes Dev. 1996;10:1917–29.
49. Hammacott JE, Williams PH, Cashmore AM. Candida albicans CFL1 encodes a functional ferric reductase activity that can rescue a Saccharomyces cerevisiae fre1 mutant. Microbiology. 2000;146 (Pt 4):869–76.
50. Marvin ME, Williams PH, Cashmore AM. The Candida albicans CTR1 gene encodes a functional copper transporter. Microbiology. 2003;149:1461–74.
51. Williamson PR. Biochemical and molecular characterization of the diphenol oxidase of Cryptococcus neoformans: identification as a laccase. J Bacteriol. 1994;176:656–64.
52. Nyhus KJ, Jacobson ES. Genetic and physiologic characterization of ferric/cupric reductase constitutive mutants of Cryptococcus neoformans. Infect Immun. 1999;67:2357–65.
53. • Ding C, Yin J, Tovar EM, et al. The copper regulon of the human fungal pathogen Cryptococcus neoformans H99. Mol Microbiol. 2011;81:1560–76. *This article describes a new* C. neoformans *Cu transporter, Ctr1, and some targets of the metalloregulatory transcription factor Cuf1*.
54. Zhao H, Eide D. The ZRT2 gene encodes the low affinity zinc transporter in Saccharomyces cerevisiae. J Biol Chem. 1996;271:23203–10.
55. Zhao H, Eide D. The yeast ZRT1 gene encodes the zinc transporter protein of a high-affinity uptake system induced by zinc limitation. Proc Natl Acad Sci U S A. 1996;93:2454–8.
56. Amich J, Vicentefranqueira R, Leal F, Calera JA. Aspergillus fumigatus survival in alkaline and extreme zinc-limiting environments relies on the induction of a zinc homeostasis system encoded by the zrfC and aspf2 genes. Eukaryot Cell. 2009;9:424–37.
57. Amich J, Leal F, Calera JA. Repression of the acid ZrfA/ZrfB zinc-uptake system of Aspergillus fumigatus mediated by PacC under neutral, zinc-limiting conditions. Int Microbiol. 2009;12:39–47.
58. Vicentefranqueira R, Moreno MA, Leal F, Calera JA. The zrfA and zrfB genes of Aspergillus fumigatus encode the zinc transporter proteins of a zinc uptake system induced in an acid, zinc-depleted environment. Eukaryot Cell. 2005;4:837–48.
59. Weissman Z, Kornitzer D. A family of Candida cell surface haem-binding proteins involved in haemin and haemoglobin-iron utilization. Mol Microbiol. 2004;53:1209–20.
60. Santos R, Buisson N, Knight S, et al. Haemin uptake and use as an iron source by Candida albicans: role of CaHMX1-encoded haem oxygenase. Microbiology. 2003;149:579–88.
61. Knight SA, Vilaire G, Lesuisse E, Dancis A. Iron acquisition from transferrin by Candida albicans depends on the reductive pathway. Infect Immun. 2005;73:5482–92.
62. Rutherford JC, Bird AJ. Metal-responsive transcription factors that regulate iron, zinc, and copper homeostasis in eukaryotic cells. Eukaryot Cell. 2004;3:1–13.
63. Scazzocchio C. The fungal GATA factors. Curr Opin Microbiol. 2000;3:126–31.
64. Lan CY, Rodarte G, Murillo LA, et al. Regulatory networks affected by iron availability in Candida albicans. Mol Microbiol. 2004;53:1451–69.
65. Hsu PC, Yang CY, Lan CY. Candida albicans Hap43 is a repressor induced under low-iron conditions and is essential for iron-responsive transcriptional regulation and virulence. Eukaryot Cell. 2011;10:207–25.
66. • Singh RP, Prasad HK, Sinha I, et al. Cap2-HAP complex is a critical transcriptional regulator that has dual but contrasting roles in regulation of iron homeostasis in Candida albicans. J Biol Chem. 2011;286:25154–70. *This article describes the roles performed by Cap2 under iron limiting conditions: activation of genes in iron uptake pathways and repression of iron-utilizing and iron-storage genes*.
67. Homann OR, Dea J, Noble SM, Johnson AD. A phenotypic profile of the Candida albicans regulatory network. PLoS Genet. 2009;5: e1000783.
68. Baek YU, Li M, Davis DA. Candida albicans ferric reductases are differentially regulated in response to distinct forms of iron limitation by the Rim101 and CBF transcription factors. Eukaryot Cell. 2008;7:1168–79.
69. Chao LY, Marletta MA, Rine J. Sre1, an iron-modulated GATA DNA-binding protein of iron-uptake genes in the fungal pathogen Histoplasma capsulatum. Biochemistry. 2008;47:7274–83.
70. Hwang LH, Seth E, Gilmore SA, Sil A. SRE1 regulates iron-dependent and -independent pathways in the fungal pathogen Histoplasma capsulatum. Eukaryot Cell. 2012;11:16–25.
71. Gauthier GM, Sullivan TD, Gallardo SS, et al. SREB, a GATA transcription factor that directs disparate fates in Blastomyces dermatitidis including morphogenesis and siderophore biosynthesis. PLoS Pathog. 2010;6:e1000846.
72. Schrettl M, Kim HS, Eisendle M, et al. SreA-mediated iron regulation in Aspergillus fumigatus. Mol Microbiol. 2008;70:27–43.
73. • Schrettl M, Beckmann N, Varga J, et al. HapX-mediated adaption to iron starvation is crucial for virulence of Aspergillus fumigatus. PLoS Pathog. 2010;6:e1001124. *This article describes the functions of transcriptional regulator HapX of* A. fumigatus*, which is important to fungus adaptation in iron starvation conditions and is crucial for virulence in a murine model of infection*.
74. Liu H, Gravelat FN, Chiang LY, et al. Aspergillus fumigatus AcuM regulates both iron acquisition and gluconeogenesis. Mol Microbiol. 2010;78:1038–54.
75. Jung WH, Sham A, White R, Kronstad JW. Iron regulation of the major virulence factors in the AIDS-associated pathogen Cryptococcus neoformans. PLoS Biol. 2006;4:e410.
76. Jung WH, Sham A, Lian T, et al. Iron source preference and regulation of iron uptake in Cryptococcus neoformans. PLoS Pathog. 2008;4:e45.
77. Jung WH, Kronstad JW. Iron influences the abundance of the iron regulatory protein Cir1 in the fungal pathogen Cryptococcus neoformans. FEBS Lett. 2011;585:3342–7.
78. Jung WH, Saikia S, Hu G, et al. HapX positively and negatively regulates the transcriptional response to iron deprivation in Cryptococcus neoformans. PLoS Pathog. 2010;6:e1001209.
79. Waterman SR, Hacham M, Hu G, et al. Role of a CUF1/CTR4 copper regulatory axis in the virulence of Cryptococcus neoformans. J Clin Invest. 2007;117:794–802.
80. Woodacre A, Mason RP, Jeeves RE, Cashmore AM. Copper-dependent transcriptional regulation by Candida albicans Mac1p. Microbiology. 2008;154:1502–12.
81. Dantas SF, Vieira de Rezende TC, Bailão AM, et al. Identification and characterization of antigenic proteins potentially expressed during the infectious process of Paracoccidioides brasiliensis. Microbes Infect. 2009;11:895–903.
82. Bailão AM, Nogueira SV. Rondon Caixeta Bonfim SM, et al. Comparative transcriptome analysis of Paracoccidioides brasiliensis during in vitro adhesion to type I collagen and fibronectin: identification of potential adhesins. Res Microbiol. 2012;163:182–91.
83. Kim MJ, Kil M, Jung JH, Kim J. Roles of zinc-responsive transcription factor Csr1 in filamentous growth of the pathogenic yeast Candida albicans. J Microbiol Biotechnol. 2008;18:242–7.
84. Nobile CJ, Nett JE, Hernday AD, et al. Biofilm matrix regulation by Candida albicans Zap1. PLoS Biol. 2009;7:e1000133.
85. Finkel JS, Xu W, Huang D, et al. Portrait of Candida albicans adherence regulators. PLoS Pathog. 2012;8:e1002525.

86. Ganguly S, Bishop AC, Xu W, et al. Zap1 control of cell-cell signaling in Candida albicans biofilms. Eukaryot Cell. 2011;10:1448–54.
87. Moreno MA, Ibrahim-Granet O, Vicentefranqueira R, et al. The regulation of zinc homeostasis by the ZafA transcriptional activator is essential for Aspergillus fumigatus virulence. Mol Microbiol. 2007;64:1182–97.
88. Kehl-Fie TE, Skaar EP. Nutritional immunity beyond iron: a role for manganese and zinc. Curr Opin Chem Biol. 2010;14:218–24.
89. Weinberg ED. Iron availability and infection. Biochim Biophys Acta. 2009;1790:600–5.
90. Ramanan N, Wang Y. A high-affinity iron permease essential for Candida albicans virulence. Science. 2000;288:1062–4.
91. Liang Y, Wei D, Wang H, et al. Role of Candida albicans Aft2p transcription factor in ferric reductase activity, morphogenesis and virulence. Microbiology. 2010;156:2912–9.
92. Chen C, Pande K, French SD, et al. An iron homeostasis regulatory circuit with reciprocal roles in Candida albicans commensalism and pathogenesis. Cell Host Microbe. 2011;10:118–35.
93. • Navarathna DH, Roberts DD. Candida albicans heme oxygenase and its product CO contribute to pathogenesis of candidemia and alter systemic chemokine and cytokine expression. Free Radic Biol Med. 2010;49:1561–73. *This article describes the heme oxygenase Hmx1 as a virulence factor in* C. albicans*. The authors observed that mutants lacking hmx1 gene were not affected during initial kidney colonization, but Hmx1 absence clearly affects infection progression*.
94. Hissen AH, Wan AN, Warwas ML, et al. The Aspergillus fumigatus siderophore biosynthetic gene sidA, encoding L-ornithine N5-oxygenase, is required for virulence. Infect Immun. 2005;73:5493–503.
95. Schrettl M, Bignell E, Kragl C, et al. Distinct roles for intra- and extracellular siderophores during Aspergillus fumigatus infection. PLoS Pathog. 2007;3:1195–207.
96. Cox GM, Harrison TS, McDade HC, et al. Superoxide dismutase influences the virulence of Cryptococcus neoformans by affecting growth within macrophages. Infect Immun. 2003;71:173–80.
97. Chun CD, Madhani HD. Ctr2 links copper homeostasis to polysaccharide capsule formation and phagocytosis inhibition in the human fungal pathogen Cryptococcus neoformans. PloS One. 2010;5.
98. Zhu X, Williamson PR. A CLC-type chloride channel gene is required for laccase activity and virulence in Cryptococcus neoformans. Mol Microbiol. 2003;50:1271–81.
99. Bignell E, Negrete-Urtasun S, Calcagno AM, et al. The Aspergillus pH-responsive transcription factor PacC regulates virulence. Mol Microbiol. 2005;55:1072–84.

Capítulo 5

Referências Bibliográficas

REFERÊNCIAS BIBLIOGRÁFICAS

Albrecht D, Guthke R, Brakhage AA, Kniemeyer O. 2010. Integrative analysis of the heat shock response in *Aspergillus fumigatus*, BMC Genomics. 11:32.

Albrecht D, Guthke R, Kniemeyer O, Brakhage AA. 2008. Systems biology of human-pathogenic fungi. In: Daskalaki A. (Ed.), Handbook of Research on Systems Biology Applications in Medicine. Vol. 1. IGI Global, pp. 403–421.

Alejandro-Osorio AL, Huebert DJ, Porcaro DT, Sonntag ME, Songdet Nillasithanukroh S, Will JL, Gasch AP. 2009. The histone deacetylase Rpd3p is required for transient changes in genomic expression in response to stress. Genome Biol. 10: R57.

Alia, Hayashi H, Chen THH, Murata N. 1998. Transformation with a gene for choline oxidase enhances the cold tolerance of *Arabidopsis* during germination and early growth. Plant Cell Environ. 21: 232–239.

Amich J, Leal F, Calera JA. 2009. Repression of the acid ZrfA/ZrfB zinc-uptake system of *Aspergillus fumigatus* mediated by PacC under neutral, zinc-limiting conditions. Int Microbiol. 12:39-47.

Amich J, Vicentefranqueira R, Leal F, Calera JA. 2010. *Aspergillus fumigatus* survival in alkaline and extreme zinc-limiting environments relies on the induction of a zinc homeostasis system encoded by the zrfC and aspf2 genes. Eukaryot Cell. 9:424-37.

Andrade RV, Paes HC, Nicola AM, Carvalho MJ, Fachin AL, Cardoso RS, Silva SS, Fernandes L, Silva SP, Donadi EA, Sakamoto-Hojo ET, Passos GA, Soares CMA, Brígido MM, Felipe MS. 2006. Cell organization, sulphur metabolism and ion transport-related genes are differentially expressed in *Paracoccidioides brasiliensis* mycelium and yeast cells. BMC Genomics. 7: 208-221.

Andreotti PF, Silva JLM, Bailão AM, Soares CMA, Benard G, Soares CP, Mendes-Giannini MJ. 2005. Isolation and partial characterization of a 30 kDa adhesin from *Paracoccidioides brasiliensis*. Microbes Infect. 7: 875-881.

Asif AR, Oellerich M, Amstrong VW, Gross U, Reichard U. 2010. Analysis of the cellular *Aspergillus fumigatus* proteome that reacts with sera from rabbits developing an acquired immunity after experimental aspergillosis. Electrophoresis. 31:1947-1958.

Baeza LC, Bailão AM, Borges CL, Pereira M, Soares CMA, Mendes-Gianini MJ 2007. cDNA representational difference analysis used in the identification of genes

expressed by *Trichophyton rubrum* during contact with keratin. Microbes Infect. 9: 1415-1421.

Bailão AM, Nogueira SV, Bonfim SMRC, Castro KP, Silva JF, Mendes-GianniniMJS, Pereira M, Soares CMA. 2012. Comparative transcriptome analysis of *Paracoccidioides brasiliensis* during in vitro adhesion to type I collagen and fibronectin:identification of potential adhesins. Res Microbiol. 163: 182-191.

Bailão AM, Schrank A, Borges CL, Dutra V, Walquíria I, Molinari-Madlum EE, Felipe MS, Mendes-Giannini MJ, Martins WS, Pereira M, Soares CMA. 2006. Differential gene expression by *Paracoccidioides brasiliensis* in host interaction conditions: representational difference analysis identifies candidate genes associated with fungal pathogenesis. Microbes Infect. 8: 2686-2697.

Bailão AM, Shrank A, Borges CL, Parente JA, Dutra V, Felipe MSS, Fiúza RB, Pereira M, Soares CMA. 2007. The transcriptional profile of *Paracoccidioides brasiliensis* yeast cells is influenced by human plasma. FEMS Immunol Med Microbiol. 51:43-57.

Bailão EFLC, Parente AF, Parente JA, Silva-Bailão MG, Castro KP, Rosa e Silva LK, Staats CC, Schrank A, Vainstein MH, Borges CL, Bailão AM, Soares CMA. 2012. Metal Acquisition and Homeostasis in Fungi. Curr Fung Infec Rep. 6: 1-10

Bagagli E, Bosco SM, Theodoro RC, Franco M. 2006. Phylogenetic and evolutionary aspects of *Paracoccidioides brasiliensis* reveal a long coexistence with animal hosts that explain several biological features of the pathogen. Infect Genet Evol. 6: 344-351.

Bagagli E, Theodoro RC, Bosco SM, McEwen JG. 2008. *Paracoccidioides brasiliensis*: phylogenetic and ecological aspects. Mycopathologia. 165: 197-207.

Barbosa MS, Báo SN, Andreotti PF, Faria FP, Felipe MS, Feitosa LS, Mendes-Giannini MJ, Soares CMA. 2006. Glyceraldehyde-3-phosphate dehydrogenase of *Paracoccidioides brasiliensis* is a cell surface protein involved in fungal adhesion to extracellular matrix proteins and interaction with cells. Infect Immun. 74: 382-389.

Barrozo LV, Mendes RP, Marques SA, Benard G, Silva ME, Bagagli E. 2009. Climate and acute/subacute paracoccidioidomycosis in a hyper-endemic area in Brazil. Int J Epidemiol. 38: 1642-1649.

Bastos KP, Bailão AM, Borges CL, Faria FP, Felipe MS, Silva MG, Martins WS, Fiúza RB, Pereira M, Soares CMA. 2007. The transcriptome analysis of early

morphogenesis in *Paracoccidioides brasiliensis* mycelium reveals novel and induced genes potentially associated to the dimorphic process. BMC Microbiol. 7: 29.

Bialek R, Ibricevic A, Aepinus C, Najvar LK, Fothergill AW, Knobloch J, Graybill JR. 2000. Detection of *Paracoccidioides brasiliensis* in tissue samples by a nested PCR assay. J Clin Microbiol. 38: 2940-2942.

Bird AJ, Gordon M, Eide DJ, Winge DR. 2006. Repression of ADH1 and ADH3 during zinc deficiency by Zap1-induced intergenic RNA transcripts. EMBO j. 25: 5726–5734.

Bird AJ, Zhao H, Luo H, Jensen LT, Srinivasan C, Evans-Galea M, Winge DR, Eide DJ. 2000. A dual role for zinc fingers in both DNA binding and sensing by the Zap1 transcriptional activator. EMBO J. 19: 3704-3713.

Blotta MHSL, Mamoni RL, Oliveira SJ, Nouér AS, Papaiordanou PM, Goveia A, Camargo ZP. 1999. Endemic regions of paracoccidioidomycosis in Brazil: a clinical and epidemiologic study of 584 cases in the southeast region. Am J Trop Med Hyg. 61: 390-394.

Boch J, Kempf B, Bremer E. 1994. Osmoregulation in *Bacillus subtilis*: synthesis of the osmoprotectant glycine betaine from exogenously provided choline. J Bacteriol. 176: 5364–5371.

Bookout AL, Cummins CL, Mangelsdorf DJ, Pesola JM, Kramer MF. 2006. High-throughput real-time quantitative reverse transcription PCR. In: Ausubel FM, Brent R, Kingston RE, Moore DD, Seidman JG, Smith JA (eds), *Current Protocols in Molecular Biology*. Hoboken NJ: John Wiley and Sons, pp. 1581–1628.

Borges CL, Bailão AM, Báo SN, Pereira M, Parente, Soares CMA 2010. Genes potentially revelant in the parasitic phase of the fungal pathogen *Paracoccdioides brasiliensis*. Mycophatogia. 171: 1-9

Bradford MM. 1976. A dye binding assay for protein. Analytical biochemistry. 72: 248–254.

Bramer CO, Silva LF, Gomez JG, Priefert H, Steinbuchel A. 2002. Identification of the 2-methylcitrate pathway involved in the catabolism of propionate in the polyhydroxyalkanoate-producing strain Burkholderia sacchari IPT101(T) and analysis of a mutant accumulating a copolyester with higher 3-hydroxyvalerate content. Applied and environmental microbiology. 68: 271–279.

Brummer E, Castaneda E, Restrepo A. 1993. Paracoccidioidomycosis: an update. Clin Microbiol Rev. 6: 89–117.

Brocker C, Lassen N, Estey T, Pappa A, Cantore M, Orlova VV, Chavakis T, Kavanagh KL, Oppermann U, Vasiliou V. 2010. Aldehyde dehydrogenase 7A1 (ALDH7A1) is a novel enzyme involved in cellular defense against hyperosmotic stress. J Biol Chem. 285: 18452-18463.

Bruneau JM, Magnin T, Tagat E, Legrand R, Bernard M, Diaquin M, Fudali C, Latgé JP. 2001. Proteome analysis of *Aspergillus fumigatus* identifies glycosylphosphatidylinositol-anchored proteins associated to the cell biosynthesis. Electrophoresis. 22 :2812-2823.

Brunori L, Giannoni F, Bini L, Liberatori S, Frota C, Jenner P, Thoresen OF, Orefici G, Fattorini L. 2004. Induction of *Mycobacterium avium* proteins upon infection of human macrophages. Proteomics. 4: 3078–3083.

Bukau B, Horwich AL. 1998. The Hsp70 and Hsp60 chaperone machines. Cell. 92: 351-366.

Cabiscol E, Belli G, Tamarit J, Echave P, Herrero E, Ros J. 2002. Mitochondrial Hsp60, resistance to oxidative stress, and the labile iron pool are closely connected in *Saccharomyces cerevisiae*. J Biol Chem. 277: 44531-44538.

Campos EG, Jesuino RS, Dantas Ada S, Brigido MM, Felipe MS. 2005. Oxidative stress response in *Paracoccidioides brasiliensis*. Genetics and molecular research. 4: 409-429.

Canteros CE, Madariaga MJ, Lee W, Rivas MC, Davel G, Iachini R. 2010. Endemic fungal pathogens in a rural setting of Argentina: seroepidemiological study in dogs. Rev Iberoam Micol. 27: 14-19.

Carberry S, Neville CM, Kavanagh KA, Doyle S. 2006. Analysis of major intracellular proteins of *Aspergillus fumigatus* by MALDI mass spectrometry: Identification and characterisation of an elongation factor 1B protein with glutathione transferase activity. Biochem Biophys Res Commun. 341:1096-1104.

Carrero LL, Niño-Vega G, Teixeira MM, Carvalho MJ, Soares CMA, Pereira M, Jesuino RS, McEwen JG, Mendoza L, Taylor JW, Felipe MS, San-Blas G. 2008. New *Paracoccidioides brasiliensis* isolate reveals unexpected genomic variability in this human pathogen. Fungal Genet Biol. 45: 605-612.

Cash P. 2002. Proteomics: the protein revolution. Biologist (London). 49: 58-62.

Castro NS, Barbosa MS, Maia ZA, Báo SN, Felipe MSS, Santana JM, Mendes-Giannini MJ, Pereira M and Soares CMA. 2008. Characterization of *Paracoccidioides brasiliensis* PbDfg5p, a cell-wall protein implicated in filamentous growth. Yeast. 25: 141-154.

Chagas RF, Bailão AM, Pereira M, Winters MS, Smullian AG, Deepe GS Jr, Soares CMA. 2008. The catalases of *Paracoccidioides brasiliensis* are differentially regulated: protein activity and transcript analysis. Fungal Genet Biol. 45: 1470-1478.

Chen Q, Haddad GG. 2004. Role of trehalose phosphate synthase and trehalose during hypoxia: from flies to Mammals. J Exp Biol. 207: 3125-3129.

Chen WP, Li PH, Chen THH. 2000. Glycinebetaine increases chilling tolerance and reduces chilling-induced lipid peroxidation in *Zea mays*. Plant Cell Environ. 23: 609–618.

Citiulo F, Jacobsen ID, Miramón P, Schild L, Brunke S, Zipfel P, Brock M, Hube B, Wilson D. 2012. *Candida albicans* Scavenges Host Zinc via Pra1 during Endothelial Invasion. PLoS pathogens. 8: e1002777.

Conesa A, Götz S, García-Gómez JM, Terol J, Talón M, Robles M. 2005. Blast2GO: a universal tool for annotation, visualization and analysis in functional genomics research. Bioinformatics. 21: 3676-3686.

Conklin DS, Culbertson MR, Kung C. 1994. Interactions between gene products involved in divalent cation transport in *Saccharomyces cerevisiae*. Mol Gen Genet. 244: 303–311.

Conklin DS, McMaster JA, Culbertson MR, Kung C. 1992. COT1, a gene involved in cobalt accumulation in *Saccharomyces cerevisiae*. Mol Cell Biol. 12: 3678–3688.

Corredor GG, Peralta LA, Castaño JH, Zuluaga JS, Henao B, Arango M, Tabares AM, Matute DR, McEwen JG, Restrepo A. 2005. The naked-tailed armadillo *Cabassous centralis* (Miller 1899): a new host to *Paracoccidioides brasiliensis*. Molecular identification of the isolate. Med Mycol. 43: 275–280.

Corte AC, Svoboda WK, Navarro IT, Freire RL, Malanski LS, Shiozawa MM, Ludwig G, Aguiar LM, Passos FC, Maron A, Camargo ZP, Itano EN, Ono MA. 2007. Paracoccidioidomycosis in wild monkeys from Parana State, Brazil. Mycopathologia 164: 225-228.

Costa M, Borges CL, Bailão AM, Meirelles GV, Mendonça YA, Dantas SF, Faria FP, Felipe MS, Molinari-Madlum EE, Mendes-Giannini MJ, Fiuza RB, Martins WS,

Pereira M, Soares CMA. 2007. Transcriptome profiling of *Paracoccidioides brasiliensis* yeast cells recovered from infected mice bring new insight into fungal response upon host-interaction. Microbiology. 153: 4194-4207.

Dainty SJ, Kennedy CA, Watt S, Bähler J, Whitehall SK. 2008. Response of *Schizossacharomyces pombe* to Zinc Deficiency. Eukaryot Cell. 7: 454-464.

Dantas AS, Andrade RV, de Carvalho MJ, Felipe MS, Campos EG. 2008. Oxidative stress response in *Paracoccidioides brasiliensis*: assessing catalase and cytochrome C peroxidase. Mycological research. 112: 747-756.

Dantas SF, Rezende TCV, Bailão AM, Taborda CP, Santos RS, Castro KP, Soares CMA. 2009. Identification and characterization of antigenic proteins potentially expressed during the infectious process of *Paracoccidioides brasiliensis*. Microbes Infect. 11: 895-903.

De Nadal E, Zapater M, Alepuz EM, Sumoy L, Mas G, Posas F. 2004. The MAPK hog1 recruits Rpd3 histone deacetylase to activate osmoresponsive genes. Nature. 427: 370-374.

Derengowski LS, Tavares AH, Silva S, Procópio LS, Felipe MS, Silva-Pereira I. 2008. Upregulation of glyoxylate cycle genes upon *Paracoccidioides brasiliensis* internalization by murine macrophages and in vitro nutritional stress condition. Med Mycol. 46: 125-134.

Desbrosses-Fonrouge AG, Voigt K, Schröder A, Arrivault S, Thomine S, Krämer U. 2005. *Arabidopsis thaliana* MTP1 is a Zn transporter in the vacuolar membrane wich mediates Zn detoxification and drives leaf Zn accumulation. FEBS Lett. 579: 4165-4174.

Doherty CP. 2007. Host-pathogen interactions: the role of iron. J Nutr. 137: 1341-1344.

Dunn MF, Ramírez-Trujillo JA, Hernández-Lucas I. 2009. Major roles of isocitrate lyase and malate synthase in bacterial and fungal pathogenesis. Microbiology. 155: 3166-3175.

Dutra V, Nakazato L, Broetto L, Silveira Schrank I, Henning Vainstein M, Schrank A. 2004. Application of representational difference analysis to identify sequence tags expressed by *Metarhizium anisopliae* during the infection process of the tick *Boophilus microplus* cuticle. Res Microbiol. 155: 245-251.

Eide DJ. 2003. Multiple regulatory mechanisms maintain zinc homeostasis in *Saccharomyces cerevisiae*. The Journal of nutrition. 133: 1532S–1535S.

Elamin AA, Stehr M, Spallek R, Rohde M, Singh M. 2011. The *Mycobacterium tuberculosis* Ag85A is a novel diacylglycerol acyltransferase involved in lipid body formation. Mol Microbiol. 81: 1577-1592.

Elbein AD, Pan YT, Pastuszak I, Carroll D. 2003. New insights on trehalose: a multifunctional molecule. Glycobiology. 13: 17R–27R.

Enjalbert B, MacCallum DM, Odds FC, Brown AJ. 2007. Niche-specific activation of the oxidative stress response by the pathogenic fungus *Candida albicans*. Infect Immun. 75: 2143-2151.

Faganello J, Dutra V, Schrank A, Meyer W, Schrank IS, Vainstein MH. 2009 Identification of genomic differences between *Cryptococcus neoformans* and *Cryptococcus gattii* by Representational Difference Analysis (RDA). Med Mycol. 47: 584-591.

Farhana A, Guidry L, Srivastava A, Singh A, Hondalus MK, Steyn AJ. 2010. Reductive stress in microbes: implications for understanding *Mycobacterium tuberculosis* disease and persistence. Adv Microb Physiol. 57: 43-117.

Fava-Netto C. 1961. Contribuição para o estudo imunológico da blastomicose de Lutz. Rev Inst Adolfo Lutz. 21: 99-194.

Finney LA and O'Halloran TV. 2003. Transition metal speciation in the cell: insights from the chemistry of metal ion receptors. Science. 300: 931–936.

Fleck CB, Brock M, 2008. Characterization of an acyl-CoA: carboxylate CoA-transferase from *Aspergillus nidulans* involved in propionyl-CoA detoxification. Molecular microbiology, 68: 642-656.

Fleck CB, Schöbel F, Brock M. 2011. Nutrient acquisition by pathogenic fungi: Nutrient availability, pathway regulation, and differences in substrate utilization. Int J Med Microbiol. 301: 400-407.

Felipe MS, Andrade RV, Petrofeza SS, Maranhão AQ, Torres FA, Albuquerque P, Arraes FB, Arruda M, Azevedo MO, Baptista AJ, Bataus LA, Borges CL, Campos EG, Cruz MR, Daher BS, Dantas A, Ferreira MA, Ghil GV, Jesuino RS, Kyaw CM, Leitão L, Martins CR, Moraes LM, Neves EO, Nicola AM, Alves ES, Parente JA, Pereira M, Poças-Fonseca MJ, Resende R, Ribeiro BM, Saldanha RR, Santos SC, Silva-Pereira I, Silva MA, Silveira E, Simões IC, Soares RB, Souza DP, De-Souza MT, Andrade EV, Xavier MA, Veiga HP, Venancio EJ, Carvalho MJ, Oliveira AG, Inoue MK, Almeida NF, Walter ME, Soares CMA, Brígido MM. 2003. Transcriptome

characterization of the dimorphic and pathogenic fungus *Paracoccidioides brasiliensis* by EST analysis. Yeast 20: 263-271.

Felipe MS, Andrade RV, Arraes FB, Nicola AM, Maranhão AQ, Torres FA, Silva-Pereira I, Poças-Fonseca MJ, Campos EG, Moraes LM, Andrade PA, Tavares AH, Silva SS, Kyaw CM, Souza DP, Pereira M, Jesuíno RS, Andrade EV, Parente JA, Oliveira GS, Barbosa MS, Martins NF, Fachin AL, Cardoso RS, Passos GA, Almeida NF, Walter ME, Soares CMA, Carvalho MJ, Brígido MM. 2005. Transcriptional profiles of the human pathogenic fungus *Paracoccidioides brasiliensis* in mycelium and yeast cells. J Biol Chem. 280: 24706-24714.

Ferreira MES, Marques ER, Malavazi I, Torres I, Restrepo A, Nunes LR, Oliveira RC, Goldman MH, Goldman GH 2006. Transcriptome analysis and molecular studies on sulphur metabolism in the human pathogenic fungus *Paracoccidioides brasiliensis*. Mol Genet Genomics. 276: 450-463.

Fonseca CA, Jesuino RS, Felipe MS, Cunha DA, Brito WA, 2001. Two dimensional electrophoresis and characterization of antigens from *Paracoccidioides brasiliensis*. Microbes and infection, 3: 535–542.

Fortes RM, Kipnis A, Junqueira-Kipnis AP. 2009. Paracoccidioides brasiliensis pancreatic destruction in Calomys callosus experimentally infected. BMC Microbiol. 7: 79-84.

Fradin C, De Groot P, MacCallum D, Schaller M, Klis F, Odds FC, Hube B. 2005. Granulocytes govern the transcriptional response, morphology and proliferation of *Candida albicans* in human blood. Mol Microbiol. 56: 397-415

Fradin C, Kretschmar M, Nichterlein T, Gaillardin C, d'Enfert C, Hube B. 2003. Stage-specific gene expression of *Candida albicans* in human blood. Mol Microbiol. 47: 1523-1543

Franco M, Montenegro MR, Mendes RP, Marques SA, Dillon NL, Mota NG. 1987. Paracoccidioidomycosis: a recently proposed classification of its clinical forms. Rev Soc Bras Med Trop. 20: 129–132.

Gaither LA, Eide DJ. 2001. Eukaryotic zinc transporters and their regulation. Biometals. 14: 251-270.

Garcia NM, Del Negro GM, Heins-Vaccari EM, de Melo NT, de Assis CM, Lacaz C da S 1993. *Paracoccidioides brasiliensis* a new sample isolated from feces of a penguin (Pygoscelis adeliae)]. Rev Inst Med Trop Sao Paulo. 35: 227-235.

George VT, Brooks G, Humphrey TC. 2007. Regulation of Cell Cycle and Stress Responses to Hydrostatic Pressure in Fission Yeast. Mol Biol of Cell. 18: 4168-4179.

Gifford AH, Klippenstein JR, Moore MM. 2002. Serum stimulates growth of and proteinase secretion by *Aspergillus fumigatus*. Infect Immun. 70: 19-26.

Gitan RS, Luo H, Rodgers J, Broderius M, Eide D. 1998. Zinc-induced inactivation of the yeast ZRT1 zinc transporter occurs through endocytosis and vacuolar degradation. J Biol Chem. 273: 28617-28624.

Goldman GH, dos Reis Marques E, Duarte Ribeiro DC, de Souza Bernardes LA, Quiapin AC, Vitorelli PM, Savoldi M, Semighini CP, de Oliveira RC, Nunes LR, Travassos LR, Puccia R, Batista WL, Ferreira LE, Moreira JC, Bogossian AP, Tekaia F, Nobrega MP, Nobrega FG, Goldman MH. 2003. Expressed sequence tag analysis of the human pathogen *Paracoccidioides brasiliensis* yeast phase: identification of putative homologues of *Candida albicans* virulence and pathogenicity genes. Eukaryot Cell. 2: 34-48.

Gónzalez-Párraga P, Alonso-Monge R, Plá J, Argüelles JC. 2010. Adaptive tolerance to oxidative stress and the induction of antioxidant enzymatic activities in *Candida albicans* are independent of the Hog1 and Cap1-mediated pathways. FEMS Yeast Res. 10: 747-756.

Gravelat FN, Doedt T, Chiang LY, Liu H, Filler SG, Patterson TF, Sheppard DC. 2008. In vivo analysis of *Aspergillus fumigatus* developmental gene expression determinedby real-time reverse transcription-PCR. Infect Immun. 76: 3632-3639.

Grose E, Tamsitt JR. 1965. *Paracoccidioides brasiliensis* recovered from the intestinal tract of three bats (Artibeus lituratus) in Colombia. Sabouraudia. 4: 124-125.

Goldani LZ. 2011. Gastrointestinal paracoccidioidomycosis: an overview. J Clin Gastroenterol. 45: 87-91.

González A, Gómez BL, Diez S, Hernández O, Restrepo A, Hamilton AJ, Cano LE. 2005. Purification and partial characterization of a *Paracoccidioides brasiliensis* protein with capacity to bind to extracellular matrix proteins. Infect Immun. 73: 2486-2495.

Gupta K, Verma I, Khuller GK, Mahajan R.2011. Evaluation of Aro-Tal-AST Complex protein as a marker for differential diagnosis of *Mycobacterium Avium* infection. J Glob Infect Dis. 3: 259-264.

Harkins AL, Yuan G, London SD, Dolan JW. 2010. An oleate-stimulated, phosphatidylinositol 4,5-bisphosphate-independent phospholipase D in *Schizosaccharomyces pombe*. FEMS Yeast Res. 17: 1-10.

Hartl FU. 1996. Molecular chaperones in cellular protein folding. Nature. 381: 571–580.

Hartmann T, Sasse C, Schedler A, Hasenberg M, Gunzer M, Krappmann S. 2011.Shaping the fungal adaptome-stress responses of *Aspergillus fumigatus*. Int J Med Microbiol. 301: 408-416.

Hayashi H, Alia, Sakamoto A, Nonaka H, Chen THH, Murata N. 1998. Enhanced germination under high-salt conditions of seeds of transgenic *Arabidopsis* with a bacterial gene (codA) for choline oxidase. J Plant Res. 111: 357–362.

Himmelreich U, Allen C, Dowd S, Malik R, Shehan BP, Mountford C, Sorrell TC. 2002. Identification of metabolites of importance in the pathogenesis of pulmonary cryptococcoma using nuclear magnetic resonance spectroscopy. Microbes Infect. 148: 2617–2625.

Ho E and Ames BN. 2002. Low intracellular zinc induces oxidative DNA damage, disrupts p53, NFkappa B, and AP1 DNA binding, and affects DNA repair in a rat glioma cell line. Proceedings of the National Academy of Sciences of the United States of America. 99: 16770–16775.

Hottiger T, Boller T, Wiemken A. 1987. Rapid changes of heat and desiccation tolerance correlated with changes of trehalose content in *Saccharomyces cerevisiae* cells subjected to temperature shifts. FEBS Lett. 220: 113–115.

Hounsa CG, Brandt EV, Thevelein J, Hohmann S, Prior BA. 1998. Role of trehalose in survival of *Saccharomyces cerevisiae* under osmotic stress. Microbiology. 144: 671–680.

Huang X, Madan A. 1999. CAP3: A DNA sequence assembly program. Genome Res. 9: 868-877.

Hubank M, Schatz AG. 1994. Identifying differences in mRNA expression by representational difference analysis of cDNA. Nucleis Acids Res. 22: 5640-8.

Hummert S, Hummert C, Schröter A, Hube B, Schuster S. 2010. Game theoretical modelling of survival strategies of *Candida albicans* inside macrophages. J Theor Biol. 64: 312–318.

Iordachescu M, Imai R 2008. Trehalose biosynthesis in response to abiotic stresses. J Integ Plant Biol. 50: 1223–1229.

James SA, Collins MD, Roberts IN. 1996. Use of an rRNA internal transcribed spacer region to distinguish phylogenetically closely related species of the genera Zygosaccharomyces and Torulaspora. Int J Syst Bacteriol. 46: 189-94.

Jenkins GM, Frohman MA. 2005. Phospholipase D: a lipid centric review. Cell Mol Life Sci. 62: 2305–2316.

Johnson L. 2008. Iron and siderophores in fungal-host interactions. Mycol Res. 112: 170-183.

Kamizono A, Nishizawa M, Teranishi Y, Murata K, Kimura A. 1989 Identification of a gene conferring resistance to zinc and cadmium ions in the yeast *Saccharomyces cerevisiae*. Mol Gen Genet. 219: 161–167

Kim Y, Nandakumar MP, Marten MR. 2007. Proteomics of filamentous fungi. Trends Biotechnol. 25:395-400.

Kim MJ, Kil M, Jung JH, Kim J. 2008. Roles of Zinc-responsive Transcription Factor Csr1 in Filamentous Growth of the Pathogenic Yeast *Candida albicans*. J Microbiol Biotechnol. 18: 242-247.

Kniemeyer O, Lessing F, Scheibner O, Hertweck C, Brakhage AA. 2006. Optimisation of a 2-D gel electrophoresis protocol for the human-pathogenic fungus *Aspergillus fumigatus*. Curr Genet. 49: 178-89.

Ktistakis NT, Delon C, Manifava M, Wood E, Ganley I, Sugars JM. 2003. Phospholipase D1 and potential targets of its hydrolysis product, phosphatidic acid. Biochem Soc Trans. 31: 94–97.

Kumamoto CA. 2008. Niche-specific gene expression during *Candida albicans* Infection. Curr Opin Microbiol. 11: 325-330.

Kurdistani SK, Grunstein M. 2003. Histone acetylation and deacetylation in yeast. Nat Rev Mol Cell Biol. 31: 248-254.

Landfald B, Strom AR. 1986. Choline–glycine betaine pathway confers a high level of osmotic tolerance in *Escherichia coli*. J Bacteriol. 165: 849–855.

Leclerc MC, Philippe H, Guého E. 1994. Phylogeny of dermatophytes and dimorphic fungi based on large subunit ribosomal RNA sequence comparisons. J Med Vet Mycol. 32: 331-41.

Lenzi HL, Calich VLG, Mendes-Giannini MJS, Xidiex CF, Miyaji M, Mota EM, Machado MP, Restrepo A. 2000. Two patterns of extracellular matrix expression in experimental paracoccidioidomycosis. Med. Mycol. 38: 115-119.

Li L, Kaplan J. 1998. Defects in the yeast high affinity iron transport system result in increased metal sensitivity because of the increased expression of transporters with a broad transition metal specificity. J Biol Chem. 273: 22181–22187.

Li L, Kaplan J. 2000. The yeast gene MSC2, a member of the cation diffusion facilitator family, affects the cellular distribution of zinc. J Biol Chem. 275: 5036–5043.

Li Q, Abrashev R, Harvey LM, McNeil B. 2008. Oxidative stress-associated impairment of glucose and ammonia metabolism in the filamentous fungus, *Aspergillus niger* B1-D. Mycological research. 112: 1049-1055.

Liao WL, Ramon AM, Fonzi WA. 2008. GLN3 encodes a global regulator of nitrogen metabolism and virulence of *C. albicans*. Fungal Genet Biol. 45: 514-526.

Lim D, Hains P, Walsh B, Bergquist P, Nevalainen H. 2001. Proteins associated with the cell envelope of *Trichoderma reesei*: A proteomic approach. Proteomics. 1:899-909.

Limjindaporn T, Khalaf RA, Fonzi WA. 2003. Nitrogen metabolism and virulence of *Candida albicans* require the GATA-type transcriptional activator encoded by GAT1. Mol Microbiol. 50: 993-1004.

Lin YF, Wu MS, Chang CC, Lin SW, Lin JT, Sun YJ, Chen DS, Chow LP. 2006. Comparative immunoproteomics of identification and characterization of virulence factors from *Helicobacter pylori* related to gastric cancer. Mol Cell Proteomics. 5: 1484-1496.

Liuzzi JP, Lichten LA, Rivera S, Blanchard RK, Aydemir TB, Knutson MD, Ganz T, Cousins RJ. 2005. Interleukin-6 regulates the zinc transporter Zip14 in liver and contributes to the hypozincemia of the acute-phase response. Proc Natl Acad Sci U S A. 102:6843-6848.

Llull D, Son O, Blanié S, Briffotaux J, Morello E, Rogniaux H, Danot O, Poquet I. 2011. Lactococcus lactis ZitR Is a Zinc-Responsive Repressor Active in the Presence of Low, Nontoxic Zinc Concentrations In Vivo. J Bacteriol. 193:1919-1929.

Löfblom J, Kronqvist N, Uhlén M, Stahl S, Wernérus H. 2007. Optimization of electroporation-mediated transformation: *Staphylococcus carnosus* as model organism. J Appl Microbiol. 102: 736-747.

Londero AT, Melo IS 1983. Paracoccidioidomycosis in childhood. A critical review. Mycopathologia. 82:49-55.

Londero AT. 1986. Paracoccidioidomicose. Patogenia, formas clínicas, manifestações pulmonares e diagnóstico. J Pneumol 12: 41-57.

Lopes DL, Araújo SA, Santos JP, Lyon AC, Dantas DV, Reis BS, de Góes AM, Pedroso ER. 2009. Prostatic paracoccidioidomycosis: differential diagnosis of prostate cancer. Mem Inst Oswaldo Cruz. 104: 33-36.

López-Avilés S, Grande M, González M, Helgesen AL, Alemany V, Sanchez-Piris M, Bachs O, Millar JBA, Aligue1 R. 2005. Inactivation of the Cdc25 Phosphatase by the Stress-Activated Srk1 Kinase in Fission Yeast. Mol Cell. 17: 49-59.

Lorenz MC, Bender JA, Fink GR. 2004. Transcriptional response *of Candida albicans* upon internalization by macrophages. Eukaryot Cell. 3: 1076-1087.

Lorenz MC, Fink GR. 2001. The glyoxylate cycle is required for fungal virulence. Nature. 412: 83-6.

Lulloff SJ, Hahn BL, Sohnle PG. 2004. Fungal susceptibility to zinc deprivation. J Lab Clin Med. 144: 208-214.

Lyons TJ, Gasch AP, Gaither LA, Botstein D, Brown PO, Eide DJ. 2000. Genome-wide characterization of the Zap1p zinc-responsive regulon in yeast. Proc Natl Acad Sci U S A. 97: 7957-7962.

MacDiarmid CW, Gaither LA, Eide D. 2000. Zinc transporters that regulate vacuolar zinc storage in Saccharomyces cerevisiae. EMBO J. 19: 2845-2855.

Maidan MM, Rop LD, Miguel R, Diez-Orejas R, Thevelein JM, Dijck PV. 2008. Combined inactivation of the *Candida albicans GPR1* and *TPS2* genes results in avirulence in a mouse model for systemic infection. Infect Immun. 76: 1686–1694.

Mackenzie GG, Zago MP, Erlejman AG, Aimo L, Keen CL, Oteiza PI. 2006. alpha-Lipoic acid and N-acetyl cysteine prevent zinc deficiency-induced activation of NF-kappa B and AP-1 transcription factors in human neuroblastoma IMR-32cells. Free radical research. 40: 75–84.

Marques ER, Ferreira ME, Drummond RD, Felix JM, Menossi M, Savoldi M, Travassos LR, Puccia R, Batista WL, Carvalho KC, Goldman MH, Goldman GH. 2004. Identification of genes preferentially expressed in the pathogenic yeast phase of *Paracoccidioides brasiliensis*, using suppression subtraction hybridization and differential macroarray analysis. Mol Genet Genomics. 271:667-677.

Martin R, Wächtler B, Schaller M, Wilson D, Hube B. 2011. Host-pathogen interactions and virulence-associated genes during *Candida albicans* oral infections. Int J Med Microbiol. 301: 417-422.

Matute DR, McEwen JG, Puccia R, Montes BA, San-Blas G, Bagagli E, Rauscher JT, Restrepo A, Morais F, Niño-Vega G, Taylor JW. 2006. Cryptic speciation and

recombination in the fungus *Paracoccidioides brasiliensis* as revealed by gene genealogies. Mol Biol Evol. 23: 65-73.

Melin P, Schnürer J, Wagner EG. 2002. Proteome analysis of *Aspergillus nidulans* reveals proteins associated with the response to the antibiotic concanamycin A, produced by Streptomyces species. Mol Genet Genomics. 267: 695-702.

Mendes-Giannini MJ, Ricci LC, Uemura MA, Toscano E, Arns CW. 1994. Infection and apparent invasion of Vero cells by *Paracoccidioides brasiliensis*. J Med Vet Mycol. 32: 189-195.

McDermott M, Wakelam MJ, Morris AJ. 2004. Phospholipase D. Biochem Cell Biol. 82: 225–253.

Mendonsa R, Engebrecht J. 2009. Phospholipase D function in *Saccharomyces cerevisiae*. Biochim Biophys Acta. 1791: 970–974.

Miele R, Barra D, Bonaccorsi di Patti MC. 2007. A GATA-type transcription factor regulates expression of the high-affinity iron uptake system in the methylotrophic yeast *Pichia pastoris*. Arch Biochem Biophys. 465: 172-179.

Missall TA, Pusateri ME, Donlin MJ, Chambers KT, Corbett JA, Lodge JK. 2006. Posttranslational, translational, and transcriptional responses to nitric oxide stress in *Cryptococcus neoformans*: implications for virulence. Eukaryot Cell. 5: 518–529.

Monteoliva L, Martinez-Lopez R, Pitarch A, Hernaez ML, Serna A, Nombela C, Albar JP, Gil C. 2010. Quantitative proteome and acidic subproteome profiling of *Candida albicans* yeast-to-hypha transition. J Proteome Res. 10: 502-517.

Moreno MA, Ibrahim-Granet O, Vicentefranqueira R, Amich J, Ave P, Leal F, Latgé JP, Calera JA. 2007. The regulation of zinc homeostasis by the ZafA transcriptional activator is essential for *Aspergillus fumigatus* virulence. Mol Microbiol. 64: 1182–1197.

Muller S. 2004. Redox and antioxidant systems of the malaria parasite *Plasmodium falciparum*. Mol Microbiol. 53, 1291–1305.

Nelson N. 1999. Metal ion transporters and homeostasis. EMBO J. 18: 4361-4371.

Neto BRS, Fátima JS, Mendes-Giannini MJ, Lenzi HL, Soares CMA, Pereira M. 2009. The malate synthase of *Paracoccidioides brasiliensis* is a linked surface protein that behaves as an anchorless adhesin. BMC Microbiol. 9: 272.

Nicola AM, Robertson EJ, Albuquerque P, Derengowski LS, and Casadevall A. 2011. Nonlytic exocytosis of *Cryptococcus neoformans* from macrophages occurs in vivo and is influenced by phagosomal pH. mBio. 2: e00167-11.

Nishikaku AS, Ribeiro LC, Molina RF, Albe BP, Cunha, Cda S, Burger E. 2009. Matrix metalloproteinases with gelatinolytic activity induced by *Paracoccidioides brasiliensis* infection. Int J Exp Pathol. 90: 527-537.

Nogueira SV, Fonseca FL, Rodrigues ML, Mundodi V, Abi-Chacra EA, Winters MS, Alderete JF, Soares CMA. 2010. *Paracoccidioides brasiliensis* enolase is a surface protein that binds plasminogen and mediates interaction of yeast forms with host cells. Infect Immun. 78: 4040-4050.

Nunes LR, Oliveira RC, Leite DB, Silva VS, Marques ER, Ferreira MES, Ribeiro DC, Bernardes LAS, Goldman MH, Puccia R, Travassos LR, Batista WL, Nóbrega MP, Nobrega FG, Yang DY, Pereira CAB, Goldman GH. 2005. Transcriptome analysis of *Paracoccidioides brasiliensis* cells undergoing mycelium-to-yeast transition. Eukaryot Cell. 4: 2115-2128.

Okagaki LH, Strain AK, Nielsen JN, Charlier C, Baltes NJ, Chrétien F, Heitman J, Dromer F, Nielsen K. 2010. Cryptococcal cell morphology affects host cell interactions andpathogenicity. PLoS Pathog. 6: 953-963.

Padilla-Guerrero IE, Barelli L, González-Hernández GA, Torres-Guzmán JC, Bidochka MJ. 2011. Flexible metabolism in *Metarhizium anisopliae* and *Beauveria bassiana*: role of the glyoxylate cycle during insect pathogenesis. Microbiology. 157: 199-208.

Palmieri L, Runswick MJ, Fiermonte G, Walker JE, Palmieri F. 2000. Yeast Mitochondrial Carriers: Bacterial Expression, Biochemical Identification and Metabolic Significance. J Bioenerg Biomembr. 32: 67-77.

Paniago AM, Aguiar JI, Aguiar ES, da Cunha RV, Pereira GR, Londero AT, Wanke B. 2003. Paracoccidioidomicose: estudo clínico e epidemiológico de 422 casos observados no estado do Mato Grosso do Sul. Rev Soc Bras Med Trop.36: 455-459.

Pao SS, Paulsen IT, Saier MH Jr. 1998. Major facilitator superfamily. Microbiol Mol Biol Rev. 62: 1-34.

Parente AF, Bailão AM, Borges CL, Parente JA, Magalhães AD, Ricart CA, Soares CMA. 2011. Proteomic Analysis Reveals That Iron Availability Alters the Metabolic Status of the Pathogenic Fungus *Paracoccidioides brasiliensis*. PLoS One. 6: e22810.

Parente JA, Salem-Izacc SM, Santana JM, Pereira M, Borges CL, Bailão AM, Soares CMA. 2010. A secreted serine protease of *Paracoccidioides brasiliensis* and its interactions with fungal proteins. BMC Microbiol. 10: 292.

Park RY, Sun HY, Choi MH, Bai YH, Chung YY, Shin SH. 2006. Proteases of a *Bacillus subtilis* clinical isolate facilitate swarming and siderophore-mediated iron uptake via proteolytic cleavage of transferrin. Biol Pharm Bull. 29: 850-853.

Pastorian K, Havell L 3rd, Byus CV. 2000. Optimization of cDNA Representational Difference Analysis for the identification of differentially expressed mRNAs. Anal Biochem. 283: 89-98.

Paulsen IT, Sliwinski MK, Nelissen B, Goffeau A, Saier MH Jr. 1998. Unified inventory of established and putative transporters encoded within the complete genome of *Saccharomyces cerevisiae*. FEBS Lett. 430: 116-125.

Pereira LA, Báo SN, Barbosa MS, Silva JL, Felipe MS, Santana JM, Mendes-Giannini MJ, Soares CMA. 2007. Analysis of the *Paracoccidioides brasiliensis* triosephosphate isomerase suggests the potential for adhesin function. FEMS Yeast Res. 7: 1381-1388.

Pereira M, Bailão AM, Parente JA, Borges CL, Salem-Izacc SM, Soares CMA. 2009. Preferential transcription of *Paracoccidioides brasiliensis* genes: host niche and time-dependent expression. Mem Inst Oswaldo Cruz. 104: 486-491.

Peres da Silva R, Matsumoto MT, Braz JD, Voltan AR, de Oliveira HC, Soares CP, Mendes Giannini MJ. 2011. Differential gene expression analysis of *Paracoccidioides brasiliensis* during keratinocyte infection. J Med Microbiol. 60: 269-280.

Peterbauer CK, Litscher D, Kubicek CP. 2002. The *Trichoderma atroviride* seb1 (stress response element binding) gene encodes an AGGGG-binding protein which is involved in the response to high osmolarity stress. Mol Genet Genomes. 268: 223-231.

Petzold EW, Himmelreich U, Mylonakis E, Rude T, Toffaletti D, Cox GM, Miller JL, Perfect JR. 2006. Characterization and regulation of the trehalose synthesis pathway and its importance in the pathogenicity of *Cryptococcus neoformans*. Infect Immun. 74: 5877-5887.

Pinzan CF, Ruas LP, Casabona-Fortunato AS, Carvalho FC, Roque-Barreira M. 2010. Immunological Basis for the Gender Differences in Murine *Paracoccidioides brasiliensis* Infection. PLoS One. 5: 10757.

Pitarch A, Sánchez M, Nombela C, Gil C. 2003. Analysis of the *Candida albicans* proteome. I. Strategies and applications. J Chromatogr B Analyt Technol Biomed Life Sci. 787:101-128.

Pocsi I, Prade RA, Penninckx MJ. 2004. Glutathione, altruistic metabolite in fungi. Adv Microb Physiol. 49: 1–76.

Pollak N, Dolle C, Ziegler M. 2007. The power to reduce: pyridine nucleotides–small molecules with a multitude of functions. Biochem J. 402: 205–218.

Prado M, da Silva MB, Laurenti R, Travassos LR, Taborda CP. 2009. Mortality due to systemic mycoses as a primary cause of death or in association with AIDS in Brazil: a review from 1996 to 2006. Mem Inst Oswaldo Cruz. 104: 513-521.

Prigneau O, Porta A, Poudrier JA, Colonna-Romano S, Noël T, Maresca B. 2003. Genes involved in beta-oxidation, energy metabolism and glyoxylate cycle are induced by *Candida albicans* during macrophage infection. Yeast. 20: 723-730.

Proft M, Struhl K. 2002. Hog1 kinase converts the sko1-Cyc8-Tup1 repressor complex into an activator that recruits SAGA and SWI/SNF in response to osmotic stress. Mol Cell. 9: 1307-1317

Puccia R, Juliano MA, Juliano L, Travassos LR, Carmona AK. 1999. Detection of the basement membrane-degrading proteolytic activity of *Paracoccidioides brasiliensis* after SDS-PAGE using agarose overlays containing Abz-MKALTLQ-EDDnp. Braz J Med Biol Res. 32: 645-9

Puttikamonkul S, Willger SD, Grahl N, Perfect JR, Movahed N, Bothner B, Park S, Paderu P, Perlin DS, Cramer RA Jr. 2010. Trehalose 6-phosphate phosphatase is required for cell wall integrity and fungal virulence but not trehalose biosynthesis in the human fungal pathogen *Aspergillus fumigatus*. Mol Microbiol. 9.

Ramírez MA, Lorenz MC. 2009 The transcription factor homolog CTF1 regulates {beta}-oxidation in *Candida albicans*. Eukaryot Cell. 8: 1604-1614.

Ramos-e-Silva M, Saraiva L do E. 2008. Paracoccidioidomycosis. Dermatol Clin. 26: 257-269.

Rappleye CA, Goldman W E. 2006. Defining virulence genes in the dimorphic fungi. Annu Rev Microbiol. 60: 281-303.

Regenberg B, Holmberg S, Olsen LD, Kielland-Brandt MC. 1998. Dip5p mediates high-affinity and high-capacity transport of L-glutamate and L-aspartate in *Saccharomyces cerevisiae*. Curr Genet. 33: 171-177.

Reis VLL, Rolla VC, Rangel CA, Sampaio MBNO, Tavares W, Praxedes H, Rocha WB 1986. Paracoccidioidomicose disseminada aguda com extenso derrame pleural. Arq Bras Med. 60: 275-280.

Restrepo A. 1985. The ecology of *Paracoccidioides brasiliensis*: a puzzle still unsolved. Sabouraudia. 23: 323-334.

Restrepo A, Cano LE, Tabares AM. 1983. A comparison of mycelial filtrate and yeast lysate paracoccidioidin in patients with paracoccidioidomycosis. Mycopathologia. 84: 49-54.

Restrepo A, Jiménez BE. 1980. Growth of *Paracoccidioides brasiliensis* yeast phase in a chemically defined medium. Journal of clinical microbiology. 12: 279-281.

Restrepo A, McEwen JG, Castañeda E. 2001. The habitat of *Paracoccidioides brasiliensis*: how far from solving the riddle Medical mycology: official publication of the International Society for Human and Animal Mycology. 39: 233-241.

Restrepo A, Trujillo M, Gomez I**.** 1989. Inapparent lung involvement in patients with the subacute juvenile type of paracoccidioidomycosis**.** Rev Inst Med Trop Sao Paulo**.** 31: 18-22.

Restrepo A, Tobón A. 2005. *Paracoccidioides brasiliensis.* In: Mandell GL, Bennett JE, Dollin R. (Eds). Principles and Practice of Infectious Diseases, Philadelphia. 3062–3068.

Restrepo-Moreno A. 2003. Paracoccidioidomycosis. In: Dismukes WE, Pappas PG, Sobel J. (Eds.), Clinical Mycology. Oxford University Press, New York, pp. 328-345.

Reuter A, Nestl A, Zwacka RM, Tuckermann J, Waldherr R, Wagner EM, Hoyhtya M, Meyer zum Gottesberge AM, Angel P, Weiher H. 1998. Expression of the recessive glomerulosclerosis gene MPV17 regulates MMP-2 expression in fibroblasts, the kidney, and the inner ear of mice. Mol Biol Cell. 9: 1675–1682.

Rezende TC, Borges CL, Magalhães AD, de Sousa MV, Ricart CA, Bailão AM, Soares CMA. 2011. A quantitative view of the morphological phases of *Paracoccidioides brasiliensis* using Proteomics. J Proteomics. 75: 572-587.

Rhee SG, Chae HZ, Kim K. 2005. Peroxiredoxins: a historical overview and speculative preview of novel mechanisms and emerging concepts in cell signaling. Free radical biology & medicine. 38: 1543-1552.

Rhodes D, Hanson AD. 1993. Quaternary ammonium and tertiary sulfonium compounds in higher plants. Annu Rev Plant Physiol Plant Mol Biol. l44: 357–384

Robert F, Pokholok DK, Hannet NM, Rinaldi NJ, Chandy M, Rolfe A, Workman JL, Gifford DK, Young RA. 2004. Global position and recruitment of HATs and HDACs in the yeast genome. Mol Cell. 16: 199-209

Rosseau P, Halvorson HO, Bulla LAJr, St. Jullan G. 1972. Germination and outgrowth of single spores of *Saccharomyces cerevesiae* viewed by scanning electron and phase contrast microscopy. J Bacteriol. 109: 1232-1238.

Roth MG. 2008. Molecular mechanisms of PLD function in membrane traffic. Traffic. 9: 1233–1239

Rutherford JC, Bird AJ. 2004. Metal-Responsive Transcription Factors That Regulate Iron, Zinc, and Copper Homeostasis in Eukaryotic Cells. Eukaryot Cell. 3: 1-13.

San-Blas G. 1993. Paracoccidioidomycosis and its etiologic agent: *Paracoccidioides brasiliensis*. J Med Vet Mycol. 31: 99–113.

San-Blas G, Niño-Vega G, Iturriaga T. 2002. *Paracoccidioides brasiliensis* and paracoccidioidomycosis: molecular approaches to morphogenesis, diagnosis, epidemiology, taxonomy and genetics. Medical mycology: official publication of the International Society for Human and Animal Mycology. 40: 225-242.

Sansó M, Gogol M, Ayté J, Seidel C, Hidalgo E. 2008. Transcription Factors Pcr1 and Atf1 Have Distinct Roles in Stress- and Sty1-Dependent Gene Regulation. Eukaryot Cell. 7: 826-835.

Sano A, Nishimura K, Miyaji M. 1999. The research encouragement award. Effects of sex hormones on sexual difference of experimental paracoccidioidomycosis. Nihon Ishinkin Gakkai Zasshi. 40: 1-8.

Schneider RO, Fogaça NS, Kmetzsch L, Schrank A, Vainstein MH, Staats CC. 2012. Zap1 regulates zinc homeostasis and modulates virulence in *Cryptococcus gattii*. PLoS One. 7: e43773

Seneviratne CJ, Wang Y, Jin L, Abiko Y, Samaranayake LP. 2010. Proteomics of drug resistance in *Candida glabrata* biofilms. Proteomics. 10:1444-1454.

Sertil O, Vemula A, Salmon SL, Morse RH, Lowry CV. 2007. Direct role for the Rpd3 complex in transcriptional induction of the anaerobic DAN/TIR genes in yeast. Mol Cell Biol. 27: 2037-2047.

Shankar J, Restrepo A, Clemons KV, Stevens DA. 2011a. Hormones and the resistance of women to paracoccidioidomycosis. Clin Microbiol Rev. 24: 296-313.

Shankar J, Wu TD, Clemons KV, Monteiro JP, Mirels LF, Stevens DA. 2011b. Influence of 17β-estradiol on gene expression of *Paracoccidioides* during mycelia-to-yeast transition. PLoS One. 6: e28402.

Shapiro RS, Uppuluri P, Kus AK, Collins C, Senn H, Perfeito JR, Heitman J, Cowen LE. 2009. Hsp90 orchestrates temperature-dependent *Candida albicans* morphogenesis via Ras1-PKA signaling. Curr Biol. 19: 621-629.

Sharma VM, Tomar RS, Dempsey AE, Reese JC. 2007. Histone deacetylases RPD3 and HOS2 regulate the transcriptional activation of DNA damage-induced genes. Mol Cell Biol. 27: 3199-3210

Sharma V, Sharma S, Bentrup KH, McKinney JD, Russell DG, Jacobs WR, Sacchettini JC. 2000. Structure of isocitrate lyase, a persistence factor of *Mycobacterium tuberculosis*. Nature. 7: 663-668.

Shi Y, Cheng D. 2009. Beyond triglyceride synthesis: the dynamic functional roles of MGAT and DGAT enzymes in energy metabolism. Am J Physiol Endocrinol Metab. 297: E10–E18.

Shin JH, Yang JY, Jeon BY, Yoon YJ, Cho SN, Kang YH, Ryu H, Hwang GS. 2001. (1)HNMR-based metabolomic profiling in mice infected with *Mycobacterium tuberculosis*. J Proteome Res. 6: 2238-2247.

Silva MG, Schrank A, Bailão EF, Bailão AM, Borges CL, Staats CC, Parente JA, Pereira M, Salem-Izacc SM, Mendes-Giannini MJ, Oliveira RM, Silva LK, Nosanchuk JD, Vainstein MH, de Almeida Soares CMA. 2011. The homeostasis of iron, copper, and zinc in *Paracoccidioides brasiliensis*, Cryptococcus neoformans var. grubii, and Cryptococcus gattii: a comparative analysis. Front Microbiol. 2:1-19.

Simm C, Lahner B, Salt D, LeFurgey A, Ingram P, Yandell B, Eide DJ. 2007. The Yeast Vacuole in Zinc Storage and Intracellular Zinc Distribution. Eukaryot Cell. 6:1166-1177.

Sirakova TD, Dubey VS, Deb C, Daniel J, Korotkova TA, Abomoelak B, Kolattukudy PE. 2006. Identification of a diacylglycerol acyltransferase gene involved in accumulation of triacylglycerol in *Mycobacterium tuberculosis* under stress. Microbiology. 152: 2717-2725.

Sõti C, Pál C, Papp B, Csermely P. 2005. Molecular chaperones as regulatory elements of cellular networks. Current opinion in cell biology. 17: 210–215.

Steen BR, Zuyderduyn S, Toffaletti DL, Marra M, Jones SJ, Perfect JR, Kronstad J. 2003. *Cryptococcus neoformans* gene expression during experimental cryptococcal meningitis. Eukaryot. Cell. 2: 1336–1349.

Strijbis K, Distel B. 2010. Intracellular acetyl unit transport in fungal carbon metabolism. Eukaryot Cell. 9: 1809-1815.

Ström K, Schnürer J, Melin P. 2005. Co-cultivation of antifungal *Lactobacillus plantarum* MiLAB 393 and *Aspergillus nidulans*, evaluation of effects on fungal growth and protein expression. FEMS Microbiol Lett. 246: 1191-24.

Sugui JA, Kim HS, Zarember KA, Chang YC, Gallin JI, Nierman WC, Kwon-Chung KJ. 2008. Genes differentially expressed in conidia and hyphae of *Aspergillus fumigatus* upon exposure to human neutrophils. PLoS One. 3: 2655-2662.

Tavares AH, Silva SS, Dantas A, Campos EG, Andrade RV, Maranhão AQ, Brígido MM, Passos-Silva DG, Fachin AL, Teixeira SM, Passos GA, Soares CMA, Bocca AL, Carvalho MJ, Silva-Pereira I, Felipe MS. 2007. Early transcriptional response of *Paracoccidioides brasiliensis* upon internalization by murine macrophages. Microbes Infect. 9: 583-590.

Taricani L, Tejada ML, Young PG. 2001. The fission yeast ES2 homologue, Bis1, interacts with the Ish1 stress-responsive nuclear envelope protein. J Biol Chem. 277: 10562-10572.

Tavares AH, Silva SS, Dantas A, Campos EG, Andrade RV, Maranhão AQ, Brígido MM, Passos-Silva DG, Fachin AL, Teixeira SM, Passos GA, Soares CMA, Bocca AL, Carvalho MJ, Silva-Pereira I, Felipe MS. 2007. Early transcriptional response of *Paracoccidioides brasiliensis* upon internalization by murine macrophages. Microbes Infect. 9: 583-590.

Taylor BL, Zhulin IB. 1999. PAS domains: internal sensors of oxygen, redox potential, and light. Microbiol Mol Biol Rev. 63: 479-506

Teixeira MM, Theodoro RC, de Carvalho MJ, Fernandes L, Paes HC, Hahn RC, Mendoza L, Bagagli E, San-Blas G, Felipe MS. 2009. Phylogenetic analysis reveals a high of speciation in the Paracoccidioides genus. Mol Phylogenet Evol. 52: 273-283.

Terçarioli GR, Bagagli E, Reis GM, Theodoro RC, Bosco SM, Macoris SA, Richini-Pereira VB. 2007. Ecological study of *Paracoccidioides brasiliensis* in soil: growth ability, conidia production and molecular detection. BMC Microbiol. 7: 92.

Teutschbein J, Albrecht D, Pötsch M, Guthke R, Aimanianda V, Clavaud C, Latgé JP, Brakhage AA, Kniemeyer O. 2010. Proteome Profiling and Functional

Classification of Intracellular Proteins from Conidia of the Human-Pathogenic Mold *Aspergillus fumigatus*. J Proteome Res. 9: 3427-3442.

Thevelein JM. 1984. Regulation of trehalose metabolism in fungi. Microbiol Rev. 48: 42-59.

Thewes S, Kretschmar M, Park H, Schaller M, Filler SG, Hube B. 2007. In vivo andex vivo comparative transcriptional profiling of invasive and non-invasive *Candida albicans* isolates identifies genes associated with tissue invasion. Mol Microbiol. 63: 1606-1628.

Thirach S, Cooper CR Jr, Vanittanakom N. 2008. Molecular analysis of the *Penicillium marneffei* glyceraldehyde-3-phosphate dehydrogenase-encoding gene (*gpdA*) and differential expression of *gpdA* and the isocitrate lyase-encoding gene (*acuD*) upon internalization by murine macrophages. J Med Microbiol. 57: 1322-1328.

Thomas ST, VanderVen BC, Sherman DR, Russell DG, Sampson NS. 2011. Pathway profiling in *Mycobacterium tuberculosis*: elucidation of cholesterol-derived catabolite and enzymes that catalyze its metabolism. J Biol Chem. 286: 43668-43678.

Thywißen A, Heinekamp T, Dahse HM, Schmaler-Ripcke1 J, Nietzsche S, ZipfelPF, Brakhage AA. 2011. Conidial dihydroxynaphthalene melanin of the human pathogenic fungus *Aspergillus fumigatus* interferes with the host endocytosis pathway. Front in microb. 2: 1-12.

Trott A, Morano KA. 2004. *SYM1* is the stress-induced *Saccharomyces cerevisiae* ortholog of the mammalian kidney disease gene *Mpv17* and is required for ethanol metabolism and tolerance during heat shock. Eukariotic cell. 3: 620-731.

Van Ho A, Ward DM, Kaplan J. 2002. Transition Metal Transport in Yeast. Annu Rev Microbiol. 56: 237-261.

Velasco-Garcia R, Jiménez CM, Mendoza-Hernández G, Muñoz-Clares RA. 1999. Rapid purification and properties of betaine aldehyde dehydrogenase from *Pseudomonas aeruginosa*. J Bacteriol. 181: 1291-1300.

Vicentefranqueira R, Moreno MA, Leal F, Calera JA. 2005. The zfrA and zrfB of *Aspergillus fumigatus* Encode the Zinc Transporter Proteins of a Zinc Uptake System Induced in an Acid, Zinc-Depleted Environment. Eukaryot Cell. 4: 837-848.

Vicentini AP, Gesztesi JL, Franco MF, de Souza W, de Moraes JZ, Travassos LR, Lopes JD. 1994. Binding of *Paracoccidioides brasiliensis* to laminin trough surface glycoprotein gp43 leads to enhancement of fungal pathogenesis. Infect Immun. 62: 1465-1469.

Vijaranakul U, Nadakavukaren MJ, Bayles DO, Wilkinson BJ, Jayaswal RK. 1997. Characterization of a NaCl-sensitive *Staphylococcus aureus* mutant and rescue of the NaCl-sensitive phenotype by glycine betaine but not by other compatible solutes. Appl Environ Microbiol. 63: 1889–1897.

Walker LA, Maccallum DM, Bertram, Gow NA, Odds FC, Brown AJ. 2009. Genome-wide analysis of *Candida albicans* gene expression patterns during infection of the mammalian kidney. Fungal Genet Biol. 46: 210-219.

Waters BM, Eide DJ. 2002. Combinatorial Control of Yeast FET4 Gene Expression by Iron, Zinc, and Oxygen. J Biol Chem. 277: 33749-33757.

Wamelink MMC, Struys EA, Jakobs C. 2008. The biochemistry, metabolism and inherited defects of the pentose phosphate pathway: A review. J Inherit Metab Dis. 31: 703-717.

Wang A, Kurdistani SK, Grunstein M. 2002. Requirement of Hos2 histone deacetylase for gene activity in yeast. Science. 298: 1412-1414

Weretilnyk EA, Hanson AD. 1990. Molecular cloning of a plant betaine-aldehyde dehydrogenase, an enzyme implicated in adaptation to salinity and drought. Proc Natl Acad Sci U S A. 87: 2745–2749.

Wheeler PR, Ratledge C. 1988. Use of carbon sources for lipid biosynthesis in *Mycobacterium leprae*: a comparison with other pathogenic mycobacteria. J Gen Microbiol. 134: 2111-2121.

Wilkins MR, Sanchez JC, Gooley AA, Appel RD, Humphery-Smith I, Hochstrasser DF, Williams KL. 1996. Progress with proteome projects: why all proteins expressed by a genome should be identified and how to do it. Biotechnol Genet Eng Rev. 13:19-50.

Winters MS, Chan Q, Caruso JA, Deepe GS Jr. 2010. Metallomic analysis of macrophages infected with *Histoplasma capsulatum* reveals a fundamental role for zinc in host defenses. The Journal of infectious diseases. 202: 1136–1145.

Winters MS, Spellman DS, Chan Q, Gomez FJ, Hernandez M, Catron B, Smulian AG, Neubert TA, Deepe GS Jr. 2008. *Histoplasma capsulatum* proteome response to decreased iron availability. Proteome Sci. 6: 36.

Wu CY, Bird AJ, Winge DR, Eide DJ. 2007. Regulation of the yeast TSA1 peroxiredoxin by ZAP1 is an adaptive response to the oxidative stress of zinc deficiency. The Journal of biological chemistry. 282: 2184–2195.

Wu CY, Roje S, Sandoval FJ, Bird AJ, Winge DR, Eide DJ. 2009. Repression of Sulfate Assimilation Is an Adaptive Response of Yeast to the Oxidative Stress of Zinc Deficiency. The Journal of biological chemistry. 284: 27544-27556.

Zhao H, Eide D. 1996a. The yeast ZRT1 gene encodes the zinc transporter protein of a high-affinity uptake system induced by zinc limitation. Proc Natl Acad Sci U S A. 93:2454-58.

Zhao H, Eide D. 1996b. The ZRT2 Gene Encodes the Low Affinity Zinc Transporter in *Saccharomyces cerevisae*. J Biol Chem. 271: 23203-23210.

Zhao H, Eide DJ. 1997. Zap1p, a metalloregulatory protein involved in zinc-responsive transcriptional regulation in *Saccharomyces cerevisiae*. Mol Cell Biol. 17: 5044-5052.

Zhao H, Butler E, Rodgers J, Spizzo T, Duesterhoeft S, Eide D. 1998. Regulation of zinc homeostasis in yeast by binding of the ZAP1 transcriptional activator to zinc-responsive promoter elements. J Biol Chem. 273: 28713-28720.